University of Novi Sad
FACULTY OF TECHNICAL SCIENCES
DEPARTMENT OF PRODUCTION ENGINEERING
21000 NOVI SAD, Trg Dositeja Obradovica 6, SERBIA

UDK 621 ISSN 1821-4932

JOURNAL OF

PRODUCTION ENGINEERING

Volume 17 Number 2

Novi Sad, November 2014

Journal of Production Engineering, Vol.17 (2014), Number 2

Publisher: FACULTY OF TECHNICAL SCIENCES
DEPARTMENT OF PRODUCTION ENGINEERING
21000 NOVI SAD, Trg Dositeja Obradovica 6
SERBIA

Manuscript submitted for publication: November 28, 2014.
Printing: 1st
Circulation: 300 copies

CIP classification:

CIP – Катаголизација у публикацији
Библиотека Матице српске, Нови Сад

621

JOURNAL of Production Engineering / editor in chief Pavel Kovač. – Vol. 12, No. 1 (2009)- . – Novi Sad : Faculty of Technical Sciences, Department for Production Engineering, 2009-. – 30 cm

Dva puta godišnje (2012-). Je nastavak: Časopis proizvodno mašinstvo = ISSN
0354-6446
ISSN 1821-4932

Printing by: FTN, Graphic Center ***GRID,*** *Novi Sad*

ISSN: 1821-4932

INTERNATIONAL EDITORIAL BOARD

Editorial

*The **Journal of Production Engineering** dates back to 1984, when the first issue of the **Proceedings of the Institute of Production Engineering** was published in order to present its accomplishments. In 1994, after a decade of successful publication, the Proceedings changed the name into Production Engineering, with a basic idea of becoming a Yugoslav journal which publishes original scientific papers in this area.*

*In 2009 year, our Journal finally acquires its present title - **Journal of Production Engineering**. To meet the Ministry requirements for becoming an international journal, a new international editorial board was formed of renowned domestic and foreign scientists, refereeing is now international, while the papers are published exclusively in English. From the year 2011 Journal is in the data base COBISS and KoBSON presented.*

The Journal is distributed to a large number of recipients home and abroad, and is also open to foreign authors. In this way we wanted to heighten the quality of papers and at the same time alleviate the lack of reputable international and domestic journals in this area.

Editor in Chief

Professor Pavel Kovač, PhD,

Journal of Production Engineering
Vol.17 No.2

Contents

REVIEW PAPER

ORIGINAL SCIENTIFIC PAPER

Journal of Production Engineering
Vol.17 No.2

Review Paper

Kovač, P., Gostimirovic M., Savkovic B., Mankova I., Pucovski V., Rodic D.

LCA ACTIVITIES - A REVIEW

Received: 17 September 2014 / Accepted: 19 October 2014

Abstract: *Mass production has also brought mass consumption of natural resources and energy, as well as mass waste disposal at the end. From development perspective, the environmental impact need to be reduced while improving the product design and the functionality in order to ensure competitiveness and satisfy customer demand. The paper summarizes the aspects of life cycle activities management, product design, maintenance and the role of assembly and disassembly. Identified was technical issues regarding activities ranging over the entire product life cycle. Assembly and disassembly play the key role in the LCM. The Eco Designed products are flexible, reliable, durable, adaptable, modular, dematerialised and reusable. This will be illustrated with a focus on processes machines for manufacturing. The Views of Manufacturer and User to the life cycle of technical products is different.*
Key words: *natural resources, life cycle, activities management, product design*

Pregled aktivnosti menadžmenta životnog ciklusa. *Masovna proizvodnja dovodi do masovne konzumacije prirodnih resursa i energije, a na kraju i do masovnog skladištenja otpada. Ljudi ne mogu kontinualno da konzumiraju resurse. Sa perspektive razvoja udar na okolinu mora da se redukuje uz poboljšanje dizajna proizvoda i njegove funkcionalnosti u cilju da se osigura konkurentnost i zadovolje zahtevi potrošača. Rad sumira sve aspekte aktivnosti menadžmenta životnog ciklusa, dizajna proizvoda, održavanja kao i uloge montaže i demontaže. Identifikovani su tehnički uslovi koji se tiču aktivnosti tokom čitavog životnog ciklusa proizvoda. Montaža i demontaža igra ključnu ulogu u životnom ciklusu. Eko dizajnirani produkti su fleksibilni, pouzdani, dugotrajni, prilagodivi, modularni, nematerijalizovani, spemni za ponovno korišćenje, modularni. Ilustracije su pokazane sa fokusom na procese i mašine za proizvodnju. Pogledi proizvođača i korisnika na životni ciklus tehničkih proizvoda se značajno razlikuju.*
Ključne reči: *prirodni resursi, životni ciklus, aktivnosti menadžmenta, dizajn proizvoda*

1. INTRODUCTION

It is widely accepted in society that our current way of living must change to diminish the damage done to the ecosystem and ensure the sustainability of future generations. Many engineering tools have been developed to assist manufacturers reduce their resource consumption and harmful environmental impact while aiming to improve existing products and processes [1]. From development perspective, the environmental impact need to be reduced while improving the product design and the functionality in order to ensure competitiveness of the manufacturer and satisfy customer demand, and be more responsible for the ecosystem. Overall environmental impact in the society is continuing to increase despite the development of many eco design tools [2]. This problem can be attributed to overlooking the issue of increasing volume of products in a wider range of functionality that are being consumed in the market [3]. Therefore, the environmental assessment of products in relation to design features need be conducted with respect to total volume to identify the required improvement at product quality level. The influence of technology change on the environmental impacts also needs to be considered in sight of new technologies in a growing market demand [4].

The purpose of the life cycle impact assessment is to interpret the inventory results into their potential impacts on the areas of protection of the LCA. The use of the LCA shall help protect in next areas:

- Human health
- Natural environment
- Natural resources
- Man-made environment

The paper, discuss life cycle assessment management for closed-loop manufacture, which could be an essential means for realize a sustainable society, and the changing role of product quality assurance from the perspective of life cycle management. Then, it is present a framework that shows management cycles of product quality assurance in the product life cycle. According to this framework, identified was technical issues regarding activities ranging over the entire product life cycle. Assembly and disassembly play the key role in the LCM. This will be illustrated with a focus on machines for manufacturing.

2. THE LIFE CYCLE MANAGEMENT IN REALIZING A SUSTAINABLE SOCIETY

People through history of industrial development have been improving the quality of human life by increasing manufacturing capability. Mass production has also brought mass consumption of natural resources and energy, as well as mass waste disposal at the end. People cannot continue to consume resources and

energy, and to dispose of waste without considering the impact of these activities on the environment. Therefore is needed to change the paradigm of manufacturing from “how to produce products most efficiently” into “how to avoid producing products while still maintaining customer satisfaction and corporate profits”. Closed-loop manufacturing has been proposed as a solution to this [5].

The concept of closed-loop manufacturing can be expressed as “renewing functions while circulating material.” There are many ways to circulate material, as shown in Figure 1, known as the comet circle TM [6]. Each orbit in the figure corresponds to a life cycle option, such as prolonged use by means of maintenance, product reuse, part reuse, material recycling, and energy recovery.

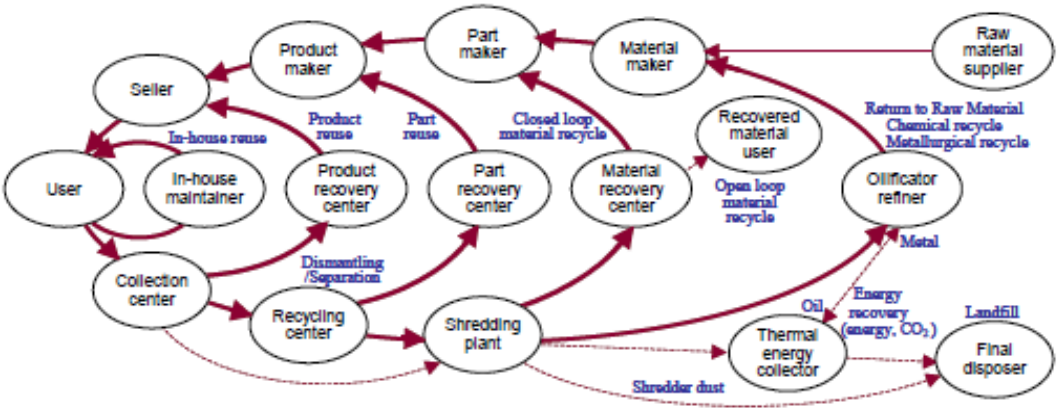

Fig. 1. Comet circle TM. [6].

In selecting life cycle options, is needed to consider eco-efficiency, which is defined as the ratio of provided value to environmental load. Therefore, cannot always be select the options with the lowest environmental load, because it is needed to consider the balance between environmental friendliness and customer satisfaction, as well as corporate profits.

3. LIFE CYCLE ACTIVITIES

The objective of product quality assurance is to preserve the condition of products so as to fulfill their required functions throughout their life cycle. It is an important part of life cycle management, whose main purpose is to enhance the eco-efficiency of the product life cycle.

As previously mentioned, there are two reasons why it is necessary to control the conditions of products: changes in the condition of products due to deterioration, and the changing needs of customers or of society. These changes generate gaps between the required function and the realized function and involve the following activities.

1. Product design:
Improving design in the product development phase and providing the design data for strategy planning and task control.
2. Strategy planning:
Selecting a strategy appropriate to each part of the product.
3. Task control:
Planning and executing the tasks based on the selected strategy.
4. Evaluation of results:
Evaluating the results of to determine quality assurance whether the strategy planning and task control are appropriate.
5. Improvement of quality assurance and products:
Improving quality assurance task control, strategy planning, and even product design based on the evaluation of the results.
6. Dismantling planning and execution:
Planning and execution of dismantling at the end of the life cycle

In life cycle, have to manage the activities listed above in an effective way throughout the life cycle of the product the following issues should be considered [7].

1. Adaptation to various changes during life cycle:
During the product life cycle, there could be various changes in the required functions, in the operating environment, in the operating conditions and in the product itself. Management should be flexible enough to adapt to these changes.
2. Continuous improvement of products:
In general, it is impossible to design a product perfectly. Therefore, should include a mechanism for continuous improvement of products based on experience and knowledge acquired during their life cycle. This mechanism is also effective for functional upgrade of products to cope with shortening the product life cycle because of rapid changes in users' needs and technology development.
3. Integration of information:
For effective quality assurance management, all information associated with should be integrated in such a way that it is available from any phase of the life cycle. In the development phase, for example, it is essential to know the real operating

situations and the problems encountered during past operations. On the other hand, it is necessary to have exact design data for strategy planning and maintenance task control product life cycle.

4. THE LIFE CYCLE MANAGEMENT PARADIGM

The new paradigm takes into account the life cycle of technical products and the optimisation of value and benefits including engineering, assembly, service, maintenance and disassembly.

Following the new paradigm of optimisation and adding value over the total life of products, a structural change in the relationship between manufacturer and user will occur. They have different views to the same business processes in the life of products, as shown in figure 2 [8].

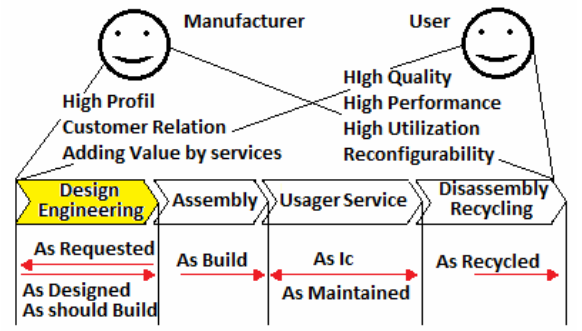

Fig. 2. The Views of Manufacturer and User to the life cycle of technical products [8]

4.1 Manufacturer's view

In general, the life cycle of products can be defined as the phase of design and engineering, manufacturing, assembly, usage, service, disassembly and recycling.

Deeper dimensions are defined in [8, 9, 10, 11, 12] and depend on the specific structure of products and production. The main objective is to fulfil the requirements of markets and customers for efficient utilisation of manufacturing resources. The new view is adding value in the usage and recycling-phases by customer near services including maintenance and disassembly for reconfiguration, reuse or recycling.

This view to the usage and recycling phases makes it necessary to take more than ever before into account aspects of life cycle design and engineering or the capability of systems for assembly, disassembly and diagnostics in all phases and especially in the phase of usage. They offer product oriented profitable services along all operations by supporting the diagnostics of the actual properties, also partial disassembly and assembly for reconfiguration, upgrading and final disassembly for recycling.

4.2 Customer's view

In general, customers are interested in achieving a high utilisation in the usage phase and lowest cost even if the processes have to be changed. Flexibility of manufacturing systems is required with minimal setup time and cost and a guaranteed process performance.

High efficiency of the usage of complex technical products depends on specific skills and know-how on the details of machines, mechatronic components, software and the optimisation of processes. This costly tendency can be overcome by specific skilled services and assistance or support by manufacturers. Users like to buy specialised services to reduce the fixed costs of products and the cost of inspection, maintenance and reconfiguration or upgrading.

The economic efficiency of capital-intensive products in industrial manufacturing depends on the profile of products, technical requirements and capacities. Requirements are changing continuously. Manufacturing systems therefore have to be adapted. So far we are lacking economic evaluation methods to control the life cycle and to find the optimal point in time for the end of a product's life or just to calculate the real life cycle costs [13,14,15,16].

4.3 Common understanding and objectives

The new paradigm of activating the product's cost-benefit is oriented on both economic aspects and fulfilling requirements for the environmental behavior of technical products applying ecological criteria. It assumes that the concentration on core competence and specialization offers new potentials to add value or to reduce cost of usage by industrialisation of service and disassembly.

The common understanding between manufacturers and users is a prerequisite to activate potentials and to get the best and maximum benefits of each technical product during its life cycle and to fulfil the Common understanding and active optimisation require technical solutions for linking products over their entire life cycle and at any phase to the information networks of manufacturers and users.

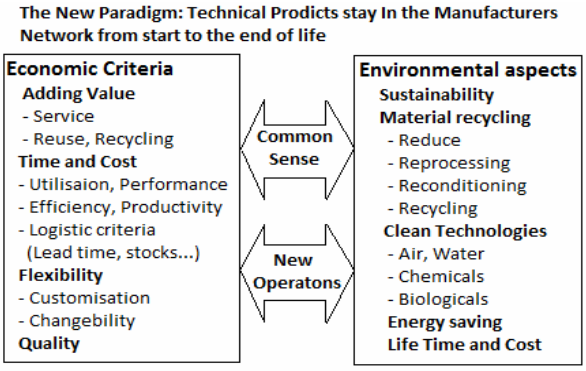

Fig. 3. Objectives of life cycle Management

5. THE ROLE OF ASSEMBLY AND DISASSEMBLY

Assembly and disassembly are the core processes in the life cycle of technical products. The usable functions of products are finalised by assembly. The result is defined as the status in which products will be delivered to users. But technical products have a ramp up phase, where specific parameters have to be set and defects to be eliminated.

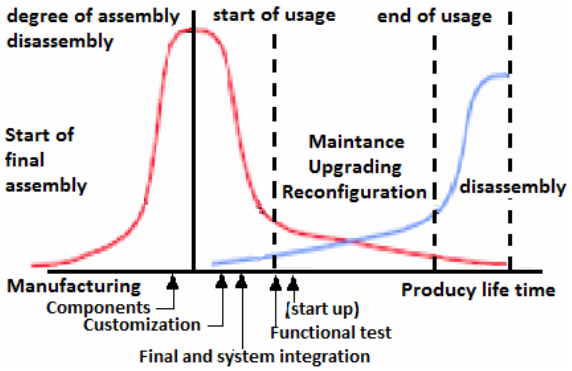

Fig. 4. Assembly and disassembly operations in the life cycle of technical products

After finalising the products, usage causes wear and defects but users try to protect capability and performance. This wear and defects are eliminated by maintenance, which includes diagnostics, disassembly, assembly and tests. During these phases it is necessary to adapt technical products permanently in their setup and by upgrading, Figure 4. Service is more and more supported by teleservice and a backup management of spare parts and spare components. These processes change the state of products permanently. Disassembly operations accumulate at the technical and economic end of life of a product. But remanufacturing and reuse demand cycles of operations: inspection, disassembly, compensation of wear, assembly, test and ramp-up. Flexible and integrated assembly and disassembly systems are discussed [17,18,19].

6. DESIGN FOR ENVIRONMENT and LC

Design for the Environment and EcoDesign are used synonymously for a systematic consideration of design issues related to environmental and human health over the life cycle of the product. The terms of EcoDesign cover approaches used by product designers in the multi-faceted field of product design and manufacture. It is viewed in various ways depending upon the context [20, 21] at all stages along the product life cycle.

According to Hill, Design for the Environment has eight axioms [22]:

- manufacture without producing hazardous waste
- use clean technologies
- reduce product chemical emissions
- reduce product energy consumption
- use non-hazardous recyclable materials
- use recycled material and reused components
- design for ease of disassembly
- product reuse or recycling at end of life.

Three design areas can be used to address the next list [23]:

- process design
- material design
- energy consumption design.

The philosophy is that Eco Designed products are flexible, reliable, durable, adaptable, modular, dematerialised and reusable. In addition to proving economical reasonability and social compatibility, these products represent an ecological necessity. The integration of environmental considerations must find its place among the many other priorities considered in the development of a new product, Figure 5 [23, 24].

If the product does not perform well in the marketplace and supersedes other less environmentally sound products, no reduction in the load on environment is obtained. The work on optimisation of the environmental performance often spurs creativity and brings innovative design solutions into the product development process which allows improvement of the overall performance together with the environmental performance.

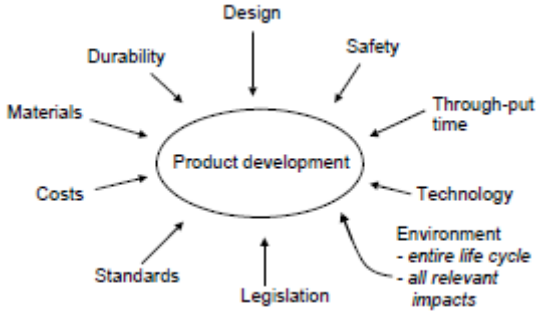

Fig. 5. Product development is the art of finding the best compromise among the many requirements to the new product set by different stakeholders [23]

Luttropp has put these common sense criteria together and called them the 10 Golden Rules of Eco Design [25]. The Eco Design rules can be summarised as:

- Do not use toxic substances, but use closed loops when necessary to do so.
- Minimize energy and resource consumption in production, use, packaging and transportation.
- Promote long life
  - o especially for passive products
  - o promote maintenance
  - o use better materials, surfaces, and structural strength
- Consider end-of-life
  - o organize for upgrading, repair and recycling
  - o use few, simple, recycled, unblended materials
  - o assemble for disassembly.

A comprehensive work on Design for Disassembly carried out Beitz [26]. He identified the more detailed areas associated with Design for Recycling as:

- Designing for ease of disassembly, to enable the removal of parts without damage.
- Designing for ease of purifying, to ensure that the purifying process does not damage the environment.
- Designing for ease of testing and classifying, to make it clear as to the condition of parts which can be reused and to enable easy classification of parts through proper markings.

• Designing for ease of reconditioning, supporting the reprocessing of parts by providing additional material as well as gripping and adjusting features.
• Designing for ease of re-assembly, to provide easy assembly for reconditioned and new parts.

7. THE LIFE CYCLE MAINTENANCE

Increasing complexity of products increases the demand for highly skilled maintenance staff and short reaction time of service. About 5 to 6 % of the products price is spent for maintenance and service yearly, with spare parts. Today's demands for maintenance in industrial manufacturing are:
- preventive maintenance and short reaction
- low cost of maintenance
- upgrading of software and control
- guarantee of output rates and quality

7.1. Prediction of potential deterioration and failures

Since the main purpose of maintenance is to manage the condition of products, it is essential to identify potential deterioration and failures. Weak points in the product design, which are indicated by deterioration and failure analysis, should be countered by design improvement or maintenance.

7.2. Design to ease maintenance operations

Disassembly and assembly operations are required for LCA. It is important to enhance assemblability and disassemblability of products by Methodologies and computer tools for evaluating serviceability.

7.3. Identification of condition of products

Identification of the product condition is one of the major maintenance tasks, not only for condition-based maintenance but also for diagnosis in the case of breakdown maintenance. The purposes of the task are:
• to check product integrity
• to detect symptoms or failures
• to analyze cause of failures or symptoms
• to predict the future trend of the condition

Terms such as inspection, monitoring, diagnosis and prognosis are used to represent these activities. While inspection implies observation and understanding of the product's current status, diagnosis and prognosis involve analysis of causality and anticipation of the progress of deterioration and functional degradation. On the other hand, monitoring implies continuous or periodic observation of the product condition for detecting symptoms or failures. In any case, the activity consists of three phases: sensing, processing, and judging.

7.4. Self-maintenance

Nowadays, most products have self-diagnostic functions executable by a build-in microprocessor. Although these functions are regarded as a kind of self-maintenance, the concept of self-maintenance discussed in this section includes not only self-diagnosis but also self-repair and self-evolution. A self-maintenance machine should be equipped with a control and reasoning processor, sensors, and actuators to perform these tasks. In contrast to biological systems, however, it is difficult for a mechanical system to repair itself physical.

8. CONCLUSION

The paper summarizes the aspects of life cycle activities management, design, maintenance and the role of assembly and disassembly. The central aspect is the concentration on the area of complex and high-value technical products like machines, manufacturing systems and even assembly systems. For technical consumer goods and low-value products, manufacturing has to develop processes and systems for disassembly and recycling. In the field of complex technical products the service, including maintenance and management systems.

9 . REFERENCES

[1] Alting L.: Life Cycle Engineering and Design. CIRP Annals – Manufacturing Technology, 1995, 44/2, pp 569–580.
[2] Zwolinski P, Kara S, Manmek S.: Comparison of Eco-Design Tools for the Conceptual Design Phase. 17th CIRP International Conference on Life Cycle Engineering, CIRP, 2010, Hefei, China.
[3] Kim SJ, Kara S, Kayis B Analysis of the Impact of Technology Changes on the Economic and Environmental Influence of Product Life-cycle Design. International Journal of Computer Integrated Manufacturing, 2013, pp 1–12.
[4] Kim SJ, Kara S Impact of Technology on Product Life Cycle Design: Functional and Environmental Perspective. 19th CIRP Conference on Life Cycle Engineering, University of California at Berkeley, USA, 2012 9Springer.
[5] Kimura, F., Suzuki H., , Product Life Cycle Modelling for Inverse Manufacturing, Life-Cycle Modelling for Innovative Products and Processes, Chapman & Hall, 1995, 80-89.
[6] Tani, T.: Product Development and Recycle System for Closed Substance Cycle Society, Proc. Of Environmentally conscious design and inverse manufacturing, 1999, 294-299.
[7] Takata S., Kimura F., F., van Houten J.A.M., E. Westkämper E., Shpitalni M., Ceglarek D., J. Lee J. Maintenance: Changing Role in Life Cycle Management, Annals of the CIRP Vol. 53, 2, 2004, pp 643-655
[8] Westkämper E.: Assembly and Disassembly Processes in Product Life Cycle Perspectives, Annals of the CIRP Vol. 52, 2, 2003, pp 579-588
[9] Westkämper, E., Alting, L., Arndt, G., Life Cycle Management and Assessment: Approaches and Visions towards Sustainable Manufacturing, Annals of the CIRP, 2000, 49/2:501-522.

[10] Seliger, G., , More use with fewer resources – a contribution towards sustainable development. In: Krause, F.-L., Seliger, G., Life Cycle Networks: Proceedings of the 4th CIRP International seminar on Life Cycle Engineering, 26-27 June 1997, Berlin, Germany, London u.a., Chapman and Hall.

[11] Feldmann, K., , Integrated Product Policy - Chance and Challenge: 9th CIRP International Seminar on the Life-Cycle Engineering, April 09-10, 2002, Erlangen, Germany, Bamberg, Meisenbach,

[12] Alting, L., Jorgensen, J.: The Life Cycle Concept as a Basis for Sustainable Industrial Production, Annals of the CIRP, 1993, 42/1:163-167.

[13] Tichkiewitch, S., Brissaud, D., 2001, Product models for life-cycle, Cirp Annals Manufacturing Technology, 50 /1:105-108.

[14] Gu, P., Hashemian, M., Sosale, S., 1997, An integrated modular design methodology for life-cycle engineering, Annals of the CIRP, 46/1:71-74.

[15] Kimura, F, 2000, A Methodology for Design and Management of Product Life Cycle Adapted to Product Usage Modes, The 33rd CIRP International Seminar on Manufacturing Systems, 5-7 June 2000, Stockholm, Sweden.

[16] Anderl, R., Daum, B., John, H., 2000, Produktdatenmanagements zum Management des Produktlebenszyklus, in: ProduktDatenManagement 1, pp. 10-15.

[17] Feldmann, K. Slama, S., 2001, Highly Flexible Assembly – Scope and Justification. Annals of the CIRP, 50/2.

[18] Westkämper, E., Feldmann, K., Reinhart, G., Seliger, G., 1999, Integrated Development of Assembly and Disassembly, In: CIRP Annals Manufacturing Technology 48/2:557-565.

[19] Feldmann, K., Meedt, O., Trautner, S., 1998, Demontage mit flexiblen Werkzeugen, in: Maschinen Anlagen Verfahren: Kennzifferzeitschrift für Produktionstechnik Automatisierung, Betriebstechnik und Betriebsausrüstung, (7/8), Leinfelden-Echterdingen: Konradin, p. 68-69.

[20] Dewberry, E., 1996, Ecodesign: Present Attitudes and Future Directions. Studies of UK Company and Design Consultancy Practice, PhD thesis, The Design Discipline, Technology Faculty, the Open University, Milton Keynes, UK.

[21] McAloone, T. C., 1998, Industry Experiences of Environmentally Conscious Design Integration: An Exploratory Study, Ph.D. thesis, The CIM Institute, Cranfield University, Cranfield, UK.

[22] Hill B.,1993, Industry's integration of environmental product design, 1993 IEEE International Symposium on Electronics and the Environment.

[23] Wang M. H., Johnston M.R., Dutta S., 1993, Design for the Environment: An imperative concept in concurrent engineering, CE & CALS, Washington.

[24] Hauschild, M., Wenzel, H., Alting, L., 1999, Life cycle design – a route to the sustainable industrial culture? Annals of the CIRP 48/1:393-396

[25] Luttropp, C., Züst, R., 1998, Ecoeffective products from a holistic point of view, 5th international CIRP seminar on life cycle engineering, Stockholm, Sweden.

[26] Beitz W., 1993, Designing for ease of recycling, Journal of Engineering Design, 4(1):11-23.

Authors: **Prof. Kovac Pavel PhD[1], Prof. Gostimirovic Marin PhD[1], Assist. Savkovic Borislav, M.Sc.[1], Prof. Mankova Ildiko PhD[2], Pucovski Vladimir, M.Sc.[1], Rodić Dragan, M.Sc.[1]**

[1]University of Novi Sad, Faculty of Technical Sciences, Institute for Production Engineering, Trg Dositeja Obradovica 6, 21000 Novi Sad, Serbia, Phone.: +381 21 450-366, Fax: +381 21 454-495.

E-mail: pkovac@uns.ac.rs, maring@uns.ac.rs savkovic@uns.ac.rs pucovski@uns.ac.rs rodicdr@uns.ac.rs

[2]Technical University of Košice, Department of Technology and Materials, Fac. of Mechanical engineering, Masiarska, 04001 Kosice 74, Slovakia

Phone: +421-55-602 2013

E-mail: ildiko.mankova@tuke.sk

***Note*: This paper presents a part of researching at the CEEPUS project and Project number TR 35015.**

Journal of Production Engineering
Vol.17 No.2

Original Scientific Paper

Vasilko, K., Murčinková, Z.

PRODUCTIVE FINISHING TURNING WITH HELICAL CUTTING EDGE TOOL

Received: 5 May 2014 / Accepted: 2 June 2014

Abstract: *When searching for paths to improve the surface quality and shorten the compilation time, it appears appropriate to know relationship between the maximum height of the machined surface roughness, the feed and the radius of the tool tip. As it is known, enlarging displacement is subject to singnificant enlargement of the corner radius. Therefore, tools have been developed with circular cutting blades and tools with corner radius $r_{\varepsilon} = \infty$ inclined opposite the axis of the workpiece at an angle λ_s. Another option is to use tools with helical cutting edge. In this case, the radius of curvature of the tool tip apex radius of curvature of the helix. We will try to identify the method of turning and its impact on the quality of machined surface.*

Key words: *machining, turning, surface roughness, chip removal*

Produktivno završno struganje zavojnim sečivom. *U potrazi za poboljšanjem kvaliteta obrađene površine i skraćenju vremena obrade, neophodno je poznavanje odnosa između maksimalne visine neravnina, pomaka i radijusa vrha alata. Kao što je poznato, značajan uticaj ima radijus vrha alata. Dakle, razvijeni su alati sa kružnim sečivom i alati sa radijusom $r_{\varepsilon} = \infty$ nagnuti prema osi obratka pod uglom λ_s. Još jedan način je korišćenje alata sa zavojnim sečivom. U ovom slučaju, radijus zakrivljenja je radijus dela spirale. Mi ćemo pokušati indetifikovati metodu struganja i uticaj na kvalitet obrađene površine.*

Ključne reči: *mašinska obrada, struganje, hrapavost površine, koren strugotine*

1. INTRODUCTION

When searching for paths to improve the surface quality and shorten the compilation time, it appears appropriate to know relationship between the maximum height of the machined surface roughness, the feed and the radius of the tool tip, [1], [2] [3], [4], [5]:

$$Rz = f^2.\frac{1}{8}.r_{\varepsilon}^{-1} = 0.125.\frac{f^2}{r_{\varepsilon}} \qquad (1)$$

Tools have been developed with circular cutting blades and tools with corner radius $r_{\varepsilon} = \infty$ inclined opposite the axis of the workpiece at an angle λ_s [6], [7], [8].
As early as 1972 LADANY [6] published the results of production finishing turning with a tool with helical cutting edge. The tool was a helical drill which was positioned against the workpiece according to Fig. 1.

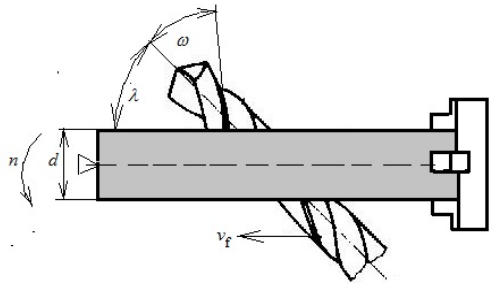

Fig. 1. Alignement of a helical drill during turning with side cutting edge

The basis of the solution is the use of unused side cutting edge of the drill for longitudinal turning of single-piece cylindrical areas. The aim is also to use damaged drills, which possess unworn longitudinal cutting edges, secondarily. Experimental tests have shown that the optimal angle of inclination of the drill against the workpiece axis is about 500 [6, 8]. STANKOVICS and KUNDRÁK [5, 10, 11] applied a similar helical tool, which rotates against the direction of workpiece rotation. At the same time, LADANY derived a relationship for the highest height of uneveness of machined surface in the following form:

$$Rz = \frac{f^2}{8.r_{\varepsilon}} + tg^2(\lambda + \omega).\left[\frac{f^2}{4.d} + \frac{f^2}{8.r_{\varepsilon}}\right] \qquad (2)$$

where d is the workpiece diameter, mm

λ - inclination angle of drill axis against workpiece axis, 0

ω - helix increase angle, 0

r_{ε}– helix top curvature angle, 0

Considering the fact that considerably large portion of cutting edge is in shift, the method is suitable for finishing turning by a large shift and shallow cut depth. Cutting edge can be renewed after becoming worn out by moving it into a new position in a clamping device. A bigger effect cannot be expected when turning carbon steels as high-speed steel requires small cutting speeds. It can be supposed that this method of turning is suitable mainly for turning light metals, titanium alloys which require small cutting forces, wood. In the following chapter there is a result of experimental evaluation of turning those selected materials. High-speed steel drill has been applied in that phase.

2. EXPERIMENTAL TOOL EVALUATION

For evaluation, a helical drill made of high-speed steel with helix inclination angle $\omega = 20^0$ attached to a holder under the angle $\lambda = 45^0$, according to Fig. 2, with the possibility to move it to a further section of cutting edge after being worn out, has been used. Therefore the actual cutting edge inclination angle is: $\lambda_s = \lambda - \omega = 25^0$.

Fig. 2. View of an experimental tool clamped in a holder.

Cutting edge has optimal geometry on the level of workpiece axis [12]. Above the workpiece axis, the working face angle increases, under the workpiece axis it decreases. Therefore turning is possible to be performed from the right to the left and vice versa, at the same time this change of working angles can be used during turning materials with different degrees of rigidity.

3. MACHINING TITANIUM

Titanium is the material with high rigidity and toughness, small heat conductivity, high friction coefficient with other metals, therefore also with cut material [13, 14]. It can be effectively machined in the conditions of a free cut, i.e. also above mentioned technology. Tests of turning with a classical tool made of high-speed steel (HS-12-1-4) with tip radius r_ε= 0.4 mm and a tool with helical cutting edge with helix increase angle $\omega = 20^0$ were performed. The result, as well as the dependence of R_z on f, can be seen in Fig. 3.

The upper curve presents classical course of a dependence, loosely copying the equation (1). However, it does not reach zero. The influence of cutting edge radius rounding under the value of a shift smaller than 0.1 mm can be seen and R_z slightly rises. The rest of the curve has parabolic course, i.e. R_z rises steeply with the increase of the shift. After turning with a helical tool shows considerably higher quality of surface in whole range of used shifts. The course of the curve is controlled by the relationship (2) and is almost linear. If we want to, for instance, reach R_z = 30 μm, a shift cca 1.5 mm is necessary for turning with a classical tool. Identical value can be obtained by a helical tool at the shift of 0.8 mm, i.e. five-times that shift. It means there is a massive shortening of machine time for machining given section of turning.

In this case, used broken helical drill was used, welded to the holder as it was too short (Fig. 4). The difference in the quality of machined surface can be visually observed at the photograph.

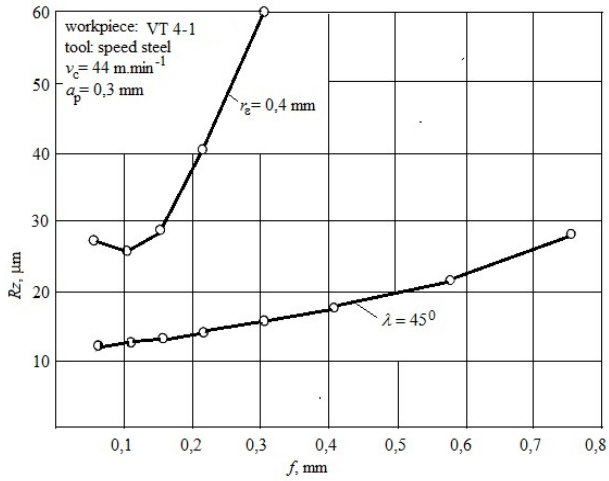

Fig. 3. Experimental dependence between the highest height of uneveness of profile R_z and shift f, obtianed during turning titanium alloy VT 4-1

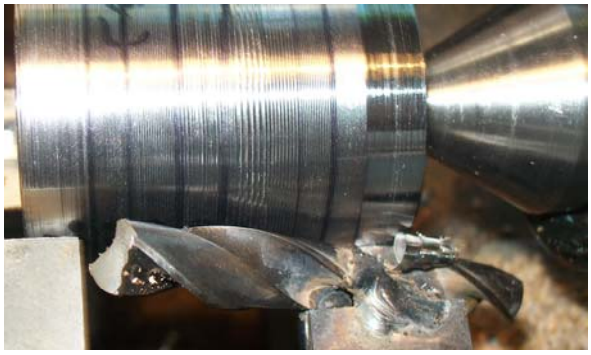

Fig. 4. View of machining process of turning titanium alloy

The left section of the workkpiece has been turned with a classical tool with the tip radius 0.4 mm. Tracks of different shifts can be seen. The right section represents turning with helical tool. The surface has mirror-like shine. The chip shape corresponds with typical free cut. In Fig. 5 there is a view of creating chips. They have considerable width, which corresponds with the length of cutting edge in shift and minimal thickness, corresponding with used shift.

Fig. 5. Shape of chips obtained at turning titanium alloy with a helical tool

4. MACHINING WOOD

Wood is organic material, which causes problems with machined surface quality when turning by fixed cut. Fissures occur in front of the cutting wedge and the

chip crumbles [7, 15]. Creating conditions of a free cut also in this case means considerable improvement of machined surface quality and enables to use much larger shifts. In Fig. 6 there is an experimental diagramme of dependence of R_z on f.

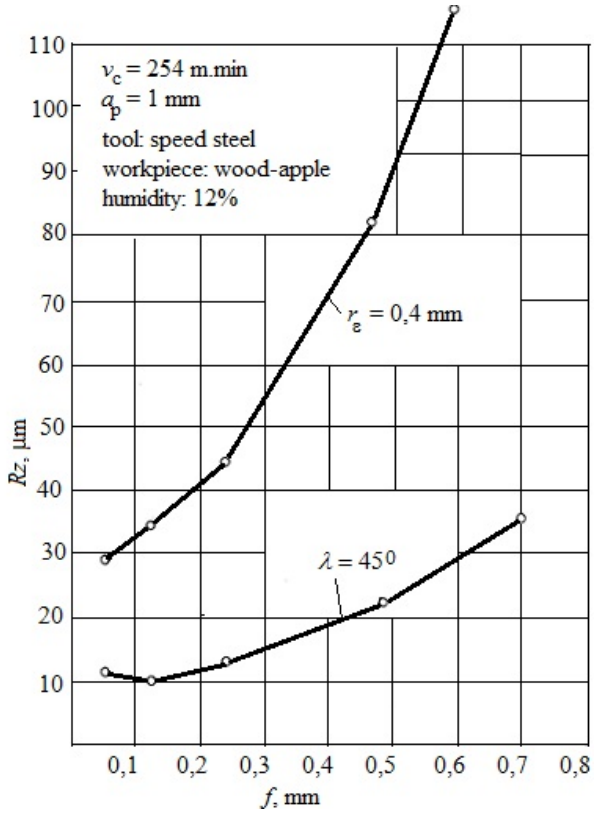

Fig. 6. Experimental dependence of R_z on f at turning apple-tree wood

The course of the diagramme is similar to the previous case. The quality of machined surface is much higher than at turning by fixed cut, mainly at higher shifts.

At fixed cut the chip is elementary, made by fissure-creating process. Free cut leads to fluent – compact chip without fissures (Fig. 7).

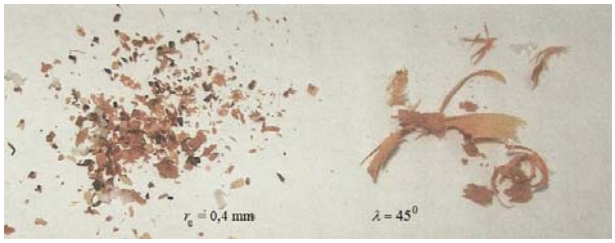

Fig. 7. Photography of chips created at classical turning and during turning with a tool with helical cutting edge

Machining process has been stopped and a cut section of chip root has been made to explain the essence of chip creation during turning (Fig.8).

Visible texture can be seen in the chip, which gives evidence of plastic deformation of machined material.

To complete the information, in Fig. 9 there is an experimental dependence between the highest uneveness of machined surface height and cutting speed during turning of soft wood with both tools.

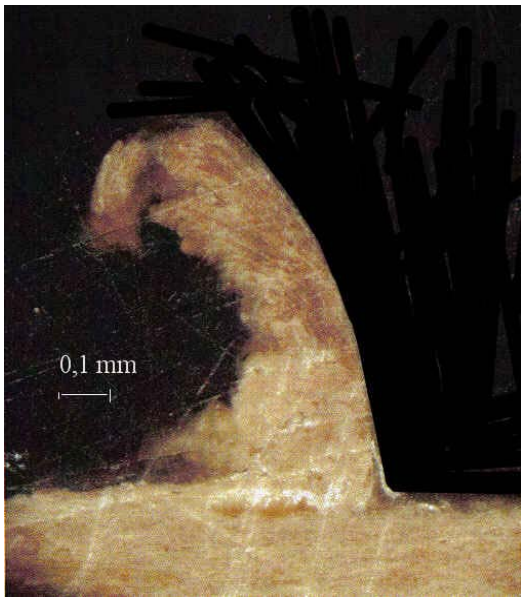

Fig. 8. Chip root obtained by immediate interruption of machining process

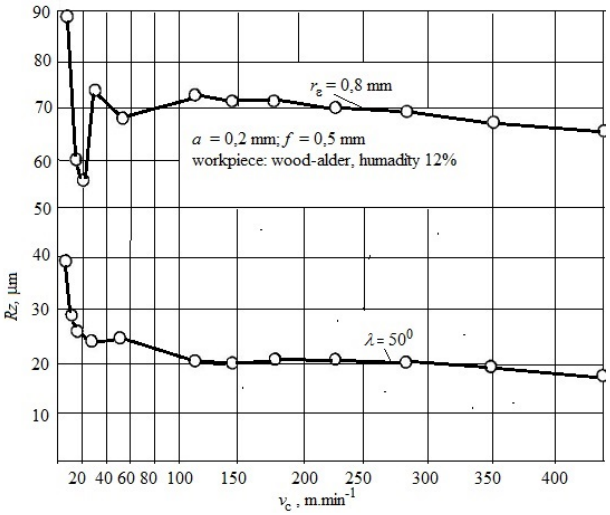

Fig. 9. Experimental dependence R_z = f(v_c)

During turning with a tool with rounded tip there occurs alternating decrease of the growth of R_z at small cutting speeds. It is accompanying sign of the fissure-creating process in front of the cutting wedge. At following increase of cutting speed the decrease of Rz is mild. The values of R_z are relatively high in whole range of v_c. During turning with a drill R_z curve has a different course. It steeply decreases at small cutting speeds, when v_c increases, it decreases minimally. In whole range of cutting speeds the absolute values of R_z are considerably lower than during turning with a classical turning tool.

5. MACHINING ALUMINIUM

Frequently used alloy of aluminium – dural, turned at the same cutting conditions as mentioned above, has been selected for experiments. The problem of

machining aluminium alloys lies mainly in considerable adhesion between cut and cutting material, the result of which is „sticking“ of material to the cutting wedge, which leads to worsening of machined surface microgeometry [16, 17]. Therefore creating the conditions of free cut is desirable [18]. In *Fig. 10* there is a view of the adjustment of the tool against the workpiece.

Fig. 10. Position of tool cutting edge against the workpiece

In Fig. 11 there is an experimental dependence R_z = f(*f*), obtained at turning with a classical tool and a tool with helical cutting edge.

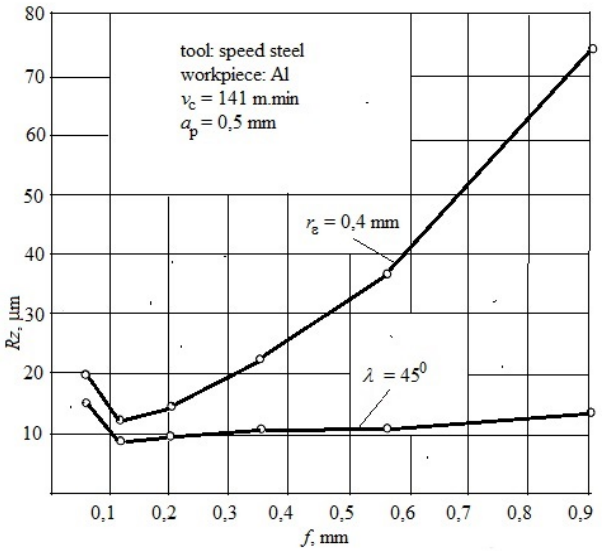

Fig. 11. Experimental courses of R_z depending on the shift

Similarly to previous materials a visible difference in the quality of machined surface can be seen. With classical tool, R_z sharply increases with the shift except for the shifts smaller than 0.1 mm. The curve for helical tool rises very mildly. R_z does not reach the value of 15 μm even at the shift of 0.9 mm.

In Fig. 12 there is an example of records of microgeometry of machined surface after turning with both tools under the same cutting conditions at the shift of 0.69 mm.

For turning with a classical tool the record shows a visible size of a shift. It is not possible to identify the shift on the record on the right. Only microuneveness of cuttined edge, transformed into machined surface, can be visible.

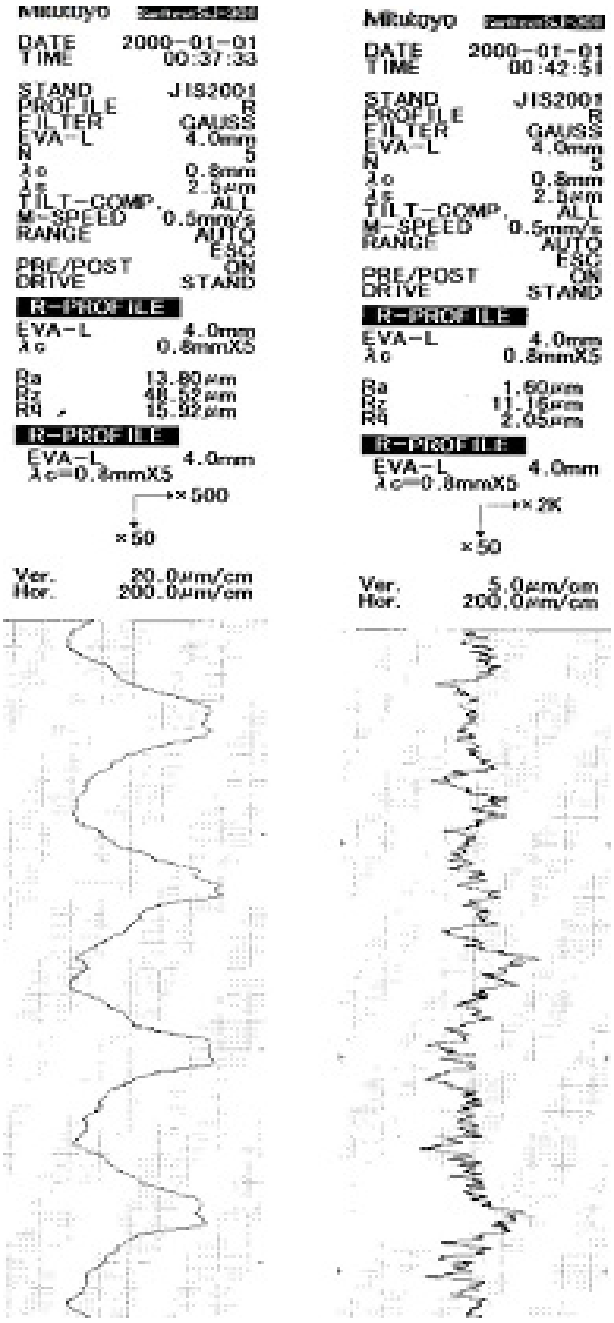

Fig. 12. Record of the profile of machined surface with a classical tool with tip radius (left) and a tool with helical cutting edge (right)

6. MACHINING BRASS

Automatic brass is characterised by a good heat conductivity, medium firmness, elementary chip. It can be realistically supposed that turning with an observed tool can improve the quality of machined surface. In Fig. 13 there is a view of an experimental workpiece with sections of turning with a classical and helical tools. Tracks of shifts can be seen on surface, created by a tool with tip radius at shifts above 0.4 mm. On the section machined with a helical tool, the size of the shift cannot be visibly identified.

Fig. 13. View of an experimental workpiece, on the right – turning with a tool with rip radius, on the left – with a helical tool

Set of measured values of R_z and R_a is presented in *Tab. 1.*

Brass, v_c= 31 m.min^{-1}, r_ε = 0.8 mm, drill λ=45^0

f, mm	Rz, μm (r_ε)	Ra, μm (r_ε)	Rz, μm (λ)	Ra, μm (λ)
0,051	15	2,52	8,69	1,41
0,075	12,97	2,28	7,06	1,06
0,1	12	2,12	7	1,02
0,14	13,24	2,51		
0,25	25,74	3,83	11	1,89
0,35	38,80	9,16		
0,4			14,34	2,50
0,45	49,08	7,46		
0,65	70	9,01	15,35	3,36
0,96	100,2	9,16	21,15	3,66

Table.1 Measured values of R_z and R_a after turning

Experimental diagramme made on the base of *Tab. 1* is shown in *Fig. 14.*

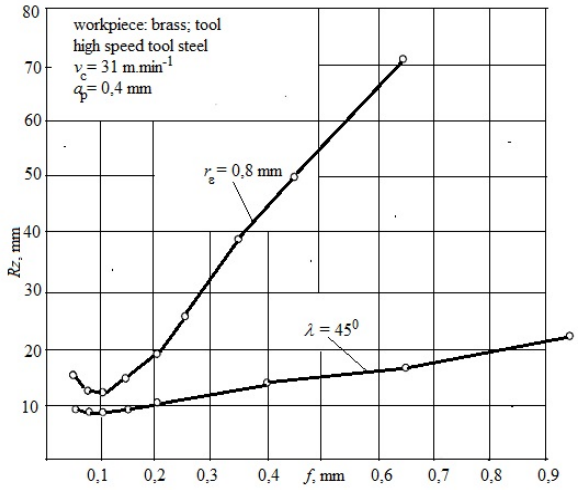

Fig. 14. Course of experimental dependencies R_z = f(f) for both tools

Similarly to previous materials, a helical tool helps to reach higher quality of machined surface. The difference in values of R_z rises with the increase of the shift. For instance, at the shift of 0.65 mm, for the classical tool, R_z is 65 μm, for the helical one it is 16 μm. Therefore this method of turning is suitable for large shifts.

An example of profiles of machined surfaces after both tools is shown in *Fig. 15*.

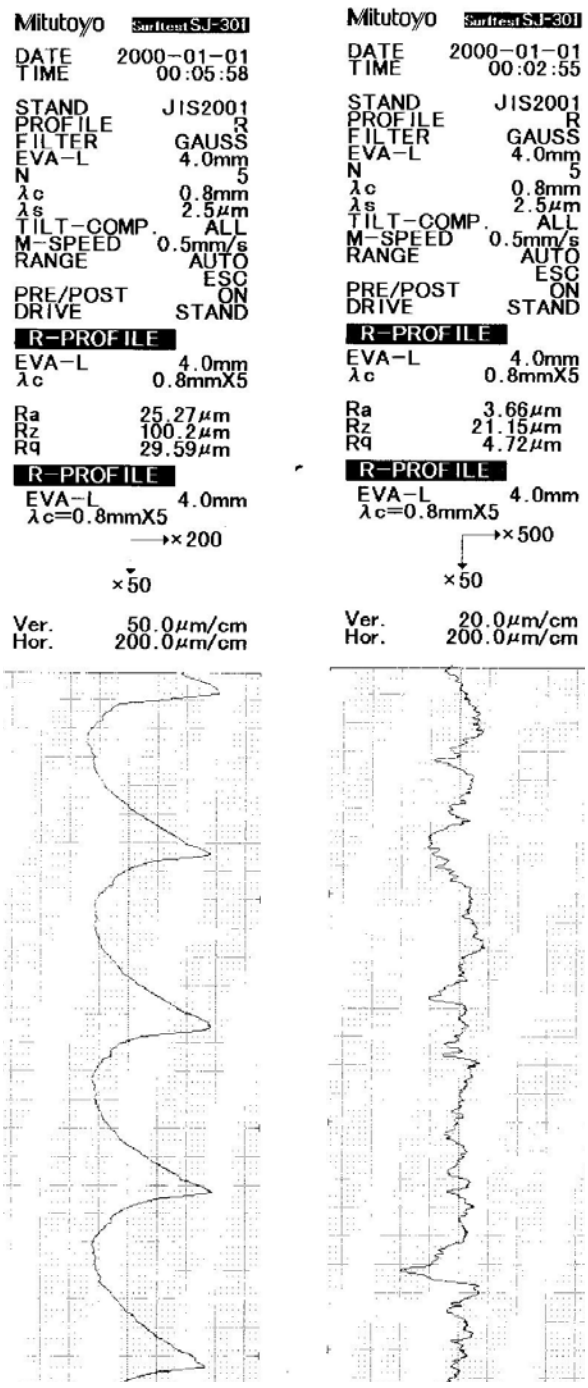

Fig. 15. Recording from profilemeter MITUTOYO of a surface machined with a classical and helical tools at the shift of f = 0.96 mm

7. CONCLUSION

Looking for non-traditional geometries of cutting tools can lead to considerable increase of the quality of machined surface, or shortening machine time at the same obtained quality of machined surface. It is obvious that creating conditions of a free cut leads to smaller intensity of chip deformation, lower inclination to creating fissures in front of the cutting wedge and smaller influence of the shift on the quality of machined surface. Secondary aspect of the presented suggestion is the possibility of the use of damaged

cutting tools of the type of helical drills and cylindrical and shank lathing machines with inclined teeth. During drilling, the long side cutting edge does not take part in the process of chip taking off therefore its wear does not occur and it can be secondarily used for machining. Possibility to vary the application of high-speed steel for selected operations and cut materials is also a positive.

8. REFERENCES

[1] BUDA,J., BÉKÉS, J.: *Teoretické základy obrábania kovov*. Bratislava: ALFA, 1967, 698 s.

[2] DMOCHOWSKI, J.: *Postawy obróbki skrawaniem*. Warszawa, 1978, 586 s.

[3] GRZESIK, W.: *Podstawy skravanija materialow metalowych*. Warszawa: Wydawnictwa Naukowo-Tchniczne, 1998, 380 s., ISBN 83-204-2311-2

[4] KOVAČ, P., MILIKIČ, D.: *Rezanje metala*. Univerzitet u Novom Sadu, 1995, 240 s., ISSN 86-499-0015-1

[5] SZTANKOVICS, I.: Theoretical Value of Arithmetic Mean Deviation in Rotation Turning. *Műszaki Tudományos Fűzetek – Fiatal Műszakiak Tudományos Ülésszaka XVIII*., pp. 391-394.

[6] LADANY, Sh.: Die wirtschaftlichen Aspekte des Drehens mit spiralförmigem Drehwerkzeug. *Microtechnic* Nr. 8, 1972

[7] MIKLES, J., MIKLES, M.: Technical Parameters of Cross-Cutting Mechanisms of Line for Wood Processing. *Manufacturing and industrial Engineering*, Vol. 11, Nr. 2, 2012, pp. 54-56, ISSN 1338-6549

[8] VASILKO, K., STROJNÝ, M.: *Progresívne metódy sústruženia*. Bratislava: ALFA, 1977, 208 s.

[9] KALPAKJIAN, S.: *Manufacturing engineering and technology*. New York: Addison Wesley Publishing Company, 1989, p. 1999, ISBN 0-201-12849-7

[10] KUNDRÁK.: Alternative machining procedures of hardened steels. *Manufacturing Technology*, No. 11, pp. 32-36, ISSN 1213-2489

[11] SZTANKOVICS, I., KUNDRÁK, J.: Effect of the Inclination Angle on the Defining Parameters of Chip Removal in Rotational Turning. *Manufacturing Technology*, March 2014, Vol.14, No.1, ISSN 1213-3489

[12] WEBER, H., LOLADZE, T. N.: *Grundlagen des Spanens*. Berlin: VEB Verlag Technik, 1985, 255 s.

[13] CZÁN, A. et al.: Studying of Cutting Zone When Finishing Titanium Alloy Application of Multificaction Measuring System. *Manufacturing Technology*, December 2013, Vol. 13, No. 4, ISSN 1213-2489

[14] MÁDL, J. et al.: Vlastnosti povrchu po tvrdém obrábění. *Strojírenská technologie*, 2008, roč. XIII, č. 3, s. 27-31, ISSN 1211-4162

[15] PŘIKRYL, Z., MUSÍLKOVÁ, R.: *Teorie obrábění*. Praha: SNTL, 1982, 235 s.

[16] KUZMAN, K. et al.: Experimental consolidation of aluminium chips by cold compression. *Journal of Production Engineering*, Vol.15, No.2, 2013 pp. 79-92, ISSN 1821-4932

[17] VASILKO, K., MÁDL, J.: *Teória obrábania*. Univerzita JEP Ústí nad Labem: 2013, 526 s., ISBN 978-80-7414-460-8

[18] KOVAC, P. et al.: Overview of Experimental Investigation of Cutting Process. *Journal of Production Engineering*, Vol.16, No.2, 2013 pp. 1-4, ISSN 1821-4932

***Authors*: Dr.h.c. prof. Ing. Karol Vasilko, DrSc., doc. Ing. Zuzana Murčinková, PhD.** Technical University of Košice, Faculty of Manufacturing Technologies, 080 01 Prešov, Bayerova 1, Slovakia. E-mail: karol.vasilko@tuke.sk; zuzana.murcinkova@tuke.sk

Journal of Production Engineering
Vol.17 No.2

Original Scientific Paper

Adedayo, S. M., Adekunle, A. S., Ajiboye, A.

EFFECT OF TEMPERING TEMPERATURE ON MICROHARDNESS AND RESIDUAL STRESSES OF QUENCHED C25 CARBON STEEL HOLLOW CYLINDER

Received: 15 September 2014 / Accepted: 10 October 2014

Abstract: *Effect of tempering temperatures on residual stresses and microhardness across quenched hollow C25 carbon steel was investigated. Residual stresses were induced by separately quenching in water and vegetable oil (Arachis hypogoe). Quenched specimens were stress relieved at 200, 400 and 600^{o}C. Two orthogonally mounted 120 ohms resistance strain gauges were used on each specimen to measure strain relaxation. Induced machining longitudinal and transverse stress were measured and factored in final stress values. Modified Sach's boring equations was applied to obtain longitudinal and transverse residual stresses across the quenched cylinder. Hardness of C25 carbon steel and cooling rate of the quenchants was also determined.*
Key words: *Residual stresses, quenching, Sach boring technique, resistance strain gauges, tempering*

Uticaj temperature temperovanja na mikrotvrdoću i zaostale napone kaljenog šupljeg cilindra od ugljeničnog čelika C25. *U ovom radu je ispitivan uticaj temperature temperovanja na zaostale napone i mikrotvrdoću kod kaljenog ugljeničnog čelika C25. Zaostali naponi su unošeni odvojenim kaljenjem u vodi i biljnom ulju (Arachis hipogoe). Kaljeni uzorci su otpuštani na 200, 400 i 600^{o}C. Dve ortogonalno montirane merne trake otpora 120 oma su korišćene na svakom uzorku za merenje napona otpuštanja. Uzdužni i poprečni naponi generisani obradom su takođe mereni i uzeti u obzir kod računanja ukupnih vrednosti napona. Modifikovana Šačova jednačina je korišćena za dobijanje vrednosti uzdužnih i poprečnih zaostalih napona u kaljenom cilindru. Tvrdoća ugljeničnog čelika C25 i brzina hlađenja medijuma je takođe određivana.*
Ključne reči: *Zaostali naponi, kaljenje, Šačova tehnika proširivanja, otporne trake, temperovanje*

1. INTRODUCTION

Residual stresses can be described as stresses which remain locked in a body which is stationary and at equilibrium with its surroundings or stresses locked in a system even though external forces are not acting on it [1-3, 10]. Liscic et al. and Palaniradja et al. [4, 5] differently studied the effect of residual stress on manufactured part and found that residual stresses arising in products being made and used govern their lifetime significantly. Residual stress analysis in thick plates using neutrons and Fe modeling showed that actual and operating stresses may differ considerably from design values due to a possible summation of working and residual stresses in separate product portions [6]. Developed model to reduce distortion of a carburized and quenched steel gear showed that determination of residual stresses is a principal problem in engineering parts [7]. Palkowski et al. [8] used numerical simulation and neutron diffraction analysis of drawn tubes to show that the magnitude and distribution of residual stresses in a component or structure is a significant source of uncertainty in mechanical engineering design and one that can affect subsequent machining as well as life prediction and assessment of structural integrity. Chinnaraj et al. [9] used numerical and experimental investigation of residual stresses in cold formed truck frame rail sections and concluded that residual stresses are an unavoidable concomitant of almost all manufacturing and fabrication processes and can also arise during service. James [10] studied residual stress influences in mechanical engineering using Fe modeling while Bin et al. [11] studied residual stresses in machined and shrink-fitted assemblies and they found that residual stress may occur under any set of circumstances that lead to differential expansion or contraction between adjacent parts of a body in which the local yield strength is exceeded; similar result was obtained by Totten et al. and Guo et al. [12, 13] in their work residual stress, nanohardness and microstructure changes in whirldwind milling of GCr15 steel. Bruch et al. [14] in his work mechanical properties and corrosion resistance of duplex stainless steel differently showed that the creation of residual stresses during heating, quenching and machining is considered as one of the key parameters since it has direct effect on the fatigue life of a machined component.

Although theoretical and numerical analyses are being widely used to estimate the residual stresses in components, it is necessary to undertake experiments to validate the predictions. Residual stress measurement techniques are generally categorized as non-destructive and fully destructive methods. Most of the non-destructive methods such as conventional X-ray and magnetic techniques are restricted to near surface measurements [15]. In contrast the neutron diffraction method is able to penetrate up to depths of about 50mm [16]. Kingston et al. [17] in his work novel application of the deep hole drilling technique for measuring through thickness residual stress distributions showed that semi-invasive methods such as the centre hole drilling provide near surface measurements up to depths of about 1mm. More recently Smith et al. [18] in the work measurement and prediction of residual stresses in thick section steel weld showed that the

deep-hole drilling technique has provided through-depth measurements to depths in excess of 700mm. Heat treatment such as induction hardening, flame hardening and quenching alters the metallurgical structure of the metal under residual stress; with such metal producing high compressive residual stresses, with fatique life improvement of up to 100% [19]. Similarly during quenching, surfaces that cools first end up in residual bi-axial compression, whilst the inner core is in a state of tri-axial tension [20-21]. Sometimes compressive stresses are intentionally introduced on the surfaces in order to increase the fatique strength of the material. Heat treatment results that are of common interest include the volume fractions of phases, hardness, residual stresses and part distortion. This paper describes the outcomes of two independent studies of the measurement of residual stresses and hardness in hollow C25 carbon steel after hardening by quenching in water and Jatropha oil with subsequent tempering.

2. EXPERIMENTAL

2.1 Materials Composition and Specimen Preparation

Photo-spectrometry tests were carried out on work piece materials. Observed composition is as shown in Table.1

Elements	Volume %
C	0.354
Si	0.351
S	0.026
P	0.007
Mn	0.742
Ni	0.202
Cr	0.172
Mo	0.017
V	0.001
Cu	0.308
W	0.004
As	0.010
Sn	0.024
Co	0.013
Al	0.004
Pb	0.001
Zn	0.004
Fe	97.76

Table 1. Chemical Composition of C25 quench metal [vol.%]

The cylindrical test specimens were cut from the parent metal and machined to an overall height of 90 mm, inner and outer diameters of 12 and 48 mm respectively. Prepared test specimens were austenised at 920^{o}C ± 3 ^{o}C in an electric furnace at the rate of 25^{o}C/min and soaked for 30 minutes to achieve complete homogenization. Test specimens were separately quenched laterally in 1000 mL of water and groundnut oil (Arachis hypogae). Thermal history of quench process was taken using a K-type thermocouple with immersion temperature of the specimen been 840^{o}C. The quench process was followed by tempering at temperatures 200, 400 and 600^{o}C. Each tempering process condition was repeated thrice with average values of residual stresses results presented.

2.2 Instrumentation and Calibration

A wheatstone bridge with the dummy arms made of electric resistance strain gauges of type FLA – 5 – 11 of resistance 120Ω and gauge factor 2.11 was constructed. Strain indications on the wheatstone bridge were carried out in order to establish a relationship between known strain values in the active arm and corresponding readings of the digital strain indicator. A variable resistor was connected in parallel with the active arm, which allowed for very small changes of resistance to be effected on the active arm as shown by Adedayo (1998). A variable resistor (Rs) setting of 1228Ω across a 133Ω resistor gave an effective resistance of 120Ω on the active arm. At this setting, all the four arms of the wheatstone bridge were balanced with read-out instrument indicating zero. The mathematical relationship used to obtain active arm strain corresponding to any resistance change is given in equation (1) below

$$\rho = \frac{1}{F}\frac{dR}{R} \qquad (1)$$

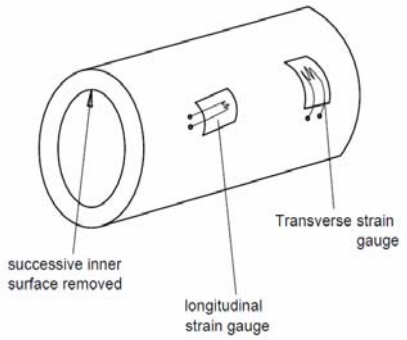

(a)

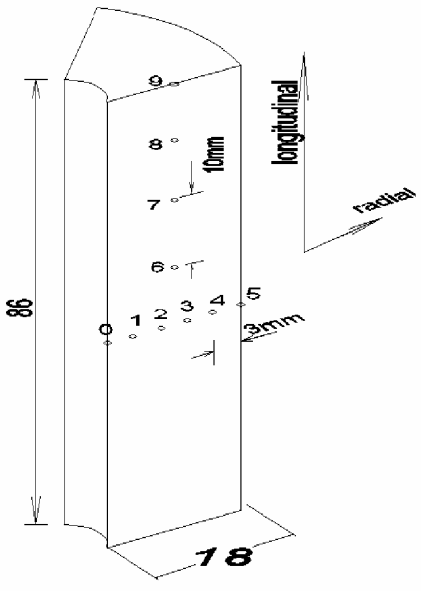

(b)

Fig.1 (a & b) Workpieces showing strain gauges and hardness test points

2.3 Longitudinal and Transverse Residual Stress Evaluation

2.3.1 Strain relaxation and measurement

Strain measurements were carried out through use of strain gauges. Specimen surfaces was properly prepared through removal of scales, dirts, burns and degreasing using different grades of emery paper. Ethanol and methylated spirit was used for degreasing the surface for proper chemical affinity. Gauge location was scribed on the specimen. Positioning and orientation of the gauge were carefully maintained during application of a cynoacrylate adhesive. Gauges were mounted on the cylindrical work-pieces in longitudinal and transverse orientations as depicted in Figure 1(a). Mild pressure was applied in mounting the gauges in order to squeeze out excess adhesive and production of a strong thin bond line. A suitable wheatstone bridge was built. A digital strain meter (Model No. E10MKII) was used to monitor strains. Bonded strain gauges were effectively protected against abrasion and moisture contacts. The zero readings of strain gauges were obtained for a period of seven days with average readings used as zero readings for the test results. Strains were read for both longitudinal and tangential directions using the successive boring technique. A Storebro lathe, Model No. GS260 was used to make the successive internal diameter cuts for strain relaxation. Machine speed was 135 rev/min and coolant was applied during the process to minimize work piece temperature. A depth of cut of 0.5 mm was taken every boring day. Relaxed longitudinal and transverse strains indicated as ε_L and ε_T respectively were measured 24 hours after the metal removal. The true values of ε_L and ε_T were obtained by subtracting the zero reading from the indicated readings on the digital strain meter and actual strain values obtained from the calibration curve. Obtained strains were fitted into modified Sach's equations to determine the transverse and longitudinal stresses.

2.3.2 Longitudinal and Transverse Residual Stresses

The longitudinal (σ_L) and transverse (σ_T) residual stresses were obtained from modified Sach's equations [2] as shown in equation 2(a & b).

$$\sigma_L = \frac{E^1}{2r}\frac{d}{dr}\left[\left(r_0^2 - r^2\right)\Lambda\right] \qquad (2a)$$

$$\sigma_T = \frac{E^1}{2}\frac{d}{dr}\left[\left(\frac{r_0^2 - r^2}{r}\right)\theta\right] \qquad (2b)$$

$$E^1 = \frac{E}{\left(1-\nu^2\right)} \qquad (3.0)$$

r_o = external radius of cylinder
r = current internal radius of cylinder after layer removal.

$$\Lambda = \varepsilon_L + \nu\varepsilon_T \qquad (4.0)$$

$$\theta = \varepsilon_T + \nu\varepsilon_L \qquad (5.0)$$

ε_L = change in longitudinal surface strain due to removal of an inner layer

ε_T = corresponding change in transverse surface strain

E = Young's Modulus (208×10^9 N/m^2)

ν = Poisson's ratio (0.3)

Strain values were obtained from the digital strain meter readings after successive relaxations. The value of the functions $\left(r_0^2 - r^2\right)\Lambda$ and $\left[\frac{r_0^2 - r^2}{r}\right]\theta$ are zero at both inner and outer surfaces so that extrapolation of functions is to zero instead of an unknown value. In this form, the stresses are calculated by plotting the functions of $\left(r_0^2 - r^2\right)\Lambda$ and $\left[\frac{r_0^2 - r^2}{r}\right]\theta$ against r, so that the longitudinal and transverse stresses can be obtained respectively at any value of r by multiplying the slope by a constant factor (see equation 2a and 2b). The radial stress values were neglected in this work due to the relatively small thickness of the cylinder walls.

The following procedures were adopted in order to evaluate the values of both longitudinal and transverse residual stresses.

(i) The value of r_0 was obtained, and it was constant for all the specimens

(ii) The values of r after each successive layer removal operation were noted.

(iii) Longitudinal strain (ε_L) and the transverse strain (ε_T) were obtained from strain gauge measurements.

(iv) The values of Λ and θ were also calculated for all the specimens from equations 4.0 and 5.0 respectively.

(v) The values of $\left(r_0^2 - r^2\right)\Lambda$ and $\left[\frac{r_0^2 - r^2}{r}\right]\theta$ were obtained for each specimen

(vi) The graphs of $\left(r_0^2 - r^2\right)\Lambda$ and $\left[\frac{r_0^2 - r^2}{r}\right]\theta$ versus r were plotted for each specimen.

(vii) The gradients of the graphs plotted in (iv) and (vii) above gave the values of $\frac{d}{dr}\left[\left(r_0^2 - r^2\right)\Lambda\right]$ and $\frac{d}{dr}\left[\left(\frac{r_0^2 - r^2}{r}\right)\theta\right]$

(viii) The constant $\frac{E}{\left(1-\nu^2\right)}$ was calculated.

(ix) The values obtained in (vi) and (vii) were substituted in equations 2(a) and 2(b) to give the longitudinal and transverse stresses.

(x) Longitudinal and transverse machining stresses

were similarly obtained by machining an annealed workpiece. Obtained Machining longitudinal and transverse stresses were applied for compensation by subtracting from the quenching stresses. The final values are presented in the results

2.3.3 Machining Residual Stresses

A fully annealed work-piece of same dimension as the quenched workpieces was fitted with strain gauges on outer diameter for longitudinal and transverse residual stresses measurement. Successive machining was carried out and results of the strain changes were fitted into the modified sach – boring expression to obtain the machining stresses.

2.4 Metallographic Examination

Test specimens were sectioned and surfaces grinded with silicon carbide papers of 240, 320, 400 and 600 grit sizes. They were subsequently polished using a cloth impregnated with alumina until a mirror surface was obtained. Grinded surface were cleaned with water and ethanol. Etching with 2% Nital was done and microstructures observed using a high powered optical microscope.

2.5 Hardness Test Measurements

The water and oil quenched C25 steel material was subjected to microhardness test along the radial direction for both tempered and untempered workpiece. Hardness measurement of the specimen at different radii locations was repetitively done three times using microhardness tester LM700AT under an applied load of 490.3 mN with a dwelling time of 10 seconds. Average values of depth of penetration of the indenter was recorded and presented. The specific locations along which the longitudinal and transverse hardness values were taken are shown in Fig.1(b).

3. RESULTS AND DISCUSSION

3.1 Effect of Tempering Temperature on Longitudinal Residual Stresses

Figs 2 and 3 show the effect of tempering temperature of 200, 400 and 600^{o}C on longitudinal residual stresses for water and oil quenched specimens respectively. The maximum values of longitudinal residual stresses of specimens quenched in water and oil under no–thermal relief conditions are 265 MN/m^2 and 202 MN/m^2 respectively as shown in Figs.2 and 3. Under stress relief temperatures of 200, 400 and 600^{o}C, maximum longitudinal residual stresses are 209, 188 and 153 MN/m^2 respectively for water quenched and 179, 150 and 140 MN/m^2 respectively for oil quenched specimens. These indicate a residual stress relief of 27.5, 34.4 and 45.3% for water and 10.9, 25.4 and 30.3% for oil at 200, 400 and 600^{o}C thermal relief temperatures respectively. Fig. 4 shows the relative magnitudes of longitudinal residual stresses of water and oil quenched specimens in a purely quenched and 400^{o}C tempered state. The quench severity of water is higher than oil thus resulting in higher values of residual stresses with or without tempering and the metallic crystal particle bonds are weakened at high temperatures thus accounting for the higher percentage stress reliefs at high temperatures.

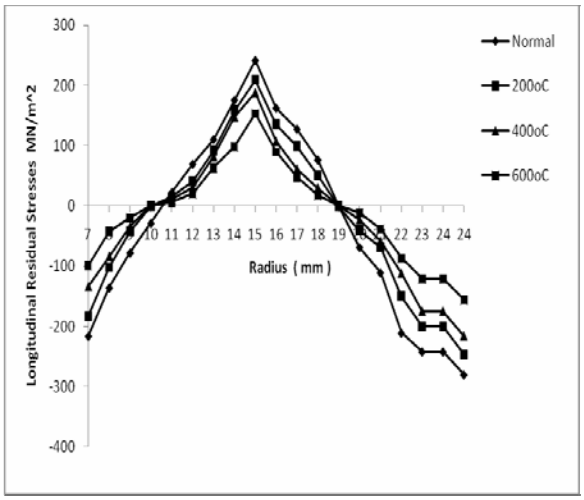

Fig.2 Effect of tempering temperature on longitudinal residual stresses in water quenched Specimen

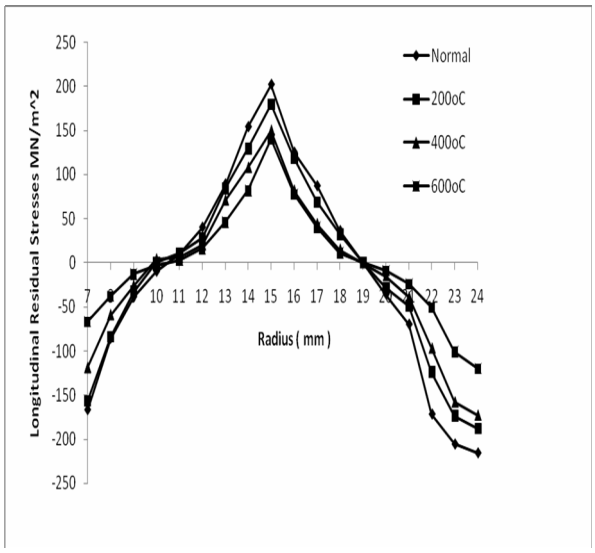

Fig.3 Effect of tempering temperature on longitudinal residual stresses of oil quenched specimen

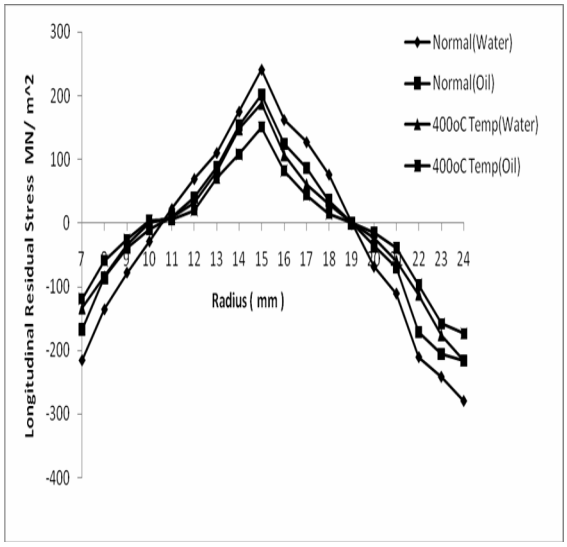

Fig 4 Distribution of longitudinal residual stresses in water and oil quenched specimen

3.2 Effect of Tempering Temperature on Transverse Residual Stresses

Figures 5 and 6 shows the effect of tempering temperatures of 200, 400 and 600°C on transverse residual stresses for water and vegetable oil quenched specimens respectively. The maximum values of transverse residual stresses of specimens quenched in water and oil under no – thermal relief conditions are 460 MN/m^2 and 411 MN/m^2 respectively. Under stress relief temperatures of 200, 400 and 600°C, maximum transverse residual stresses are 436, 426 and 345 MN/m^2 respectively for water quenched and 387, 363 and 311 MN/m^2 respectively for oil quenched specimens.. These indicate a residual stress relief of 2.5, 7.4 and 25 % for water and 5.8, 11.7 and 24.6 % for oil at 200, 400 and 600°C thermal relief temperatures respectively. Fig.7 compares magnitudes of water and oil quenched specimens with and without tempering at 400°C. The quench severity of water is higher than oil thus resulting in higher values of transverse residual stresses.

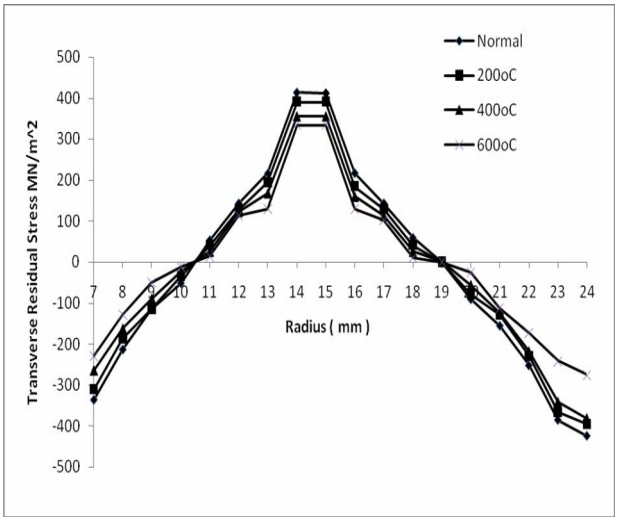

Fig.5 Effect of tempering temperature on transverse residual stresses of water quenched specimen

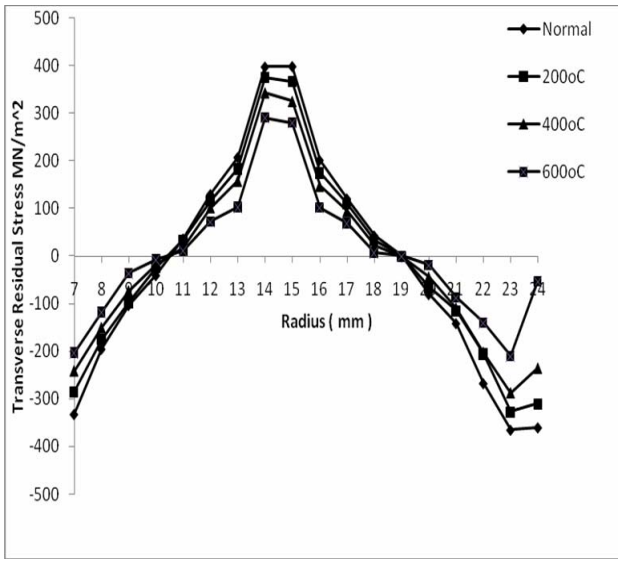

Fig.6 Effect of tempering temperature on transverse residual stresses of oil quenched specimen

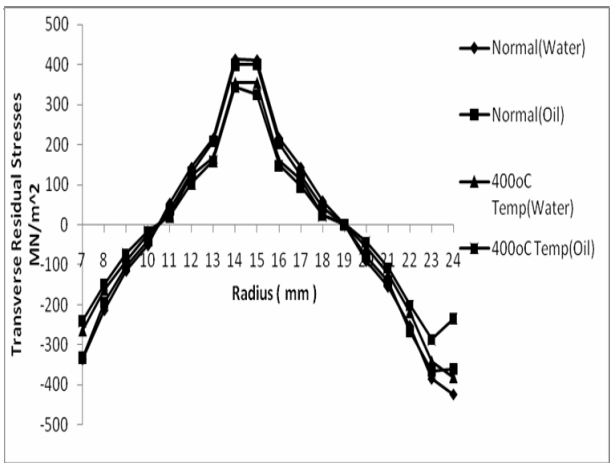

Fig.7 Distribution of transverse residual stresses in water and oil quenched specimen

3.3 Machining Longitudinal and Transverse Residual Stresses

Table.2 shows the values of the machining longitudinal and transverse residual stresses at every successive machining stage.

Cut No	Radius (mm)	Longitudinal (MN/m^2)	Transverse (MN/m^2)
1	6.5	-20.52	-45.56
2	7.0	-16.62	-27.33
3	7.5	-11.64	-19.43
4	8.0	-9.43	-12.15
5	8.5	-5.61	-7.43
6	9.0	-3.94	-3.17
7	9.5	-1.89	-2.66
8	10.0	-0.80	-1.71
9	10.5	0.00	0
10	11.0	0.60	1.83
11	11.5	2.67	4.23
12	12.0	6.95	5.94
13	12.5	8.61	13.14
14	13.0	12.97	18.66
15	13.5	15.13	21.44
16	14.0	19.20	25.81
17	14.5	21.63	30.10
18	15.0	25.78	23.21
19	15.5	18.03	19.81
20	16.0	14.43	13.03
21	16.5	12.34	9.03
22	17.0	7.64	6.97
23	17.5	4.60	4.46
24	18.0	1.94	1.71
25	18.5	0.06	0.57
26	19.0	0.00	0
27	19.5	-0.47	-1.60
28	20.0	-1.46	-2.57
29	20.5	-3.91	-5.63
30	21.0	-6.27	-8.54
31	21.5	-9.25	-13.38
32	22.0	-12.16	-17.41
33	22.5	-14.20	-22.75
34	23.0	-21.67	-44.98
35	23.5	-24.24	-48.20
36	24.0	-26.41	-52.52

Table 2. Machining Residual Stresses

Maximum tensile machining longitudinal and transverse residual stresses of 25.78 MN/m^2 and 30.10 MN/m^2 was attained at the 18th and 17th cut with internal radius of 15.0 and 14.5 mm respectively. The corresponding maximum compressive stresses was -26.41 MN/m^2 and -52.52 MN/m^2 occuring at radius 24 mm for longitudinal and transverse residual stresses respectively. Magnitudes of the machining stresses are small relative to the quenching stresses. This is due to the relatively low cutting forces due to small depths of cut and corresponding low thermal gradients across material thickness.

3.4 Effect of tempering temperature on metal hardness

The microhardness for both water and oil quenched C25 material at tempering temperature of 200^{o}C, 400 ^{o}C and 600 ^{o}C is as shown in Fig. 8 and 9 respectively. Slight increase in microhardness values is observed between radii 3 and 6 mm for all tempering temperature with highest value been 298 H_v at tempering temperature of 600 ^{o}C; while for oil quenched material the hardness only increases between radial distances 3 and 6 mm for tempering temperature of 200 ^{o}C with highest attained hardness value of 172.5 VHN Fig. 9. Beyond radial distance of 6 mm for the water and oil quenched material the hardness values decreases for all tempering temperatures. The hardness of water quench C25 material was higher than that of oil quenched for all tempering temperatures which shows higher quench severity and cooling rate of water than oil as shown in Fig 11. In general highest hardness was obtained for the C25 material at tempering temperature of 400 ^{o}C for both water and oil quenched. Fig. 10.

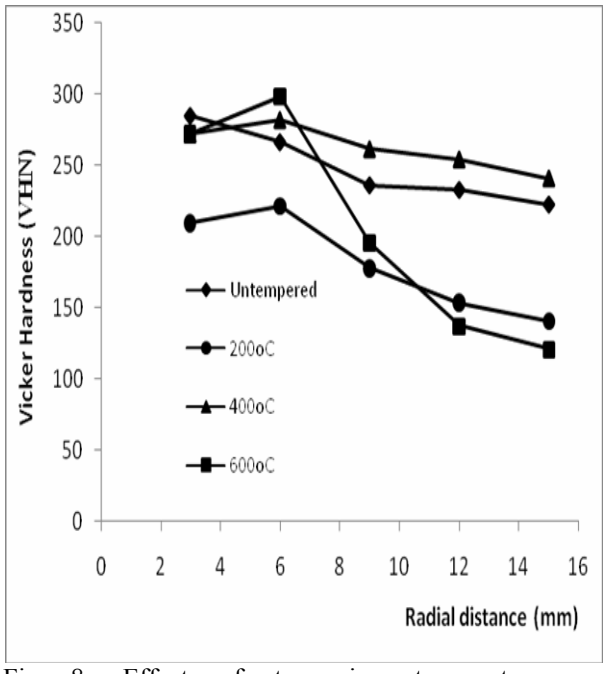

Fig 8. Effect of tempering temperature on microhardness in water quenched C25 material

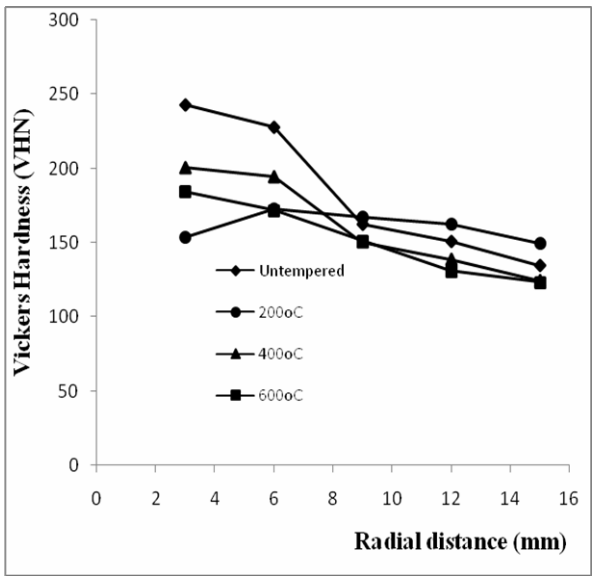

Fig 9. Effect of tempering temperature on microhardness of oil quenched C25 material

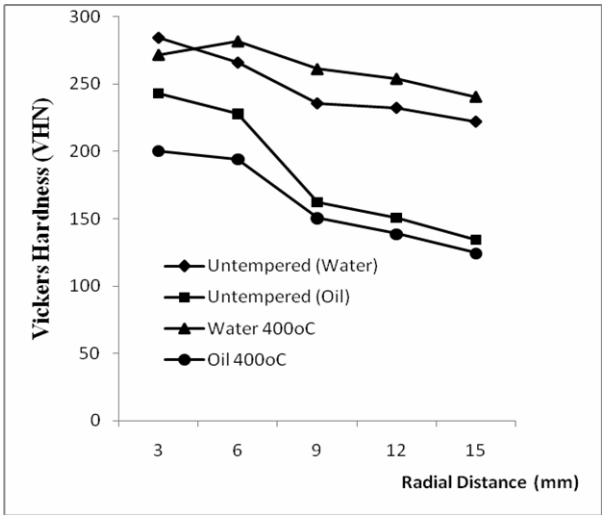

Fig 10. Variation of hardness in water and oil quenched at 400^{0}C tempering temperature

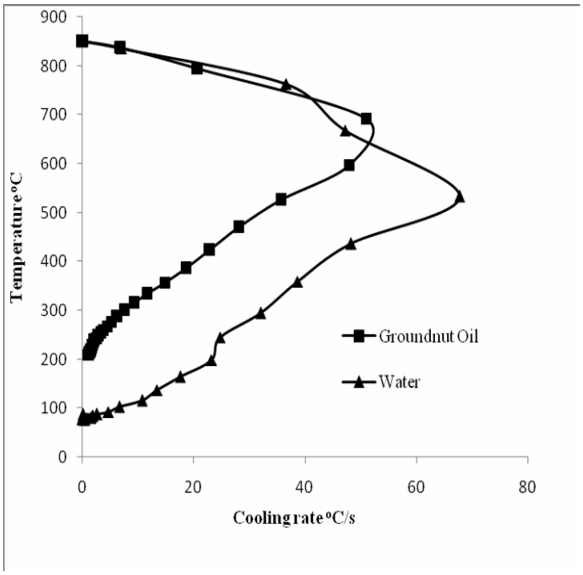

Fig. 11. Cooling rate for various quenchants

3.5 Microstructures of Quenched Specimens

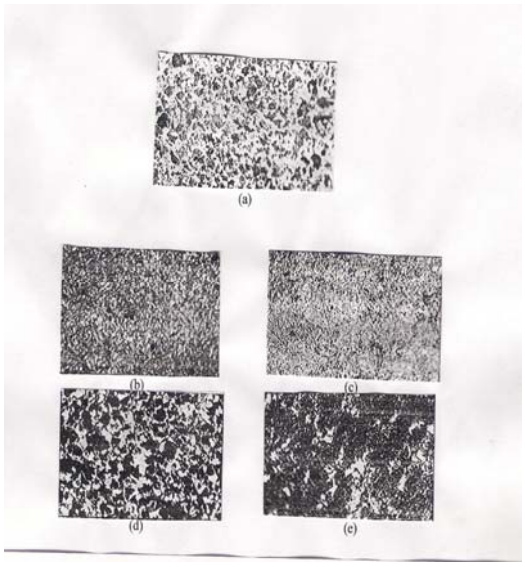

Magnification: x200

Figs. 12 (a÷e): Microstructures of water quenched 0.3% C steel specimens

(a) As received (annealed)
(b) Water quenched
(c) Water quenched and tempered at 200^0C
(d) Water quenched and tempered at 400^0C
(e) Water quenched and tempered at 600^0C

Fig.12(a) Comprises of coarse pearlite in a ferrite matrix indicative of fully annealed condition. Figs.12(b - e) shows a mixture of martensite and fine pearlite indicative of quenching condition but the grain structures are finer than the specimens quenched in oil, which shows that water has higher severity of quenching.

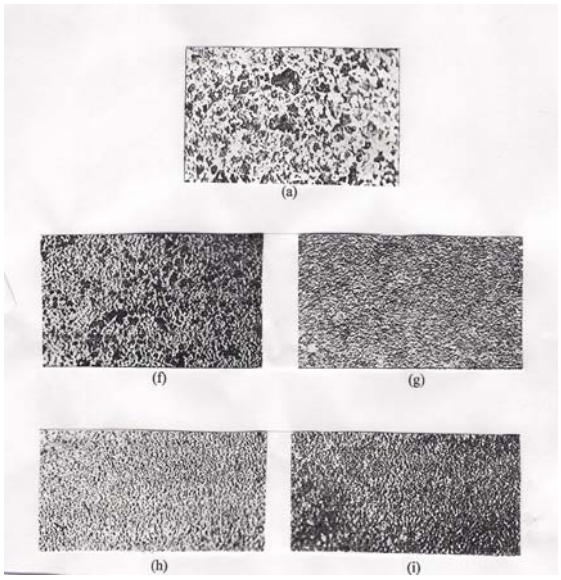

Magnification: x200

Fig.12 (a, f-i): Microstructures of oil – quenched 0.3% C steel specimens

(f) Oil quenched
(g) Oil quenched and tempered at 200^0C
(h) Oil quenched and tempered at 400^0C
(i) Oil quenched and tempered at 600^0C

Figs.12(f-h) shows mixture of martensite and fine pearlite indicative of quenching condition but the grain structures are not as fine as the specimens quenched in water, which indicates that oil has lower severity of quenching.

4. CONCLUSIONS

To study the effect of tempering temperature on residual stresses of quenched C25 carbon steel hollow cylinders, successive stress relaxation are performed with strain gauges used to monitor the strain changes. Modified sach boring technique is applied to obtain values of longitudinal and transverse residual stresses. Also effect of tempering temperature on hardness was studied and the variation of hardness along the radial distances was determined for the quenched material using water and oil. From the experimental results the following conclusions are deduced:

(1) Higher levels of residual stresses of as much as 24% are induced in water quenched materials in comparison with vegetable oil quenched materials.

(2) Residual stresses across the quenched hollow cylinder are compressive at inner and outer surfaces and tensile in the inner part thus maintaining equilibrium across the cross section.

(3) Tempering reduces magnitude of residual stresses induced by quenching by as much as 40%.

(4) The higher the tempering temperature the more the residual stresses relieved in both longitudinal and transverse direction.

(5) Maximum tensile transverse residual stress of water quenched and untempered material is higher than that of longitudinal stress by as much as 73.5%.

(6) Maximum longitudinal machining stresses are as high as 25.78 MN/m^2 and transverse 30.1 MN/m^2 in tension. They are significant enough and therefore deducted to obtain actual quench residual stresses.

(7) Tempering at 400 ^{o}C gives higher hardness for C25 material than other tempering temperatures and the highest hardness was 281.5 VHN and 200.4 VHN for water and oil quenched respectively. Hardness decreases with increase in radial distance beyond 6 mm.

5. REFERENCES

[1] James, M. N., Hughes, D. J., Chen, Z., Lombard, H., Hattingh, D. G., Asquith, D., Yates, J. R., Webster, P. J. *Residual Stresses and Fatigue Performance*, *Engineering Failure Analysis*. England, 2010, p384-385.

[2] Gorkunov, E. S., Zadvorkin, S. M., Goruleva, L. S. *Estimating Residual Stresses in heat-treated Carbon Steels by Magnetic Parameters*, 18th World Conference for Nondestructive Testing, South Africa, April 16 – 20 2012, www.ndt.net/article/wcndt2012/papers/pdf, [online] accessed 4th February 2014

[3] Totten, G. E. *Steel Heat Treatment, Metallurgy and*

Technologies; 2ed., Taylor & Francis Group, 2007.

[4] Liščić, B., Singer, S., Smoljan, B. *Prediction of Quench-hardness Within the Whole Volume of Axially-symmetric Workpieces of Any Shape*, Journal of Mechanical Engineering. Vol. 56, p.p. 104-114, 2010.

[5] Palaniradja, K., Alagumurthi, N., Soundararajan, V. *Residual Stresses in Case Hardened Materials*, The Open Materials Science Journal. Vol. 4, p.p 92-102, 2010.

[6] Chobaut, N., Repper, J., Pirling, T., Carron, D., Drezet, J. M. *Residual Stress Analysis in AA7449 as-Quenched Thick Plates Using Neutrons and Fe Modelling*, The Minerals, Metals & Materials Society, 13th International Conference on Aluminum Alloys (ICAA13), p.p. 285-291, W. Hasso, D. Anthony, A. William, Ed, London, 2012.

[7] Li, Z. C., Ferguson, B. L., Freborg, A. *Modeling Application to Reduce Distortion of a Carburized and Quenched Steel Gear*, ASM International, p.p 200 – 210, 2012.

[8] Palkowski, H., Brück, S., Pirling, T., Carradò, A. *Investigation on the Residual Stress State of Drawn Tubes by Numerical Simulation and Neutron Diffraction Analysis*. Materials, Vol. 6, p.p 5118-5130, 2013. http://www.mdpi.com/1996-1944/6/11/5118, [online] accessed 6th February 2014

[9] Chinnaraj, K., Sathya, P. M., Lakshmana, R. C. *Numerical and Experimental Investigation of Residual Stresses in Cold Formed Truck Frame Rail Sections*, SAE Technical paper, 2013. http://papers.sae.org/2013-01-2796/ [online] accessed 8th February 2014.

[10] James, M. N., *Residual Stress Influences in Mechanical Engineering*, Congreso Nacional de Ingeniería Mecánica, XVIII, 2010, [online] accessed 10th February 2014, www.uclm.es/actividades/2010/CongresoIM/pdf/penarias/James.pdf

[11] Bin, **S.,** Foroogh, O., Chris, T., David, S. *Residual Stresses in Machined and Shrink-fitted Assemblies,* JCPDS-International Centre for Diffraction Data, p.p 675 – 682, 2009,

[12] Totten, G., Howes, M., Inoue, T., *Handbook of Residual Stress and Deformation of Steel*. ASM International. Vol. 4, p.p 60-66, 2002.

[13] Guo, Q., Chang, L., Ye, L., Wang, Y., Feng, H., Cao, Y., Lian, Q., Li, Y. *Residual Stress, Nanohardness, and Microstructure Changes in Whirlwind Milling of GCr15 Steel*, Materials and Manufacturing Processes, Vol. 28, 1047-1052, 2013, http://www.tandfonline.com/doi/abs/10.1080/10426914.2013.763963#preview [online] accessed 4th February 2014.

[14] Bruch, D., Henes, D., Leeibenguth, P., Holzapfel, C., *Mechanical Properties and Corrosion Resistance of Duplex Stainless Steel Forgings with Large Well Thicknesses*, Proceedings Duplex international, Grado, 2007.

[15] Yelbay, H. I., Cam, I., Gur, C. H. *Non-Destructive Determination of Residual Stress State in Steel Weldments by Magnetic Barkhansen Noise technique*, NDT&E International, Vol. 43, p.p 29 – 33, 2010.

[16] George, D., Kingston, E., Smith, D. J. *Measurement of Through Thickness Stresses Using Small Holes*, Journal of Strain Analysis, Vol. 37, p.p 125-139, 2002.

[17] Kingston, E. J., Stefanescu, D., Mahmoudi, A. H., Truman, C. E., Smith, D. J. *Novel Applications of the Deep Hole Drilling Technique for Measuring Through Thickness Residual Stress Distributions*, Journal of ASTM International, Vol. 3, p.p. 1-12, 2006.

[18] Smith, D. J., Bouchard, P. J., George, D. *Measurement and Prediction of Residual Stresses in Thick-section Steel Welds*, Journal of Strain Analysis, Vol.. 35, p.p. 287-303, 2000.

[19] Adedayo, S. M. *Temperature and Residual Stress Distribution in arc-Welded Steel Plates*, Unpublished Ph.D Thesis, University of Ilorin, Ilorin, p.p. 34-38, 1998.

[20] Adeyemi, M. B. *Isothermal Stress-relief and Stress-relaxation of Cold-extruded Mild Steel Rods*, Unpublished Ph.d Thesis, Loughborough University of Technology, p.p. 5-10, 1979.

[21] Adedayo, S. M., Adeyemi, M. B. *Effect of Preheat on Residual Stresses Distribution in Arc-welded Mild Steel Plate*, Journal of Materials Engineering and performance. Vol. 9, p.p. 7-11, 2000.

Authors:

Associate Professor. Dr. Segun M. Adedayo, University of Ilorin, Department of Mechanical Engineering, P.M.B. 1515, Ilorin, Nigeria. Phone: 234-8033821984, e- mail: amsegun@unilorin.edu.ng

Lecturer. Dr. Adebayo S. Adekunle, University of Ilorin, Department of Mechanical Engineering, P.M.B. 1515, Ilorin, Nigeria. Phone: 234-8033591465, e-mail: adekunlebayor@gmail.com

M. Eng. Arasanmi Ajiboye, University of Ilorin, Department of Mechanical Engineering, P.M.B. 1515, Ilorin, Nigeria.

Journal of Production Engineering
Vol.17 No.2

Original Scientific Paper

Salokyová, Š.

EVALUATION OF THE VIBRATION MEASUREMENTS DURING MILLING OPERATIONS

Received: 9 September 2014 / Accepted: 2 October 2014

Abstract: *Vibrations are an inseparable accompanying occurrence, which occurs during the operation of every technical device. The main contribution of this text is to measure the extent of the vibrations on the head of the milling machine during the material processing. During the realization of the experiments one type of milling machine was used, the rpm of the spindle head was changed as well as the reduction of the material. The vibrations sensor recorded created vibrations. Original graphic relations were created based on measured values, based on which new knowledge and conclusions were formulated.*
Key words: *Milling operation, material processing, vibrations acceleration amplitude, frequency spectrum*

Ocena merenja vibracija u toku operacija glodanjem. *Vibracije su sastavni deo pratećih pojava, koje proizlaze iz rada bilo koje mehaničke opreme. Glavni doprinos ovog rada je relativna veličina vibracija glave za glodanje glodalice tokom obrade materijala. U eksperimentima je korišćen jedan tip glodalice, variran je broj obrtaja vretena i dubina glodanja. Dobijene vibracije su beležene pomoću senzora vibracija. Originalni grafičkiprikazi su sačinjeni na osnovu dobijenih podataka, na osnovu kojih su formulisana nova saznanja i zaključci.*
Ključne reči: *Glodanje, obrada materijala, amplituda vibracija, spektar frekvencije*

1. INTRODUCTION

Despite advanced technologies devices still fight the creation of vibrations during their operation. These vibrations are unwanted from the point of view of accuracy of the products‘ production and every company should aim to eliminate these vibrations as much as possible. Vibrations during the milling operations occur because of two reasons. Especially because the fact, that during the milling operations the splinter is removed intermittently during the alternating angle of the cutter. These are vibrations caused by the operation of the machine and we view them as a common consequence of this type of processing. The second reason is the fact, that the cutters of the milling machine process a warped surface. In cases when the spindle and the machine get under the influence of the dynamic forces generated by the oscillation caused by the cutting process, we talk about a regenerative oscillation and oscillation in positional relation. The goal of this text is to point to the possibility of vibration generation during the milling process as a consequence of the changing rpm of the spindle head and as a consequence of the changing thickness of the removed layer of the material [1-6].

2. CONDITIONS DURING THE VIBRATIONS MEASUREMENT

The vibrations were examined on the milling stand Zayer 3000 BF 3 depicted on Fig. 1. The milling stand consists of steel construction, electromotor drive with 26 kW power, spindle and the cutter. The rpm of the spindle can be steadily regulated in the interval 28 – 1800 rpm. Vibrations of the spindle head during the milling were measured and recorded under constant and changing parameters of the operating conditions. Four consequent measurements were performed, which were split into two experiments. Conditions of the experiments execution are stated in Tab. 1.

Table 1. Conditions of the experiments execution

	constant parameters			changing parameters	
	type of material	shift	milling cutters	the reduction of the material	the rpm of the spindle head
1.exp.	1.1213	150 mm/min	monolithic cutter type NR TiN 50x36	2,7 mm	200 rpm
2.exp.				4,8 mm	250 rpm

Fig. 1. Milling machine of the Zayer 3000 BF 3 type

3. TECHNICAL SYSTEM FOR MEASUREMENT AND EVALUATION OF THE EXPERIMENTS

A piezoelectric sensor of the 4514B-62887 type from the company Brüel & Kjaer was used for the monitoring of the frequency analysis of the oscillation, which was mounted on the spindle head through the means of a magnet (Fig. 2). The piezoelectric vibrations sensor monitors vibrations during milling in the direction of the milling course axis. In the data collector the acceleration of the vibration signal is being recorded and it is integrated with the speed of the vibration signal [7].

The vibrations acceleration amplitudes in the axis of the milling recorded in this way are written into the memory of the measuring device NI 9233 of the National Instruments Company and are evaluated in the frequency spectrum thanks to the fast Fourier transformation. This allows the determination of the harmonic frequencies rate in the monitored signal. The evaluated signal can then be immediately observed on the portable computer thanks to the SignalExpress software. The SignalExpress program contains several functions necessary for the correct evaluation, recording of the measurements and their analysis [7].

Fig. 2. Detail depiction of the vibrations sensor mounting

4. RESULTS OF THE EXPERIMENTS

The vibration signal measured during the milling in the time period is transformed thanks to the quick Fourier transformation to the frequency spectrum in the range 3,0 – 8,0 kHz [8]. As an example, the course change of the vibrations acceleration amplitude based on the frequency of the spindle head of 200 rpm and material removal of 2,7 mm is depicted in Fig. 3 and the spindle rotations of 250 rpm with material removal of 2,7 mm are depicted in Fig. 4. Similarly the graphical relation of the vibration acceleration amplitude and the vibrations frequency for 200 and 250 rpm with material removal of 4,8 mm was depicted [9].

Based on graphical relations of the vibrations acceleration amplitude (Fig. 3, 4), covers of the vibrations frequency spectrum on the spindle head were created and from the comparison, graphs of the frequency spectrum covers for the common set of experiment sets were created.

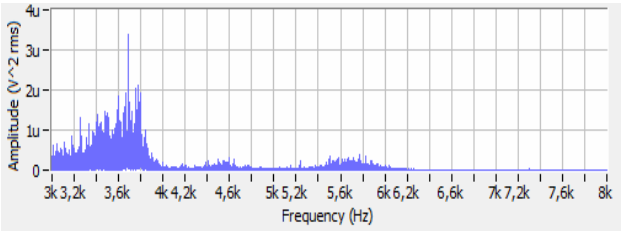

Fig. 3. Graphical relation of the acceleration amplitude and vibrations frequency of a monolith milling machine with material removal of 2,7 mm and 200 rpm

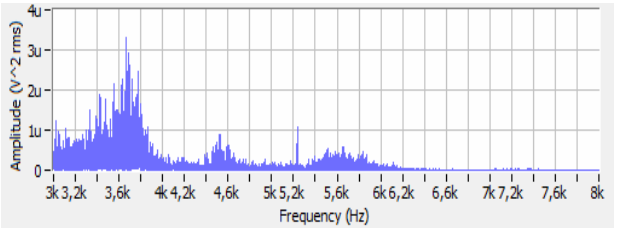

Fig. 4. Graphical relation of the acceleration amplitude and vibrations frequency of a monolith milling machine with material removal of 2,7 mm and 250 rpm

Fig. 5 depicts the comparison graph of frequency spectrum covers jointly for the selected examined set of the spindle rotations of 200 and 250 rpm with material removal of 2,7 mm. The comparison graph of the frequency spectrum covers for spindle rotations of 200 and 250 rpm with material removal of 4,8 is depicted on Fig. 6.

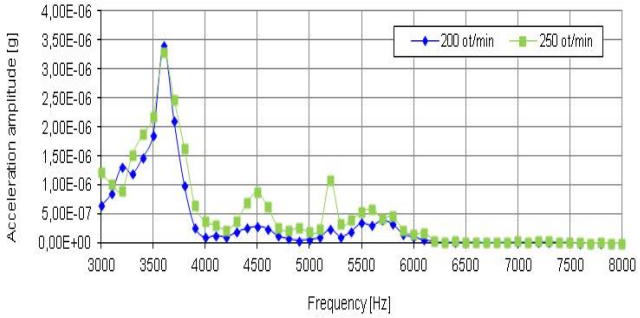

Fig. 5. Comparison graph of the frequency spectrum covers for material removal of 2,7 mm and spindle head rotations of 200 and 250 rpm

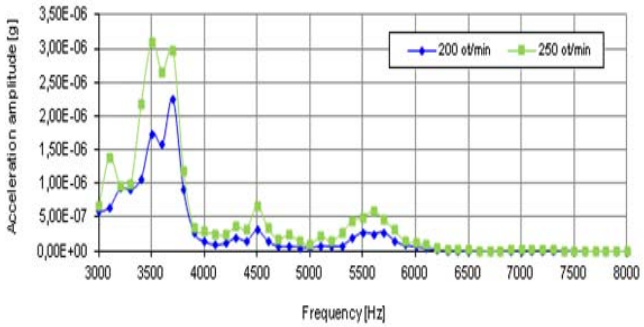

Fig. 6. Comparison graph of the frequency spectrum covers for material removal of 4,8 mm and spindle head rotations of 200 and 250 rpm

Experiments results contain also the evaluation of the comparison graphs of the frequency spectrums covers in the structure separately for the two examined spindle rotations and jointly for the material removal. The comparison graph of the vibrations accelerations amplitude covers and the frequency spectrums of the spindle head vibrations at 200 rpm and with material removal of 2,7 and 4,8 mm is depicted in Fig. 7 and in Fig. 8 the comparison graph at 250 rpm is depicted.

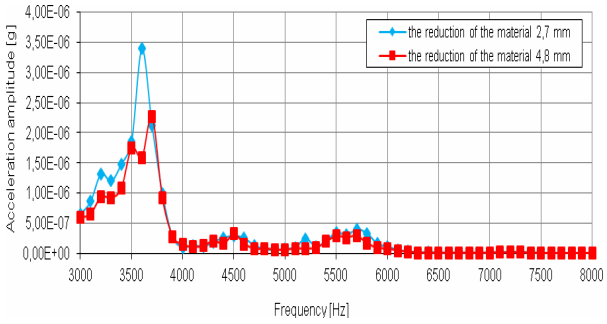

Fig. 7. Comparison graph of the frequency spectrum covers with material removal of 2,7 and 4,8 mm and spindle head rotations of 200 rpm

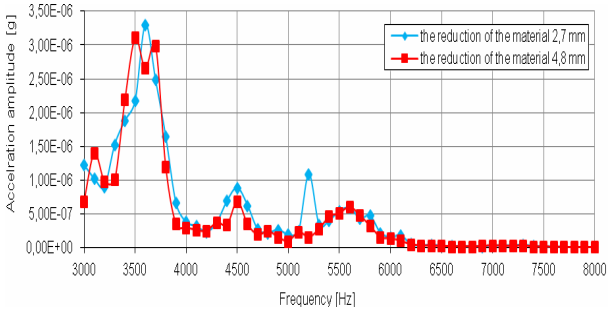

Fig. 8. Comparison graph of the frequency spectrum covers with material removal of 2,7 and 4,8 mm and spindle head rotations of 250 rpm

Chart with the maximum values of the vibrations acceleration amplitude is created based on the comparison graph of the frequency spectrum covers (tab. 2).

Table. 2. Maximum values of the vibration acceleration amplitudes

the rpm of the spindle head	maximum values of the vibration acceleration amplitudes [g]	
	1. experiment	2. experiment
200 rpm	3,4E-06 – 3,6 kHz	2,26E-06 – 3,7 kHz
250 rpm	3,3E-06 – 3,6 kHz	3,1E-06– 3,5 kHz

5. DISCUSSON

The text observes the effect of the spindle head rotations and the factor of removed thickness from the examined material on the creation of mechanical oscillation on the milling machine head during milling and the results are new knowledge and recommendations:

- for the two examined rotations of the spindle head of 200 and 250 rpm with material removal of 2,7 and 4,8 mm the increased vibrations values in the observed range of 3,0-8,0 kHz can be found in the frequency spectrum of 3,0 to 3,9 kHz
- the size of the vibrations acceleration amplitude with material removal of 2,7 mm in the comparison range reaches the highest value 3,4E-06 g for the frequency 3,6 kHz and spindle head rotations of 200 rpm
- with the growing numeric value of the spindle head rotations with material removal of 2,7 mm in the examined range the vibrations acceleration amplitude ix approx. the same and is reduced 2,94% in comparison for the rotations of 200 rpm and 250 rpm
- the size of the vibrations acceleration amplitude with material removal of 4,8 mm in the comparison range reaches the highest value 3,1E-06 g for the frequency 3,5 kHz and spindle head rotations of 250 rpm
- with the growing numeric value of the spindle head rotations with material removal of 4,8 mm in the examined range the vibrations acceleration amplitude ix approx. the same and is reduced 27,09% in comparison for the rotations of 200 rpm and 250 rpm
- during milling operations at 200 rpm the maximum value of the vibrations reached the value of 3,4E-06 g for material removal of 2,7 mm and for material removal of 4,8 mm the vibrations acceleration amplitude value of 2,26E-06 g, which is a 33,53 % decrease
- during milling operations at 250 rpm the maximum value of the vibrations reached the value of 3,3E-06 g for material removal of 2,7 mm and for material removal of 4,8 mm the vibrations acceleration amplitude value of 3,1E-06 g, which is a 6,06 % decrease

6. CONCLUSION

Based on the analysis of the graphic relations of the vibrations acceleration amplitude and the frequencies we can state, that with the increased speed of the rotations of the spindle head of the milling machine the values of the mechanical oscillation grew slightly. With the growing thickness of the removed material the vibrations acceleration amplitude values decreased steadily. From the view point of optimization of the milling process on the Zayer 3000 BF 3 milling machine it is necessary to state, that the worst case in respect to the vibrations accelerations amplitude values is the combination of conditions of the cutting process under low cutting speed and material removal of 2,7 mm.

Under the ISO 10816-3 regulation the milling machine of the Zayer 3000 BF 3 type with 26 kW power belongs into the group 3, along with machines of middle size without special foundations or immovably stored machines with foundations up to 30 kW [10]. As per the maximum value of the vibrations acceleration amplitude we can asses, that not even long-term processing under given conditions does not cause vibrations on our milling machine, which would

shorten the life-span, since we have measured the maximum vibrations acceleration amplitude of 3,4E-06 g.

7. ACKNOWLEDGEMENTS

This work was partially supported by EU Structural Funds, R&D 2.2, Project ITMS 26220220103 "Research and development of intelligent unconventional actuators based on artificial muscles" and by Institutional research task IU 5/2011.

8. REFERENCES

[1] STAREK, L.: Kmitanie mechanických sústav. Bratislava: STU Bratislava, 2006. 316 s. ISBN 80-227-2491-2.

[2] KOCMAN, K., PROKOP, J.: Technologie obrabění. Brno: Vysoké učení technické: Akademické nakladatelství CERM, 2005. 270 s. ISBN 80-214-3068-0.

[3] KOCMAN, K.: Frézovaní. Brno: Vysoké učení technické, 1999. 191 s. ISBN 80-214-1425-1.

[4] BUGÁR, T.: Experimentálne metódy a technická diagnostika. Košice: TU, 2000. 49 s. ISBN 80-7099-539-4.

[5] Fabian, S., Krenický, T.: Využitie vybraných vibrodiagnostických metód v monitoringu prevádzkových charakteristík strojových zariadení. 2010. In: Spravodaj ATD SR. Č. 1,2 (2010), s. 32-34. - ISSN 1337-8252.

[6] Kreheľ, R.: Vibračná diagnostika rotujúcich strojov. 2007. In: MM. Průmyslové spektrum. No. 7,8 (2007), p. 29. ISSN 1212-2572.

[7] Salokyová, Š.: Analýza, modelovanie a simulácia vibrácií vo výrobných systémoch s technológiou vodného prúdu, Dizertačná práca. Prešov, 2012. 303 p.

[8] ŠOLTÉSOVÁ, S., BARON, P., SIMKULET, V., MARCINKOVÁ, M.: Konkrétne metódy technickej diagnostiky určené pre sledovanie a monitorovanie stavu výrobných strojov a zariadení. 2013. In: Posterus. Roč. 6, č. 9 (2013), s. 1-6. - ISSN 1338-0087.

[9] Panda, A., Prislupčák, M.: Technologické faktory pôsobiace na obrábanie. In: Trendy a inovatívne prístupy v podnikových procesoch : 16. medzinárodná vedecká konferencia : 7. - 8.november 2013, Košice, 2013 S. 1-7. ISBN 978-80-553-1548-5.

[10] ISO 10816-3: Mechanické kmitanie. Hodnotenie kmitania strojov meraním na nerotujúcich častiach. 2009.

Authors: **Ing. Štefánia Salokyová**, [1]Technical University of Košice, Slovakia, Faculty of Manufacturing Technologies, Department of Manufacturing Processes Operation, Bayerova 1, 080 01 Prešov, Phone.: 051/ 77 23 504
E-mail: stefania.salokyova@tuke.sk

Journal of Production Engineering
Vol.17 No.2

Original Scientific Paper

Dhakar, K., Pundir, H., Dvivedi, A.

OPTIMIZATION AND COMPARISON OF NEAR-DRY EDM AND DRY EDM OF INCONEL 718

Received: 21 October 2014 / Accepted: 16 November 2014

Abstract: *Near-dry electric discharge machining (EDM) and dry EDM are the process variants of the EDM process. This article presents experimental investigation on near-dry and dry EDM to achieve the high material removal rate (MRR), and low tool wear rate (TWR) on Inconel 718. Two-phase dielectric (liquid and air) was utilized in near-dry EDM while only air was used in dry EDM. L_9 orthogonal array was used to determine the effect of pulse current, pulse on time, pulse off time and gap control on MRR and TWR in near-dry and dry EDM. Experimental results reveal that near-dry EDM achieved higher MRR while dry EDM obtained lower TWR.*
Key words: *Electric discharge machining, Material removal rate, Tool wear rate.*

Optimizacija i poređenje skoro-suve EDM i suve EDM obrade INCONEL-a 718. *Skoro - suva elektro erozivna obrada (EDM) i suva EDM obrada su varijante EDM procesa. Ovaj rad predstavlja eksperimentalno istraživanje na skoro-suvom i suvom EDM procesu u cilju postizanja velike proizvodnosti (MRR) i niskog trošenja alata (TVR) pri obradi INCONEL-a 718. Dvofazni dielektrikum (tečnost i vazduh) je korišćen pri skoro suvoj EDM obradi dok je kod suve EDM korišćen samo vazduh. L9 ortogonalni plan eksperimenta je korišćen da se odredi uticaj struje impulsa, dužine impulsa, vreme pauze i veličinu zazora na MRR i TVR u delimično suvoj i suvoj EDM obradi. Eksperimentalni rezultati pokazuju da skoro suva EDM obrada postiže veću proizvodnost dok suva EDM obrada daje manje trošenje alata.*
Ključne reči: *Elektro erozivna obrada, proizvodnost, trošenje alata.*

1. INTRODUCTION

Electrical discharge machining (EDM) has become a well-known non-conventional machining process because of its widely application in die making industries, aerospace and surgical equipment manufacturing industries [1]. Inconel 718 is a high strength, temperature resistant nickel-based super alloy. It is widely used in aerospace industries. It is difficult to machine, because of its poor thermal properties, high toughness, high hardness, presence of highly abrasive carbide particles and strong tendency to weld with the tool to form build up edge [2]. EDM process is based on removing material from a part by means of a series of repeated electrical discharges between tool called the electrode and the work piece in the presence of a dielectric fluid. The material is removed with the erosive effect of the electrical discharge from tool and work piece [3]. EDM also has the advantage of being able to machine difficult-to-cut material like Titanium, Inconel etc. However, its low machining efficiency, higher tool wear rate (TWR), poor surface finish and environmental pollution constrained its further applications. The EDM process utilizes hydrocarbon oils as dielectric medium. This dielectric medium results in serious toxic fumes and pose a health hazard to machine operator [4].

Near-dry and dry EDM are the process variants of the EDM process. Both are the environmental friendly process. Theses processes do not produce toxic fumes and consequent health hazards. Near-dry utilizes liquid-air mixture as dielectric medium and dry EDM uses high velocity air or gases as dielectric medium through a tubular electrode.

NASA published first research paper on dry EDM process in 1985. It was reported that the EDM drilling could be feasible with gases if argon and helium used as the dielectric medium [5]. Kunieda et al. [6] investigated that MRR improves with oxygen dielectric medium. It also reported that the high velocity gas flow through hollow tool electrode improves debris flushing from IEG. Kunieda et al. [7] reported that the accuracy of machined surface deteriorates with the debris deposition.

Near-dry EDM was reported by Tanimura et al. in 1989 first time [8]. Further Tao et.al [9] reported that liquid phase in the dielectric medium enhances debris flushing and eliminates debris reattachment. This results in the better surface finish and increases process efficiency in the near-dry EDM. Better surface finish obtained in near-dry EDM as compared to the wet and dry EDM at the same discharge energy level [10].

In this comparative study near-dry and dry EDM were investigated to analyze the effect of current, pulse on time, pulse off time and gap control on MRR and TWR. Taguchi's L_9 orthogonal array was used for design of experimentation.

2. EXPERIMENTAL SETUP

2.1. Material and Methods

The experiments were conducted on the EMS 5030 die sinking EDM by Electronica India. An attachment was designed and fabricated in house for a dielectric

mixing unit for near-dry EDM process. This attachment was placed on the tool holder head. It mixes up liquid with air. The liquid dielectric fluid was supplied to the dielectric mixing unit at a constant flow rate. The air was supplied to the mixing unit at a regulated pressure, subsequently this air-water mix dielectric was injected through tubular electrode between the inter electrode gap (IEG). In case of dry EDM only air was supplied at IEG.

The flow rate of the water was constantly maintained at 5 ml/min and air pressure was regulated at 5.62 kg/cm^2 during experimentation. Figure 1 shows a schematic of near-dry EDM setup. In the present work, tubular electrode of copper with external diameter 5.5 mm and internal diameter 3 mm has been used to drill Inconel 718 material at 10 mm depth.

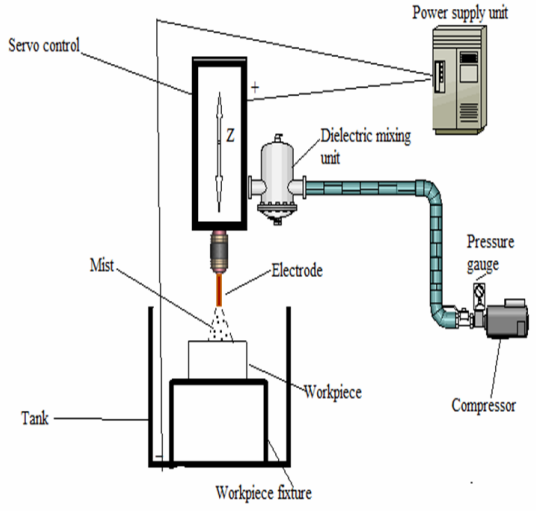

Fig. 1. Schematic of Near-dry EDM setup

2.1 Process Parameters

The selection of process parameters was based on literature review and subsequently pilot experimentation. The following parameters were selected to study their effect on performance measures of the near-dry and dry EDM process.

- Pulse current (Ip)
- Pulse-on time (T_{on})
- Pulse-off time (T_{off})
- Gap control

These parameters were used at 3 levels (Table 1). The parameters that were kept constant during experimentation are also tabulated in Table 1.

S. No	Variable	Code	Level 1	Level 2	Level 3
1	Current (A)	A	12	15	21
2	T_{on} (µs)	B	400	500	700
3	T_{off} setting	C	4	5	6
4	Gap control setting	D	4	5	6
Constant					
Lift	: 5				
Voltage	: 60 V				
Tool	: 99.9% Copper tube				
Workpiece	: Inconel 718 (10 mm thick)				
Polarity	: Straight (+)				
Liquid	: water (5 ml/min)				

Table 1. Process parameters and their levels

A standard Taguchi orthogonal array L_9 was used to study this four factor system. The 9 experiments were performed on the trial conditions with near-dry EDM and dry EDM given in Table 2. Data from a designed experiment is traditionally used to analyse the mean response.

Trial No.	Process parameter				Near-dry EDM Avg. MRR (mm^3/min)	Dry EDM Avg. MRR (mm^3/min
	A	B	C	D		
1	12	400	4	4	1.286	1.236
2	12	500	5	5	1.704	1.522
3	12	700	6	6	1.883	1.649
4	15	400	5	6	2.087	1.960
5	15	500	6	4	2.112	2.300
6	15	700	4	5	2.294	2.192
7	21	400	6	5	3.294	2.439
8	21	500	4	6	4.091	2.898
9	21	700	5	4	4.976	3.129

Table 2. Experimental design matrix for near-dry and dry EDM

3. RESULT AND DISCUSSION

The average value of MRR and S/N ratios for each parameter were calculated and tabulated in Table 3 for near dry EDM. The effect of each parameter on MRR is plotted in Figure 2. The higher MRR is desirable, so the parameter at levels A_3, B_3, C_2 and D_1 are best choice with respect to both mean response and variation.

	Parametric designation	Average value of QC		
		Level 1	Level 2	Level 3
MRR (raw data)	A	1.624	2.127	4.120
	B	2.185	2.636	3.051
	C	2.557	2.885	2.430
	D	2.791	2.431	2.650
MRR (S/N data)	A	4.099	6.534	12.166
	B	6.142	7.782	8.875
	C	7.202	8.158	7.440
	D	7.534	7.385	7.881

Table 3. Average value of raw data and S/N data for near-dry EDM and dry EDM

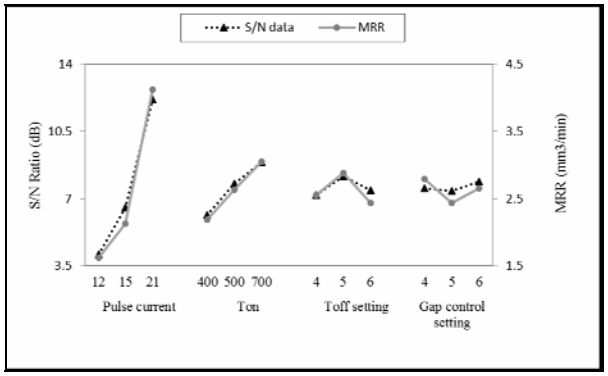

Fig. 2. Curve showing the effect of process parameters in near-dry EDM

Analysis of variance (ANOVA) was performed for experimental results (Table 4) using the help of Qualitec software. ANOVA of raw data revealed that contribution of current was highest towards MRR in near-dry EDM. The analysis of S/N data also produced the similar results.

	Source	DOF	SS	V	F- ratio	S'	% P
MRR	A	2	31.365	15.682	2345.127	31.351	86.013
	B	2	3.374	1.687	252.334	3.361	9.222
	C	2	.994	0.497	74.382	0.981	2.692
	D	2	.594	0.297	44.469	0.581	1.595
	Error	18	.120	0.006			0.478
S/N Data	A	2	102.718	51.359		102.718	88.589
	B	2	11.357	5.678		11.357	9.794
	C	2	1.485	0.742		1.485	1.281
	D	2	0.387	0.193		0.387	0.334
	Error	0					

Table 4. ANOVA for near-dry EDM

	Parametric designation	Average value of QC		
		Level 1	Level 2	Level 3
MRR (raw data)	A	1.469	2.594	2.822
	B	2.155	2.407	2.323
	C	2.109	2.480	2.296
	D	2.389	2.051	2.446
MRR (S/N data)	A	3.248	8.214	8.959
	B	6.153	7.248	7.021
	C	5.962	7.45	7.01
	D	6.896	6.039	7.487

Table 5. Average value of raw data and S/N data for dry EDM

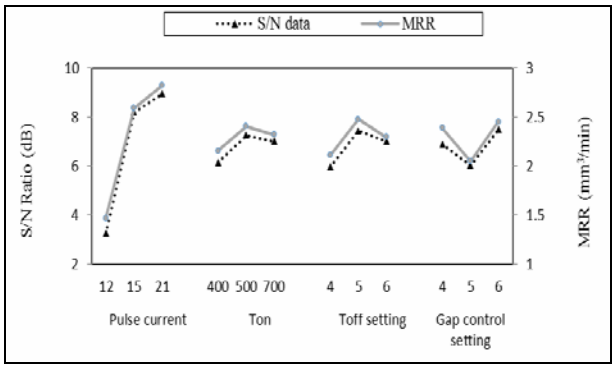

Fig. 3. Curve showing the effect of process parameter in dry EDM

	Source	DOF	SS	V	F- ratio	S'	% P
MRR	A	2	9.447	4.723	650.203	9.432	83.356
	B	2	0.296	0.148	20.377	0.281	2.488
	C	2	0.622	0.311	42.861	0.608	5.374
	D	2	0.819	0.409	56.388	0.804	7.111
	Error	18	0.129	0.007			1.671
S/N Data	A	2	57.831	28.915		57.831	86.933
	B	2	2.003	1.001		2.003	3.011
	C	2	3.509	1.754		3.509	5.275
	D	2	3.179	1.589		3.179	4.779
	Error	0					

Table 6. ANOVA for dry EDM

For dry EDM, the average values of MRR and S/N ratios for each parameter were calculated and tabulated in Table 5. The effect of parameter on MRR is shown in Figure 3. Maximized MRR is desirable, hence the parameter values at levels A_3, B_2, C_2 and D_3 are best choice with respect to both mean response and variation. Table 6 shows ANOVA for dry EDM.

3.1. Estimation of MRR at optimum condition for near-dry EDM and dry EDM

Recommended levels of factors for higher MRR are A_3, B_3, C_2 and D_1. MRR at optimum condition can be computed as:

$$\mu_{MRR} = A_3 + B_3 + C_2 + D_1 - 3\bar{\bar{X}}_{MRR} \qquad (1)$$

Where

μ_{MRR} is mean value of MRR,

$\bar{\bar{X}}_{MRR} = 2.624$ mm^3/min,

A_3, B_3, C_2 and D_1 are the average value of MRR (Table 3).

So $\mu_{MRR} = 4.975$ mm^3/min

Therefore, the expected increase in MRR at optimum machining conditions is 89.60% over the current average MRR (2.624 mm3/min).

CI for the predicted value of μ_{MRR} can be calculated as:

$$CI = \sqrt{F_\alpha(1, f_e) V_e \left[\frac{1}{n_{eff}} + \frac{1}{R}\right]} \qquad (2)$$

Where

Error DOF (fe) = 18 and Error variance Ve = 0.006 (Table 4), R = sample size of confirmation experiment = 3

At the 95% CI for the expected optimum MRR in near-

dry EDM is 4.842 < μ_{MRR} < 5.108 mm^3/min.

Similarly process follow for estimation of MRR at optimum condition in dry EDM.

$\bar{\bar{X}}_{MRR}$ = 2.295 mm^3/min, and μ_{MRR} = 3.270 mm^3/min. At the 95% CI for the expected optimum MRR in dry EDM is 3.127 < μ_{MRR} < 3. 413 mm3/min.

3.2. Analysis of MRR in Near-dry

Contributions of current and pulse on time (T_{on}) towards the MRR are 86.013% and 9.222% respectively (Table 4). MRR increases with increase in current and T_{on} (Figure 2). The increase in pulse current results in increased heat intensity and increase in Ton increased sparking time at inter electrode gap (IEG). These results in more material to melt in molten puddle and thus MRR increases. This result concurs with findings of Tao et al. [11].

Contribution of pulse off time (T_{off}) is 2.692%. MRR increases with an increase in T_{off} at a certain level and then decreases. It was occurred due to increase in T_{off} provides sufficient time to flushing at IEG. It flushes out debris effectively from the working gap and efficient sparking occurs between electrodes, which subsequently enhances MRR. However, higher level of T_{off}, reduces sparking time per cycle so that heat generated at workpiece per cycle decreases and therefore less material gets eroded from workpiece.

Contribution of gap control setting towards MRR is 1.595%. MRR decreases with an increase in gap control setting up to a certain point and then increases. Dielectric gets more space in IEG to flush away the debris and therefore proper sparking occurs which results in increased MRR. However, if gap is further increased, then plasma would expand due to which heat intensity at the least IEG decreases and therefore MRR reduces.

3.3. Analysis of MRR in Dry EDM

Contribution of pulse current is 83.356% towards MRR. The contribution of T_{on} is 2.488% towards MRR (Table 6). MRR increases with Ton up to a certain point and then decreases (Figure 3). At higher value of T_{on}, spark energy is higher (since spark energy is directly proportional to T_{on}) so large discharge craters are formed on work surface and therefore more material removed per spark. Further increase in T_{on} then T_{off} also reaches to a higher value (since T_{off} is proportional to T_{on}) and therefore non-machining time increases due to which MRR is reduced.

The contribution of T_{off} setting is 5.374% towards MRR (Table 6). MRR increases with T_{off} up to a certain point and then decreases (Figure 3).

The contribution of gap control setting is 7.111% towards MRR.

3.4. Analysis of TWR in Near-dry and Dry EDM

In this investigation, it was found that TWR was approximately negligible in both EDM. Because wear ratio of the process was less than one percent. It can be considered as satisfactory.

3.5. Confirmation Experiments

The confirmation experiment is the final step in verifying the conclusions drawn based on Taguchi's parameter design approach. Three trial experiments were performed at the optimum levels of the process parameters, which was obtained by this investigation. At this optimum setting of process parameters of near-dry EDM and dry EDM, average value of MRR was 4.896 mm^3/min and 3.149 mm^3/min (Table 7) respectively. It was close to the predicted value of 5.108 mm^3/min and 3.413 mm^3/min respectively. This result was within the 95% confidence interval (CI) of the expected optimal value of quality characteristics.

Process	Process parameters				Avg. MRR (mm^3/min)
	A	B	C	D	
Near-dry EDM	21	700	5	4	4.896
Dry EDM	21	500	5	6	3.149

Table 7. Results of confirmation experiments

3.6. Comparison of Near-dry and Dry EDM

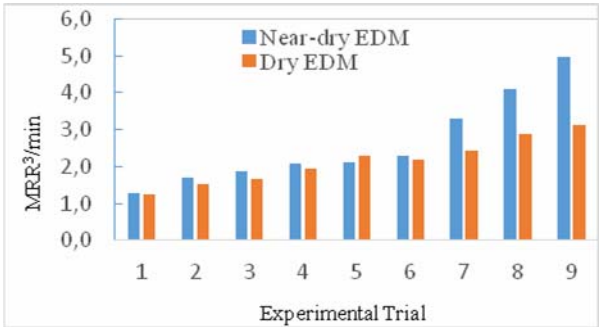

Fig. 4. Comparison of near-dry EDM and dry EDM for MRR

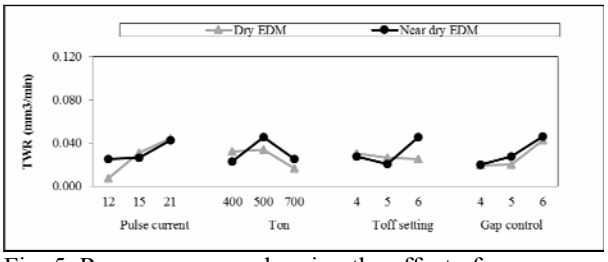

Fig. 5. Response curve showing the effect of process parameters on TWR for wet, near-dry and dry EDM

Experiments were performed on the same input parameters setting for near-dry EDM and dry EDM. Comparison of results are shown in Figure 4 and 5. It was observed that MRR in near-dry EDM is more than the dry EDM. However TWR in dry EDM is less than the near-dry EDM. It was occurred due to the debris reattachment on the tool tip and consequent over cut on the work piece. This is severe problem in dry EDM process. Effective flushing of debris at IEG in near-dry EDM provides higher MRR.

4. CONCLUSION

Based on the experimental results following conclusions was drawn for the effective machining of Inconel 718 in near-dry EDM and dry EDM process.

- Discharge current was the most significant factor in both EDM process. In near-dry EDM contribution of current towards MRR was highest followed by T_{on},

T_{off} and gap control. While in dry EDM current was highest followed by gap control, T_{off} and T_{on}.

- Near-dry EDM provided higher MRR than dry EDM.
- TWR was negligible in both EDM process.
- Near-dry EDM and dry EDM are environment friendly processes.

5. REFERENCES

[1] Norliana, M. A., Darius, G. S., Bahari M. F.: A review on current research trends in electrical discharge machining (EDM), International Journal of Machine Tools & Manufacture, 47, p.p. 1214–1228, 2007.

[2] Ojha, K., Garg, R. K., and Singh., K. K.: MRR Improvement in Sinking Electrical Discharge Machining: A Review, Journal of Minerals & Materials Characterization & Engineering, 9, p.p. 709-739, 2010.

[3] Sharman, A. R. C., Hughes, J. I., Ridgway, K.: (Workpiece surface integrity and tool life issues when turning Inconel 718 nickel based superalloy. Machining Science & Technology, 8, p.p.399–414, 2004.

[4] ElHofy, H., and Youssef, H.: Environmental hazards of nontraditional machining, Proceedings of the IASME/WSEAS International Conference on Energy & Environment, 4, p.p. 140-146, 2009.

[5] NASA: Inert-Gas Electrical-Discharge Machining NASA Technical Brief No. NPO-15660, 1984.

[6] Kunieda, M., and Yoshida, M.: Electrical Discharge Machining in Gas, CIRP Ann., 46, p.p. 143–146, 1997.

[7] Kunieda, M., and Furuoya, S.: Improvement of EDM Efficiency by Supplying Oxygen Gas into Gap, Annals of the CIRP, 40, p.p. 215-218, 1991.

[8] Tanimura, T., Isuzugawa, K., Fujita, I., Iwamoto, A., and Kamitani, T.: Development of EDM in the Mist, Proceedings of Ninth International Symposium of Electro Machining (ISEM IX), p.p. 313–316, Nagoya, Japan 1989.

[9] Tao, J., Shih, A. J., Ni, J.: Investigation of dry and near-dry electrical discharge milling processes, Journal of Manufacturing Science and Engineering, 130, p.p. 011002-9, 2008.

[10] Kao, C. C., Tao, J., Shih, A. J.: Near dry electrical discharge machining, International Journal of Machine Tools & Manufacture, 47, p.p. 2273–2281, 2007.

[11] Tao, J., Shih, A. J., Ni, J.: Near-dry EDM milling of mirror-like surface finish, International Journal of Electrical Machining, 13, p.p. 29-33, 2008.

Authors: **Krishnkant Dhakar, Research Scholar., Harsh Pundir, Mtech Student, Dr. Akshay Dvivedi, Assistant Professor.,** Department of Mechanical and Industrial Engineering, Indian Institute of Technology Roorkee – 247 667, INDIA.

Email: kk_jec@yahoo.co.in
harshpundirsiet@gmail.com
akshaydvivedi@gmail.com

Journal of Production Engineering
Vol.17 No.2

Original Scientific Paper

Pankaj Kumar Gupta*, Akshay Dvivedi, Pradeep Kumar

A STUDY ON THE PHENOMENON OF HOLE OVERCUT WITH WORKING GAP IN ECDM

Received: 20 October 2014 / Accepted: 15 November 2014

Abstract: *Electrochemical discharge machining (ECDM) is a combined phenomenon of spark and electrolysis action of EDM and ECM respectively. Spark strikes locally on a nonconductive glass workpiece during electrolysis for micromachining.*
This article represents phenomenon of material removal as hole overcut (HOC) with the help of ECD from cylindrical tool. Investigations are performed for working gap (between tool and workpiece) to result minimum HOC. Results reveal reduction in HOC at minimum working gap till the tool comes in contact with work piece. The maximum limit of tool workpiece gap was 250 µm, beyond which no material removal was observed.
Key words: *ECDM, Working gap, Hole overcut.*

Studija pojave povećanja rupe usled radnog zazora pri obradi ECDM. *Elektrohemijsko-erozivna obrada (ECDM) je kombinacija obrade iskrom i elektrolize, procesa EDM resp ECM. Varnica se pojavljuje lokalno na neprovodljivom obratku od stakla tokom elektrolize pri mikro obradi.*
Ovaj rad predstavlja pojavu skidanja materijala uz povećanje rupe (HOC) pomoću ECM i cilindričnog alata. Istraživanja su vršena preko posmatranja radnog zazora (između alata i obratka) da bi se utvrdilo minimalno povećanje rupe. Rezultati ukazuju na smanjenje HOC pri minimalnom radnom zazoru sve dok se ne ostvari kontakt između alata i obratka. Gornja granica radnog zazora je iznosila 250 µm, posle čega nije primećeno skidanje materijala.
Ključne reči: *ECDM, Radni zazor, povećanje rupe.*

1. INTRODUCTION

Glass has the special properties of being transparent, chemically inert, low electrical and thermal conductive. Its applications are increasing in micro fabricated devices like solid oxide fuel cells, micro pumps, and micro reactors [1]. The presently available micromachining processes for glass are ultrasonic machining, laser machining, abrasive jet machining and chemical etching. These technologies have certain process and application limitations. Laser and ultrasonic technique produce surface cracks and leads to poor surface finish [2]. Chemical etching with hydrogen fluoride is a very slow process. It also has health hazards. On the other hand, conventionally available sawing techniques are used for simple structures only [3]. In spite of fabrication limitations, glass is very good choice. It has wide applications in manufacturing of DNA arrays [4] and micro solid oxide fuels [5]. High aspect ratio micro fabrication can drastically increase the application of glass in biomedical and energy fields.
Electrochemical discharge machining (ECDM) is a process that has the ability to face the challenges of micromachining of glass. Machining is conducted in an electrochemical cell, when a DC voltage is applied between two electrodes. Electrical discharge takes place at critical voltage on the negatively charged electrode (cathode). The critical voltage aggravates to break the gas films formed by gas bubbles in electrolytic solution. The gas film developed around the tool electrode is never stable. Machined structure locally destroyed by occurrence of micro explosions with gas film. During machining, this causes increase in local temperature to an extent, resulting in hole overcut and heat affected zones or sometimes cracking of glass work piece. This discharge action and electrochemical action are responsible for material removal from the work piece [6]. This machining phenomena is also termed as electrochemical spark machining (ECSM) [7]. A schematic of the ECDM process is shown in Figure 1.

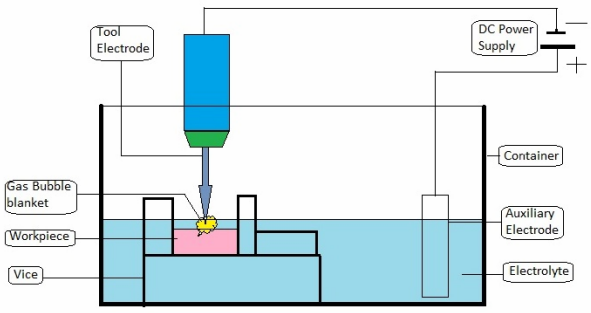

Fig. 1. Schematic of the ECDM process [8].

2. LITERATURE REVIEW

In ECDM, the tool work piece gap depends on tool geometry and it is typically less than 25 micron for glass [9, 10]. Material removal takes place when the material is kept in close proximity of the tool while

mataining gap [9-15]. Literature reveals ECD drilling processes by different methods [16]. The gravity feed drilling is used as one of the prevalent method and proved as most effective for glass drilling process [17-18]. The tool and workpiece remains in continuous contact during gravity feed drilling [19-22]. This gravity feed drilling device contains a workpiece holding platform installed in electrolyte chamber. The chamber has constant upward force due to downward movement of dead weight through pulleys connected by string. A digital indicator placed under chamber checks immediate surveillance of the contact between the tool and workpiece [23]. A force of about 1 N was exerted by counterweight to maintain a contact between the tool and workpiece [24]. The contact force of 30 g was maintained between the tool and workpiece during gravity feed drilling process [25-26]. The machining performances is affected by feeding mechanism of the tool during drilling.

Another alternative for maintaining contact between the tool and workpiece is applying a spring force. This is achieved by locating a compression spring under the work table. It is simpler than gravity feeding device. This delivers the necessary pressure required between the workpiece and tool. The spring pressure also fulfils an additional function of fracturing the passivation layer. The passivation layer in the form of oxide film is generally formed as a results of electrolytic chemical reactions [27].

The literature review determines, some of the investigations in maintaining a gap between tool and workpiece while some made continuous contact. Hence a void in research investigaton exist in, either maintaining or removing the working gap (WG). If kept then what should be its minimum and maximum limits. In this article, investigations were performed by varying the WG from 0 to 300 µm. This variation resulted in a machined surface on workpiece as HOC. The micro drilled hole as HOC is extra material removal around the tool at entry. Material removal phenomenon occurred at tool surface is also discussed.

3. EXPERIMENT DESIGN

3.1 Experimental setup

In the present setup of ECDM as shown in Figure 2, 70 V DC rectangular pulse programmable power supply was used. Rectangular pulse waves were generated by the pulse width controller. The pulse width can be adjusted within a time range of 5-499995 µs.

Workpiece (glass) was fixed on non-reactive work holding device (perspex) in an electrolyte container (perspex). The container was fixed on a worktable which can be given a 2D movement in x-y direction. However, the tool movement takes place along the perpendicular z-axis. Tool movement was further controlled by a microcontroller. The least count of this microcontroller was 3µm against 0.015 degree of motor rotation.

A cylindrical tool of SS, with circular cross section was used as cathode. The schematic geometry of tool used and actual tool form are presented in Figure 3. The tool working surface is made smooth from its periphery and its bottom suface of cross-section. The counter electrode (anode) was made of graphite and kept at a distance of 95 mm from the tool electrode (cathode).

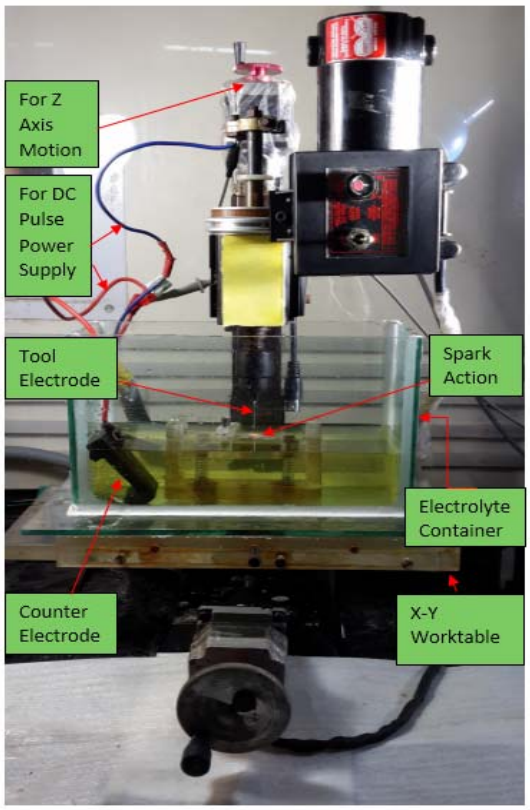

Fig. 2. ECDM Setup

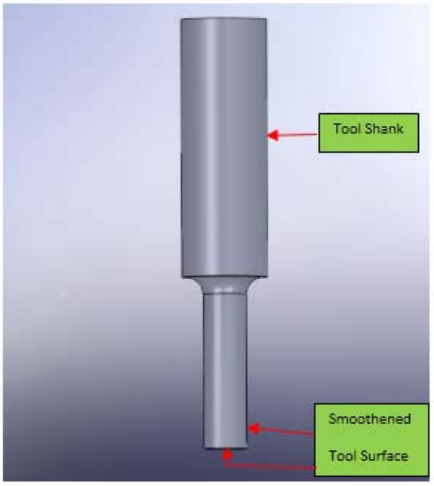

(a)

(b)

Fig. 3. (a) Schematic of tool and (b) actual tool form

3.2 Machining Procedure

The NaCl electrolyte was used in the experiment with 20% w/v concentration at room temperature. The work piece used was microscopic glass slide. Experiments were conducted by varying WG in steps of 50 microns using micro controller. Three sample were machined for each WG setting for 5 minutes. All other details of working conditions are listed in Table 1.

Process parameters	**Description**
TWG	0-300 µm
Pulse on time (T_{on})	10 ms
Pulse off time (T_{off})	1 ms
Duty factor [T_{on} / (T_{on} + T_{off})]	90.9%
Applied voltage	70 V
Tool Material	Stainless Steel
Cross section area of tool	Circular
Tool Diameter	1100 µm
Machining time	5 min
Size of couter electrode	60 mm x 50 mm x 20 mm

Table 1. Working Conditions

Blind holes were produced on the glass slide after fixed time of machining. These specimen were cleaned in ultrasonic cleaner at 50 ^{o}C for 30 min. Images of cleaned micro drilled blind holes were taken on Stereoscopic microscope (SMZ745T).

The image consist of two circles, first in which material removal was observed and second in which material removal was not observed. These two circles were traced by touching three extreme points on optical images of produced blind holes, as the circularity of the hole was not adequate. The first circle was considered as HOC and second circle was considered as central un removed material (CURM). diameter of these circles were measured at 10 X magnification. The images of these blind holes were observed in the shape of a donut as shown in Figure 4.

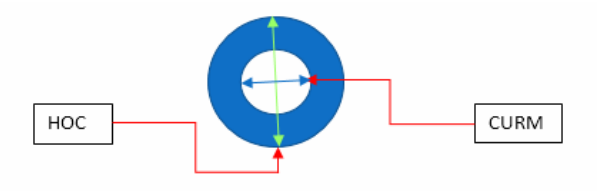

Fig. 4. Schematic of blind hole (donut) with HOC and CURM

3. RESULTS

The results obtained from machining of glass slide with cylindrical tool are shown in Figure 6. The images taken from microscope show that the size of the micro drilled hole increased with increase in WG. HOC increases with increase in tool work piece gap slightly when the WG increases from 0 to 150 µm and this increase is higher thereafter. There was very low increase in CURM at 250 µm as compared to intial value of CURM at 0 µm . However, it was approximately constant with increase in WG. The results show that there is minimum HOC and CURM when the WG is zero. Material removal was not observed after 250 µm WG. The HOC and CURM are shown in Figure 6 at minimum and maximum condition of WG.

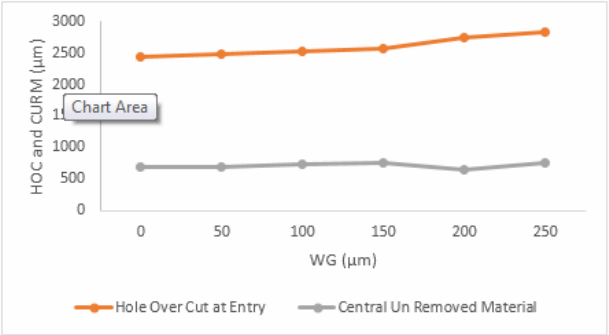

Figure 5. Variation of HOC and CURM with WG

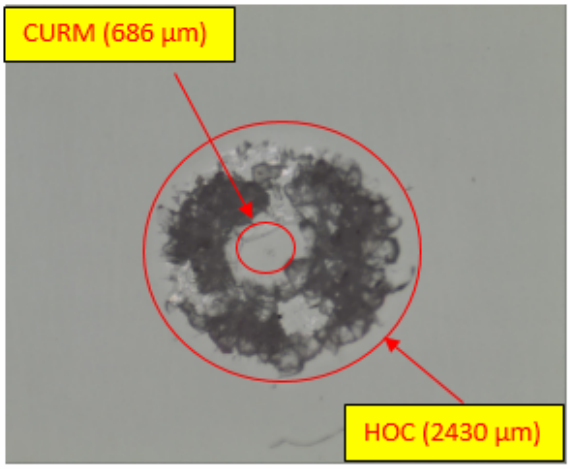

(a) WG=0 µm

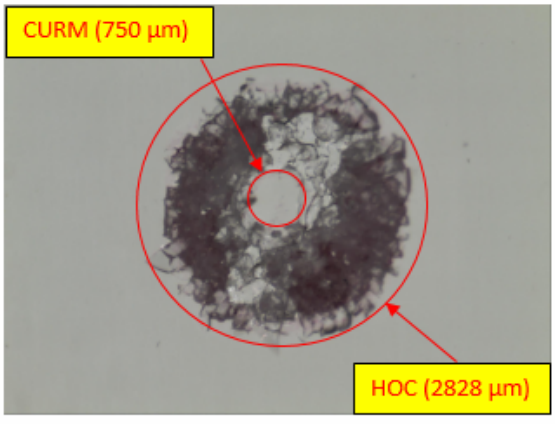

(b) WG=250 µm

Fig. 6. Microscopic image of blind hole with HOC and CURM at minimum and maximum WG

4. DISCUSSION

4.1 Phenomenon material removal and hole overcut at entry

Material removal in terms of HOC and CURM occurred during ECDM attributed to following main reasons. First reason is that the material removal starts from the sides of tool in case of cylindrical tool (intersecting edge of periphery of cylindrical surface and bottom surface). This proceeds with time towards centre of tool. Since intersecting surface of tool acts like a multiple trace of points on the periphery. The increase in spark intensity was observed due to this point effect. Thus, higher material removal occurs on the sides of the tool as compared to flat surface of the bottom of the tool. This phenomenon leads to overcut formation. In addition, electrons are discharged from the location where the electrical field strength is maximum or resistance is minimum. It is located where the radius of curvature of the surface is minimum. It refers to the sharp point or edge rather than a flat surface of the tool. It became easiest to pull electrons from a sharp or pointed electrode edge (corona discharge) [28].

Second reason is that the higher number of gas bubble are formed near the side of the tool due to abundant space availability. This causes stable gas film formation and leads to higher material removal as compared to centre part of the tool as shown in Figure 7.

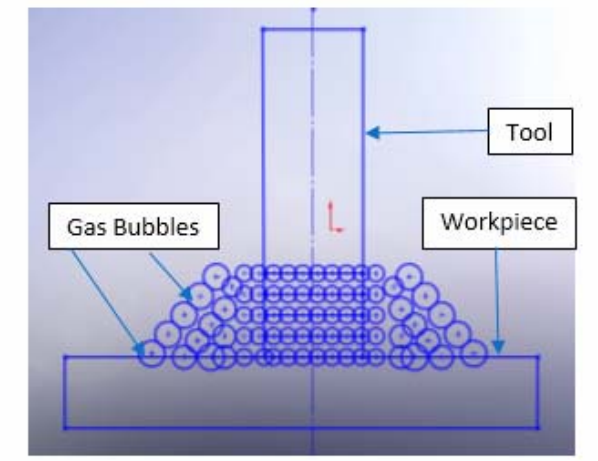

Figure 7. Schematic of bubble formation near the tool end

4.2 Tool WG and HOC

It is found that when WG is theoretically zero, overcut is minimum and it increases with the WG. The first reason of increase in overcut with WG is that the coverage area of spark as subtended by constant angle of spark lines increases with WG as shown in Figure 8. The increase in arc length is responsible for larger number and size of bubbles. The formation of gas film through these bubbles is very rapid. This gas film last longer and results in higher material removal which causes increase in overcut.

Second, after certain distance between tool and work piece there is no material removal. Bubbles do not coalesces due to higher distance between the bubbles and lack of cohesion. Hence gas film is not formed and result as no material removal.

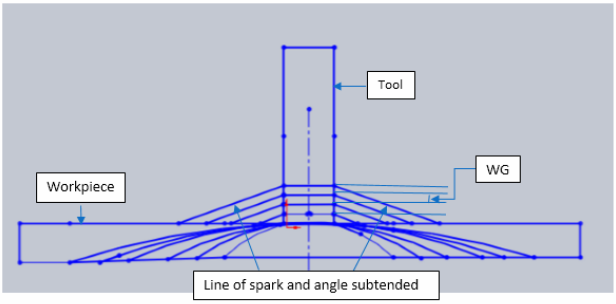

Figure 8. Schematic of subtended arc with WG

5. CONCLUSION

It is experimentally investigated that when the tool work piece gap is practically zero then HOC and CURM were found minimum. This is attributed to minimum coverage of spark subtended by a constant angle in between the line of spark of intersecting edges. There was no material removal observed beyond 250 µm WG. A tool with sharp edges can be used in order to minimize the CURM and maximize the material removal. The sharp edges provide better discharge quality and flow of electrolyte under the tool point to result reduction in HOC.

ACKNOWLEDGMENT

This work was financially supported under research project by Science & Engineering Research Board (SERB), Department of Science & Technology, India. The authors acknowledge the assistance and support. Grant Code : SR/S3/MERC/0070/2012.

6. REFERENCE

[1] Tolke, R.B.H., Evans, A., Rupp, A., Gauckler, J.L.M., Ludwig, J.: Processing of Foturan glass ceramic substrates for micro-solid oxide fuel cells, Journal of the European Ceramic Society, 32, 3229–38, 2012.

[2] Thoe, T.B.A., Aspinwall, D.K., Wise, M.L.H.: Review on ultrasonic machine, International Journal of Machine Tools and Manufacture, 38, 239–55, 1998.

[3] Plaza, J.A., Lopez, M.J., Moreno, A., Duch M., Cane C.: Definition of high aspect ratio glass columns, Sensors and Actuators A: Physical, 105, 305–10, 2003.

[4] Khan, M.C., Robert, L., Boy, J-J, Blind, P.: Deep micro structuring in glass for microfluidic applications, Microsystem Technologies, 13, 447–53, 2007.

[5] Evans, A., Bieberle, H.A., Rupp, J.L.M., Gauckler L.J.: Review on micro fabricated micro-solid oxide fuel cell membranes, Journal of Power Sources, 194, 119–29, 2009.

[6] Basak, I., Ghosh, A.: Mechanism of material removal in electrochemical discharge machining: a theoretical model and experimental verification, Journal of Materials Processing Technology, 71, 350–9, 1997.

[7] Jain, V.K., Dixit, P.M., Pandey, P.M., On the analysis of the electrochemical spark machining process, Machine Tools and Manufacture, 39, 165-189, 1999.

[8] Gupta, P.K., Dvivedi, A., Kumar, P.: Developments on ECDM: A review of experimental investigations on tool electrode process parameters, Journal of Engineering Manufacture, June 2013. DOI: 10.1177/0954405414534834.

[9] Fascio, V., Wuthrich, R., Viquerat, D., Langen, H.: 3D Micro structuring of glass using electrochemical discharge machining (ECDM), International Symposium on Micro mechatronics and Human Science. (MHS'. 99), 179–183, 1999.

[10] Abou Ziki, J.D., Wuthrich, R., Forces exerted on the tool electrode during constant-feed glass micro-drilling by spark assisted chemical engraving, International Journal of Machine Tools and Manufacture, 73, 47–54, 2013.

[11] Wuthrich, R., Fascio, V.: Machining of non-conducting materials using electrochemical discharge phenomenon—an overview, International Journal of Machine Tools and Manufacture, 45, 1095–1108, 2005.

[12] Yang, C.T., Ho, S.S., Yan, B.H.: Micro hole machining of borosilicate glass through electrochemical discharge machining (ECDM), Key Engineering Materials, 196, 149–166, 2001.

[13] Kulkarni, A., Sharan, R., Lal, G.K.: An experimental study of discharge mechanism in electrochemical discharge machining, International Journal of Machine Tools and Manufacture. 42, 1121–1127, 2002.

[14] Fascio, V., Wuthrich, R., Bleuler, H.: Spark-assisted chemical engraving in the light of electrochemistry, Electro chim. Acta 49, 3997–4003, 2004.

[15] Wuthrich, R., Spaetler U., Bleuler H.: The current signal in spark-assisted chemical engraving (SACE), what does it tell us?, Journal of Micromechanics and Microengineering, 16, 779–785, 2006.

[16] Yang, C.K., Wu, K.L., Hung, J.C., Lee, S.M., Lin, J.C., Yan, B.H.: Enhancement of ECDM efficiency and accuracy by spherical tool electrode, International Journal of Machine Tools & Manufacture, 51, 528–535, 2011.

[17] Wei, C., Xu, K., Ni, J., Brzezinski, A. J., Hu. D., A finite element based model for electrochemical discharge machining in discharge regime, International Journal of Machine Tools & Manufacture, 54, 987–995, 2011. DOI 10.1007/s00170-010-3000-0.

[18] Cheng, C. P., Wu , K. L., Mai, C. C., Yang, C. K., Hsu, Y. S., Yan, B. H.: Study of gas film quality in electrochemical discharge machining. International Journal of Machine Tools & Manufacture, 50, 689–697, 2010.

[19] Yang, C.K., Cheng, C.P., Mai, C. C., Wang, A. C., Hung, J, C. Yan, B, H.: Effect of surface roughness of tool electrode materials in ECDM performance, International Journal of Machine Tools & Manufacture 50, 1088–1096, 2010.

[20] Fascio, V., Wuthrich, R., Viquerat, D., Langen, H.: In situ measurement and micro-machining of glass, International Symposium on Micromecatronics and Human Science (MHS'99), pp. 185–191, Nagoya, 1999.

[21] Gautam, N., Jain, V.K.: Experimental investigations into ECSD process using various tool kinematics, International Journal of Machine Tools and Manufacture, 38, 15–27, 1998.

[22]] Cheng, C. P., Wu , K. L., Mai, C. C., Hsu, Y. S., Yan, B. H.: Magnetic field-assisted electrochemical discharge machining, Journal of Micromechanics and Microengineering. 20, 075019 (7pp), 2010. doi:10.1088 / 0960-1317 / 20 / 7 / 075019.

[23] Wuthrich, R., Spaetler U., Bleuler H.: A systematic characterization method for gravity-feed micro-hole drilling in glass with spark assisted chemical engraving (SACE), Journal of Micromechanics and Microengineering. 16, 1891–6, 2006.

[24] Yang, C.T., Ho, S.S., Yan, B.H,: Micro hole machining of borosilicate glass through electrochemical discharge machining (ECDM), Key Engineering Materials, 196, 149–166, 2001.

[25] Tokura, H., Kondoh, I., Yoshikswa, M.: Ceramic material processing by electrical discharge in electrolyte, Journal of Material Science 24, 991–998, 1989.

[26] Lim, H. J, Lim, Y. M., Kim, S.H., Kwak, Y. K., Self-aligned micro tool and electrochemical discharge machining (ECDM) for ceramic materials, Proceedings of SPIE, 4416, 348–353, 2001.

[27] Coteata, M. Schulze, H. P., Atineanu L.S.: Drilling of Difficult-to-Cut Steel by Electrochemical Discharge Machining, Materials and Manufacturing Processes, 26: 1466–1472, 2011. DOI: 10.1080 / 10426914.2011.557286.

[28] Goldman, M., Goldman A., Sigmond R.S.: The corona discharge, its properties and specific uses. Pure & Appi. Chem., Vol. 57, No. 9, pp. 1353—1362, 1985.

***Corresponding author:**

Pankaj Kumar Gupta,
Mechanical & Industrial Engineering Department, Indian Institute of Technology Roorkee,
Roorkee-247667 (Uttarakhand), India.
Mobile: +919456333923
Email: pankaj_tnk@rediffmail.com

Journal of Production Engineering
Vol.17 No.2

Original Scientific Paper

Horvath, R., Mátyási, Gy., Drégelyi-Kiss, Á.

THE EXAMINATION OF HOMOGENEITY IN THE FINE TURNING OF ALUMINIUM ALLOY

Received: 16 September 2014 / Accepted: 18 October 2014

Abstract: *Aluminium alloys are increasingly used by the automotive and aerospace industries because of their numerous advantageous mechanical and chemical properties. Surface roughness is an essential characteristic of a machined surface. The most widespread aluminium alloy used in cutting is the die-cast type, alloyed with silicon. Industries prefer using two types of such alloys, the so-called eutectic and hypereutectic alloys. In this article the machinability of two die-cast aluminium alloys are examined with different edge-geometry tools (conventional - ISO, nonconventional - Wiper) and edge materials. The cutting experiments were carried out with design of experiment – DOE (the so-called central composite design – CCD). In the course of the examination three factors were altered (cutting speed – vc, m/min; feed – f, mm; depth of cut – a, mm), and the main surface roughness parameters used in the industries were taken as output parameters. The parameters of the manufactured surface roughness and their standard deviation in the case of different workpiece materials, tool materials and edge materials were analysed with statistical methods. Besides minimizing surface roughness, another important criterion of the manufacturing system (machine – tools – chuck – workpiece) is its surface roughness maintaining capacity, which was analysed with the coefficient of variation (CV).*

Key words: *fine turning, surface roughness measurement, design of experiments, RSM method, statistical analysis, cutting capacity*

Ispitivanje homogenosti fino strugane legure aluminijuma. *Legure aluminijuma se sve više koriste u automobilskoj i avio industriji zbog njihovih brojnih prednosti usled mehaničkih i hemijskih osobina. Površinska hrapavost je ključna karakteristika obrađene površine. Najkorišćenija legura aluminijuma kod rezanja je livena pod visokim pritiskom sa silikonom kao legirajućim elementom. Industrija preferira dva tipa takvih legura, tzv. eutektičke i nadeutektičke legure. U ovom radu je istraživana obradljivost dve legure aluminijuma, livene pod pritiskom, sa različitim reznim geometrijama alata (konvencionalna – ISO, nekonvencionalna – Wiper) i različitim materijalom rezne ivice. Eksperimenti rezanja su izvršeni po planu eksperimenta (centralnim kompozitnim planom eksperimenta). Tokom trajanja eksperimenta varirana su tri faktora (brzina rezanja – vc, m/min; pomak – f, mm; dubina rezanja – a, mm) i vrednosti hrapavosti obrađene površine su praćeni kao izlazni parametri. Parametri hrapavosti obrađene površine i njihova standardna devijacija u slučaju različitih materijala obratka, materijala alata i materijala reznih ivica su analizirani statističkim metodama. Pored minimiziranja površinske hrapavosti, još jedan važan kriterijum proizvodnih sistema (mašina – alat – pribor – obradak) je mogućnost održavanja hrapavosti površine, koji je analiziran koeficijentom varijacije.*

Ključne reči: *fino struganje, merenje hrapavosti površine, plan eksperimenta, RSM metoda, statistička analiza, kapacitet rezanja*

1. INTRODUCTION

Surface roughness measurements are essential in the characterization of machined surfaces. To thoroughly examine the effect of cutting parameters on surface roughness, a large number of experiments are needed, depending on the number of parameters. With the method of design of experiments (DOE), the number of experiments can be reduced. If only linear effects of cutting parameters are considered, fractional factorial design is sufficient, but to examine quadratic terms and the cross effect of parameters, the RSM method has to be used [1].

DoEs are often employed in cutting research. Aouchi et al. [2] and Noordin et al. [3] examined hard turning with a CBN and a hard metal tool and the resulting surface with the help of DoE. Asiltürk et al. [4] examined stainless steel turning with coated hard metal tools. Dry, wet, and MQL turning were examined with DoE by Hwang [5]. Harničárová et al. studied the topography of laser-cut surfaces [6]. Lazarevic et al. examined the surface roughness of engineering polymers by using the Taguchi method [7]. Mankova et al. examined the chip deformation of coated and uncoated drills with the Taguchi method and built a mathematical model with the machining parameters as input [8]. Pokorádi showed the theoretical background of mathematical modelling [9] and importance of parametrical uncertainties caused by measurement [10]. Horvath et al. examined the fine-turning of aluminium with the help of DOE; they set up empirical equations to estimate the roughness producing capacity of the examined tools (*Ra*, *Rz*) [11], as well as defining surface roughness and productivity target functions, and looking for optimal parameters [12, 13].

We carried out cutting experiments to determine the

connection between cutting parameters and surface roughness values in the case of different edge geometry diamond tools, different edge materials and different workpiece materials. Our aim was to compare and describe the effect of the tools on surface roughness with statistical methods. Another aspect of our research was to examine the behaviour of the workpiece materials under HSC turning. Besides minimizing surface roughness, another important characteristic of the manufacturing system (machine – tools – chuck – workpiece) is its surface roughness maintaining capacity.

2. SUBJECT AND METHODS

2.1 Workpiece and tool materials

Increased silicon content means difficulties in the cutting of aluminium. The primary silicon crystals found in the aluminium matrix make the chip break more easily, but their presence leads to faster tool wear (which can be most often observed in the case of hard metal tools) and makes cutting more difficult. The workpiece materials were AS12 (eutectic) and AS17 (hypereutectic), frequently used in the automotive, aerospace and defence industries. The advantage of the eutectic workpiece material is its perfect castability while the benefits of hypereutectic alloys are their bigger fatigue limit and their better resistance to abrasion. The chemical composition (in wt.%) and hardness of the workpiece were: for AS12 the Al content is 88.43%, the Si content is 11.57%, and the hardness is 64±2 $HB_{2,5/62,5/30}$. For AS17 the Al content is 74.35%, the Si content is 20.03%, the Cu content is 4.57%, the Fe content is 1.06%, and the hardness is 114±3 $HB_{2,5/62,5/30}$.

The examined part was a cylinder with a diameter of 110 mm. The experimental runs were made at every 10 mm, at twelve reference lines equally positioned at 30 degrees as can be seen in Fig. 1.

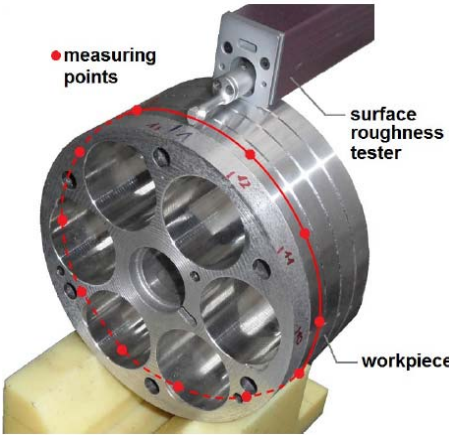

Fig. 1. The measurement of surface roughness

The two metallographic specimens of the workpiece materials (machined surface) are shown in Fig. 2. In the figures the difference between the eutectic and hyper-eutectic fabrics can be seen. The hard primary silicon crystals appear in the case of the hypereutectic material (AS17), while the photo of the AS12 material shows a typical eutectic fabric.

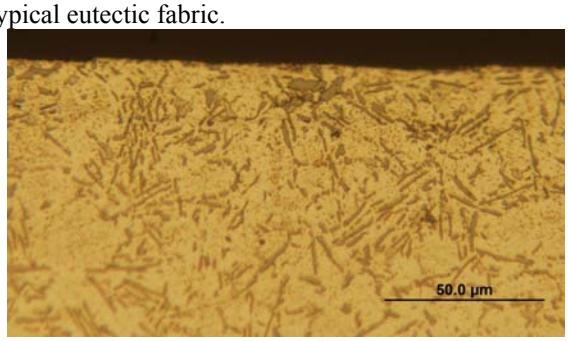

a)

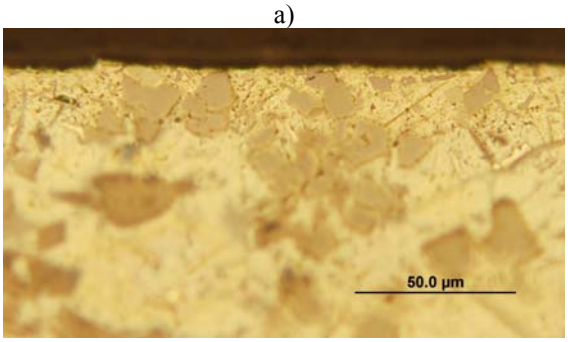

b)

Fig. 2. Metallographic specimen of the workpiece materials; a) Material: AS12 material; cutting parameters: $v_c = 1833$ *m/min*, $f = 0.118$ *mm*, $a = 0.733$ *mm*; tool material: CVD-D, tool geometry: Wiper; b) Material: AS17 material; cutting parameters: $v_c = 1833$ *m/min*, $f = 0.058$ *mm*, $a = 0.733$ *mm*; tool material: CVD-D, tool geometry: ISO

The standard designation of the tools selected were DCGW 11T304 with ISO and Wiper edge geometry. The edge materials were PCD, CVD-D, MDC and they were manufactured by TiroTool (PCD, CVD-D) and WNT (MDC). The holder of the tool was codified as SDJCR 1616H 11. The average surface roughness (Ra) and maximum height values (Rz) were measured by a Mitutoyo SJ-301 surface roughness tester. Parameters relating to surface roughness measurement were: $l = 4$ *mm*, $\lambda c = 0.8$, $N = 5$. The measurements were repeated at twelve reference lines (Fig. 1.) and the values were averaged.

2.2 Experimental design

Response surface methodology (RSM) is a procedure able to determine a relationship between independent input process parameters (e.g. cutting parameters) and output data (process response, e.g. Rz, Ra). In the course of DOE, a response surface method was chosen, the central composite design (CCD) method. The CCD method was set up for three controllable factors: cutting speed *(v_c)*, feed rate *(f)* and depth of cut *(a)*. Each factor had 5 different levels. The number of experimental runs was 16, in which two trials were examined in the centre of the design (Table 1).

The limits of the studied cutting parameters are set to meet the values used by industries currently and the requirements of high speed cutting (HSC) applications

as well. Wiper tool geometry is known to produce the same roughness at twice as high or even higher feed as ISO geometry [14]. Therefore, to enable proper comparison of the surfaces machined with the different geometry tools, the feed of the Wiper tools are different from the feed of the ISO tools (Table 2 and Table 3). The minimum and maximum values of the cutting parameters used in the examination can be seen in Table 2 and Table 3.

2^3 central composite design			
Runs	v_c	f	a
1	-1	-1	-1
2	-1	-1	1
3	-1	1	-1
4	-1	1	1
5	1	-1	-1
6	1	-1	1
7	1	1	-1
8	1	1	1
9	-1.28719	0	0
10	1.28719	0	0
11	0	-1.28719	0
12	0	1.28719	0
13	0	0	-1.28719
14	0	0	1.28719
15 (C)	0	0	0
16 (C)	0	0	0

Table 1. Design of experiments with the levels of factors

v_{cmin} = 500 m/min	v_{cmax} = 2000 m/min
f_{min} = 0.05 mm	f_{max} = 0.12 mm
a_{min} = 0.2 mm	a_{max} = 0.8 mm

Table 2. The limits of used cutting parameters (ISO geometry)

v_{cmin} = 500 m/min	v_{cmax} = 2000 m/min
f_{min} = 0.10 mm	f_{max} = 0.24 mm
a_{min} = 0.2 mm	a_{max} = 0.8 mm

Table 3. The limits of used cutting parameters (Wiper geometry)

3. RESULTS AND STATISTICAL ANALYSIS

The experiments were performed with five types of tools and two types of workpiece materials in the range of the examined cutting parameters. The results are grouped according to these two types of tools.

3.1. The results of ISO geometry tools

The averages of the measured results belonging to each experimental setting can be seen in Fig. 3., for different materials and types of tool. The averages of the *Ra* and *Rz* parameters show that there is no clear difference between the workpiece materials. It can also be seen that the behaviours of the different tools are quite similar to each other.

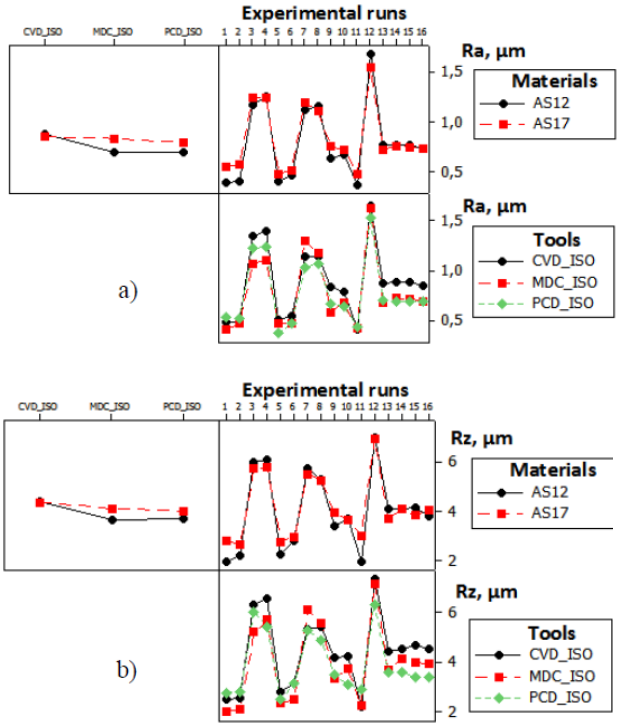

Fig. 3. The means of the *Ra* and *Rz* values in different experimental runs with ISO geometry; a) The means of the average surface roughness values regarding different workpiece materials and different tools; b) The means of the maximum height surface roughness values regarding different workpiece materials and different tools

The index number of the surface roughness measured on the cylinder (twelve times, every 30 degrees) may be the value of the coefficient of variation (*CV*), which is calculated as follows:

$$CV = \frac{s}{\bar{x}} \quad (1)$$

where is the mean and s is the standard deviation of the twelve repeated measurements in each case.

The *CV* values of each experimental run were shown with regard to *Ra* (Fig. 4.a) and *Rz* (Fig. 4.b). On the bar charts it can be seen that there is no difference between the tools in the deviation of the measured values. When the workpiece materials are compared, it is clear that the variations measured in the case of AS17 are much lower than in the case of AS12.

The differences of the *CV* values were examined with a nonparametric test (Wilcoxon Sign test). These values were produced by subtracting the *CV* values for the two types of workpiece materials in identical sets (delta $CV = CV_{AS12} - CV_{AS17}$).

Wilcoxon Estimated				
	N	Statistic	P	Median
delta CV_{Ra}	48	1123.0	0.000	9.345
delta CV_{Rz}	48	1103.0	0.000	6.518

Table 4. The results of the Wilcoxon Sign test for tools of ISO geometry

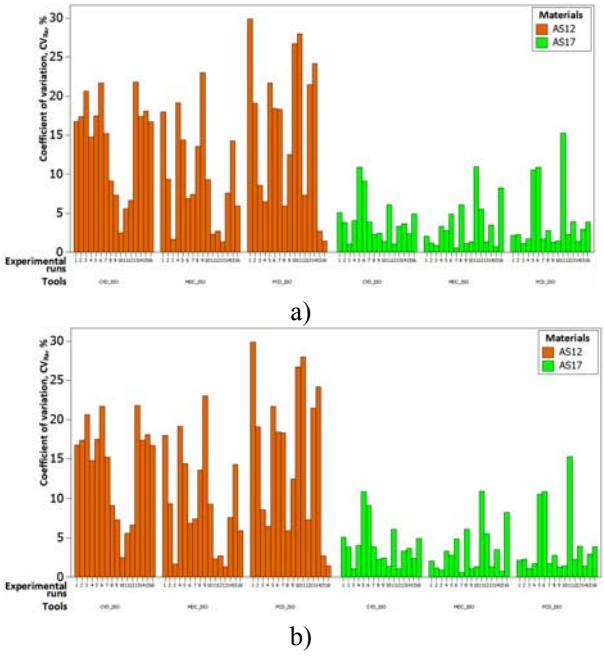

Fig. 4. Analysis of the coefficients of variation in the case of ISO geometry; a) *CV* values in the case of *Ra*; b) *CV* values in the case of *Rz*

Based on the test results (Table 4.) it can be stated that the surface roughness of AS17 has significantly lower deviations, than the surface roughness of AS12.

3.2. The results of the Wiper geometry tools

For Wiper tools the average values of the *Ra* and *Rz* parameters of each set can be seen in Fig. 5. When the experiments carried out with two types of Wiper geometry tools are compared, it is evident that in the case of both tools the mean values of surface roughness are lower when AS17 is cut.

For the measured values the nonparametric Mood median test was carried out. The results of the test show that the *Ra* values do not differ significantly for the two workpiece materials, although the *Rz* values are smaller when the workpiece material is AS12 (at 95% significancy level) (Table 5).

Chi-Square = 13.88 DF = 1 P = 0.000					
					Individual 95.0% CIs
Material	N<=	N>	Median	Q3-Q1	--------+---------+---------+--------
AS12	137	184	3.110	1.215	(---------*------)
AS17	196	147	2.790	0.770	(---*----)
					--------+---------+---------+--------
					2.85 3.00 3.15
Overall median = 2.870					
A 95.0% CI for median (AS12) – median (AS17): (0.150;0.430)					

Table 5. The Mood median test for Rz

The *CV* values of Wiper tools can be seen in Fig. 6. It is clear that the variations of surface roughness are significantly smaller in the case of AS17.

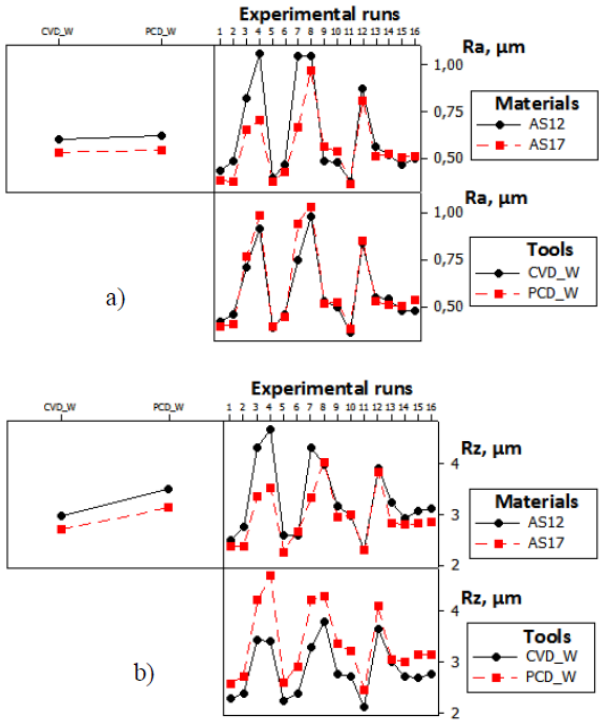

Fig. 5. The means of *Ra* and *Rz* values of different experimental runs in the case of Wiper geometry; a) The means of the average surface roughness values regarding different workpiece materials and different tools; b) The means of the maximum height surface roughness values in the case of different workpiece materials and different tools

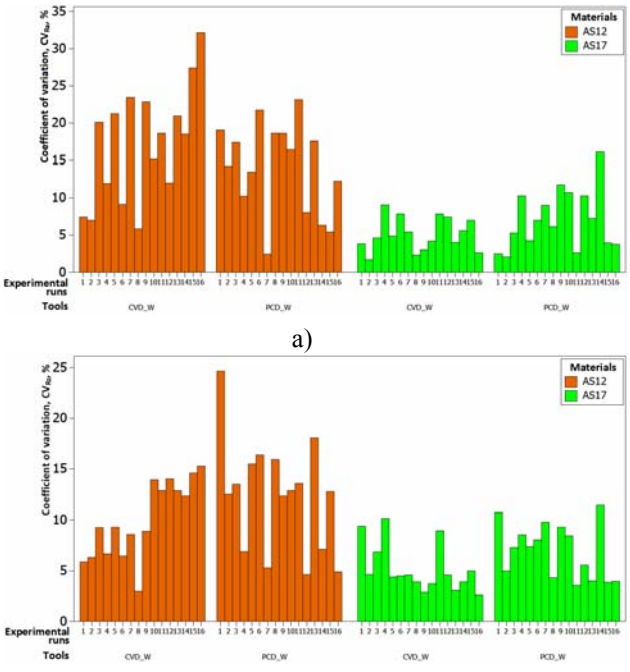

Fig. 6. Analysis of the coefficients of variation in the case of Wiper tools; *CV* values for *Ra*; b) *CV* values for *Rz*

The differences of *CV* values were analyzed with the non-parametric Wilcoxon Sign test (Table 6.).

Wilcoxon Estimated				
	N	Statistic	P	Median
delta CV_{Ra}	32	497.0	0.000	9.700
delta CV_{Rz}	32	472.0	0.000	5.217

Table 6. The results of the Wilcoxon Sign test for the tools of Wiper geometry

The results show that the variations within the surface (for *Ra* and *Rz*) for AS17 workpiece materials are significantly smaller than in the case of AS12.

4. CONCLUSION

In this article the machinability of two types of die-cast aluminium alloys were examined with different type and edge-material diamond tools. The results are as follows:

- the ISO geometry tools cut both workpiece materials in a similar way;
- the Wiper geometry tools produced significantly lower surface roughness when the workpiece material was AS17;
- even at double feed the Wiper geometry tools produced lower surface roughness values than the ISO geometry tools;
- statistical analysis showed that the surface of the workpiece material was more homogeneous in the case of AS17 than in the case of AS12.

In summary, it can be stated that the roughness-maintaining ability of the manufacturing system depends only on the workpiece material.

5. REFERENCES

[1] Drégelyi-Kiss, Á., Horváth, R., Mikó, B.: *Design of experiments (DOE) in investigation of cutting technologies*, Development in Machining Technology/Scientific-Research Reports, 3, p.p. 20-34, 2013

[2] Hamadi, A., Mohamed, A. Y., Kamel C., Tarek, M., Jean-François, R.: *Analysis of surface roughness and cutting force components in hard turning with CBN tool: Prediction model and cutting conditions optimization*, Measurement, 45, p.p. 344-353, 2012

[3] Noordin, M. Y., Kurniawan, D., Tang, Y. C., Muniswaran, K.: *Feasibility of mild hard turning of stainless steel using coated carbide tool*, Int J Adv Manuf Technol, 60, p.p. 853–863, 2012

[4] Asiltürk, I., Neseli, S.: *Multi response optimisation of CNC turning parameters via Taguchi method-based response surface analysis*, Measurement, 45, p.p. 785–794, 2012

[5] Hwang Y. K., Lee , C. M.: *Surface roughness and cutting force prediction in MQL and wet turning process of AISI 1045 using design of experiments*, Journal of Mechanical Science and Technology, 24, p.p. 1669-1677, 2010.

[6] Harničárová, M., Valíček, J., Kušnerová, M., Grznárik, R., Petrů, J., Čepová, L.: *A New Method for the Prediction of Laser Cut SurfaceTopography*, Measurement Science Review, 12, p.p. 195-204, 2012

[7] Lazarević, D., Madić, M., Janković, P., Lazarević, A.: *Surface roughness minimization of polyamide pa-6 turning by Taguchi method, Journal of Production Engineering*, 15, p.p. 29-32, 2011

[8] Maňková, I., Vrabel, M., Beňo, J., Kovac, P., Gostimirovic, M.: *Application of Taguchi method and surface response methodology to evaluate of mathematical models to chip deformation when drilling with coated and uncoated twist drills*, Manufacturing Technology, 13 (4), p.p. 492-499, 2013

[9] Pokorádi, L.: *Systems and Processes Modelling*, Campus Kiadó, Debrecen, p.p. 242, (in Hungarian), 2008

[10] Pokorádi, L.: *Uncertainties of Mathematical Modelling*, Proc. of the 12th Symposium of Mathematics and its Applications, Timisoara, Romania, 2009.11.05-2009.11.07. p.p. 471-476, 2009

[11] Horváth, R., Drégelyi-Kiss, Á.: *Analysis of surface roughness parameters in aluminium fine turning with diamond tool*, Measurement 2013 Conference,13 may 2013 p.p. 275-278, Smolenice, Slovakia.

[12] Horváth, R., Drégelyi-Kiss, Á., Mátyási, Gy.: *Application of RSM method for the examination of diamond tools*, Acta Polytechnica Hungarica, Acta Polytechnica, 11, p.p. 137-147, 2014

[13] Horváth R, Mátyási Gy, Drégelyi-Kiss Á: *Optimization of machining parameters for fine turning operations based on the response surface method*, ANZIAM Journal 55, p.p. C250-C265, 2014

[14] Grzesik, W., Wanat, T.: *Surface finish generated in hard turning of quenched alloy steel parts using conventional and wiper ceramic inserts*, International Journal of Machine Tools & Manufacture, 46, p.p. 1988–1995, 2006

Authors: **Richárd Horváth, assistant Professor**
Dr. Ágota Drégelyi-Kiss, PhD, **Associate Professor**
Óbuda University Donát Bánki Faculty of Mechanical and Safety Engineering Budapest, H-1081, 8 Népszínház Street, Hungary.
Dr. Gyula Mátyási, PhD, **Associate Professor**
Budapest University of Technology and Economics Budapest, H-1111 1 Egry József Street, Hungary
E-mail: horvath.richard@bgk.uni-obuda.hu
dregelyi.agota@bgk.uni-obuda.hu
matyasi@manuf.bme.hu

Journal of Production Engineering
Vol.17 No.2

Original Scientific Paper

Radiša, R., Manasijevic, S., Mandic, V., Stefanovic, M., Komadinic, V.

OPTIMIZATION GEOMETRY OF THE BODY PRESSES FOR THE FINE PUNCHING USING FEM ANALZSIS

Received: 25 August 2014 / Accepted: 25 September 2014

Abstract: *During the design process of vital structural components it is necessary to consider all engineering design aspects including the initial geometry, material selection, nominal loads, global and detailed stress-strain calculations. The objective of the present article is to outline the process of such multiparametric geometry optimization of a press for fine sheet-metal punching by using FEM analysis. An iterative process of the geometry optimization is illustrated on an example of the press exposed to high static loads under strict allowable deflection requirements. The initial press geometry is modified based on the obtained FEM simulation results. The static calculations are then performed repeatedly on the modified press models until the obtained stress and deflection values fell within the permissible limits. The press model adopted in the described process of iterative geometry modifications represents an input for the calculations under dynamic loads.y*
Key words: *optimization of geometry, press, stress, deflection*

Optimizacija geometrije tela prese za fino prosecanje primenom FEM analize. *Pri projektovanju vitalnih strukturalnih komponenti neophodno je razmatrati sve aspekte konstrukcije uključujući početno geometrijsko definisanje, izbor materijala, nominalna opterećenja, globalni i detaljni proračun naponsko-deformacionih stanja. U radu je ilustrovan iterativni proces optimizacije geometrije prese za fino prosecanje lima primenom FEM analize. Prikazan je postupak optimizacije na primeru prese izložene velikim statičkim opterćenjima u uslovima strogih zahteva u pogledu dozvoljenih vrednosti ugiba strukturnih komponenti. Nakon obavljenih proračuna na inicijalnom modelu prese izvršena je modifikacija njene geometrije. Potom su proračuni ponavljani na modifikovanim modelima prese sve dok nisu dobijene vrednosti napona i ugiba u dozvoljenim granicama. Na taj način usvojena, poboljašana geometrija tela prese predstavlja ulazni model za strukturni proračun pod dejstvom dinamičkog opterećenja.*
Ključne reči: *optimizacija geometrije, presa, naponi, ugibi*

1. INTRODUCTION

It has been estimated that 80% of the product price is already determined in the early phase of engineering design, which prompts companies to focus on finding ways to make quick design decisions regarding crucial issues of costs, quality and market demand. This is precisely the main goal of engineering design (hereinafter referred to as »design« for brevity): to develop and manufacture products that are optimized in terms of reliability and quality in the shortest possible time and with minimum cost [1]. In order to achieve this goal the ideal design process must function, as much as possible, in the virtual product development environment. The virtual product models are flexible and allow any number of iterations necessary to reach the optimal solution. The defined virtual model facilitates better visualization and understanding, which results in improvements of both product quality and development efficiency and consequently provides an optimal design solution without any need for avoidable costly and time-consuming redesigns [2].

The virtual product model prepared in a CAD (computer-aided design) package contains all necessary input data that fully describe geometry of all structural components including boundary conditions, as well as information about materials, needed for CAE (computer-aided engineering) analysis. The numerical simulation setup is based on in-depth understanding of the process physics and reliable experimental results used to predict the material flow and determine the distribution of material, stress, temperature, and strain on tools as well as the potential sources of defects and cracks (apptly called the »hot spots« in damage mechanics). The necessary inputs should also take into account properties and microstructure of the product, as well as the assessment of elastic correction and residual stresses. The most widely applied and the most powerful tool for numerical simulation in the CAE is the finite element method (FEM): a discrete analysis technique based on the physical discretization of the computational domain representing the analized structure[3]. In short, the observed continuum with an infinite number of degrees of freedom (DOF) is approximated by a discrete model of interconnected finite elements with finite number of DOF. There are many different types of elements, depending on their shape, linearity and order.

The selection of element types is influenced by various diverse factors including, but not limited to, the nature of the physical problem problem, model geometry, required accuracy, availability within the software[4].

2. SIMULATION TECHNIQUE

The body of the press for fine sheet metal punching (the press body, hereinafter) is the basic module of the sheet metal working unit. Fig. 1 shows a layout of the press body with hydraulic power unit and static and movable parts, which constitute the initial model. Given the complexity of the punch tool geometry and the high tool production price, this type of metalworking is used in large-scale production of parts made of sheet metal.

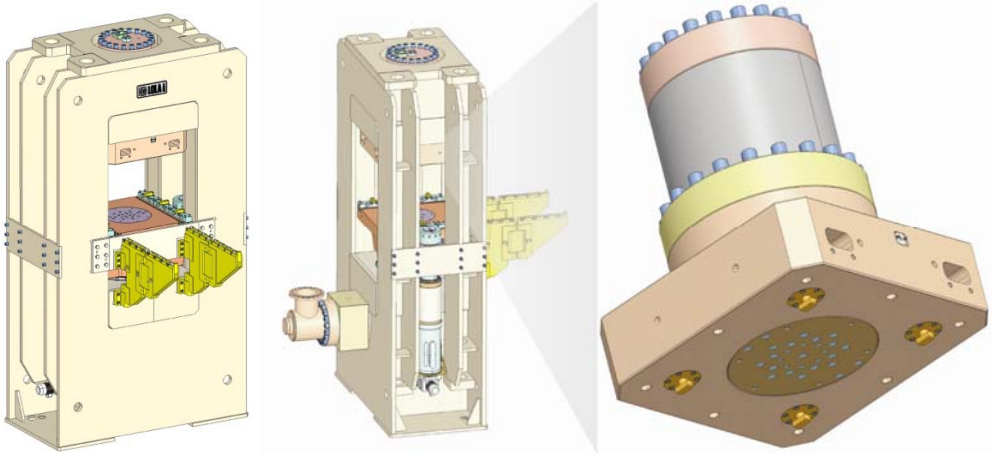

Fig. 1. Three-dimensional (3D) model of the press body

2.1 Initial conditions and constraints of FEM analysis

The computational model of the press body is developed based on the following inputs and assumptions:

- Technical drawing of the initial (draft) version of the press body;
- Mechanical properties of the selected press component materials;
- Load case simulating a static (time invariant) pressure on the appropriate areas of the top and bottom press plates;
- Structure discretization performed by using the 3D quadratic finite elements (number varies between 80 000 and 100 000 elements.)
- Boundary conditions that simulate the press base as rigidly connected to a concrete block that "floats" on an air bag.

2.2 FEM analysis

The main objective of the computation is to determine the deformation and stress fields of the press body resulting from the gravity load and the set of static forces proposed and evaluated by designers. This set of static force values mimics the load transferred from the tool to the press support structure in the course of the press operation [5].

The initial design of the support structure press (called hereinafter the **initial model**) is the first numerical model discretisized by finite elements and supplied with the boundary conditions to simulate the operating conditions. Based on the simulation results obtained by using this model, a series of geometry modifications are gradually introduced accompanied necessarily by their respective FEA calculations. This iterative analytical effort (over ten simulations) resulted eventually in the improved geometry of the press support structure called the **improved model** throughout this article.

The obtained version of the press body model characterized by the static stability is necessary to analyze under the real working conditions—that is, the dynamical loading—before the recommendation for the optimal version of the press body structure is given. The corresponding FEA computation is performed by using the I-DEAS Master Series 12NX software package[6].

1.3 Initial and improved models of the press body and their discretization

As explained before, the initial press body model (Fig. 2a) is used as the starting point for a series of FEM simulations and resulting sequance of successive geometry modifications. This iterative process of gradual geometrical improvements leads finally to the improved model characterized by a strengthened structure of the decreased overall height (Fig. 2b). The strengthening of the improved model is achieved by increase of the widths of the supporting frame and of the horizontal plate placed on the top of the press body[7].

The model coordinate system is positioned in such a way that the *x*-axis is horizontal and oriented to the right, the *y*-axis is vertical and oriented upwards, and the *z*-axis is oriented toward the observer (Fig. 2a).
Fig. 2b illustrates the 3D geometry model of the existing improved version of the press body. The structural analysis culminated in the upgraded version of the improved press body model preloaded with four M140 bolts (150 mm in diameter) and the preloading force of 1500 kN per bolt (Fig. 2b).

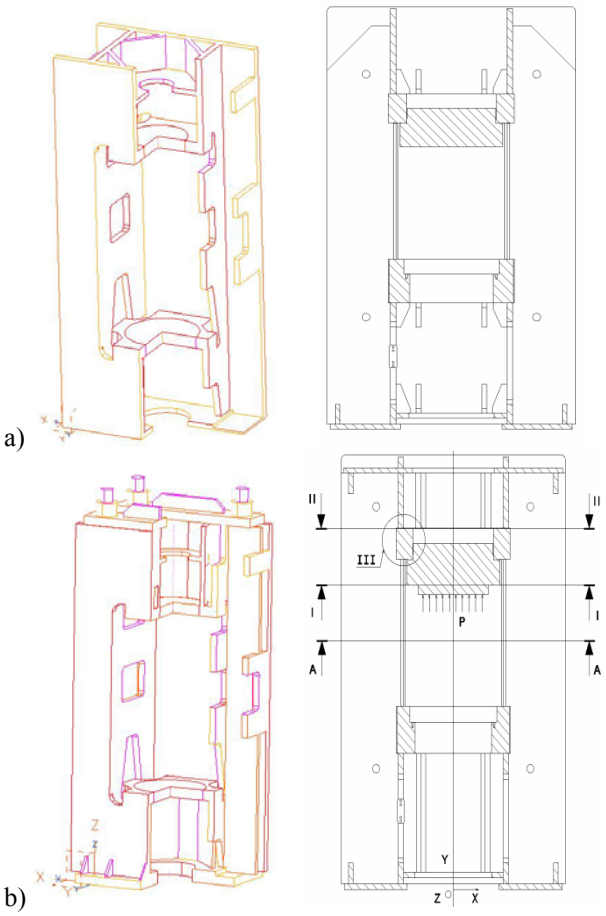

Fig. 2. The press body: a) initial model, b) improved model

The deformation and stress fields of the press body are obtained for the boundary conditions which simulate the its footing rigidly fixed to the concrete block "floating" on an air bag. Note that the influence of the concrete block and the air bag is disregarded. In other words, the problem of boundary conditions is solved by disabling displacement on the bottom surface of the press body footing in all directions [8,9].

The static FEA simulation is performed for the worst-case load scenario by simulating the pressure on the appropriate surfaces of the top clamping plate and the bottom plate of the press body. The simulation is performed for the static force of 6300 kN resulting from the punching tool, that is, it from the movement of the top and bottom movable parts of the press body [10].

The centered load is applied on both the initial and the improved model, while the eccentric load on the later only. These load cases represent the static-force variants of the load encountered under regular operating conditions, and encompass two extreme cases of eccentric load that can occur during operation [11,12]. The load consists of the weight of the press body itself and the static force, which has three variants:

- centered load: F=6300 kN (Figure 3a),
- eccentric load shifted along the x-axis by 235 mm: where the force F_1=4800 kN is centered, and the force F_2=1500 kN is exerted eccentrically (Fig. 3b),
- eccentric load shifted along the z-axis by 150 mm; where the force F_1=4800 kN is exerted centrally, and the force F_2=1500 kN is exerted eccentrically (Fig. 3c).

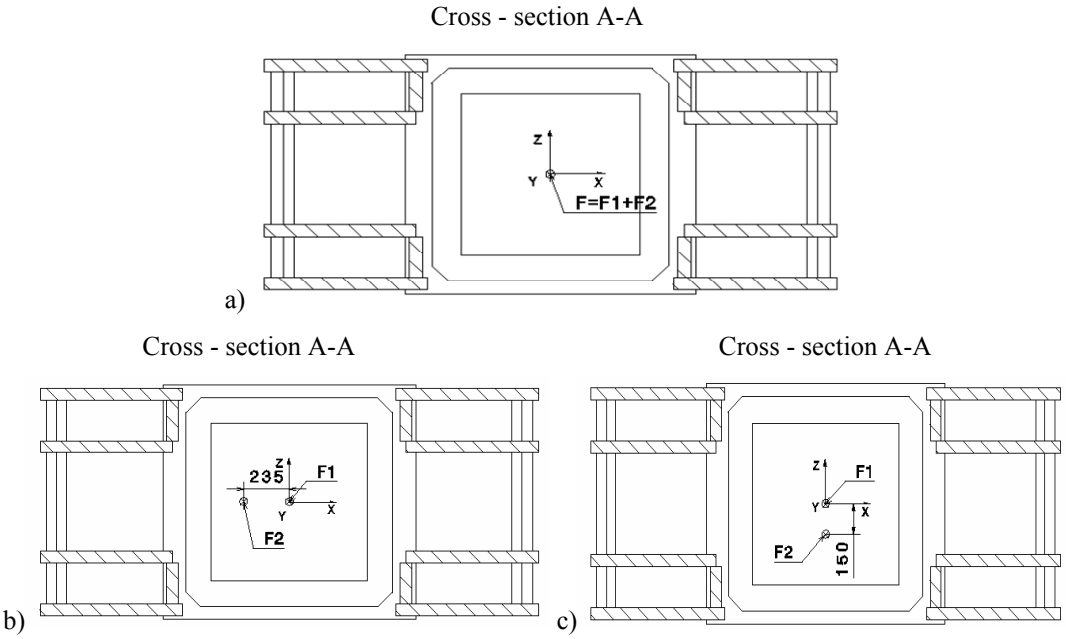

Fig. 3. Loads: a) Centered, b) Eccentric shifted along the x-axis and c) Eccentric shifted along the z-axis

3. RESULTS AND DISCUSSION

3.1. Simulation results for the initial model

The deformation field of the entire press body is presented in Fig. 4a. The maximum value of deformation (depicted by red color) is 1.56 mm on the upper plate. The lower part of the model exposed to the

static load behaves in stable manner with less pronounced deformation (up to 0.863 mm – the yellow-green areas). The top part of the structure exhibits a much more significant distortion by opening toward the top. The ends of the outer plates bend outwards, while the two transversal ribs bend considerably along the *z*-axis. When the overall deformation is decomposed into displacements along three coordinate axes, it can be observed again that the displacement along the *y*-axis is small for the bottom plate of the press body (−0.144 mm), but considerable on the top plate (0.328 mm). This deformation is along the load direction and is therefore expected. However, a considerable displacement along the *x* and *z*-axis is also noticeable (in excess of 0.320 mm at the top part of the structure).

Von Mises equivalent stress has a uniform distribution in the press body, with a value up to 80 N mm^{-2} (Fig. 4b). The maximum stress value (500 N mm^{-2}) appears locally at the points of connection of the upper/bottom plates with the press body (vertical walls). σ_{xx} and σ_{zz} values are 80 N mm^{-2} in contrast to σ_{yy} which reaches 156 N mm^{-2}.

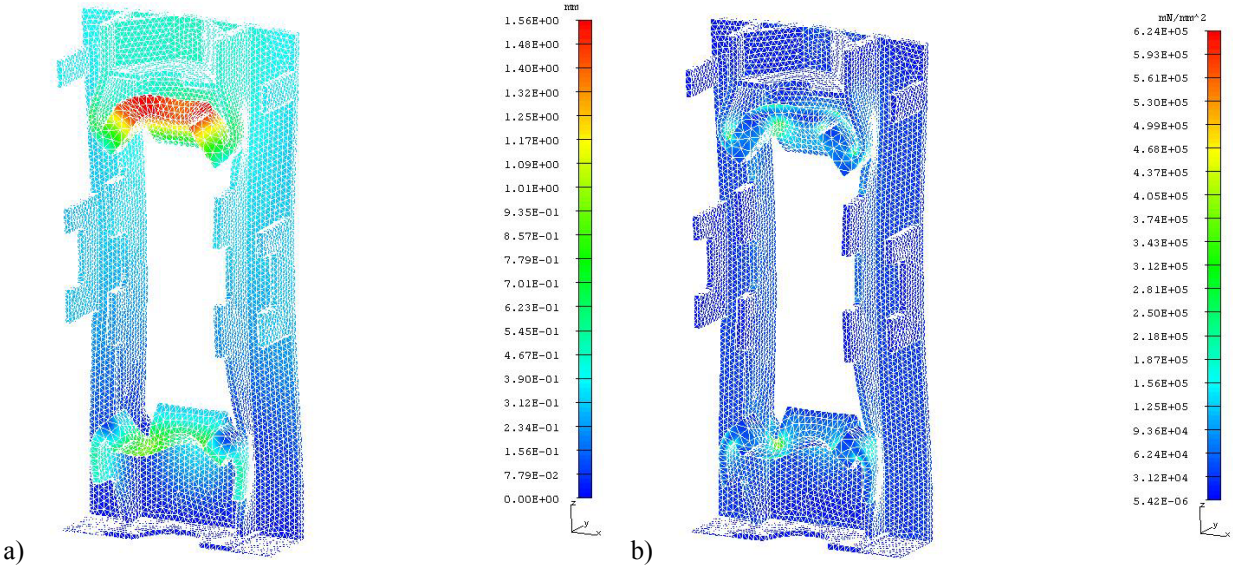

a) b)

Fig. 4. Initial model: a) deformation field, b) von Mises stress field

3.2. Simulation resulats for the improved model

An FEA computation is performed on the press working plate as a separate part to verifying the computation results of the press body. Fig. 5 illustrates a 3D geometry model of the working plate, which is statically loaded with the same force used previously to mimics the the operational load of the press (6300kN). The boundary limitations are defined at the connection points of the working plate and of the body presses.

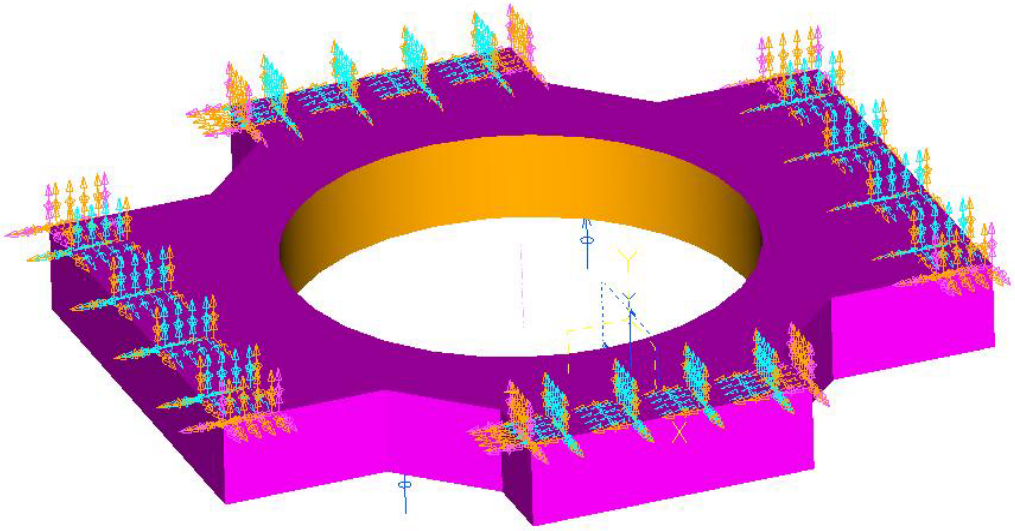

Fig. 5. 3D geometry model of the press body working plate

The maximum deformation of the working plate (depicted with red color in Fig. 6a) is 0.5 mm. This deformation of the working plate affects the total press-body deformation by superposing it with the deformation of the press body wall at their mutual connection points. Von Mises stress distribution (Fig. 6b) in the working plate is of the same maximum value and spatial distribution as in the case when the working plate is an integral part of the initial press model.

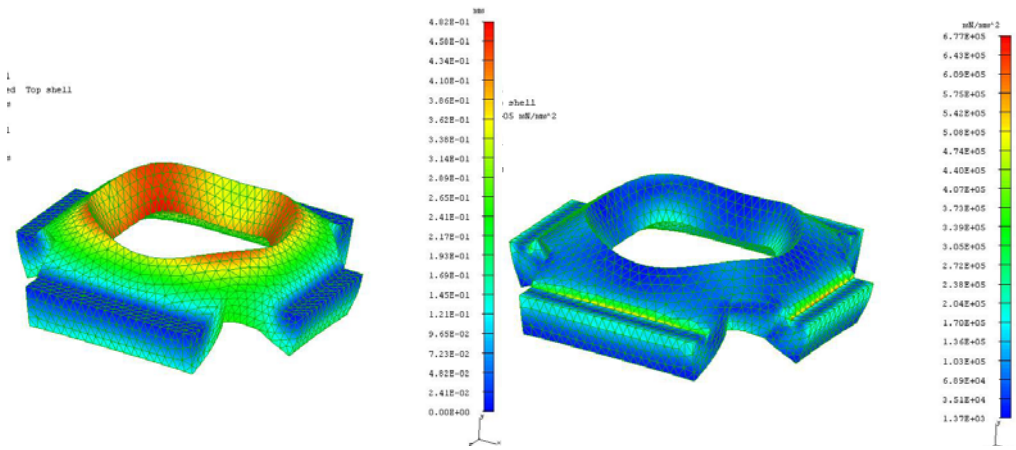

Fig. 6. Press working plate: a) deformation fiels, b) von Mises stress field

Fig. 6a shows that the structural deformation at the connction points of the press wall and the upper working plate is 0.8 mm. Therefore, the press wall deformation superposed on the deformation of the working plate results in total deformation of 1.5 mm of the initial model at the point of the upper working plate.

The accuracy of the analysis is confirmed by the deformation value computed for the plane corresponding to the upper surface of the lower working plate as shown in Fig. 6b. The structure deformation is 0.3 mm at the connection points of the press wall and the lower working plate. By superposing this deformation on that of the working plate as a separate part a total deformation of 0.8 mm of the initial model at the point of lower working plate is obtained.

The von Mises stress distribution at the lower surface of the upper working plate (Fig. 8.) reveals a stress increase at the point of connection of the working plate and the press wall.

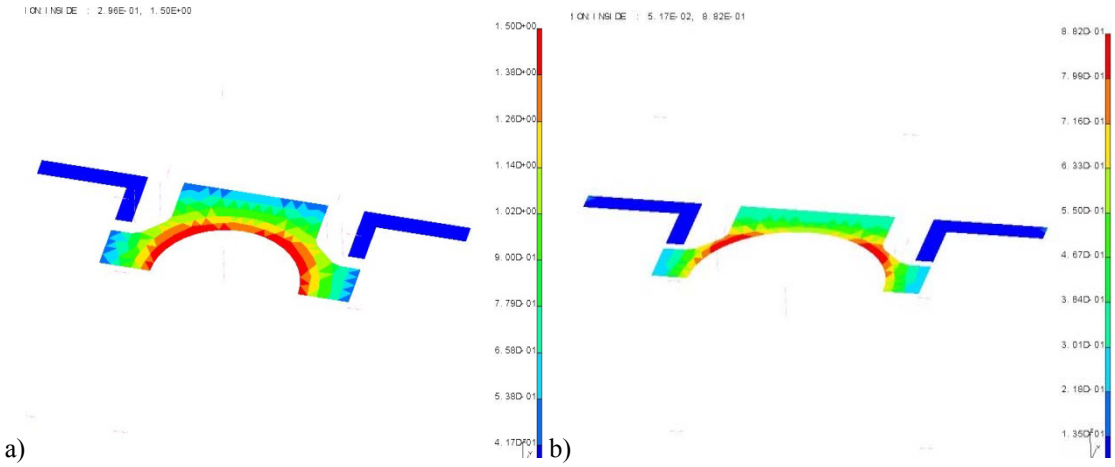

a) b)

Fig. 7. Deformation distribution in the plane corresponds to: a) the lower surface of the upper working plate, b) the upper surface of the lower working plate

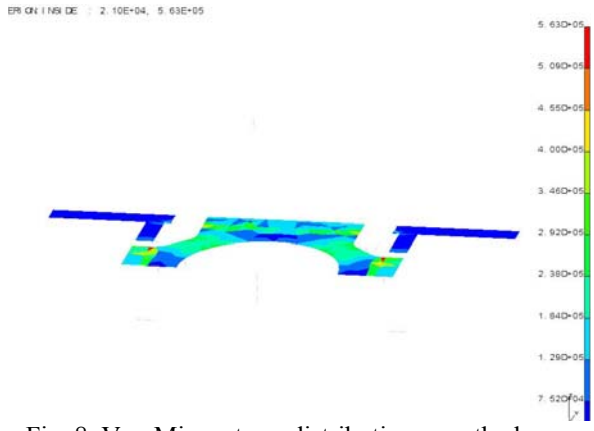

Fig. 8. Von Mises stress distribution over the lower surface of the upper working plate

3.3. Deformation and stress of the improved press model

The deformation distribution of the improved press model (Fig. 9a) reaches a maximum value of 0.51 mm on the upper plate. The Fig. 9a illustrates a steadier behavior of the whole model of the press body compared to the corresponding deformation of the initial model (1.5 mm). The von Mises stress distribution in the upgraded model (Fig. 9b) is uniform and the value is up to 30 N mm^{-2}. The stress increase at the point of connection of the lower plate to the press body reaches 260 N mm^{-2}.

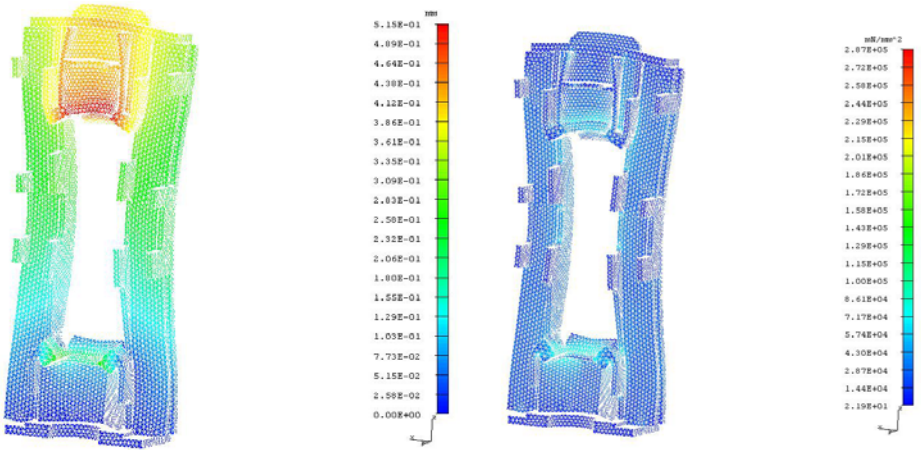

Fig. 9. Upgraded model: a) deformation distribution, b) von Mises stress distribution

The press body models defined so far do not capture realisticaly the actual stress and deformation fields since the press body is given without clamping plates for tools and other structural elements that affect rigidity of the press. When the clamping plates and additional bracings are oncluded into the FEA model, a completely different stress and deformation distributions are obtaines as illustrated henceforth.

3.4. Deformation and stress for the improved press model with additional bolts for preloading

The maximum deformation of the upgraded press body model with additional bolts for preloading (Fig. 10a) reaches 0.27 mm at the lower clamping plate. This implies that the use of bolts for preloading reduces the deformation of the press wall, which leads to a lower total value of deformation.

Von Mises stress distribution in the upgraded model with additional preloading bolts (Fig. 10b) is relatively uniform with a very low value of up to 30 N mm^{-2}. A localized stress increase, limited to just a few finite elements, at the point of recline of the upper plate on the upper press body reaches 180 N mm^{-2}.

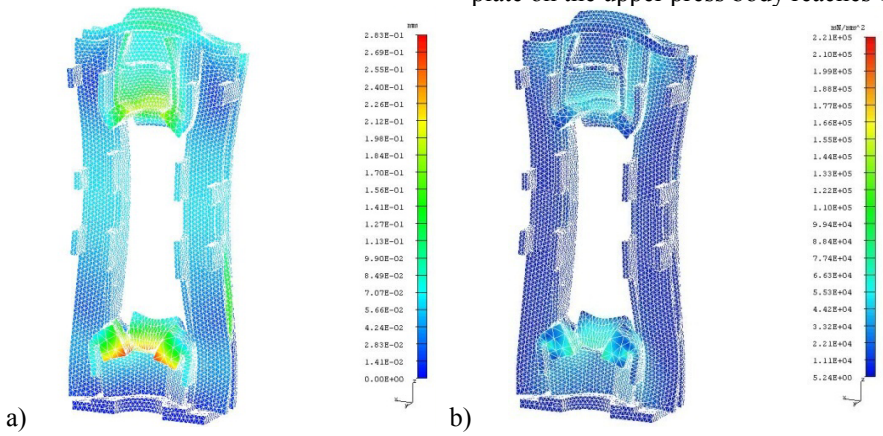

a) b)

Fig. 10. The upgraded model with additional preloading bolts: a) deformation distribution and b) von Mises stress distribution

Fig. 10 shows that the deformations in the x and z directions are 0.116 mm and 0.109 mm, respectively, while it reaches 0.306 mm along the y-axis. This means that the improved model deformations in the x and z directions decreased threefold in comparison with the respective initial model displacements.

Von Mises stress distribution in the improved model (Fig.10b) is uniform with relatively low maximum value, 33.5 N mm^{-2}. A stress increase appears at the point of recline of the top clamping plate on the top plate and reaches 168 N mm^{-2}. σ_{xx} and σ_{zz} maximum values are below 95 N mm^{-2}, while in σ_{yy} maximum value reaches 177 N mm^{-2}.

3.5. Characteristic values of displacement and stress

Fig. 11 illustrates the points on the top plate and on the top clamping plate of the press body at which the values of deflection and stress are evaluated. The cross-section I-I shows the disposition of evaluation points on the top clamping plate (the horizontal surface on the bottom side), from point 1 to point 4 (Fig. 11a). The cross-section II-II shows the disposition of evaluation points on the top plate of the press body (the horizontal plate on the top side), from point 1 to point 4 (Fig.11b).

Planarity of the loaded surfaces of the clamping plate is 0.025 mm, 0.110 mm, and 0.100 mm in the cases of the centered load, the eccentric load along the x-axis, and the eccentric load along the z-axis, respectively.

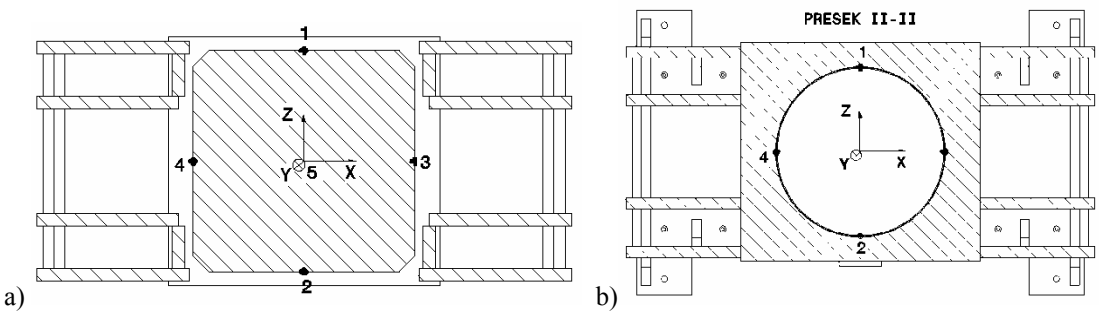

a) Cross - section I-I b) Cross - section II-II

Fig. 11. The evaluation points disposition on: a) the top clamping plate and b) the top plate.

4. CONCLUSION

The static FEA simulations performed in the present article enable an insight into the deformation and stress distributions of the initial press model and emphasized the need for necessary changes in geometry. These structural modifications that have been made in the initial model resulted in the improved model, which have proved to be statically more stable. These geometry modifications also proved to be beneficial from the standpoint of the press overall mass which decreased 450 kg.

In order to interpret properly the stress and deformation values in the postprocessing phase of the FEM analysis, it is necessary to focus on certain press parts. The simulation results indicate that the maximum stress values in the two models are not significantly different (81 N mm^{-2} and 90.3 N mm^{-2}). It is important emphasized, thought, that these stress values, for both the centered and the eccentric loads, are well below the distortion limit of the selected steel, which is 248 N mm^{-2}. Although the simulation results on the upgraded model with additional clamping plates indicate, the stress criterion (σ=0.5 σ_{02}) is not satisfied for the corresponding sheet metal Č.0361. The deformation criteria for the press body are satisfied.

Finally, it cannot be overstated that in order to accept the improved model conceptual design, it is necessary perform an adequate dynamic FEA simulation with realistic loads and perform an analysis of obtained solutions.

5. ACKNOWLWDGEMENTS

The results presented in this paper originated partially from Research Project TR funded by the Ministry of Education and Science of the Republic of Serbia.

6. REFERENCES

[1] Jedrzejewski, J., Kwasny, W. (2001). XII *Workshop, on Supervising and Diagnostic of Machining Systems*, Wroclaw University of Technology.

[2] Mandic V. (2012). *Physical and numerical modeling of metal forming processes.* Faculty of Engineering, University of Kragujevac, Kragujevac, Serbia.

[3] Weck, M., Hessel, C. (2002), *Flächenrückführung topologieoptimierter FE-Modelle*, WT Werkstattstechnik online 92 H. 7/8, Springer-VDI-Verlag, Düsseldorf, pp. 377-381.

[4] Kojic M., Slavkovic R., Živkovic M., Grujovic N. (2010). *Finite element method*. Faculty of Engineering, University of Kragujevac, Kragujevac, Serbia.

[5] Cook, R., Malkus, D., Plesha, M. (1988). *Concepts and Applications of Finite Element Analysis*, 3 Edition, John Wiley, Madison.

[6] Altintas Y., Brecher., Weck M., Witt S. (2005). Virtual machine tool, *CIRP Annals - Manufacturing Technology*, Volume 54, Issue 2, pp. 115–138.

[7] Bern M., Plassmann P. (2000). *Mesh generation*. Handbook of computational geometry, Elsevier Science, Amsterdam, pp. 291–332.

[8] Herz E., Hertel O., Vormwald M. (2011). Numerical simulation of plasticity induced fatigue crack opening and closure for autofrettaged intersecting holes. *Engineering Fracture Mechanics*, vol. 78, pp. 559–572.

[9] Döring R., Hoffmeyer J., Seeger T., Vormwald M. (2003). A plasticity model for calculating stress–strain sequences under multiaxial nonproportional cyclic loading. *Computational Materials Science,* vol. 28, no. 3–4 pp. 587–596.

[10] Dowling N., (2003). *Local strain approach to fatigue, comprehensive structural integrity*. Elsevier, vol 4, pp. 77–94.

[11] Sauve R.G., Morandin G.D. (2004). Simulation of contact in finite deformation problems–algorithm and modeling issues. *International Journal of Mechanics and Materials in Design*, vol. 1, pp. 287–316.

[12] Belytschko T. (1986). Hughes T.J.R., (eds.) *Computational Methods in Mechanics*, Vol. 1. North-Holland Elsevier Science.

Authors: **M.Sc. Radomir Radisa, Dr. Srecko Manasijevic, M.Sc. Velimir Komadinic,** Lola Institute, Belgrade, Serbia, www.li.rs, **Prof. Dr. Vesna Mandic, Prof. Dr. Milentije Stefanovic,** Faculty of Engineering, University of Kragujevac, Kragujevac, Serbia, www.mfkg.rs.
E-mail: radomir.radisa@li.rs,
srecko.manasijevic@li.rs

Journal of Production Engineering
Vol.17 No.2

Original Scientific Paper

M. Prakash Babu, Balla Srinivasa Prasad

PREDICTION OF VIBRATION INDUCED DISPLACEMENT AND ITS EFFECT ON TOOL WEAR IN TURNING USING 3D FINITE ELEMENT SIMULATION

Received: 11 September 2014 / Accepted: 12 October 2014

Abstract: *This paper presents the three dimensional (3D) finite element analysis to predict the workpiece displacement amplitude and tool wear in face turning of AISI 1040 steel under dry machining condition. 3D vibration induced turning models have been developed and validated by comparing with experimental results so as to identify the correlation. Extensive experimentation and investigators carried out on CNC lathe machine and the details are reported in [1] have been considered for present work. Commercial FE programme is used for simulating turning process. The effect of workpiece displacement due to vibration on the tool wear is critically evaluated.*

Key words: *Vibration amplitude, 3D finite element simulation, tool wear, face turning.*

Predviđanje vibracijama uzrokovanog pomeranja i njegov efekat na habanje alata kod struganja pomoću 3D simulacije konačnim elementima. *U ovom radu je predstavljena trodimenzionalna (3D) analiza konačnim elementima radi predviđanja amplitude pomeranja i habanje alata kod poprečnog struganja AISI 1040 čelika pod uslovima suve obrade. 3D vibracije su uvedene u razvijeni model rezanja i izvršena je provera upoređivanjem sa eksperimentalnim rezultatima zarad dobijanja zavisnosti. Realizovana obimna eksperimentalna istraživanja, vršena na CNC strugu, predstavljena u [1] su uzeti kao osnova ovog rada. Komercijalni program konačnih elemenata je korišćen za simulaciju procesa struganja. Efekat vibracija obratka na habanje alata je kritički vrednovano.*

Ključne reči: *Amplituda vibracija, 3D simulacija konačnim elementima, habanje alata, čeono rezanje*

1. INTRODUCTION

In metal cutting as a result of the cutting motion, cutting tool wear will be influenced by cutting parameters, cutting force, and vibrations, etc. But the effects of vibrations have been paid less attention. The dynamic phenomena of cutting tool induced by the interaction of elastic system in the cutting process causes the relative displacement between tool and work piece, which generates the vibration during machining [2]. Vibrations in the turning process can be a good way to monitor online growth of the tool wear in turning and, therefore, it can be useful for establishing the end of tool life in these operations [3]. This is very important when the goal is to monitor the cutting process in real time and to establish automatically the end of tool life [4]. Therefore, it is necessary to study on effect of cutting tool vibrations during the machining. Therefore, it is necessary to study on effect of cutting tool vibrations during the machining [5]. In modern machining processes [6] due to continuous demand for higher productivity and product quality asks for better understanding and control of the machining process. A better understanding can be achieved through finite element modelling and simulations of machining process. Thus, in recent years, finite element method has particularly become the main tool for simulating metal cutting processes. Predictions of the physical parameters such as displacement amplitude, tool wear, cutting forces, tool chip interface temperature and stress distributions accurately play a pivotal role for predictive process engineering of machining processes. Simulations of various machining operations using the finite element method have been reported over the last three decades; in Reference [7] a collection of such papers can be found. Vytautas Ostasevicius et al. [8] developed a finite element model of the vibration milling tool and verified experimentally. Rimkeviciene J et al. [9] reported a combined numerical experimental approach for the reduction of surface roughness based on exciting higher-order transverse modes in the vibration turning tool. Tuğrul Özel et al. [10] proposed a FEM model and simulation strategy for orthogonal cutting of AISI 1045 steel is by using dynamics explicit Arbirary Lagrangian Eulerian method in simulating plastic flow around the round edge of the cutting tool and eliminates the need for chip separation criteria. W. Grzesik [11] created a FEM simulation model in order to obtain numerical solutions of the cutting forces, specific cutting energy and adequate temperatures occurring at different points through the chip/tool contact region and the coating/substrate boundary for a range of coated tool and uncoated tool materials and defined cutting conditions. A. G. Mamalis et al. [12] results reported simulation of high speed hard turning when using the finite element method for both orthogonal and oblique cutting models. Yung-Chang Yen et al. [13] developed a methodology to predict the tool wear evolution and tool life in orthogonal cutting using FEM simulations. D. Umbrello et al. [14] deals with the 3D FE simulation of cutting processes in order to estimate tool wear development during turning operations and proposed a new subroutine for tool wear

calculation and tool mesh and geometry updating is has been proposed in a commercial 3D code. Maňková et al. [15] identified the influence of cutting parameters in hard turning of hardened steel with hardness of HRC 55 with mixed oxide ceramic inserts. Zhang Wei et al. [16] presented the construction of a 3-D finite element simulation of turning process with an updated Lagrangian method. From literature, it is understood that most of the research work is limited to experimental results. But numerical modelling of turning process can provide a useful data for better understanding of the process. Limited literature available on this topic and this is mainly focused on 2D problems while 3D models are rather rare in the relevant literature. A considerable amount of research has focused on 2D finite element simulations for turning, but studies on 3D finite element simulations (FES) for turning process are not widely available. Major drawback of a cutting simulation is that it does not provide direct information on the increase of tool wear, as opposed to the experimental approach. Nevertheless, it is expected that the tool wear growth (crater and flank wear) is dependent on the relative displacement amplitude due to vibration, cutting temperature, contact stresses, and sliding velocity produced during cutting. In order to overcome the above mentioned limitations and to improve the performance of finite element simulations 3D FE models can be effectively used to simulate actual machining processes. Thus, an extensive investigation on the effect of displacement amplitude of workpiece due to vibration on tool wear in face turning processes is important to realize an accurate finite element simulation (FES) method for the vibration induced machining (VIM).

2. PROPOSED METHODOLOGY IN PRESENT STUDY

In the present work, tool – chip and tool – work piece interfaces is strongly influenced by the displacement amplitude due to vibration, tool wear, cutting temperature and relative sliding velocity at the interface. Therefore, understanding of the tool wear behavior and the capability of predicting it is the key to successful process control and optimization. To achieve this goal, the effect of different cutting variables and process mechanics has been investigated using finite element method (FEM). Overview of proposed methodology in present study is presented in figure 1.
Hence ultimate objective of the present study is to develop a 3D finite element simulation based methodology to predict the evolution of displacement amplitude and tool wear in vibration induced face turning. Implementation of machining model(s) in the commercial FEM code (DEFORM®-3Dv6.1) that relates the displacement amplitude and tool wear during machining to the predicted process variables. This approach consists of development of tool wear model for the specified tool–work piece pair via a calibration set of tool wear cutting tests in conjunction with FE cutting simulations. Second part includes the validation FS simulation results with experimental results considered in the literature. Turning operation is a steady-state process when continuous chip is formed. The implementation of tool wear estimation is relatively easier and studied first. A tool wear estimation models have been developed for turning operation as part of the work.

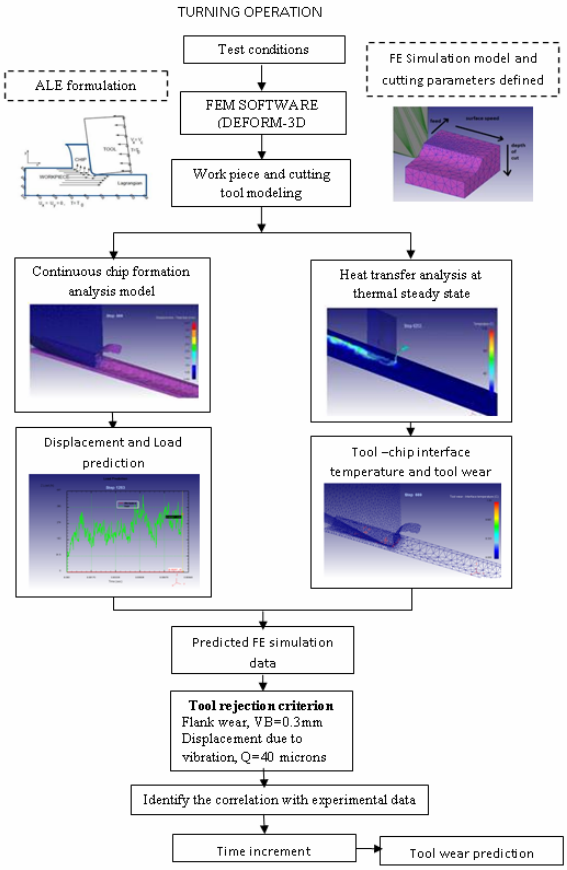

Fig. 1. Overview of proposed research work

Present study is planned to carry out in following stages, first stage concentrates on chip formation analysis in which a new chip formation modeling method for continuous steady state chip formation is developed. It can simulate the entire chip formation process from initial chip formation, chip growth to steady state by making use of Arbitrary Lagrangian Eulerian technique. Second stage concentrates on tool chip interface temperature analysis. In order to save the calculation time and the temperature distribution in the cutting tool at thermal steady state is studied by performing pure heat transfer analysis. Present analysis is confined to only to study the temperature distributes in the cutting tool. Last stage involves in modeling the displacement amplitude and its corresponding predicted load. Through previous stages, the present commercial FE code also predicts the tool wear along with normal stress, sliding velocity and tool temperature at steady state according to the test conditions.

3. THREE DIMENSIONAL (3D) FINITE ELEMENT METHOD SIMULATION OF TURNING PROCESS

The 3D model, implemented in DEFORM 3D v6.1, is reported in figure 2 where it is possible to see the work

piece with the growing chip and the tool. The tool, a rigid object meshed with more than 1, 00,000 elements, is oriented according to the cutting angles set in experimental test and reported in table 2 and it moves along the feed direction. Work piece considered as a rigid-plastic object meshed with more than 30,000 elements, is fully constrained on the lower and lateral sides so it cannot move. On the same faces thermal boundary conditions are set so to simulate the heat diffusion. The thermal exchange between tool and chip is regulated by heat diffusion relationship whose characteristic parameters are reported in table 1. The friction is modeled considering a shear factor equal to 0.82. An adaptive re-meshing scheme is implemented to optimize between the computational time and accurate prediction. The top and back surfaces of the tool are fixed in all directions. The workpiece is constrained in vertical (Z) and lateral (Y) directions on the bottom surface and moves at the cutting speed in the horizontal direction (X) toward the stationary tool. Tool wear estimation models for turning mainly composed of chip formation analysis, heat transfer analysis, wear calculation procedure and tool geometry updating, as shown in figure 2.

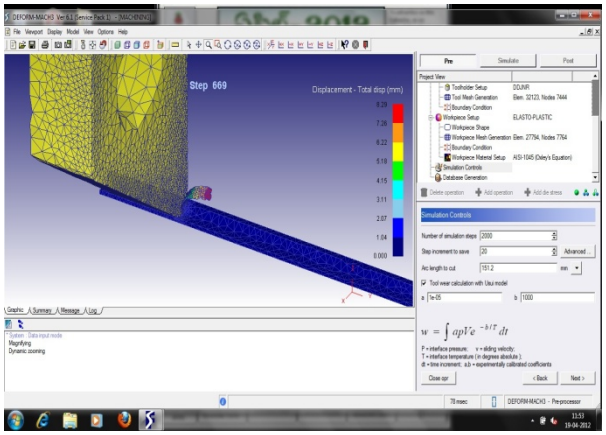

Fig. 2. FE modelling of displacement amplitude due to vibration in turning

In this work, a commercial software code, DEFORM 3D and explicit dynamic ALE modeling approach is used to conduct the FEM simulation of oblique cutting process. The chip formation is simulated via adaptive meshing and plastic flow of work material. Therefore, there is no chip separation criterion is needed. In this approach, the elements are attached to the material and the un-deformed tool is advanced towards the work piece. The programme menus are designed in such a way that they allow the user to minimize the model preparation time.

The thermo-mechanical FEM simulation schemes (models) are created by including tool and work piece thermal and mechanical properties, boundary conditions, contact conditions between tool and work piece as shown in figure 2 and as per the conditions given in table 1. As discussed in literature, this research is aimed to the 3D numerical prediction of tool wear using the knowledge acquired in 2D studies. Thus, in order to validate 3D predictions for both flank wear and displacement amplitude due to vibration, experimental details are reported in [1] have been considered for the present research work. Tool rejection criterion developed based on both ISO 3685 and ISO 10816 standards for evaluate the cutting tool condition in turning.

3.1. Material flow properties

According to a comparative analysis described by [16], Johnson- Cook model is one of the most convenient material models which also produce excellent results describing the material behaviour and chip formation. In this work, the Johnson- Cook constitutive model was used to predict the post-yield behaviour of AISI 1040 steel is given by equation 1 is used.

$$\bar{\sigma} = \left(A + B\bar{\varepsilon}^{n} \left[1 + C \ln\left(\frac{\dot{\bar{\varepsilon}}}{\dot{\bar{\varepsilon}}_0} \right) \right] \left[1 - \left(\frac{\theta - \theta_{room}}{\theta_{malt} - \theta_{room}} \right)^{m} \right] \right) \quad (1)$$

where $\dot{\bar{\varepsilon}}$ is plastic strain rate, ε is equivalent plastic strain, $\dot{\bar{\varepsilon}}_0$ is reference strain rate, A is initial yield stress, B is hardening modulus, C is strain rate dependency coefficient, n is work hardening exponent, m is thermal softening coefficient, θ is the process temperature, θ_{malt} is the melting temperature of the workpiece and θ_{room} is the ambient temperature (35^0C).

Oblique cutting parameters: Rake angle (°): -5, Clearance angle (°) :5, Flank face length (mm) : 0.75, Rake face length (mm) :1		
Cutting speed (N rpm)	Feed rate (mm rev)	Depth of cut (mm)
538	0.08 0.4 0.8	0.5 0.8 1.5
836	0.08 0.4 0.8	0.5 0.8 1.5
1135	0.08 0.4 0.8	0.5 0.8 1.5
Work piece material AISI 1040 steel of size (O 80 x 150mm)	Carbide Tool Properties: DNMA 432 (uncoated, WC as base material), Tool holder: DDJNR	
Coefficient of thermal expansion (µm m°C) 11 (at 20°C)	Coefficient of thermal expansion 4.7 (at 20 °C) (µm m°C) 4.9 (at 1000 °C)	
Density (g/cm³) 7.8	Density (g cm³) 15	
Poisson's ratio 0.3	Poisson's Ratio 0.2	
Specific heat (J kg °C) 432.6	Specific heat (J kg °C) 203	
Thermal conductivity (W m°C) 47.7	Thermal conductivity (W m°C) 46	
Young's modulus (GPa) 200	Young's Modulus (GPa) 800	

Table 1 Test conditions for experimental investigation

4. RESULTS AND DISCUSSIONS

As part of the present research work, finite element simulations have been carried out for 27 cases of experiments consisting of 3 different feed rates, cutting speeds and depth of cuts. Table 2 presents results of both experimental and predicted FE simulation values at different test cutting conditions under which simulations are carried out. FE predicted results are verified with experiment results. In FE simulations, the resultant field variables have been extracted after 5 milliseconds (ms) of cutting time. This short cutting time is assumed sufficient for the field variables to reach a steady-state. Effect of displacement amplitude on tool wear and analysis is done for all test conditions. Effect displacement on tool wear is studied and correlation is established. Results of test conditions TC 1-1, TC 2-5 and TC 3-9 are discussed in detail whereas table 2 gives the details of entire experimentation.

4.1. Case 1 (TC1-1: Rotational speed 538 rpm, feed at 0.08mm/rev, depth of cut 0.5 mm)

The 3D models, implemented in Deform 3D v6.1, are reported in figure 3, figure 4 and figure 5 where it is observed that workpiece with the growing chip and the tool. Figure 3 presents the 3D FE modeling of oblique metal cutting process for TC 1-1 which shows the predicted displacement amplitude due to vibration during cutting in the work piece and the chip separation.

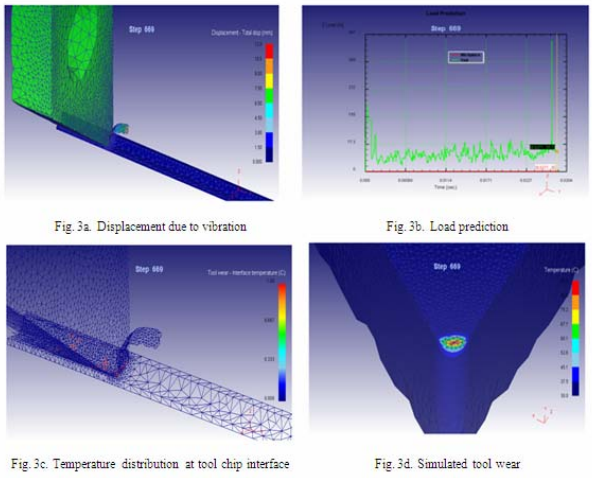

Fig. 3a. Displacement due to vibration

Fig. 3b. Load prediction

Fig. 3c. Temperature distribution at tool chip interface

Fig. 3d. Simulated tool wear

Fig. 3. 3D FE modeling of oblique metal cutting process for TC 1-1

In agreement with experimental results [1] the chip is a continuous one due to material model and cutting condition chosen. Displacement predicted from FEM simulation are also maintains good agreement with the results of experiment. In addition, chip separation achieved by continuous re-meshing which is triggered by sharp tool penetration is presented in figure 3(a). It is a known fact that the friction between the tool and the workpiece is little when the tool is new (sharp) and accordingly the amplitude of vibration will also be low. Due to the presence of dominant signals vibration is measured in the feed direction (Z direction). Predicted load in Z direction each test condition are presented in figure 3(b), 4(b) and 5(b) are showing the good correlation with dominant signals vibration is measured in the feed direction (Z direction) as part of the results discussed in [1]. Figure 3(b) shows a typical cutting force versus time increment, where it can be seen that after some point steady-state is reached. Therefore all the results presented in this work are gathered under steady state conditions. Pure heat transfer analysis is performed after chip formation analysis and it is shown in figure 3(c). At the end of the chip formation analysis in turning operation, temperatures at nodes inside the cutting tool are climbing while those at tool-chip interface nodes approach steady state as shown in figure 3(c). As mentioned earlier, this analysis is presents the temperature distributes in the cutting tool. Figure 3(d) presents the profile of 3D tool flank wear after simulation. Figure 3(d) shows the simulated tool flank wear corresponding to initial point of the test for each of the cutting conditions for AISI 1040. It is observed that as long as values of VB≤0.14mm the tool flank wear developed gradually without any BUE formation.

4.2. Case 2 (TC 2-5 Rotational speed 836 rpm, feed at 0.4 mm/rev, depth of cut 0.8 mm)

Results of test condition 2-5 are given in figure 4. In figure 4(a) an increase in displacement amplitude due to vibration is clearly found. As the length of the workpiece decreases, the stiffness of the workpiece increases and a corresponding increase in vibration will occur is [17] clearly observed in figure 4(b).

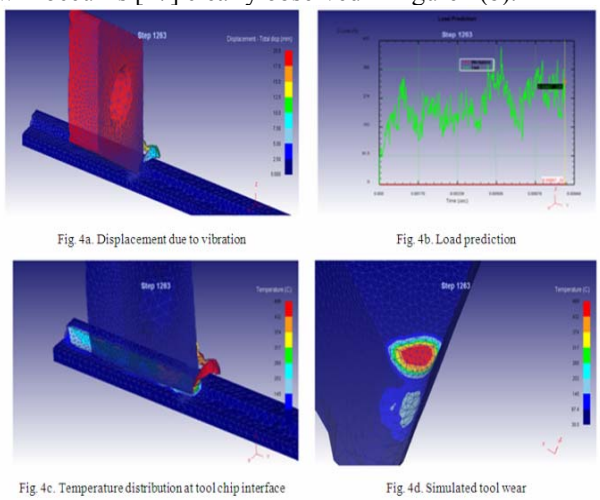

Fig. 4a. Displacement due to vibration

Fig. 4b. Load prediction

Fig. 4c. Temperature distribution at tool chip interface

Fig. 4d. Simulated tool wear

Fig. 4. Results of test condition 2-5

This increased level of vibration due to increase in tool wear. At the end of TC 2-5 condition, temperatures at nodes inside the cutting tool are still climbing whereas at tool-chip interface nodes approach steady state as shown in figure 4(c). The highest temperature is at the rake - chip interface and most part of the tool is still at room temperature. Figure 4(d) shows the simulated tool flank wear corresponding to middle point of the test for each of the cutting conditions for AISI 1040. Increase in tool wear profile is clearly shown in figure 4(d). It is found that when the flank wear developed further

near VB=0.2mm formation of workpiece built-up on the edge and material smearing on the flank wear face can be observed. It is observed that as long as values of VB≥0.25 mm the tool flank wear developed gradually with significant BUE formation.

4.3. Case 3 (TC 3-9 Rotational speed 1135 rpm, feed at 0.8 mm/rev, depth of cut 1.5 mm)

FEM simulation results corresponding to test condition TC 3-9 is presented in figure 5. In figure 5(a) a further increase in vibration amplitude is found when compare to previous cases and this is because of the increasing friction between the workpiece and cutting tool which is due to increase in tool wear.

Any displacement amplitude beyond this value is showing excessive vibration which increases tool flank wear and reducing the tool life. Figure 5(b) shows a highest predicted load in all test cases presented in results and discussions. Result of pure heat transfer analysis for TC 3-9 is shown in figure 5(c).

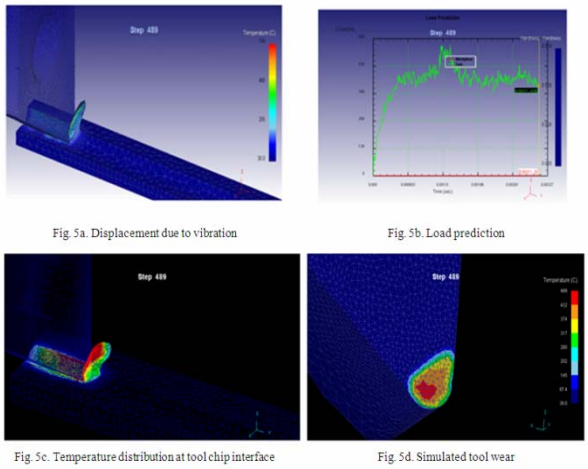

Fig. 5a. Displacement due to vibration

Fig. 5b. Load prediction

Fig. 5c. Temperature distribution at tool chip interface

Fig. 5d. Simulated tool wear

Fig. 5. FEM simulation results corresponding to test condition TC 3-9

Test condition	Cutting Speed (N)	Feed rate(f)	Depth of cut(d)	Displacement (microns)		Flank wear,VB (mm)		Machining Time. (min)
				Experimental	FE-predicted	Experimental	FE predicted	Experimental
TC 1-1	530	0.08	0.5	12	12.60	0.08	0.084	8.22
TC 1-2	538	0.08	0.8	14	12.88	0.10	0.092	12.22
TC 1-3	538	0.08	1.5	16	16.80	0.12	0.1260	16.22
TC 1-4	538	0.4	0.5	18	16.56	0.14	0.1288	20.22
TC 1-5	538	0.4	0.8	20	21	0.17	0.1785	24.22
TC 1-6	538	0.4	1.5	26	23.92	0.19	0.1748	28.22
TC 1-7	538	0.8	0.5	28	29.40	0.2	0.21	32.22
TC 1-8	538	0.8	0.8	30	27.60	0.24	0.2208	36.22
TC 1-9	538	0.8	1.5	32	33.60	0.26	0.2730	40.22
TC 2-1	836	0.08	0.5	16	14.72	0.15	0.1380	4.10
TC 2-2	836	0.08	0.8	20	21	0.19	0.1748	6.05
TC 2-3	836	0.08	1.5	22	20.24	0.17	0.1564	8.11
TC 2-4	836	0.4	0.5	24	25.20	0.21	0.2205	10.04
TC 2-5	836	0.4	0.8	32	29.44	0.26	0.2392	11.58
TC 2-6	836	0.4	1.5	40	42	0.31	0.3255	13.33
TC 2-7	836	0.8	0.5	50	46	0.32	0.2944	15.48
TC 2-8	836	0.8	0.8	60	63	0.32	0.3360	17.33
TC 2-9	836	0.8	1.5	72	66.24	0.33	0.3036	19.28
TC 3-1	1135	0.8	0.5	12	12.60	0.21	0.2205	1.5
TC 3-2	1135	0.8	0.8	16	14.72	0.24	0.2205	2.25
TC 3-3	1135	0.8	1.5	22	23.10	0.26	0.2730	3.03
TC 3-4	1135	0.4	0.5	26	23.92	0.36	0.3312	3.78
TC 3-5	1135	0.4	0.8	38	39.90	0.39	0.4095	4.58
TC 3-6	1135	0.4	1.5	48	44.16	0.41	0.3772	5.45
TC 3-7	1135	0.8	0.5	60	65	0.43	0.4515	6.15
TC 3-8	1135	0.8	0.8	72	66.24	0.46	0.4232	6.9
TC 3-9	1135	0.8	1.5	84	88.20	0.49	0.5145	7.66

Table 2. Experimental and FE simulated values

In figure 5(c) it is observed that, temperatures at nodes inside the cutting tool are climbing while those at tool-chip interface nodes approach steady state condition. Figure 5(d) gives the profile of 3D tool flank wear after simulation. In figure 5(d) flank wear (VB) values are found to be more than 0.3 mm. Flank wear value more than 0.3 mm is clear indication of the end of the tool life as per ISO 3685 and rejection criterion adopted in present study. From table 2, it is found that according to ISO 10816 displacement amplitude values up to 20 µm do not have any effect on tool flank wear. Tool flank wear is found to be effected by the measured displacements in the range between 20 and 60 µm. A displacement value beyond 60 µm is not a acceptable as per ISO 10816. From table 2 it is clear that in all conditions i.e, TC 1-1 to TC 1-9 displacement values is found to be less than 60 microns and VB≤0.3 mm.

With increase of flank wear, displacement amplitude due to vibration is found to be increase in all test conditions. As it can be observed from table 2, the tool life is reduced significantly with the increasing vibration amplitude at all test conditions.

5. CONCLUSIONS

In this work, a finite element model of chip formation process in face turning is combined with a dynamic model of machine tool system in order to obtain a comprehensive model which realistically predicts the effects of various cutting parameters on displacement amplitude of the workpiece in face turning. A Lagrangian FE approach is used in combination with mesh adaptation techniques to deal with severe mesh distortion in machining process simulations. Using the combined model, the displacement amplitude of the work piece is determined at different cutting conditions. In particular, the effects of depth of cut at constant cutting speed is studied which defines the onset of instability. Also, the effect of cutting speed on the vibration amplitude is investigated. The simulation results show a good agreement with experimental results in the range of cutting speed and feed rate considered. It is shown that the stability borders obtained at mid-to high speeds are in agreement with the results considered in the present work for investigation. Furthermore, 3D FE models are able to predict the tool wear and corresponding load during the cutting process. It is demonstrated that the FE simulations can be used successfully to distinguish between new and worn tools. This is very meaningful for the scientific research and education. A high degree of identified between the experimental and FE simulated results in identifying the effect of vibration amplitude on tool wear state.

6. REFERENCES

[1] Balla Srinivasa Prasad, M. M. M. Sarcar, B. Satish Ben.: Development of a system for monitoring tool condition using acousto-optic emission signal in face turning—an experimental

approach, International Journal of Advanced Manufacturing Technology 51, p.p.57–67, 2010.
[2] Chih-Cherng Chen, Nun-Ming Liu, Ko-Ta Chiang and Hua-Lun Chen.: The use of D-optimal design for modelling and analyzing the vibration and surface roughness in the precision turning with a diamond cutting tool, International Journal of Advanced Manufacturing Technology 54, p.p.465–478, 2011.
[3] Ning Fang, P.Srinivasa Pai, S.Moquea.: Effect of tool edge wear on cutting forces and vibrations in high-speed finish machining of Inconel 718: an experimental study and wavelet transform analysis, International Journal of Advanced Manufacturing Technology 52, p.p.65–77, (2011).
[4] Mer A, Diniz AE.: Correlating tool wear, tool life, surface roughness and tool vibration in finish turning with coated carbide tools, Wear 173, p.p.137–144(1994).
[5] Dimla DE.: The correlation of vibration signal features to cutting tool wear in a metal turning operation, International Journal of Advanced Manufacturing Technology 19, p.p.705–713(2002).
[6] A. G. Mamalis, J. Kundrák, A. Markopoulos, D. E. Manolakos.: On the finite element modelling of high speed hard turning, International Journal of Advanced Manufacturing Technology 38, p.p.441–446(2008).
[7] Mackerle J.: Finite element analysis and simulation of machining: an addendum a bibliography, International Journal of Machine Tools and Manufacture 43, p.p.103–114(2003).
[8] Vytautas Ostasevicius, Rimvydas Gaidys, Rolanas Dauksevicius, Sandra Mikuckyte.: Study of Vibration Milling for Improving Surface Finish of Difficult-to-Cut Materials, Journal of Mechanical Engineering 59(6), p.p.351-357, (2013).
[9] Ostasevicius, V., Gaidys, R., Rimkeviciene, J., Dauksevicius, R.: An approach based on tool mode control for surface roughness reduction in high-frequency vibration cutting, Journal of Sound and Vibration, 329(23), p.p.4866-4879, (2010).
[10] Tuğrul Özel, Erol Zeren.: Determination of work material flow stress and friction for FEA of machining using orthogonal cutting tests, Journal of Materials Processing Technology, 153, p.p.1019-1025(2004).
[11] Grzesik W.: Determination of temperature distribution in the cutting zone using hybrid analytical-FEM technique, International Journal of Machine Tools and Manufacture 46, p.p.651–658(2006).
[12] Yung-Chang Yen, JörgSöhner, Blaine Lilly and Taylan Altan.: Estimation of tool wear in orthogonal cutting using the finite element analysis, Journal of Materials Processing Technology,146, p.p.82–91(2004).
[13] A. Attanasio, E. Ceretti1, C. Giardini, L. Filice and D. Umbrello.: Criterion to evaluate diffusive wear in 3D simulations when turning AISI 1045 steel, International Journal of Material Forming suppl 1, p.p.495–498(2008).
[14] Maňková, I., Kovac, P., Kundrak, J., Beňo, J.: Finite element analysis of hardened steel cutting, Journal of production engineering, 14, p.p.7-10(2011).
[15] Zhang Wei and Sun Chuan-qiong.: The Three-dimensional Numerical Simulation of Turning, E-Product E-Service and E-Entertainment (ICEEE), 2010 International Conference on. IEEE, (2010).
[16] Fazar Akbar, Paul T. Mativenga. M.A.Sheikh.: An experimental and coupled thermo-mechanical finite element study of heat partition effects in machining, International Journal of Advanced Manufacturing Technology 46, p.p. 491-507(2010).
[17] G.H Lim.: Tool wear monitoring in machine turning, Journal of materials processing technology 51, p.p. 25-36, (1995).

INFORMATION

Dept.of Mechanical Engineering,
GITAM Institute of Technology, GITAM University,
Visakhapatnam, India-530045
Tel: +91-891-2840250

Acknowledgements
The authors would like to acknowledge Dr. R V S Subrahmanyam Scientist 'G' & Director, CNC Center NSTL, Visakhapatnam, India for providing both computational and experimental support.

Authors:
M.Prakash Babu, Corresponding author, Ph.D. scholar, Dept.of Mechanical Engineering, GITAM Institute of Technology, GITAM University, Visakhapatnam, India-530045**,** Tel: +91-0-9573219821
e-mail: m.prakashbabu1535@mail.com

Dr Balla Srinivasa Prasad, Research guide, Assistant Professor, Dept.of Mechanical Engineering, GITAM, Institute of Technology, GITAM University, Visakhapatnam, India-530045, Tel.: +91-0-98483210710 Fax: (+381 21) 454-495
e-mail: bsp.prasad@gmail.com

Journal of Production Engineering
Vol.17 No.2

Original Scientific Paper

Kovačević D., Antić A., Budak I., Okuka R.

AxisVM® 12 - ACTUAL VERSION OF CASA FEM SOFTWARE

Received: 04 November 2014 / Accepted: 28 November 2014

Abstract: *This is a review of new version of AxisVM® - CASA (Computer Aided Structural Analysis) software. AxisVM® is a combination of pre-processor based on graphic user interface, processor with advanced modeling possibilities and post-processor for presentation of modeling results. The software performs linear/nonlinear, static and dynamic analysis of line and surface structures. Design section treats various structural materials and 17 national design codes. On Department for Civil Engineering and Geodesy, FTN - Novi Sad, AxisVM® is used in education in structural design area, research work and design practice.*
Key words: *AxisVM, FEM modeling, CASA*

AxisVM® 12 - aktuelna verzija CASA MKE softvera. *Ovo je prikaz aktuelne verzije AxisVM® softvera za MKE analizu konstrukcija. AxisVM® je kombinacija pre-procesora zasnovanog na grafičkom unosu podataka, procesora sa naprednim mogućnostima modeliranja i post-procesora za prikaz rezultata modeliranja. Softver omogućava linearnu/nelinearnu, statičku i dinamičku analizu linijskih i površinskih konstrukcija. Sekcija za dimenzionisanje obuhvata sve građevinske konstrukcijske materijale i 17 različitih nacionalnih standarda. Na Departmanu za građevinarstvo i geodeziju, FTN - Novi Sad AxisVM® se koristi u obrazovanju u oblasti projektovanja konstrukcija, u istraživačkog radu i za potrebe projektantske prakse.*
Ključne reči: *AxisVM, MKE modeliranje, numerička analiza konstrukcija*

1. INTRODUCTION

AxisVM is FEM based 32/64bit software developed for a Microsoft Windows® by structural engineers and intended for structural engineers [1]. Due to its wide modeling capabilities, AxisVM is verified as successful in design ranging from large complex structures to small and simple buildings.

The software performs linear and nolinear, static and dynamic analysis of beam, membrane, plate, and shell structures. It enables use of an unlimited number of nodes and unlimited number of FE freely combined in a models by use of: plane/space frames/truss FEs, elastically embedded beams/membranes/plates/shells, plane stress/strain membranes, ribbed plates, spatial shell structures and any combination of mentioned structures.

2. AXISVM® PRE-PROCESSOR

AxisVM (Visual Modeling) provides a leading edge graphical user interface with multi window model creation and display. Each graphics window has its independent settings. During any command it is possible to switch to the graphics window that shows the best model view or results of your action. Fig. 1 shows typical AxisVM working environment.

AxisVM pre-procesor editor enables:

- geometry modeling in 2D or 3D,
- geometry generation commands (translate, rotate, mirror, scale, with multiple copy or move),
- structural grid lines support (helps precise positioning of structural elements),

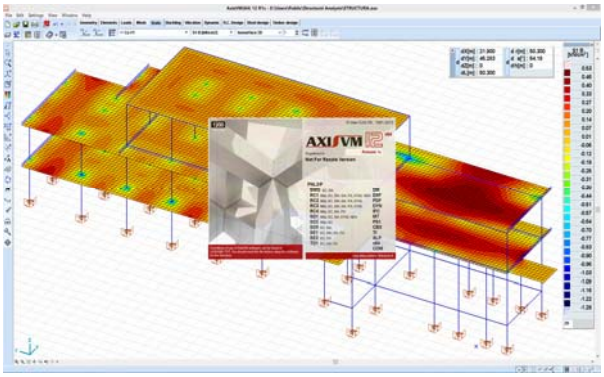

Fig. 1. AxisVM working environment

- pictograms help though the generation processes, in conjunction with online help,
- graphical editing of the model in any view including the perspective view,
- powerful selection tools (filtered selection available),
- view changes at the click of the mouse,
- complete set of zoom in/out, fit to page, pan, view undo/redo commands,
- working on parts (allows easy editing of most complex 3D geometries and includes advanced part management),
- wire frame modeling,
- rendered display for better model check (see Fig. 2),
- section lines for surface element results display,

- toolbars can be positioned on the screen in any area, selected on a one-time basis or set to appear until no longer needed,

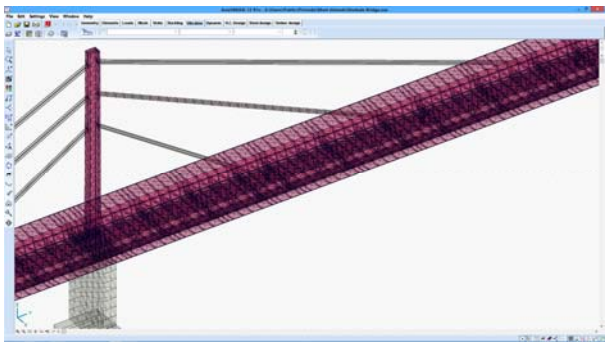

Fig. 2. AxisVM rendered model display example

- search for entities by type and index,
- automatic duplication check feature,
- graphically created joints, members, finite elements, properties, constraints, releases and loadings,
- display settings for the most appropriate model display and configure symbol and labeling display for each finite element,
- configurable 3D grid and mouse step,
- steel cross-section libraries with most of the available European and U.S. shapes and creation of custom libraries and
- fully integrated graphical cross-section editor for complex shapes (all cross-sectional properties are automatically calculated based on the graphical input).

Structural geometry, materials, cross-sections, loads, supports etc. can also be imported from latest version of IFC files, as well as curved elements and elements with variable cross-section, loads, load cases and load groups.

The user can merge other AxisVM models to create a new model, thus allowing parts of the structure to be modeled by different users/departments.

3. AXISVM® PROCESSOR

AxisVM implements an object-oriented finite element architecture that inherits more reliability than the classical systems. It provides a variety of finite elements for modeling frames and/or surface structures, special elements for modeling boundary conditions and connections and elements with nonlinear capabilities:

- line elements: truss, beam, rib (the truss and the cubic beam element are the most widely used finite elements for bar, beam, or column modeling. The rib element is a 3-node isoparametric element with quadratic displacement interpolation that can be used similar to the beam element (but takes into account the shear deformations) or in conjunction with surface elements for eccentric rib modeling),
- surface elements: membrane, plate, shell (these elements are isoparametric quadrilateral (8/9-node) or triangular (6-node) elements, that use quadratic shape functions to interpolate displacements, and pass the patch test for arbitrary shape (the plate and shell elements use Mindlin's plate assumptions in a Heterosis formulation, see Fig. 3)), [2]
- conversion of line elements (beams, ribs) with steel cross section to shell elements,

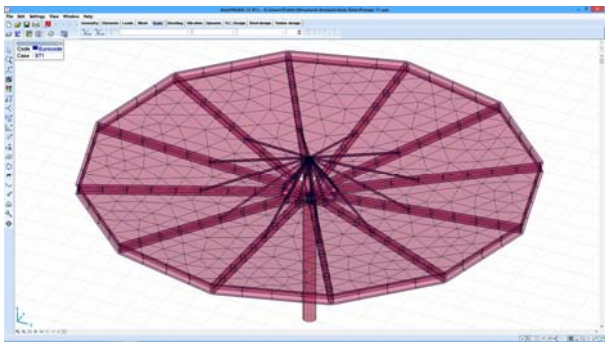

Fig. 3. AxisVM shell FEs modeling example

- conversion of beam connections to shell elements,
- Winkler type elastic supports for line and surface elements can model elastic foundation support conditions of line and surface elements with nonlinear characteristics - tension or compression only, limited resistance,
- joint support elements with arbitrary orientation and stiffness can have a specified stiffness, and the resulting internal forces are the support reactions with nonlinear characteristics - tension or compression only, limited resistance,
- gap elements for contact modeling can model point-to-point contact conditions and have a large stiffness when active and a small, but non-zero stiffness when in an inactive state (the active state can be for compression or for tension and initial opening can be specified for the elements),
- spring elements for linear/nonlinear support or semi-rigid connection modeling can be taken into account for linear or nonlinear elastic support or connection behavior,
- link elements for connection modeling can be node-to-node (connect nodes to nodes), or line-to line (connect ribs, ribs to surfaces, or surface sides) and
- rigid elements can model rigid parts of your structures without assigning large stiffness values to an element, that can have any number of nodes,
- global imperfections can be generated in accordance with the requirements of the Eurocode.

Various loads can be applied on the nodes and the finite elements. Up to 99 load cases can be applied on a model and any number of load combinations can be generated from these load cases. Load cases can be classified in load groups for automatic critical internal force calculations.

Finite element mesh generation is possible using triangular, quadrilateral, as well as mixed triangle-quadrilatetal finite elements.

AxisVM performs most of the analyses, typical in the practical design of civil engineering structures:

- linear static analysis,
- buckling analysis: critical force and shape computation (Fig. 4),

- nonlinear static analysis: displacement/force controlled incremental iterative solution,
- free vibration analysis: eigen-shape and -frequency computation (Fig. 5),
- dynamic and earthquake analysis - response spectrum, time history and push over analysis - Eurocode 8, ISA (Italian), STAS (Romanian) and MSz (Hungarian).

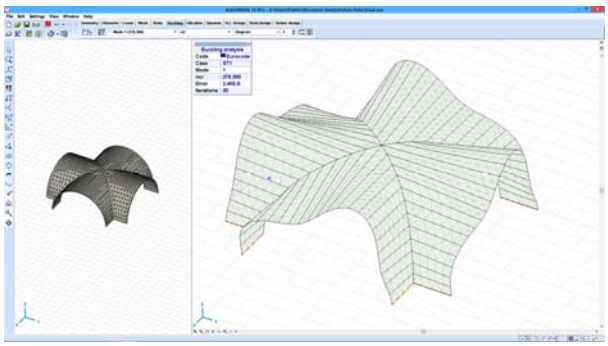

Fig. 4. AxisVM 3rd order buckling analysis

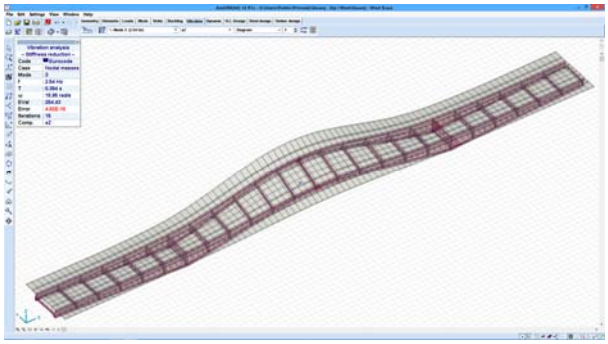

Fig. 5. AxisVM free vibration analysis of bridge

Clearly, in application of CASA software, it is not sufficient to know only the basic problem and the essence of the applied method, but also to know the software performances (in sense of possibilities and limits), numerical methods and a critical approach in interpretation and application of the obtained results [3, 4].

4. AXISVM® POST-PROCESSOR

Civil engineers use AxisVM for the analysis of structures with confidence that their final engineering product will meet their country specific design codes. The ease of results exporting allows each user to connect AxisVM to almost every locally produced and national code compliant design and detailing software. AxisVM is committed to assisting each user in connecting the results of the finite element calculations to the programs they use every day.

AxisVM provides multi-window model analysis results display and design capabilities:

- diagram analysis results display,
- analysis results display for section lines,
- analysis results display for structure parts,
- analysis results display in 2D or 3D (Fig. 6-8),
- piled foundations design regards Eurocode 7,
- plate deflection calculation according to Eurocode 2, NEN (Dutch), MSz (Hungarian, STAS (Romanian),
- steel design according to Eurocode 3, NEN 6770/74 (Fig. 9),

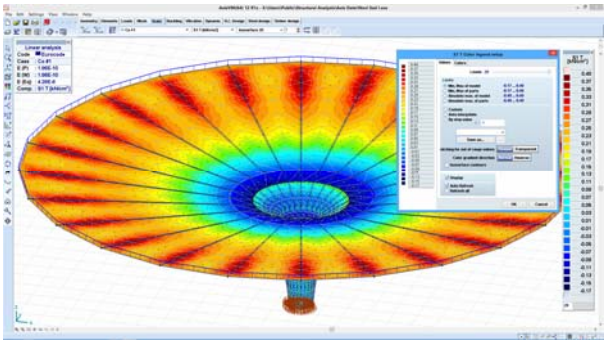

Fig. 6 – Analysis results display - space roof

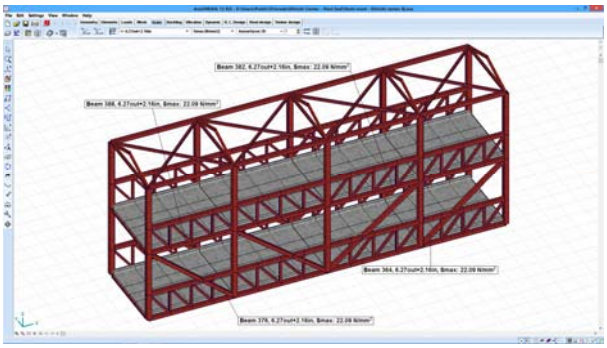

Fig. 7. Analysis results display - space truss

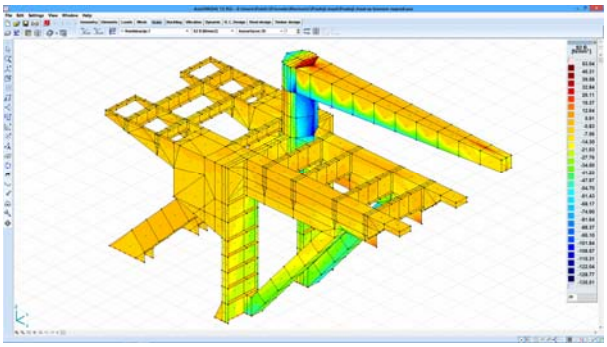

Fig. 8. Analysis results display - space crane structure

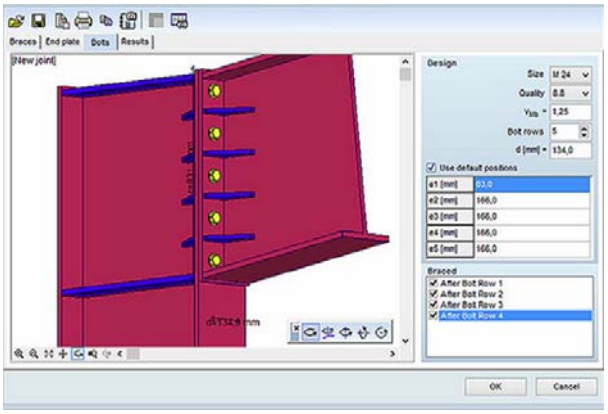

Fig. 9. Steel design example

- timber design according to Eurocode 5 EN 1995-1-1:2004 (Fig 10),

- reinforced concrete design (beams, columns, plates, membranes, shells) according to Eurocode 2 (Fig. 11), NEN (Dutch), DIN (German), SIA (Swiss),
- integrated Report Generator to create report templates for every construction partner: design approval, steel detailer, bid estimates, component producers, and departmental specialties,
- detailed documentation of strength and stability checks using formulas and substituted values,
- 3D PDF file export of the graphical content, which can be rotated and zoomed in and out within the PDF reader.

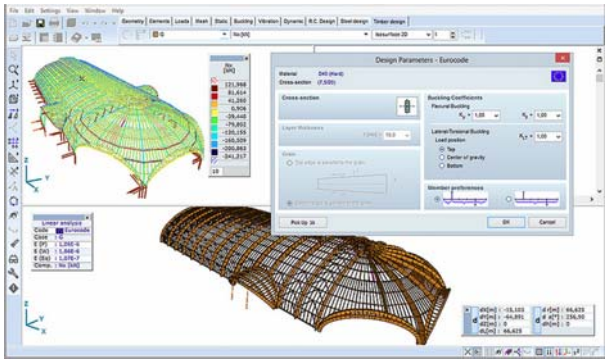

Fig. 10. Timber design example

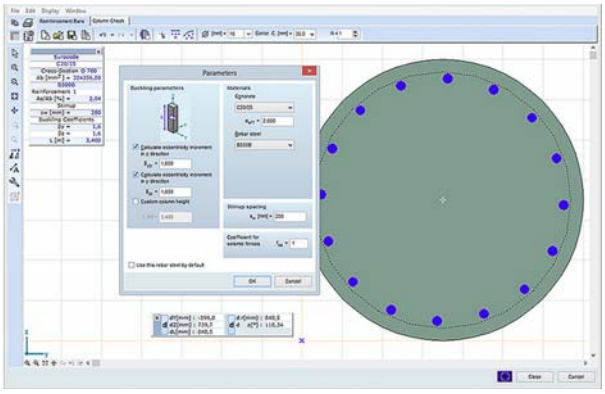

Fig. 11. Concrete design example

5. CONCLUSIONS

The software implementation quality decides how much the advantages of FEM in modeling would be expressed. Thus, as the key one, the problem of choice of the CASA software is imposed.

AxisVM is based on FEM as a dominant numerical concept. Due to great possibilities of software implementation (automatic FE mesh creation, the formation and solving of constitutive equations, numerical and graphic presentation of the results, etc.) FEM has become a dominant method of numerical modeling of complex structural problems.

Development, distribution and application of CASA software is the area where the professional competence is essential, but provided that rather high education in the field of computer sciences is also possessed. Very similar relations apply when distribution and, particularly, program application are in question. AxisVM is developed by engineers for engineers.

The question of educational concept rises in connection to this. In addition to high knowledge in the primary profession (structural analysis and design) also is needed knowledge, providing that the software being developed has good performances (numerical mathematics, software design and programming), to have a good quality in software distribution (computer technology knowledge at the advanced user level, sense for marketing and public relations) and for competent use of the software (numerical mathematics and use of computer technology at the advanced user level). The authors consider that each and every technically oriented faculty should make this concept in education possible.

Education and, especially, examination of the knowledge in the primary profession should be adapted, first of all, to need of complete understanding of the essence of structural behavior. Gaining of the "encyclopedia like" knowledge by studying of many methods for analysis possibly provides wide education and contributes to the technical culture, but it takes away attention and energy and ruins enthusiasm of students. Such knowledge is insufficiently used and is not necessary if the analysis of the CASA software is applied in competent manner. All this reasons cause introduction of AxisVM software in program of subject "FEM Modeling in Structural Analysis".

ACKNOWLEDGEMENTS The paper has been done within the scientific research project "Theoretical, experimental and applied research in Civil Engineering", developed at the Department of Civil Engineering and Geodesy, Faculty of Technical Sciences, University of Novi Sad.

6. REFERENCES

[1] AxisVM® 12: "User's manual", InterCAD, Budapest, 2013
[2] R.D. Cook: "Finite Element Modeling for Stress Analysis", John Wiley & Sons, Inc. , 1995
[3] D. Kovačević: "FEM Modeling in Structural Analysis" (in Serbian), Građevinska knjiga, Belgrade, 2006
[4] D. Kovačević: "Some aspects of FEM modeling of nonlinear behavior of civil engineering structures" (in Serbian), Invited lecture, Mathematical Institute of SANU, Belgrade, 2007

Authors: **Prof. Dr Dušan Kovačević, Civ. Eng.**
Ass. Prof. Dr Aco Antić, Mech. Eng.
Ass. Prof. Dr Igor Budak, Mech. Eng.
Ass. Ranko Okuka, Civ. Eng.
University of Novi Sad
Faculty of Technical Sciences
Trg Dositeja Obradovica 6
21000 Novi Sad, Serbia
E-mail: dusan@uns.ac.rs
antica@uns.ac.rs
budaki@uns.ac.rs
okukaranko@yahoo.com

Journal of Production Engineering
Vol.17 No.2

Original Scientific Paper

Mangat, H.S., Kohli, G.S.

INVESTIGATION FOR SHEET WIDTH AND THICKNESS DURING PIPE MANUFACTURING BY ROLL FORMING IN A ROLLING MILL

Received: 26 October 2014 / Accepted: 17 November 2014

Abstract: *The paper experimentally investigate the anisotropic elastic properties of sheet metal and to find the satisfactory correlation between the strip widths, thickness to the diameter of steel pipe. The work has been focused to investigate the variation in strip thickness, while forming the strip in a rolling mill for constant roller loads and constant line velocity. It was found that there is negligible change in the thickness of the strip while forming. In other words, the strain in the thickness direction is negligible while the stretch in the width direction of the strip is almost increasing linearly with the increase in the thickness. In other words, the strain in the circumferential direction is considerable.*

Key words: *steel pipe, anisotropic elastic properties, rolling mill, strip thickness & width, steel pipe diameter, strain*

Istraživanje širine i debljine ploča u procesu proizvodnje cevi profilnim savijanjem valjcima. *U ovom radu su ispitivane anizotropne elastične osobine lima i tražena je zavisnost između širine i debljine trake lima u odnosu na prečnik cevi. Istraživanje je fokusirano na variranje debljine lima tokom oblikovanja lima u cev pri konstantnoj sili valjaka i brzini proizvodne linije. Primećena je neznatna promena debljine trake lima pri oblikovanju. Drugim rečima napon u pravcu debljine lima je zanemarljiv dok je rastezanje u pravcu širine trake približno linearno sa povećanjem debljine. Što znači da je napon po obimu popriličan.*

Ključne reči: *čelične cevi, anizotropne elastične osobine, linija za profilisanje pomoću valjaka, debljina i širina trake, prečnik čelične cevi, deformacije*

1. INTRODUCTION

Pipe manufacturing refers to how the individual pieces of pipe are prepared in a pipe mill; it does not refer to how the pieces are connected in the field to form a continuous pipeline. Each piece of pipe formed by a pipe mill is called a length. Steel pipes are long, hollow tubes that are used for a variety of purposes [1]. The majority of steel products are made from these four primary forms of raw steel: ingots, billets, blooms and slabs. These forms can be produced in huge volumes and are easily re-heated, extruded, squeezed or formed into many other configurations so as to make nearly every steel product used today. Steel pipe is produced from these two fundamental forms of steel, the round billet and the slab. A billet is a solid round bar of steel used to make many other downstream products such as seamless pipe. The other types of steel pipe are manufactured from slabs that are solid rectangular blocks of steel. The slabs are reheated and processed into plate and coils. Broadly, production of steel pipe is grouped into two general categories: Welded and Seamless. In both, raw steel is first cast into a more workable preparatory form. It is then made into a pipe by stretching the steel out into a seamless tube or forcing the edges together and sealing them with a weld. Further, there can be following methods used to produce steel pipe: Lap Weld, Electric Resistance Weld, Flash Weld, Double Submerged Arc Weld and Seamless [2].

The first methods for producing steel pipe were initiated in the early 1800s and they have gradually progressed into the new processes we utilize today. Different authors have explained the manufacturing of pipes in their unique way. Here two best elaborated descriptions are presented so as to understand the basics and concepts involved in pipe manufacturing. As per the first explanation, historical aspect along with evolution of production processes for pipe manufacturing is clearly stated. At first, pipe was manufactured by hand – by heating, bending, lapping, and hammering the edges jointly. The foremost automated pipe manufacturing process was commenced in 1812 in England. The utilization of lap welding to manufacture pipe was introduced in the early 1920's. In the lap welding process, steel was heated in a furnace and then rolled into the shape of a cylinder. The edges of the steel plate were then "scarfed". Scarfing involves overlaying the inner edge of the steel plate and the tapered edge of the reverse side of the plate. The seam was subsequently welded using a welding ball and the heated pipe was passed between rollers which forced the seam together to build a bond. The welds formed by lap welding are not much reliable as compared to shaped using more modern methods. Based on the type of manufacturing process, the American Society of Mechanical Engineers (ASME) has developed an equation for calculating the permissible operating pressure of pipe. This equation comprises a variable called a joint factor, which is dependent on the type of weld used to create the seam of the pipe. A joint factor of seamless pipe 1.0. Lap welded pipe has a joint factor of 0.6. Electric resistance welded (ERW) pipe is manufactured by cold-forming a sheet of steel into a cylindrical shape. Current is subsequently passed

between the two edges of the steel to heat the steel to a point at which the edges are forced together to make a bond without the utilization of welding filler material. In the beginning this manufacturing process used low frequency alternating current to heat the edges. This low frequency process was used from the 1920's until 1970. In 1970, the low frequency process was outmoded by a high frequency ERW process which produced a higher quality weld. Eventually, the welds of low frequency ERW pipe was found to be prone to selective seam corrosion, hook cracks and poor bonding of seams. Accordingly low frequency ERW is not used to manufacture pipe these days. The high frequency process is still being utilized to manufacture pipe for use in new pipeline construction. Electric flash welded pipe was first manufactured in 1927. Flash welding was carried out by forming a steel sheet into a cylindrical shape. The edges were heated until semi-molten, then forced together until molten steel was forced out of the joint and formed a bead. Like low frequency ERW pipe, the seams of flash welded pipe are vulnerable to corrosion and hook cracks, but to a lesser extent than ERW pipe. This type of pipe is also at risk to failures due to hard spots in the plate steel. Because the bulk of flash welded pipe was produced by a single manufacturer, it is supposed these hard spots arised due to accidental quenching of the steel during the manufacturing process utilized by that particular manufacturer. Flash welding is no longer employed to manufacture pipe. The manufacture of Double Submerged Arc Welded Pipe also involves first forming steel plates into cylindrical shapes. The edges of the rolled plate are formed so that V-shaped grooves are created on the interior and exterior surfaces at the location of the seam. The pipe seam is then welded by a single pass of an arc welder on the inner and outer surface (therefore double submerged). The welding arc is submerged under flux. The benefit of this process is that welds pierce 100% of the pipe wall and make a very strong bond of the pipe material. Seamless pipe has been manufactured since the 1800's. Seamless pipe is manufactured by piercing a hot round steel billet with a mandrel. The hollowed steel is then rolled and stretched to attain the desired length and diameter. The main benefit of seamless pipe is the eradication of seam-related defects but the cost of manufacture is higher. Early seamless pipe was liable to defects caused by impurities in the steel. Though the steel-making techniques have improved but they have not been totally eradicated. Seamless pipe is presently available in lower grades and wall thicknesses than welded pipe [3].

As per the second explanation, different types of processes that have been used to manufacture various type of pipes along with their specific applications are clearly stated. Steel tubes and pipe can be generally classified according to manufacturing method as seamless tubes and pipe made by hot rolling or hot extrusion, and welded pipe and butt-welded pipe made by bending and welding sheets or plates. When seamless pipe is prepared by rolling, the rolling method involves piercing the material while it is being rolled, and is appropriate for mass production. The Figure 1 shows the manufacturing process utilized in the Mannesmann plug mill, which is a usual rolling process. The Mannesmann-type piercer lessen the material by rolls that are inclined diagonally to each other. When the round billet is rotated while being compressed in the diametric direction, the central part of the billet becomes slack, which makes it simple to pierce a hole through the center. This is called the Mannesmann effect. The pierced portion is enlarged by the elongator and the wall thickness is then thinned and elongated by the plug mill. The internal and external surfaces are smoothed by the reeler and the final dimensional adjustments are prepared by the sizer. The hot-extrusion method involves working in the compressive-stress field. Therefore, it is feature of this method that high-alloy steel pipe of low deformability can be formed along with heavy-wall and large-diameter pipes. Seamless pipe has exceptional homogeneity in the circumferential direction and is thus highly resistant to internal pressure and torsion. Hence, seamless pipe is commonly used for drilling and pumping petroleum and natural gas. Welded pipe is divided into electric-resistance welded (ERW) pipe, spiral pipe, and UO pipe based on the the forming and welding method. ERW pipe and butt-welded pipe are manufactured by continuously forming a hot-rolled coil into a tubular shape by forming mills. ERW pipe is manufactured by cold forming, and the seam is welded by electric-resistance welding. This type of steel pipe is utilized in large quantities as line pipe for transporting petroleum and gas. Butt-welded pipe is manufactured by hot forming after the entire material has been heated and seams are then butt welded. This type of pipe is hot-dip galvanized and uilized for transporting water and gas. The outer diameter of ERW pipe and butt-welded pipe is determined by the width of the material coil. Spiral pipe is made by forming the coil into a spiral shape, that makes it doable to attain a large outer diameter despite of the width of the material. UO pipe is typically large in diameter and manufactured one piece at a time by forming plates. Firstly, the plate is pressed into a U shape by the U-press and then into an O shape by the O-press. Because comparatively thick material is utilized for building spiral and UO pipes and submerged arc welding is utilized for joining. The major purpose of spiral pipe is pipe piles.

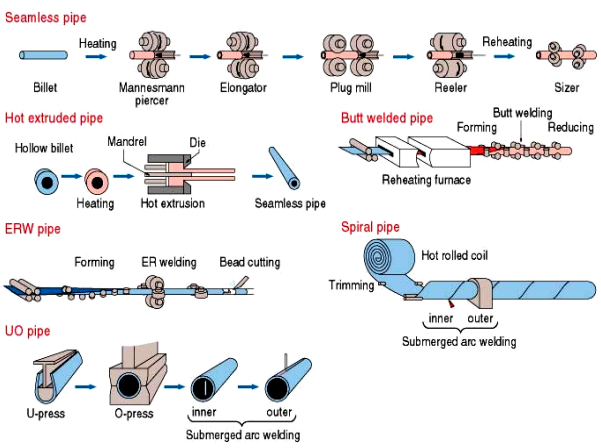

Fig. 1. Manufacturing Processes for pipes[4]

UO pipe is chiefly utilized as line pipe for transporting petroleum and natural gas in huge quantity over long distances [4].

Originally category of pipes that contains a solid phase butt weld was manufactured by means of resistance heating to create the longitudinal weld (ERW), however most pipe mills currently use high frequency induction heating (HFI) for better control and consistency. Figure 2 shows a diagrammatic representation of the HFI welding. The process occupies the relevance of a high-frequency alternating current in the range 200 to 500 kHz with the tube forming and energy input operations being performed by separate units. This welding method again simultaneously utilizes pressure and heat in order to join the strip edges of the open-seam tube together without the addition of a filler metal. Squeeze and pressure rolls in the welding stand bring the edges of the open-seam tube gradually together and apply the pressure necessary for welding. The open-seam tube 1 to be welded is introduced in the direction of the arrow to the welding table where it is engaged by the squeeze rolls 5. These initially press together the incoming open seam edges approaching at angle 2. The high-frequency current supplied by the welding generator 4 forms an electro-magnetic field around the induction coil 3 which induces an AC voltage in the open-seam tube corresponding to a current travelling around the tube circumference. This current is focused at the open seam edges and travels next to edge a through point 6 to edge b and back to the circumferential plane of the induction coil, with the circuit being closed at the rear of the tube. The heated edges are pressed together and welded by the squeeze rolls 5. The internal and external ridges (weld flashes) which form are trimmed from the finished weld 7 [5].

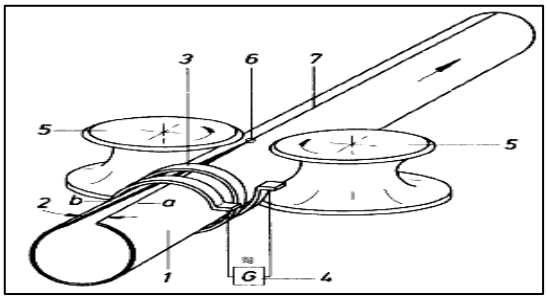

1. Open seam tube 2. Welding gap entry angle 3. Induction coil 4. Welding generator 5. Squeeze rolls 6. Welding point 7. Weld

Fig. 2. High-frequency induction welding [5]

Figure 3 shows the stretch bend test when a sheet of thickness t_o is bended over radius R, the stresses produced in the sheet material are given by:

σ_3 (in radial direction)

σ_1 (circumferential stress or in the direction of strip width)

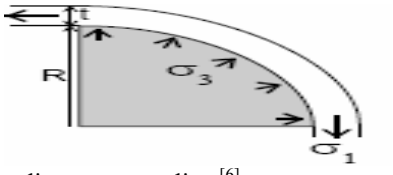

Fig. 3. Bending over a radius [6]

If the plain strain conditions are assumed in this condition, the strain in circumferential direction is given by [6]

$$\varepsilon_1 = n(1+\square t_0) = n\left(1+\frac{t_0}{aR}\right) \quad (1)$$

where: ε_1=Strain

t_o= Initial Thickness

R=Radius of roller

a= material and geometry dependent constant

n= hardening coefficient

Every year, millions of tons of steel pipe are produced. Its adaptability makes it the most frequently used product produced by the steel industry. Steel pipes are found in a different places. Because they are tough so they are mostly used underground for transporting water and gas all the way through cities and towns. They are too utilized in construction to guard electrical wires. As steel pipes are strong, they can as well be lightweight. This makes them ideal for utilization in cycle frame manufacture. Steel pipes also find its application in vehicles, refrigeration plants, heating and plumbing systems, flagpoles, street lamps etc. The first manufacturing plant to use welded pipe is formed by rolling steel strips through a series of grooved rollers that mold the material into a circular shape as shown in Figure 4. Subsequently, the un-welded pipe passes by welding Electrodes. These devices close the two ends of the pipe together [1].

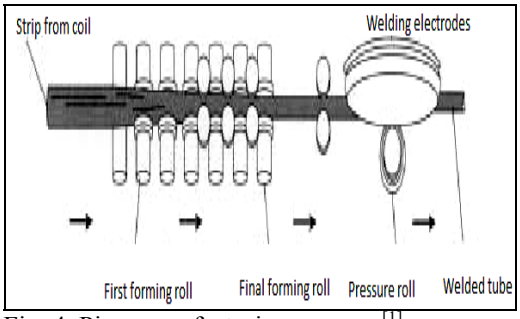

Fig. 4. Pipe manufacturing process [1]

Table 1 shows chronological survey of pipe material used and its manufacturing techniques

Year	Material used and manufacturing Techniques
2000 BC	Clay tubes were used by Chinese for transporting water.
1652	Bamboo tubes were used to transport water.
1800's	Welded Steel Tubes.
1820's	Edges of a flat iron strip were joined to produce tubes Patented by James Russell.
1880's-1890's	Tube was made by drilling a hole through the center of a solid cylinder.
1950's	Roll forming of strips to make pipes in large quantity.
Upto 2000	Continuous research in the pipe/tube manufacturing by joining seam of strip.

Table 1. Chronological Survey of Pipe material used and its Manufacturing Techniques

If a strip is draged over a curved tool then there is a contact stress acting on the strip. This contact stress alters the stress state in the material that was investigated by a few of the researchers with a simple

model. It has been found that the yield stress in tension is reduced. Forecasting by these models concur with observation from a 90^0 bending test found in literature and not directly with observation from a stretch-bend test also found in literature [6]. In accordance with the great importance given to the subject of stiffness degradation, in particular with regard to metal forming, this work aims to experimentally investigate the anisotropic elastic properties of sheet metal (steel IS:10748, also IS:6240). In the past, many researchers investigated the pipe manufacturing processes, but the satisfactory correlation between the strip widths, thickness to the diameter of steel pipe has not been found. So the present work aims to investigate the minimum strip width required for different thicknesses of steel strips while manufacturing the pipes.

2. LITERATURE REVIEW

Cage roll forming process was simulated with the explicit elastic–plastic finite element method in the MSC Marc Mentat software. Simulation results have shown that by increasing the initial strip width, more circumferential length reduction was induced to the deformed strip in the fin-pass stands. The difference of longitudinal strains at the edge and center of the deformed strip has been incrased by this effect. As a result, it has lead to a high longitudinal compression at the strip edge. Thus, edge buckling would be unavoidable if the initial width is selected bigger than a specific limit. The circumferential length and the horizontal distance between two deformed strip edges were obtained from the simulation and were compare with the experimental data from a production line. The comparison has shown that a good concurrence was found with the finite element simulations [7]. The whole cage roll-forming process was simulated with the explicit elastic–plastic finite element method. The strip deformation during the cage roll forming process was investigated. The “non-bending area” phenomenon was found and the ranges of the non-bending area at different forming stands were obtained through simulation. As well, the longitudinal strain at the inside edge and center were predicted. Further by comparison it has been observed that the deformation of the strip edge was usually larger and edge buckling is most likely to occur at the entry sides of No.1–No.3 fin-pass stands. Lastly, the circumferential length, opening distance and the profiles of the deformed strip were measured on the cage roll-forming mill. A good agreement between the experimental and simulated results were obtained [8]. Influences of foremost process parameters of thermomechanical tube-spinning process i.e. preform thickness, thickness decrease, mandrel rotational speed, rollers feed rate , solution treatment time & aging treatment time on internal diameter growth and wall thickness changes for manufacturing of 2024 aluminum spun tubes using design of experiments were determined by authors. It has been found that lower thickness reduction with thin preform thickness, high feed rate of rollers, low mandrel rotational speed and low solution treatment time have benefits for obtaining smaller internal diameter growth and wall thickness changes [9]. Two aluminum killed draw quality (AKDQ) steels and one high strength low alloy (HSLA) steel were selected to foresee the performance of tube from sheet tensile tests. Tensile properties and plastic strain ratios were measured on sheet material in the longitudinal and transverse directions. Residual stresses in the production and quasi tube were established by displacement methods. Effective strains resulting from tubemaking were calculated for two discrete operation i.e. bending and sizing. A linear relationship was found between a load factor (strength times thickness) and effective sizing strain for the production tubes. The association between load factor and residual stress was also linear [10]. The effect of thickness reduction on mechanical properties and spinning accuracy were experimentally investigated on 7075-O aluminum tube. A prototype spinning machine was designed and manufactured. It has been shown that with augmentation of thickness reduction; the yield point strength, ultimate strength, crystal refining iand surface hardness, increase. In contrast, it has bad effect on growth of diameter, accuracy of geometry, surface roughness and percentage elongation of spun tube [11]. 15 tensile coupon tests and 12 full section tests on VHS tubes were performed. The tested VHS tubes had a diameter varying from 31.8 -75 mm with wall thickness varying from 1.6 -2.0 mm. The non-heat-treated tubes were also tested for comparison purposes. The ultimate strength to yield stress ratio of VHS tubes was compared with different cold-formed hollow sections, sheet steels and quenched/tempered steels. It has revealed that the VHS tubes fulfilled the material ductility requirement specified in the Australian/New Zealand Standard for Cold-Formed Steel Structures AS/NZS4600 [12]. The tube and pipe industries face many challenges that are requests for tube products in a wider variety of shapes and sizes by the end users, applications that require special materials, and demand for improved product quality from manufacturer to produce high quality tubing in a cost effective and productive way in today's marketplace. Different facets of manufacturing, processing, design, utilization, quality control, handling, cost and safety in tube and pipe production has been reviewed to present a general idea relating to these issues [13]. The results of the numerical study of rectangular cup drawing of steel sheets using finite element methods were discussed. For the intention of the results of the numerical solutions, an experimental study was performed where the material behavior under deformation was analyzed. A 3D parametric finite element model was made using the commercial FE-package ABAQUS/Standard. It has been found that plastic anisotropy of the matrix in ductile sheet metal has influence on deformation behavior of the material. Once the material and friction anisotropy were considered in the finite element analysis, it gives better approximate numerical results for real processes. The maximum wall thickness in all directions was observed near the edge of blank, while minimum thickness is at the punch shoulder. The variation of thickness at bottom is relatively small as compared with deformation on the corner. It has been

suggested that FEM method for optimization of initial blank shape is an attractive approach which eliminates time-consuming experimental methods [14]. An experimental investigation to check an accuracy of skelp profile-geometry prediction that can be used to model the strain history during forming was described. Skelp geometries predicted from roll-stand geometries were compared to profiles measured on an actual 16" rolling mill. A method of correcting theoretically-predicted geometry was developed and found to produce good agreement with mill-measured geometry. Also, it was suggested that skelp geometry predicted from theoretical roll-stand geometries was not sufficiently accurate to adequate define strain state in deformed skelp [15].

3. EXPERIMENTAL DETAILS

To investigate the behavioral relationship between the stretching of the strip in the width direction to form a pipe of certain diameter, the pipe forming line was studied under different working conditions. The parameters which are assumed to be affecting the forming of strips in to pipes are: strip width, strip thickness, speed of rolling mill line, roller loads, strength of the steel strip and type welding method used to join the seam. In the present study, the roller loads, speed of rolling mill line and the welding technique are assumed to be non variable. For investigations in the various geometrical quantities of the steel strip to form a pipe under constant roller loads and line speed, the material for the steel strip was selected as IS:10748 and IS: 6240. The thickness of the strip is measured with the help of micrometer with vernier scale. The variation of initial to final thickness of strip is discussed below: The observations obtained for thickness reduction were given in Table 2.

The pipe diameter is also measured with the help of micrometer. An initial strip width and final pipe diameter for steel IS: 10748 and IS: 6240 were observed. The observations obtained for width elongations for steel IS: 10748 and IS: 6240 are given in Table 3 and Table 4 respectively.

4. RESULTS AND DISCUSSIONS

From the observation obtained in Table 2, it has been observed that there is a negligible change in the thickness of strip during forming. The figure below represents the Initial Vs. Final strip thickness.

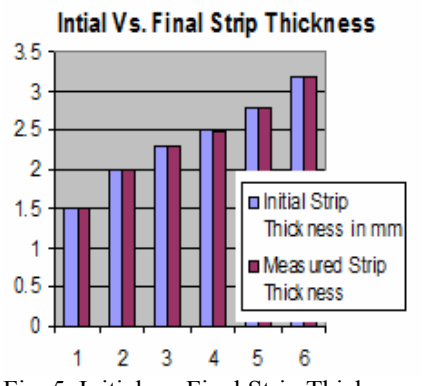

Fig. 5. Initial vs. Final Strip Thickness

S.No	Initial Strip Thickness in mm	Measured Value	Mean of four measured values	% Reduction in thckness
1	1.5	1.499	1.498	0.13
		1.498		
		1.498		
		1.497		
2	2	1.999	1.999	0.05
		1.998		
		2		
		1.999		
3	2.3	2.298	2.298	0.86
		2.299		
		2.298		
		2.298		
4	2.5	2.498	2.498	0.08
		2.5		
		2.498		
		2.499		
5	2.8	2.799	2.798	0.07
		2.798		
		2.799		
		2.798		
6	3.2	3.198	3.198	0.06
		3.198		
		3.199		
		3.198		

Table 2. Percentage reduction in thickness

S. No	Strip Width	Avg. Initial Strip Thickness	Avg. Pipe Outside Dia.	Theor-etical Dia. r	% Stretch
1	129.5	1.7	43	41.24	4.09
2	129	2.6	42.9	41.08	4.24
3	128	2.9	43.1	40.76	5.42
4	127	3.6	42.8	40.44	5.5
5	126	4	42.9	40.12	6.4

Table 2. Percentage stretch in width for steel IS: 10748

S. No	Strip Width	Avg. Initial Strip Thickness	Avg. Pipe Outside Dia.	Theor-etical Dia. r	% Stretch
1	184.5	2	60.7	58.59	3.47
2	184	2.6	60.8	58.59	3.6
3	182	3.2	60.5	57.96	4.1
4	180	4	60.8	57.32	5.7
5	179	4.5	60.6	57	5.9

Table 3. Percentage stretch in width for steel IS: 6240

From the observation obtained Table 3, it has been observed that there is a considerable change in the width of sheet while forming. From the observation Table 4, it has been observed that there is a considerable change in the width of sheet while forming. From above it is cleared that there is negligible change in the thickness while a considerable change has been observed in width. This refers to a plain strain condition in which the strain in the circumferential direction is inversely proportional to the radius of the roller and is given by Equation 1.

$$\varepsilon_1 = n(1+\square t_0) = n\left(1+\frac{t_0}{aR}\right) \qquad (1)$$

Further for Roll forming process, this relation can be extended as shown in equation number 2:

$$\varepsilon_1 = n.1 + \frac{t_0}{a}\left(\frac{1}{R_1} + \frac{1}{R_2} + \frac{1}{R_3} + \cdots + \frac{1}{R_n}\right) \qquad (2)$$

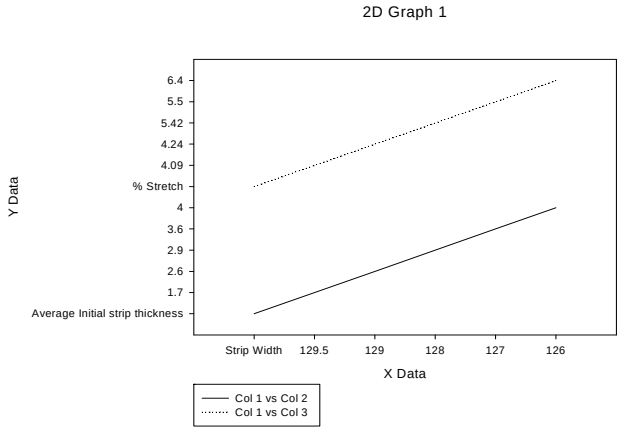

Fig. 5. Strip width Vs. Percentage Stretch and Initial thickness for steel IS: 10748

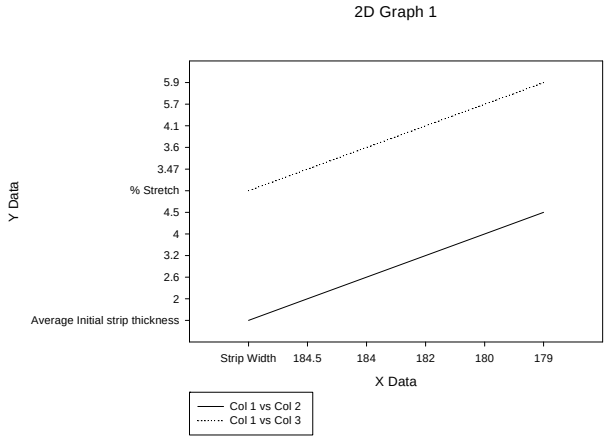

Fig. 6. Strip width Vs. Percentage Stretch and Initial thickness for steel IS: 6240

5. CONCLUSION

1. From the results of the study it has been concluded that there is negligible change in the initial thickness of a strip while forming/stretching over a roller. In other words, the strain in the thickness direction (radially outward from roller) is negligible.
2. The stretch in the width direction of the strip is increasing almost linearly with the increase in initial thickness. In other words the strain in circumferential direction is considerable.

From above two conclusions, it may be assumed that for the calculation of strain in width and thickness direction can be calculated on the basis of equation available in the plain strain conditions.

6. REFERENCES

[1] Steel Pipe from website http://www.madehow.com/Volume-5/Steel-Pipe.html asessed on 25.10.2014.

[2] Buckland, B.: An Introduction into the Production and Specification of Steel Pipe from website http://www.piledrivers.org/files/uploads/3074194E-A642-491F-A948-C6E81E04C1F5.pdf assessed on 25.10.2014.

[3] Fact Sheet: Pipe Manufacturing Process from website http://primis.phmsa.dot.gov/comm/FactSheets/FSPipeManufacturingProcess.htm assessed on 25.10.2014.

[4] Methods of manufacturing steel tubes and pipe from website http://www.jfe-21stcf.or.jp/chapter_3/3e_1.html assessed on 25.10.2014.

[5] Brensing, K.H., Sommer, B.: Steel tube and pipe manufacturing processes from website http://www.smrw.de/files/steel_tube_and_pipe.pdf assessed on 25.10.2014.

[6] Emmens, W.C., Boogaard, A.H. V.: Contact effects in bending affecting stress and Formability, International Journal of Material Forming, Volume Number 3(1), p.p. 1159-1162, 2010.

[7] Kasaei, M.M., Naeini, H.M., Tafti, R. A., Tehrani, M. S.: Prediction of maximum initial strip width in the cage roll forming process of ERW pipes using edge buckling criterion, Journal of Materials Processing Technology, Volume number 214 (2), p.p.1 90-199, 2014.

[8] Jiang, J., Li, D., Peng, Y., Li, J.: Research on strip deformation in the cage roll forming process of ERW round pipes, Journal of Material Processing Technology, Volume number 209 (10), p.p. 4850-4856, 2009.

[9] Fazeli, A.R., Ghoreishi, M.: Statical analysis of dimensional changes in thermomechanical tube spinning process, International Journal of Advanced Manufacturing Technology, Volume Number 52 (5-8), p.p. 597-607, 2010.

[10] Levy, B.S., Tyne, C.J.V., Stringfield, J.M.: Characterizing steel tube for hydroforming applications, Journal of Material Processing Technology, Volume number 150 (3), p.p. 280-289, 2004

[11] Molladavoudi, H.R., Djavanroodi, F.: Experimental study of thickness reduction effects on mechanical properties and spinning accuracy of aluminium 7075-O, during flow forming, International Journal of Advanced Manufacturing Technology, Volume number 52 (9-12), p.p. 949-957, 2011.

[12] Jiao, H., Zhao, X.L.: Material ductility of very high strength (VHS) circular steel tubes in tension, Thin walled structures, Volume number 39 (11), p.p. 887-906, 2001.

[13] Hashmi, M.S.J.: Aspects of Tube and Pipe manufacturing; meter to nanometer diameter, Journal of Material Processing Technology, Volume number 179 (1-3), p.p. 5-10, 2006.

[14] Trzepiecinski, T. , Gelegele, H.L.: Investigation of anisotropy problems in the sheet metal forming using finite element method, International Journal of Material Forming, Volume number 4 (4), p.p. 357-369, 2011.

[15] Walker, T.R., Pick, R.J.: Development in the geometric modeling of an ERW pipe skelp, Journal of Material Processing Technology Volume number 25(1), p.p. 35-54, 1991.

Authors:

***Harjit Singh Mangat, Assistant Professor,** Department of Mechanical Engineering, Baba Banda Singh Bahadur Engineering College, Fatehgarh Sahib, Punjab, India affiliated to Punjab Technical University, Kapurthala, Punjab, India ***(Corresponding Author)**

Gagandeep Singh Kohli, Assistant Professor, Department of Mechanical Engineering, Baba Banda Singh Bahadur Engineering College, Fatehgarh Sahib, Punjab, India affiliated to Punjab Technical University, Kapurthala, Punjab, India

E-mail: mangat84@gmail.com (Correspondence E-mail)
engg_kohli@yahoo.co.in

Journal of Production Engineering
Vol.17 No.2

Original Scientific Paper

Kovač P., Gostimirović M., Ješić D., Savković B., Kulundžić N.

THE ROLE OF MATERIAL QUALITY CONTROL IN MODERN MANUFACTURING

Received: 15 September 2014 / Accepted: 10 October 2014

Abstract: *Quality and characteristics of a material are important factor for successful manufacturing. Quality control of the material at the beginning of a production process is usually based on mechanical characteristics control and rarely on identification of structure and chemical composition. Measurement of tribological characteristics of materials (anti-frictional and anti-wear) and their abrasive resistance is still not performed in our country.*

Key words: *Block on Disk, friction force, EDM, nodular cast iron, Vikers piramide*

Merenje i kontrola kvaliteta materijala uslov za uspešnu proizvodnju. *Za uspešnu proizvodnju svakog proizvoda karakteristike i kvalitet osnovnog materijala su veoma važni. Kontrola kvaliteta osnovnog materijala koja se vrši na njegovom ulazu u proizvodni sistem obično se svodi na merenje mehaničkih karakteristika a redje na identifikaciju strukture i hemijskog sastava. Merenje triboloških svojstava materijala (antifrikcion i antihabajućih) kao i merenje njihove abrazivne otpornosti još uvek se ne vrši u industrijskim sistemima u našoj zemlji.*

Ključne reči: *Zaostali naponi, sila trenja, EDM, nodularni liv, Vikersova piramida*

1. INTRODUCTION

In larger industrial systems function of admission control of material is reduced to dimensional, mechanical and rarely on chemical control and structural characteristics [1]. This is performed in industrial systems which have adequate laboratories. In smaller and medium sized factories admission control is usually only quantity and dimension check. Very few cases are noticed that small and medium sized manufacturing companies are using university or institute laboratories for quality control of materials. This fact can be one of the reasons for various differences in product quality [2].

Assessment of tribological characteristics of the materials entering the production is not performed in domestic companies due to the lack of laboratory equipment. Also in domestic industry a systematic analysis of materials is not performed mostly because a procedure is much complex resp. lack of knowledge from this area. This paper presents the results of tribological properties assesment of specific group of materials [3, 4].

2. MEASUREMENT OF ANTIFRICTION CHARACTERISTICS OF MATERIALS

Determination of antifriction properties of material is performed by measuring friction forces in the contact zone with another material during presence of lubricant as the third element in contact. As it is known friction force is the resistance of one solid body movement on another with presence of a normal load [5].

Antifriction characteristics of material depends on conditions under which that contact is achieved (sliding, rolling, impact…) and contact geometry (contact in point, line or surface). This means that friction force as an anti-friction characteristic of a material can have different values. Because of this, antifriction characteristic is considered to be relative value.

Measurement of friction and determination of friction coefficient is performed on tribometers which have the possibility to achieve all three types of contact under different conditions meaning sliding speed and load.

Example of tribometer from family ″Block on Disk″ is shown on Fig. 1.

Fig.1 Tribometer ″Block on Disk″ TPD 2000

On fig. 2, 3, 4 shows the types of possible contacts for “Blok on Disk” metod.

Fig.2 Contact on line

Fig.3 Contact at the point of

Fig.4 contact the surface

Measuring instruments of mentioned type (tribometers) are connected with personal computer. Through this is, with help of adequate software, monitored friction process and measured friction force, auxiliary load and coefficient of friction.
On Fig. 5 and Fig. 6 are shown examples of measurement results performed on Tribometer TPD 2000 during program of defining tribological characteristics of a group of nodular cast iron in contact with EN-GJL-250 and steel C45.

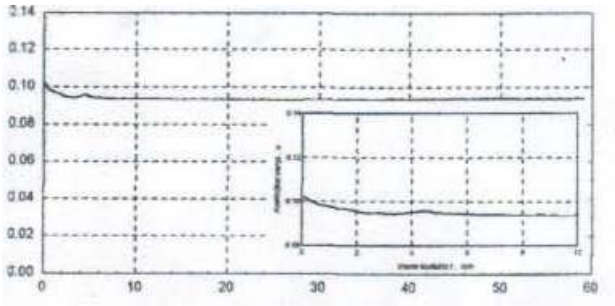

Fig.5 Experimental dependence μ-$f_1(t)$ Contact: EN-GJS-600-3/ steel C45

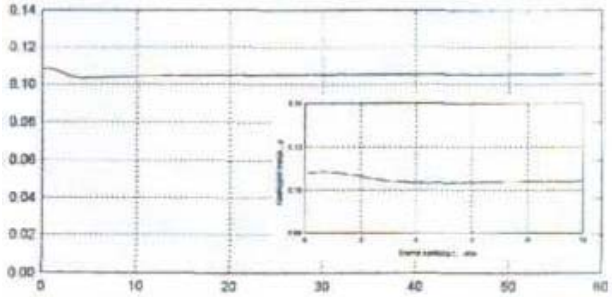

Fig.6 Experimental dependence μ-$f_2(t)$ Contact: EN-GJS-600-3/ steel C45.

Friction coefficient in contact zone of nodular cast iron EN-GJS-600-3 and steel C45 was measured to be 0,095. In contact zone of nodular cast iron EN-GJS-600-3 and nodular cast iron EN-GJL-250 coefficient of friction was greater with value 0,105.
Both experiments were performed under normal load of 200 N, sliding speed 2 m/s with lubricant HVL-22 manufactured by Rafinerija Modrica [6].
By comparing the friction coefficient values of both cases a conclusion is made about differences in tribological characteristics of tested materials.

3. ABRASIVE RESISTANCE MEASUREMENT OF MATERIALS

Presence of abrasive mechanism in industry and transport can be found in almost 60% of tribomechanical systems. Contact surfaces of many machine and devices parts are coated with various types of coatings so the overall abrasive resistance of critical part of tribomechanical system is increased. Measurement of coatings and other material abrasive resistance is performed on measuring system called Scratch tester. Measuring methodology is based on forming of scratches on contact surface of element which resistance is about to be measured [7].
On Fig. 7 domestic Scratch tester ST-99 is shown together with the principle of measurement.

Fig.7 Scratch tester ST-99

Measurement of abrasive resistance can be performed on two ways.
First is to vary normal load from zero to maximum value, starting from establishing the contact between the tip of the tool (Vikers piramide) made from cemented carbide and surface of the part which is to be measured.

Maximum force is chosen according to material or coating type and will usually range from 20 N for soft materials up to 200 N for hard materials.
Second way to measure abrasive resistance is to hold the normal load constant during experiment.
Software which is responsible for machine operation and monitoring of phenomena during experiment allows the choice of different sliding speeds and variation of normal force.
On fig.8 and fig.9 result of scratch tests are shown.

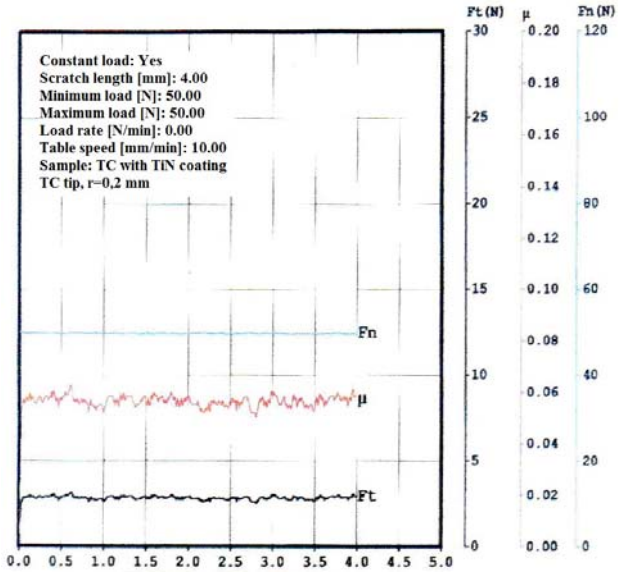

Fig. 8. Result of horizontal scratch tester displasment

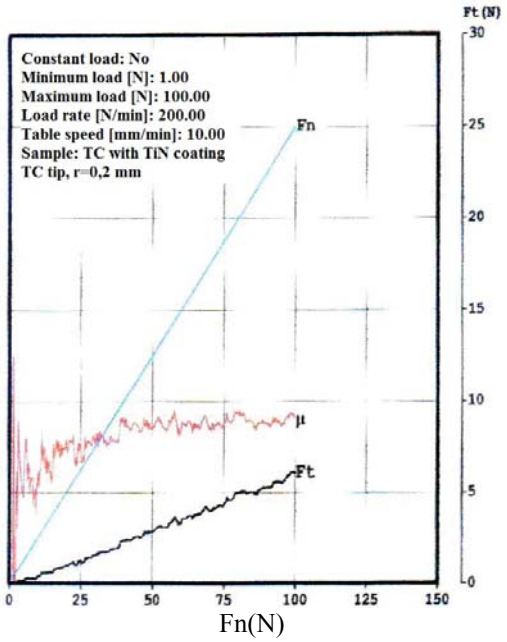

Fig. 9. Result of scratch tester force

4. EXAMINATION OF MATERIALS MACHINABILITY

Analyzing the status of production technologies application in contemporary manufacturing, conclusion can be made that widest area of industrial application belongs to the technology of material removal. This specific technology covers conventional and nonconventional material forming by material removal. Conventional processes of material removal are based on chip forming with hard tool of specific geometric shape. Nonconventional machining is performed by material removal with various physical-chemical mechanisms.

4.1. Term of Material Machinability

Contemporary manufacturing is putting an accent on development of new and high-quality products made by various materials with different properties. There is a prevailing trend to use more and more materials with high mechanical, metallurgical, tribological and physical-chemical properties. In order to implement these materials into everyday use, one of the most important research directions is to determine technological characteristics of the machining process, which is finding a data and functions about machinability of materials. This is about functional dependencies in relation with: manufacturing procedure, elements of procedure parameters, construction and geometry of the tool and other machining conditions which are responsible for convenient machining.

Machinability of materials is a complex term which defines the ability of the machining process to machine the part by economic methods. Defining the machinability of materials is a complex task due to multiple factors and their interactions. The most influential factors are:

- Metalurgical characteristics
- Technological characteristics
- Techno-economical characteristics

Defining of the material machinability is implemented through array of functional characteristics of a machining process with which can be directly or indirectly assessed machining suitability of a material. Since the machining process with chip removal is complex, there is no specific definition of a suitability material for machining, but it is assessed based on multiple criterions resp partial functions of machinability.

4.2 Material Machinability by Electroerosion

Electrical discharge machining (EDM) is a material removal procedure which can be used to machine all electro conductive materials regardless on their physical-metalurgical properties. But not all electro conductive materials are machined equally efficiently so each of them has its own characteristic EDM machinability. As an indicator can be taken different criteria such as: erosion speed, quality of machined surface, wear of electrode-part, specific energy consumption etc.

Material removal in EDM is performed by periodic transformation of electric energy into heat, during which a local meltdown is caused and evaporation of material as a consequence. Basic parameters which define process of material removal are electric impulse parameters resp. energy of impuls.

Research regarding machinability by EDM in industrial conditions, depending on electric impulse parameters, are performed by Gostimirovic et al. [8]. On Fig. 10 is shown a systematic dependency of basic technological parameters from impulse energy, as a groundwork for selection of optimal parameters electrical impulse in EDM.

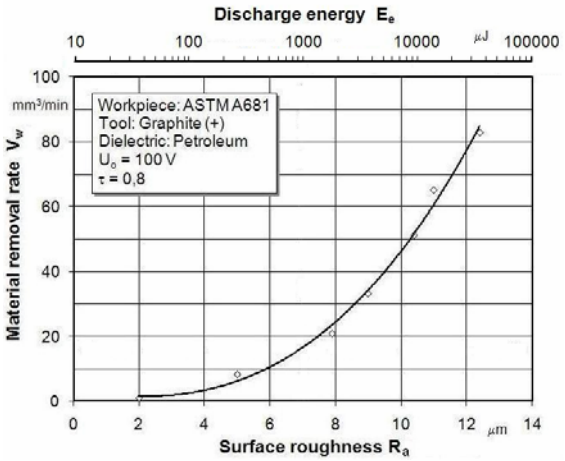

Fig.10 Dependency of EDM productivity on roughness of machined surface in function of impulse energy

With installation of EDM machine in Laboratory for machining processes by chip removal on Faculty of Technical Sciences in Novi Sad – Serbia, conditions are met for detail laboratory investigation of machinability by EDM. Specific machine is a CNC die sink electrical discharge machine, type Agie Charmilles SP 1U Fig. 11 Technical specifications of the EDM machine: axis travel X/Y/Z 320x250x250 mm, max. workpiece dimensions 790x480x235 mm, electrode weight 60 kg, machining current 50 A, max. removal rate 330 mm3/min and best surface finish 0,3 μm.

Investigation of machinability will be performed based on availability of copper/graphite-steel technologies and copper/copper tungsten-carbide but also for specific types of part material and tools with defined characteristic and quality.

Fig.11. CNC die sink EDM machine, type Agie Charmilles SP 1U

Metallographic investigations show that there is heat affected zone and a recast layer (white layer) at low and high discharge energies, Fig. 12. The recast layer manifests through uneven thickness, microstructure transformations and a modified microhardness compared to the bulk material. That means that for all cases of EDM, for longer or shorter intervals, the surface layer temperature exceeded the temperature of previous tempering, which equals 520°C for the tool steel AISI 02 (62 HRc) examined in these investigations.

The analysis of typical metallographic photos reveals four characteristic layers: melted layer, hardened layer, interface layer and tempered layer (Fig. 12). The melted layer is a sludge of lightly welded particles, which is a residue left after the ejection of melted material from the crater. The hardened layer consists of martensite, residual austenite and cementite. The interface layer consists of martensitic-austenitic grid and cementite, where the ratio of austenite diminishes with the distance from the tempered layer. The microstructure of the tempered layer is tempered martensite and cementite, which gradually phase into basic microstructure consisting of martensite with fine globular cementite [8].

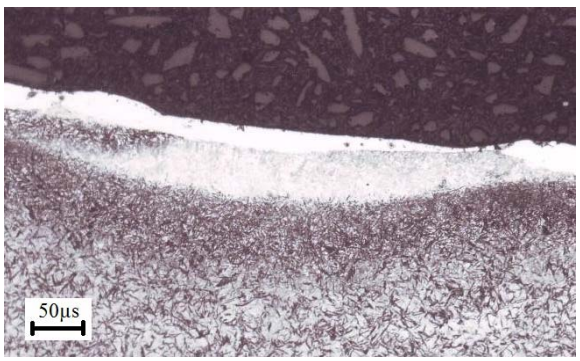

Worpiece: AISI 02; Tool: Cu 99,9% (+); Dielectric: Petroleum; U_O=100V; τ=0,8; t_i=10µs; I_e=9A

Fig. 12 Metallographic photos of recast layer for tool steel after EDM

5. CONCLUSION

Quality control of materials and coatings, from tribological aspects, can be performed only with instruments which can support reliable measurements of friction forces resp. coefficient of friction in specific time of experiment duration and performing scratch tester.

Unfortunately this type of measuring instruments is not often represented in our country, not only in industry but also in laboratories of institutes and universities.

6. REFERENCES

[1] Adedayo, S. M., Adeyemi, M. B. Effect of Preheat on Residual Stresses Distribution in Arc-welded Mild Steel Plate, Journal of Materials Engineering and performance. Vol. 9, p.p. 7-11, 2000.

[2] Golubović D., Kovač P., Ješić D., Gostimirović M., Pucovski (Pucovsky) V.: Wear Intensity of Different Heat Treated Nodular Iron, Metalurgija, 2012, Vol. 51, No 4, pp. 518-520

[3] Golubovic D., Kovac P., Jesic D., Gostimirovic M.: Tribological properties of adi material, Journal of the Balkan Tribological Association, Vol 18, No 2, pp. 165-173, 2012.

[4] Ješić D.: MERNA TEHNIKA, Univerzitetski udžbenik, Banja Luka, 2004.

[5] Kovac P., Mankova I., Gostimirovic M., Sekulic M., Savkovic B.: A review of machining monitoring systems, Journal of Production Engineering, Vol 14, No 1, pp. 1-6, 2011.

[6] Ješić, D., Pulić, J., Kovač, P., Savković, B., Kulundžić, N.: Application of nodular castings in the modern industry of tribo-mechanical systems today and tomorrow, Journal of Production Engineering, Vol 17, No 1, pp. 55-58, 2014.

[7] Golubovic D., Kovac P., Savkovic B., Jesic D., Gostimirovic M.: Testing the tribological characteristics of nodular cast iron austempered by a conventional and an isothermal procedure, Materiali in tehnologije, Vol 48, No 2, pp. 293-298, 2014.

[8] Gostimirovic, M., Kovac, P., Sekulic, M., Skoric, B.: Influence of discharge energy on machining characteristics in EDM, Journal of Mechanical Science and Technology, Vol. 26, No 1, pp.173–179, 2012.

Authors: **Prof. Kovac Pavel PhD[1], Prof. Gostimirovic Marin PhD[1], Prof. Ješić Dusan PhD[2], Assist. Savkovic Borislav, M.Sc.[1], Kulundzic Nenad, M.Sc.[1]**

[1]University of Novi Sad, Faculty of Technical Sciences, Institute for Production Engineering, Trg Dositeja Obradovica 6, 21000 Novi Sad, Serbia, Phone.: +381 21 450-366, Fax: +381 21 454-495.

E-mail: pkovac@uns.ac.rs, savkovic@uns.ac.rs nenadts@gmail.com

[2]Tribotehnik, Croatia, Titov trg 6/4, 51000 Rijeka

***Note*: This paper presents a part of researching at the CEEPUS project and Project number TR 35015.**

Journal of Production Engineering
Vol.17 No.2

Original Scientific Paper

R.K.Suresh., P.Venkataramaiah., G. Krishnaiah

MULTI RESPONSE OPTIMIZATION IN TURNING OF AISI 8620 ALLOY STEEL WITH CVD TOOL USING DFA AND GRA- A COMPARITIVE STUDY

Received: 20 October 2014 / Accepted: 10 November 2014

Abstract: *In the present day scenerio of manufacturing industry, quality and productivity play a significant role. Surface roughness and material removal rate are indicators of quality and productivity. Hence surface roughness and material removal rate are considered as response characteristics. This article focusses on an approach based on Grey relational analysis and Desirability function analysis for optimizing the process parameters during turning of AISI 8620 alloy steel with CVD coated tool with multiple performance characteristics. Experimentation were carried out on a CNC lathe using L9 orthogonal array based on Taguchi design of experiments. The influence of spindle speed, feed and depth of cut were analysed on the performance of surface roughness and material removal rate. The optimal turning parameters are determined by composite desirability index and grey relational grade. Analysis of variance (ANOVA) is used to determine the influence of parameters which significantly affect the responses. From the study, it is concluded that machining performance is significantly improved.*

Key words: *AISI 8620 alloy steel, CVD coated tool,Surface roughness, Material removal rate, Grey relational analysis, Desirability function nalysis, ANOVA, CNC lathe*

Optimizacija višestrukih odaziva kod struganja legiranog čelika AISI 8620 sa CVD presvučenim alatom korišćenjem DFA i GRA – poređenje metoda. *U današnje vreme u industriji, kvalitet i proizvodnost igraju značajnu ulogu. Zbog toga se površinska hrapavost i proizvodnost smatraju odazivnim parametrima. U ovom radu se fokusira na pristup zasnovan na Grejevoj relacionoj analizi (GRA) i analizi funkcije povoljnosti (DFA) za optimizaciju parametara procesa pri struganju legiranog čelika AISI 8620 sa CVD presvučenim alatom i višestrukim osobinama učinka. Eksperimenti su sprovedeni na CNC strugu korišćenjem L9 ortogonalnog plana Tagučijevog planiranja eksperimenta. Analiziran je uticaj broja obrtaja vratila, pomaka i dubine rezanja na promenu površinske hrapavosti proizvodnosti. Optimalni parametri struganja su određeni pomoću „composite desirability index" i „grey relation grade". Analiza ANOVA se koristi za određivanje uticaja parametara koji značajno utiču na odazive. Ova stuija je dovela do zaključka da su se porformanse obrade značajno poboljšale.*

Ključne reči: *AISI 8620 legura čelika, CVD presvučen alat, hrapavosti površine, proizvodnost, Grejeva relaciona analiza, analiza funkcije povoljnosti, ANOVA, CNC strug*

1. INTRODUCTION

The important goal in the modern industries is to manufacture the product with lower cost and with high quality in short span of time. There are two main practical problems that engineers face in a manufacturing process, the first is to determine the product quality (meet technical specifications) and the second is to maximize manufacturing system performance using the available resources. The challenge of modern machining industry is mainly focused on achievement of high quality ,in terms of work piece dimensional accuracy, surface finish ,high production rate, less wear on the cutting tools ,economy of machining in terms of cost saving and increase the performance of the product with reduced environmental impact. Today metal cutting process places major portion of all manufacturing rocesses .Within these metal cutting processes the turning operation is the most fundamental metal removal operation in the manufacturing industry. Increase in productivity and the quality of the machined parts are the main challenges of metal based industry. There has been increased interest in monitoring all aspects of machining process. Surface finish and material removal rate are two important parameters are need to be considered in manufacturing industry to ensure aesthetic appeal to the product as well as improved productivity. Surface roughness has become the most significant technical requirement and is an index of product quality in order to improve the tribological properties, fatigue strength, corrosion resistance and aesthetic appeal of the product reasonably good surface finish is required. Now a day's manufacturing industries especially concerned to dimensional accuracy and surface finish. In order to obtain better surface finish and increased material removal rate, proper setting of cutting parameters is crucial before the process takes place factors such as spindle speed ,feed rate, depth of cut that control the cutting operation can be set up in advance . values of process parameters that will yield the desire In the present work, AISI 8620 alloy steel was selected as work material which finds applications in the manufacture of gears. pinions, lay shaft, cam shafts, mining haulage, cage suspensions, lifting gears, fasteners, chains and many more.For the purpose of experimentation, factorial design experiments are considered as per Taguchi DOE. By

advocating Taguchi design, a clear understanding of the nature of variation and economical consequences of quality engineering in the world of manufacturing can be clearly got through. In the present study, Desirability function analysis and Grey relational analysis were performed to combine the multiple performance characterstics in to one numerical score which is an indicative of the optimal process parameter setting. Analysis of variance (ANOVA) is also performed to investigate the most inflencing parameters on the surface roughness and material removal rate.

2. LITERATURE REVIEW

W.H.Yang & Y.S Tang [1] envisages that the Taguchi method is a powerful tool to design optimization for quality and is used to find the optimal cutting parameters for turning operations. An orthogonal array , the signal to noise ratios and ANOVA are employed to investigate the cutting characteristics of S45C steel bars using Tungsten carbide cutting tools. Through this study, not only optimal cutting parameters for turning operations obtained, but also the main cutting parameters that affect the cutting performance in turning operations are found.

M.P. Jenarthanan & R. Jeyapaul [2] presents a new approach for optimizing machining parameters on milling glass-fibre reinforced plastic(GFRP) composites. Optimization of parameters was done by an analysis called desirability function analysis(DFA) which is a useful tool for optimizing multi response problems. A composite desirability value is obtained for multi- responses viz., surface roughness. Delamination factor and machining force using individual desirability values from DFA. Based on composite desirability value, the optimum levels of parameters have been identified and significant contribution of parameters is determined by analysis of variance.

T.Saravanan & R. Udaykumar [3] presents the machining of hybrid metal matrix using a mediumduty lathe. The optimum machining parameters have been identified by a composite desirability value obtained from desirability function analysis as the performance index and significant contribution of parameters can then be determined by analysis of variance.

P.S. Kao & H.Hocheng [4] explains the usefulness of Grey relational analysis for multi-input, discrete data and experimental study. Developed an application of grey relational analysis for optimizing the electropolishing of 316L stainless steel with multiple performance characteristics. The processing parameters(temperature, current density and electrilyte composition) are optimized with consideration of the multiple performance characteristics(surface roughness and passivation strength). The conducted experiments approve the effectiveness of the grey relational analysis.

S.Khalilpourazary etal [5] depicts the influencing parameters such as cutting speed, feed rate, depth of cutand tool rake angle on surface roughness and tool life. ST37 steel and M1 high speed steel (HSS) were selected as workpiece material and tool respectively.Grey relational analysis was performed to elicit the optimal values for the mentioned data. To achieve this, grey relational generating, grey relational coefficient and grey relational grade are calculated step by step. Finally it was shown that ST37 led to higf surface quality and tool life.

R.K.Suresh, P.Venkataramaiah and G.Krishnaiah [6] envisages an experimental investigation on turning of AISI 8620 alloy steel using PVD coated cemented carbide CNMG inset. Nine experimental runs based on Taguchi factorial design were performed to find out optimal cutting level condition. The main focus of present experimentation is to optimize the process parameters namely spindle speed, feed and depth of cut for desired response characteristics i.e. surface roughness, VMRR and interface temperature. To study the performance characteristics in this work orthogonal array (OA), analysis of means (ANOM) and analysis of variance(ANOVA) were employed.The experimental results showed that the spindle speed affects more on surface roughness, feed affects more on VMRR and feed affects more on interface temperature. Confirmation tests also been performed to predict and verifythe adequacy of models for determining optimal values of response characteristics.

M.Y Wang & T.S. Lan [7] presents Orthogonal array of Taguchi experiment where in four parameters like cutting speed, feed rate, tool nose run off with three levels in optimizing the multi-objective such as surface roughness, tool wear and material removal rate in precision turning on CNC lathe.For the purpose of multi resonse optimization, Grey relational analysis was employed.

Bala Murugan Gopalsamy, etal [8] deals with experimental investigations carried out for machinability study of hardened steel and to obtain optimumprocess parameters by Grey relational analysis. An orthogonal array, grey relations, grey relational coefficients and analysis of variance are applied to study the performance characteristics of machining process parameters such as cutting speed, feed, depth of cotand width of cut with consideration of multiple responses i.e., volume of material removed, tool wear and tool life.

From the literature survey, it is evident that no work has been reported on AISI 8620 alloy steel work with combination of CVD coated tool. Also little work has been reported on Desirability functin Analysis and Grey relational analysis simultaneously on various machining operations. Hence the experimentation is done on above said combination of work piece and tool and optimization method-Desirability function analysis and Grey relational analysis are put forth.

3. EXPERIMENTATION

In the present study, three turning parameters were selected with three levels os shown in Table.1. The experimentation was carried out using L9 orthogonal array based on Taguchi design of experiments. The work material selected for this experiment is AISI 8620 alloy steel of 30 mm diameter, length 215 mm. The

chemical composition of AISI 8620 alloy steel is given in Table.2.

Element	carbon	silicon	Mn	Ni	Cr	Mo	S	P
% composition	0.18-0.23	0.3-0.6	0.6-0.1	0.4-0.7	0.4-0.6	0.15-0.25	0.04	0.035

Table 1.

Turning parameters	Level 1	Level 2	Level 3
Spindle speed,S(rpm)	450	580	740
Feed, F(mm/rev)	0.05	0.07	0.09
Depth of cut, D(mm)	0.10	0.20	0.25

Table 2.

The turning tests were carried out on FANUC series OI Mate-TD(Super jobber 500) CNC lathe machine to determine the surface roughness and material removal rate for various runs of experiment. Surface roughness is measured using stylus type surface roughenn tester "Mitutoyo Surfest SJ-201P".The material removal rate (mm^3/min) is calculated using formula:

$MRR = [\pi/4(D_1^2-D_2^2)L]/t \ mm^3/min$

Where,

D_1 = Diameter of the work piece before turning.mm

D_2 = Diameter of the work piece after turning.mm

L = Length of turning, mm

t = Machining time, min

4. METHODS USED

Desirability Function Analysis:

Desirability function analysis is widely accepted method used in manufacturing industry. Desirability function analysis is used to convert multi response characteristics in to single response characteristic. Derringer and suich [9] popularized the concept of DFA as a simultaneous optimization technique which proved to be useful in solving multi response optimization problems. In view of this, complicated multi response characteristics can be converted in to single response characteristic which is termed as composite desirability. In the present study, multi responsed such as surface roughness and material removal rate are combined as composite desirability using desirability function analysis

The steps involved in the optimization process are detailed as follows

Step 1: The first step isto calculate desirability index(d_i) for each of the process parameters i.e surface roughness and material removal rate. The desirability index values are tabulated. It is calculated based on the desirability function shown in equations (1) and (2) respectively for the cases smaller is better and larger is better. In this study, surface roughness need tobe minimized and material removal rate need to be maximized.

Step 2: The second step is to evaluate the composite desirability based on equation (3)

Step 3: The third step is to determine optimality condition based on highest composite desirability index. Also the ranking of process parameters is estimated.

Step 4: The next step is to perform ANOVA by which contribution made by each parameter influencing the combined objective is estimated

Step 5: The last stage is to calculate the values from confirmity test based on optimum level of parameters is found out.

For smaller is better,

$$d_i = \frac{y_i - y_{\max}}{y_{\min} - y_{\max}} \qquad (1)$$

For larger is better,

$$d_i = \frac{y_i - y_{\min}}{y_{\max} - y_{\min}} \qquad (2)$$

where

d_i - is desirability index for a particular level

y_i - is i^{th} normalized value

y_{min} - is minimum of particular column values(response characteristic)

y_{max} - is maximum of particular column values(response characteristic)

$$d_c = \sqrt[w]{d_1^{w1} d_2^{w2} d_3^{w3} \ldots d_n^{wn}} \qquad (3)$$

where

w_1 and w_2 are the weights assigned. Since both surface roughness and material removal rate plays a significant role in machining operation, equal weightages are assigned ($w_1 = 0.5$ and $w_2 = 0.5$)

Grey relational analysis:

In the procedure of GRA, the experimental result of MRR and TWR are normalized at first in the range between zeros to one due to different measurement units. This data pre-processing step is termed as 'grey relational generating'. Based on the normalized experimental data, grey relational coefficient is calculated to correlate the desired and actual experimental data using equation (4). The overall Grey Relational Grade (GRG) is determined by averaging the grey relational coefficient corresponding to selected responses using equation (5). This approach converts a multiple response process optimization problem into a single response optimization by calculating overall grey relational grade. The normalized experimental results can be expressed as follows.

For larger is better,

$$xi(k) = \frac{yi(k) - \min yi(k)}{\max yi(k) - \min yi(k)}$$

For smaller is better,

$$xi(k) = \frac{\max yi(k) - yi(k)}{\max yi(k) - \min yi(k)}$$

Where

$\max yi(k)$ and $\min yi(k)$ are the largest and smallest values of $yi(k)$ respectively

The Grey relational coefficient ξ(k) for $yi(k)$ is calculated as

$$\xi(k) = \frac{\Delta \min + \psi \Delta \max}{\Delta oi(k) + \psi \Delta \max} \qquad (4)$$

where

$\Delta oi(k)$ is reference sequence deviation which is equal to mod $(\max yi(k) - \min yi(k))$

ψ is a distinguishing coefficient which varies from 0 to 1, the value of ψ is set as 0.5 to maintain equal weightage of surface roughness and material removal rate.

Greyrelationalgrade,

$$\gamma i = \frac{1}{n}\sum_{i=1}^{n} \xi i(k) \qquad (5)$$

5. RESULTS

A series of turning tests were conducted to assess the effect of turning parameters on surface roughness and material removal rate and the resuts of experimentation are shown in table 3.

SNo	Spindle speed (rpm)	Feed (mm/rev)	Doc (mm)	Surface roughness (µm)	Material removal rate (mm^3/min)
1	450	0.05	0.10	1.2130	51.870
2	450	0.07	0.20	1.1250	288.613
3	450	0.09	0.25	0.9678	476.167
4	580	0.05	0.20	1.3120	261.906
5	580	0.07	0.25	1.2250	541.901
6	580	0.09	0.10	1.0950	206.916
7	740	0.05	0.25	1.1967	407.997
8	740	0.07	0.10	1.2860	226.108
9	740	0.09	0.20	1.0882	544.693

Table 3. Experimental data and results for 3 parameters, corresponding Ra and MRR for CVD tool

Tables 4,5.6,7,8, 9 and 10 depicts the results related with Desirability function analysis and Grey relational analysis.

Expt No	Normalized values (SR)	Normalized values (MRR)	Weighted desirability index (SR)	Weighted desirability index (MRR)	Composite desirability	Rank
1	0.2876	0.0000	0.5363	0.0000	0.0000	9
2	0.5433	0.4804	0.7371	0.6931	0.5109	3
3	1.0000	0.8609	1.0000	0.9278	0.9278	1
4	0.0000	0.4262	0.0000	0.6528	0.0000	8
5	0.2528	0.9943	0.5028	0.9971	0.5013	4
6	0.6304	0.3146	.7939	0.5609	0.4453	6
7	0.3349	0.7226	0.5739	0.8501	0.4919	5
8	0.0755	0.3536	0.2748	0.5946	0.1634	7
9	0.6502	1.0000	0.8063	1.0000	0.8063	2

Table 4. Evaluated results of composite desirability

Process parameters	Average composite desirability				
	Level 1	Level 2	Level 3	Max-Min	Rank
Spindle speed (S)	0.4796	0.3155	0.4870 *	0.1715	3
Feed(F)	0.1639	0.3918	0.7264 *	0.5625	1
Depth of cut (D)	0.2029	0.4391	0.6403 *	0.4374	2
Total mean value of the composite desirability = 0.4274 *Optimum levels					

Table 5. Response table for composite desirability

Source of variation	Degrees of freedom	Sum of squares	Mean sum of squares	F-ratio	Percent contribution
Spindle speed	2	0.056393	0.0281965	0.5922	6.667
Feed	2	0.409946	0.204973	4.3049	48.465
Depth of cut	2	0.284285	0.1421425	2.98537	33.609
Error	2	0.095226	0.047613		11.258
`	8				100.000

Table 6. ANOVA based on Composite desirability

Expt No	Experimental data		Normalized values		Grey relational coefficient		GRG	Rank
	SR	MRR	SR	MRR	SR	MRR		
1	1.2130	51.870	0.2876	0.0000	0.4124	0.3729	0.3729	9
2	1.1250	288.613	0.5433	0.4804	0.5226	0.5065	0.5065	5
3	0.9678	476.167	1.0000	0.8609	1.0000	0.8912	0.8912	1
4	1.3120	261.906	0.0000	0.4262	0.3333	0.3995	0.3995	7
5	1.2250	541.901	0.2528	0.9943	0.4009	0.6948	0.6948	3
6	1.0950	206.916	0.6304	0.3146	0.5749	0.4984	0.4984	6
7	1.1967	407.907	0.3349	0.7226	0.4292	0.5362	0.5362	4
8	1.2860	226.108	0.0755	0.3536	0.3510	0.3934	0.3934	8
9	1.0822	544.693	0.6502	1.0000	0.5884	0.7942	0.7942	2

Table 7. Grey relational analysis for surface roughness and material removal rate

Process parameters	Average relational grade				
	Level 1	Level 2	Level 3	Max-Min	Rank
Spindle speed(S)	0.5902*	0.5309	0.5746	0.0593	3
Feed (F)	0.4362	0.5315	0.7279*	0.2917	1
Depth of cul(D)	0.4216	0.5667	0.7074*	0.2858	2
Total mean value of the Grey relational grade = 0.5652 *Optimum levels					

Table 8. Response table for Grey relational grade

Source of variation	Degrees of freedom	Sum of squares	Mean sum of squares	F-ratio	Percent contribution
Spindle speed	2	0.00567	0.00284	0.4788	2.078
Feed	2	0.13270	0.06635	11.2077	48.644
Depth of cut	2	0.12259	0.06129	10.3520	44.937
Error	2	0.01184	0.00592		4.340
`	8	0.27280			100.000

Table 9. ANOVA based on Grey relational grade

Prediction at optimum levels

The objective of the prediction at optimum levels is to validate the conclusions drawn during the analysis phase. Once the optimal level of process parameters is selected, the next step is to verify the improvement in response characteristics using optimum level ofparameters. A confirmity test is conducted using the following equation:

$$\gamma = \gamma_m + \sum_{i=1}^{n} \gamma i - \gamma_m ,$$

where is:

γ_m - is total mean of the required responses

γi - is the mean of the required resposes at optimum level

n - is the number of process parameters that significantly affects the multiple perfrmance characteristics

GRA	Optimum process parameters		
	Intial process parameters	Predicted values	Experimental values
Level of parameters setting	S1-F1-D1	S1-F3-D3	SI-F3-D3
Surface roughness (μm)	1.213	0.946	0.9678
MRR (mm^3/min)	51.870	285.439	476.167
Grey relational grade	0.3729	0.8951	0.8912
DFA			
Level of parameters setting	S1-F1-D1	S3-F3-D3	S3-F3-D3
Surface roughness (μm)	1.213	0.98986	0.9453
MRR (mm^3/min)	51.870	406.155	426.868
Composite desirability	-	0.9992	0.94924

Table 10. Comparison of predicted and Experimental results using GRA and DFA

6. CONCLUSIONS

➢ **Grey relational analysis**

1. The optimal parameters setting with Grey relational analysis lies at 450 rpm spindle speed, 0.09 mm/rev feed and 0.25 mm depth of cut. The optimum predicted value for surface roughness is 0.946μm, MRR 285.439 mm^3/min and grey relational grade is 0.895. Also the experimental value for surface rougness is 0.9678 μm, MRR is 476.167 mm^3/min and grey relational grade is 0.8912.

2. In case of Grey relational analysis, it is found that both predicted and experimental respnse characteristics are better as compared to initial machining parameters. To be specific predicted surface roughness(0.946µm) and experimental surface roughness (0.9678µm) are very much lower than surface roughness at initial setting level. Also predicted MRR (285.439 mm^3/min) and experimental MRR(476.167 mm^3/min) are much higher as compared to MRR at initial setting leval. It may be noted that there is a good agreement between the predicted GRG (0.8951) and experimental GRG(0.8912) and therefore the condition **S1-F3-D3** of process parameters combination was trested as optimal. Further significant improvement in machinability is observed and measured that there is 20.2% improvement in surface roughness(Experimental value), 22% improvement in surface roughness (Predicted value) as compared with initial machining parameters and at the same time there is a substantial incresed in MRR (both experimental and predicted) as compared with initial setting. This encourages applying Grey relational analysis for optimizing multi response problems.
3. Further, from Analysis of variance (ANOVA) depicts that feed is the most significant parameter followed by depth of cut affecting multi response characteristics with feed 48.64%, depth of cut 44.94% and speed 2.08% respectively

➢ **Desirability function analysis**

4. The optimal parameters setting with Desirability function analysis lies at 740 rpm spindle speed, 0.09 mm/rev feed and 0.25 mm depth of cut. The optimum predicted value for surface roughness is 0.98986µm, MRR 406.155 mm3/min and composite desirability is 0.9992. Also the experimental value for surface rougness is 0.9453 µm, MRR is 426.868 mm^3/min and composite desirability is 0.9492
5. In case of Desirability function analysis, it is found that both predicted and experimental respnse characteristics are better as compared to initial machining parameters. To be specific predicted surface roughness(0.98986µm) and experimental surface roughness (0.9453µm) are very much lower than surface roughness at initial setting level. Also predicted MRR (406.155 mm^3/min) and experimental MRR(426.868 mm^3/min) are much higher as compared to MRR at initial setting leval. It may be noted that there is a good agreement between the predicted Composite desirability (0.9992) and experimental Composite desirability(0.9492) and therefore the condition **S3-F3-D3** of process parameters combination was trested as optimal. Further significant improvement in machinability is observed and measured that there is 22% improvement in surface roughness(Experimental value), 18.4% improvement in surface roughness(Predicted value) as compared with initial machining parameters and at the same time there is a substantial incresed in MRR (both experimental and predicted) as compared with initial setting. This encourages applying Composite desirability analysis for optimizing multi response problems.
6. Further, from Analysis of variance(ANOVA) depicts that feed signifies the most followed by depth of cut affecting multi response characteristics with feed 48.46%, depth of cut 33.60% and spindle speed 6.67% respectively

7. REFERENCES

1. W.H Yang & Y.S Tang, Design optimization of cutting parameters based on Taguchi method, Journal of Materials processing Technology 84(1998) 122-129
2. M.P. Jenartanan and R.Jeyapaul,Optimization of machining parameters on milling of GFRP composites by desirability function analysis using Taguchi method, International journal of Engineering, science and Technology, vol.5, No.4, 2013, pp.23-36
3. T.Saravanan and R. Udaykumar, Optimization of machining hybrid matal matrix composites using Desirability Analysis, Middle-East Journal of Scientific Research15(12), 2013
4. P.S. Kao and H.Hocheng, Optimization of electrochemical polishing of stainless stees by grey relational analysis, Journal of Materials processing Technology 140(2003) pp.255-259
5. S.Khalilpourazary, P.M.Kshtiban and N.Payam, Optimizing turning operation of St37 steel using grey relational analysis, Journal of Computational and Applied research in Mechanical Engineering, Vol.3, No.2, Spring 2014, pp.135-144
6. R.K.Suresh, P.Venkataramaiah and G.Krishnaiah, Experimental investigation for finding optimum surface roughness, VMRR and interface temperature during turning of AISI 8620 alloy steel using CNMG insert, International Jornal of current Engineering and Technology, Vol.4, No.4, 2014
7. M.Y. Wang and T.S. Lan, Parametric optimization on multi-objective precision turning using Grey relational analysis, Information Technology Journal 7(7), 2008, pp.1072-1076
8. Bala Murugan Gopalsamy, Biswanth Mondal and Sukamal Ghosh, Optimization of machining parameters for hard machining: grey relational theory approach and ANOVA, Int. J. Manufacturing Technology(2009) 45, pp.1068-1086.
9. D.C. Montgometry, Design and analysis of experiments, 4th edition, New York: Wiley; 1997.

Authors:

R.K.Suresh[1], P.Venkataramaiah[2], G.Krishnaiah[3]

[1]Department of Mechanical Engineering, Srikalahasteeswara Institute of Technology, Srikalahasti, India,

[2,3]Department of Mechanical Engg, SVU College of Engg, S.V University, Tirupati, India

E-mail: rayakuntapalli@gmail.com

Journal of Production Engineering
Vol.17 No.2

Original Scientific Paper

Singh, G., Mangat, H.S., Sodhi, H.S.

OPTIMIZATION OF END MILLING PROCESS FOR D2 (DIE STEEL) BY USING RESPONSE SURFACE METHODOLOGY

Received: 20 October 2014 / Accepted: 15 November 2014

Abstract: *An approach for determination of the best cutting parameters leading to maximum material removal rate in machining D2 (Die Steel) on vertical milling centre is used. The Response Surface Methodology technique is applied to obtain optimum values of considered parameters in machining D2 (Die Steel) with four flutes carbide end mill tool having diameter 12 mm. The experimental study was carried out on MITSUBISHI M70 V series CNC vertical machining center (VMC). Spindle speed (N), Feed Rate (F) and Depth of Cut (DC) are the considered machining parameters. The effect of machining parameters on material removal rate is evaluated and the optimum cutting condition for maximizing the material removal rate is determined using Minitab Software.*

Key words: *D2 (Die Steel), Carbide End Mill Tool, Vertical Machining Center, Response Surface Methodology, Optimum Cutting Condition*

Optimizacija završne obrade procesa glodanja čelika D2 (alatni čelik) koristeći metodologiju odaziva površina. *U ovom radu je korišćen pristup za određivanje najboljih parametara rezanja koji rezultuju maksimalnim skidanjem materijala pri obradi D2 čelika (alatnog čelika) na vertikalnoj glodalici. Metoda odaziva površina je primenjena za dobijanje optimalnih vrednosti parametara procesa obrade D2 čelika sa glodalom sa četiri rezne ivice prečnika 12 mm. Eksperimentalna studija je sprovedena na CNC vertikalnom obradnom centru marke MITSUBISHI M70 serije V. Broj obrtaja vretena (N), pomak (f) i dubina rezanja (DC) su varirani parametri obrade. Uticaj parametara obrade na količinu skinutog materijala je ocenjivan, a optimalni režimi rezanja za maksimizovanje skinutog materijala je određeno korišćenjem softvera Minitab.*

Ključne reči: *D2 (alatni čelik), karbidno glodalo za završnu obradu, vertikalni obradni centar, metoda odaziva površine, optimalni režimi rezanja*

1. INTRODUCTION

Optimization of cutting parameters is valuable in terms of providing high precision and efficient machining. Many computation techniques were used for the optimization of cutting parameters in different machining operations. Titanium Aluminum Nitrite coating play a key role in milling cutter to produce better surface finish and tool life with minimum cost. An experimental investigation of face milling operation of Oil Hardened Non Shrinkable (OHNS) steel plates with different process parameters like spindle speed, feed rate and depth of cut was done to find out an optimal machining conditons of minimum surface roughnes (Ra). The experiments were designed and conducted based on Taguchi's design of experiments using L9 orthogonal array and analyzed by ANOVA. Feed rate was a dominating and influencing parameter [1]. The selection of optimal machining parameters (i.e., spindle speed, depth of cut and feed rate) for face milling operations was investigated in order to minimize the surface roughness and to maximize the material removal rate. Effects of selected parameters on process variables (i.e., surface roughness and material removal rate) were examined using Response Surface Methodology (RSM) and artificial neural networks [2]**.** The surface finish and material removal rate were recognized as quality attributes and were assumed to be directly related to productivity. The use of Principal Component Analysis (PCA) based hybrid Taguchi method was proposed and adopted for solution of multi objective optimization in CNC end milling operation [3]. While numerous computation techniques have been developed for combinatorial optimization problems, Particle swarm optimization (PSO) has been principally developed for continuous optimization problem. An Artificial Neural Network (ANN) predictive model was used to calculate cutting forces during machining and then PSO algorithm was used to obtain optimum cutting speed and feed rates [4]. One of the effects of cutting force in the end milling operation with low diameter tool is tool deflection. Assuming that machining errors frequently begin from tool deflection, effort was made to optimize machining parameters using Genetic Algorithm (GA) so as to minimize tool deflection. As compared to other optimizations in which machining time and cost are defined as the objective functions, here algorithm considers tool deflection as the objective function while surface roughness and tool life are the constraints [5]. As the actual milling operation is exceedingly constrained and nonlinear in nature, the traditional optimization techniques are not suitable in such cases. Consquently Genetic Alogrithm with a Self-Organizing Adaptive Penalty (SOAP) approach was used for quick convergence by focusing the search near the boundary of the feasible and infeasible solution space. The optimum feed rate and cutting speed for a specific

depth of cut of end milling operation were determined by minimizing the machining time. This new approach is limited for single pass milling and depth of cuts (axial and radial) are taken as constants [6]. High speed end milling of AISI D3 cold-work tool steel hardened to 35 HRC was examined using coated carbide, coated cermet, alumina (Al_2O_3) based mixed ceramic and cubic boron nitride (CBN) cutting tools. The best cutting performance was obtained with CBN tool [7]. Details of machining experiments with hardened AISI D2 cold work tool steel (about 58 HRC) using indexable insert ball nose end mills employing carbide and cermet tools, and solid carbide ball nose end mills were given. The aim was to identify tool wear mechanisms and appropriate cutting parameters [8]. Optimisation of multi-response CNC turning parameters has been done by by means of central composite design technique of 'Response Surface Methodology' (RSM) through Minitab 16 Software. Further statistical testing of results is verified through ANOVA. An experimental study on Al-7020 alloy turned with un-coated carbide tip tool with a 'CNC TL-250 turner' was done that has a broad relevance in aerospace, machine tools and automobiles sector [9].

In the present work, an effort has been made to optimize the CNC milling parameters for D2 (Die steel) material using response surface method (RSM) to maximize material removal rate (MRR). The major parameters that are considered for optimization in milling operation are as follows: Spindle Speed (rpm), Feed Rate (mm/min) and Depth of Cut (mm). The effects of other influencing noise parameters on the milling operation such as operator skill, type of tool, work material, machining conditions, type of coolant etc. are not considered. Material Removal Rate is the considered response. Machining was done on Mitsubishi M70 V series CNC Vertical Milling Machine with 4 flute carbide tool using the RSM matrix of input parameters. Then analysis work was carried out using regression test. Further, the optimized values were obtained for cutting speed, feed and depth of cut. The material removal rate has been noticed under these set of parameters.

Fig. 1. D2 (Die Steel) Slabs

Fig. 2. Mitsubishi M70 V Series Milling Center at Sood Industries, Chandigarh

2. EXPERIMENTAL DETAILS

Several experiments were conducted to investigate the effect on process state variable (MRR) due to the change in process parameters. The considered cutting parameters were cutting speed, feed and depth of cut as shown in Table 1. Experiments were conducted at two levels of machining parameters. Twenty experiments were conducted and material removal rate was measured. Results are tabulated in Table 2.

Process Variables	Lower Limit	Upper Limit
Spindle Speed (rpm)	1500	2500
Feed (mm/min)	300	1200
Depth of cut (mm)	0.04	0.12

Table 1: Process Variables and their limits

2.1 Calculation of Material Removal Rate

Once the cutting operations were accomplished, the Material Removal Rate was calculated with Equation given below:

$$\frac{W_i - W_f}{\rho} \times t \quad (1)$$

where,
"W_i" = Initial Weight in grams
"W_f" = Final Weight in grams

"**ρ**" = Density of Die Steel (0.007696 g/mm^3)

"t" = time in seconds
"MRR" = Material Removal Rate in mm^3/sec
(M.R.R Results are tabulated in Table 2)

St	Run	Spindle Speed (rpm)	Feed rate (mm/min)	Depth of cut (mm)	MRR (mm^3/sec)
16	1	2000	750	0.08	48.13
10	2	2841	750	0.08	103.95
20	3	2000	750	0.08	48.73
9	4	1159	750	0.08	47.73
5	5	1500	300	0.12	18.12
4	6	2500	1200	0.04	86.63
1	7	1500	300	0.04	18.56
12	8	2000	1507	0.08	32.48
6	9	2500	300	0.12	95.36
7	10	1500	1200	0.12	21.66
15	11	2000	750	0.08	47.97
13	12	2000	750	0.01	37.13
19	13	2000	750	0.08	48.21
3	14	1500	1200	0.04	19.48
8	15	2500	1200	0.12	64.97
18	16	2000	750	0.08	48.69
14	17	2000	750	0.15	16.24
17	18	2000	750	0.08	48.69
11	19	2000	-7	0.08	16.24
2	20	2500	300	0.04	52.99

Table 2: Execution of Experiments

2.2 Response Surface Methodology: Importance and Applications

Box and Wilson (1951) introduced the Response Surface Methodology (RSM) and others developed it for designing experiments and consequent analysis of experimental data [10]. The method uses Design of Experiments techniques or DOE [11] such as Two-level Full & Fractional Factorial Designs, and regression analysis methods [12] where DOE techniques can be employed before, during, and after the regression analysis to assess the accuracy of the model. The core thought is to substitute a complicated response function with an approximate function by studying the relative significance of the effects of several factors supposed to have control on the response of interest. The response surface methodology (RSM) is a combination of statistical and mathematical techniques to analyze, model, and optimize processes. The intention of this method is to create the unknown relationship between the independent variables (input factors) and the process responses. Surface experiments were performed to fit either a first order model (linear function) or a second-order model to the observations [13]. RSM consist of of three methods [14]: (a) Statistical experimental design/two-level factorial or fractional factorial design, (b) Regression modeling techniques and (c) Optimization methods. RSM can be sighted from three major viewpoints [15] (a) If the system response is rather well-discovered, RSM techniques are used to hit upon the best (optimum) value of the response, (b) If discovering the paramount value is ahead of the available resources of the experiment, then RSM techniques are used to at least achieve a better understanding of the overall response system, (c) If obtaining the system response demands a very complex analysis that requires hours of run-time and advanced computational resources then a simplified equivalent response surface may be obtained by a few numbers of runs to replace the complex analysis. The objective is to optimize a response (output variable) which is influenced by several independent variables (input variables). Response-surface methodology comprises a body of methods for exploring for optimum operating conditions through experimental methods. Typically, this involves doing several experiments, using results of one experiment to provide direction for what to do next .This next action could be to focus the experiment around a different set of conditions, or to collect more data in the current experimental region in order to fit a higher order model or confirm what seems to have found. An experiment is a series of tests, called runs, in which changes are made in the input variables in order to identify the reasons for changes in the output response.

Response Surface Methodology has been thriving its roots in various fields of science and engineering. Concepts and techniques of Response Surface Methodology (RSM) have been broadly applied in many fields of engineering, especially in the chemical and manufacturing sections. The application of RSM is also intended to reduce the expenses of other difficult analytical methods like Finite Element Method or CFD analysis etc. and their related numerical noises [16]. The problem can be approximated with smooth functions of Central Composite Design of RSM that improve the convergence of the optimization process because they trim down the effects of noises and inherent errors, significantly [17]. The responses can be represented graphically, either in the three-dimensional space or as contour plots that further assist to envision relation of response surfaces with input variables more clearly. The application of RSM is aimed at reducing the cost of pricey analysis methods and their linked mammoth investment of resources and volumes of numerical data analysis. This particular advantage has paved the way for its thriving application in different disciplines such as chemical and pharmaceutical processes, biological/biochemical processes, food science, production engineering, air quality analysis and toxicological research and computational and simulation studies. Researchers from different fields in recent years have published several interesting applications of response surface methodology. In one such study, C J Stevens (Jr) of NASA, United States, integrated RSM with computational fluid dynamics (CFD) for the prediction of combined cycle propulsion components in hypersonic jet fighter.

3. RESULTS AND DISCUSSIONS

3.1. Considered Responses:

An analysis is done through Minitab Software. In this study, while performing the experiments one response is kept under consideration that is Material Removal Rate (MRR). Firstly data has been checked for its normality by probability plot (see first plot of figure 3). As data points are distributed all along the normal line and having few outliers, so data can be concluded as normally distributed. The second plot doesn't show any trend while plotting residual versus fitted values of data which implies RSM model chosen is well fitted with given data set. Third plot is frequency histogram showing data distribution and at last residue versus order plot highlights the random data points which signifies non-significance of experimental order as far as first response (MRR) is concerned.

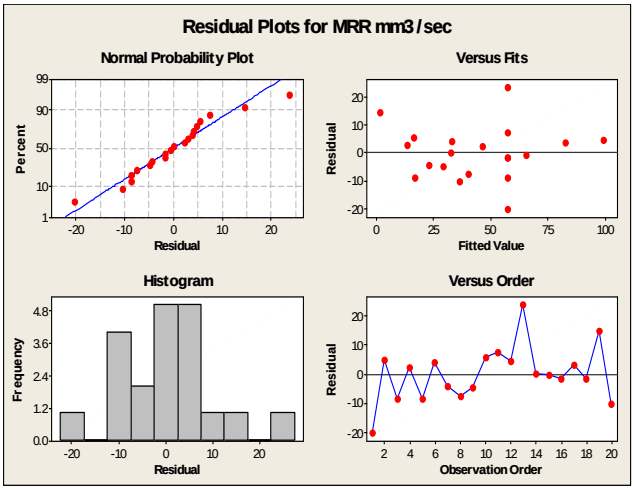

Figure 3: Data Normality Testing for MRR

RSM for MRR has been applied at 95% confidence, so all factors and their interactions having p (probability) value less than 0.05 will be statistically significant for MRR and must be further taken care of. Refer Table 3. on next page for more details of statistical analysis of RSM for MRR. As p values are more than 0.05 for (cutting speed × feed) and (feed × depth) and hence can be ignored during optimization of MRR because of their negligible analytical affect.

3.2 Graphical Inferences for MRR:

The software has deduced the results in graphical form also. Figure 4 highlights the one factor at a time affect on response (MRR).

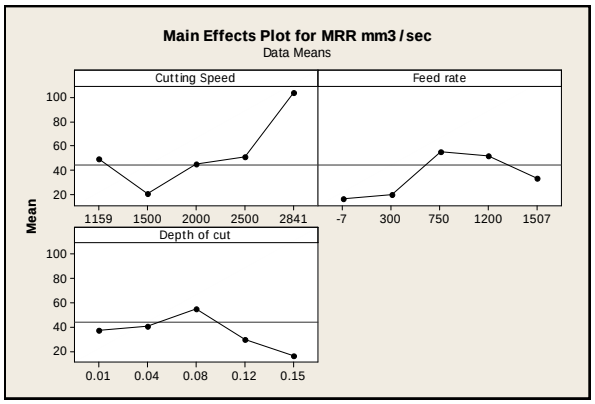

Fig. 4. Main Effect Plots for MRR

Term	Coef	SE Coef	T	P	Sig./NS
Cutting Speed	26.345	5.963	4.41	0.001	Sig.
Feed rate	19.110	5.964	3.20	0.009	Sig.
Depth of cut	-11.108	6.120	-1.815	0.010	Sig.
Cutting Speed × Cutting Speed	15.3955	9.759	1.578	0.046	Sig.
Feed rate × Feed rate	-36.6020	9.762	-3.750	0.004	Sig.
Depth of cut × Depth of cut	-36.0462	10.265	-3.512	0.006	Sig.
Cutting Speed × Feed rate	26.0972	13.100	1.992	0.074	NS *
Cutting Speed × Depth of cut	-0.7293	13.433	-0.054	0.048	Sig.
Feed rate × Depth of cut	-7.4065	13.435	-0.551	0.594	NS*
S = 13.0952				PRESS = 6223.25	
R-Sq = 96.85%				R-Sq(adj.) = 95.01%	
Here, Sig. means Significant & NS means Not Significant					

Table 3: Statistics for MRR

Figure 5 represents the main effects of varying cutting speed, feed and depth of cut on material removal rate.

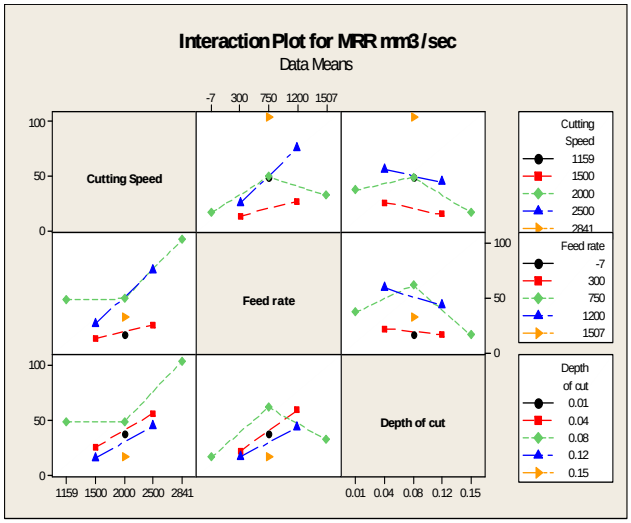

Fig. 5. Two-Way Interaction Plot for MRR

The 3-D surface plots as a function of two factors at a time, maintaining all other factors at fixed levels not only provides understanding of both the main and the interaction effects of these two factors, but also helps to identify the optimum level of each variable for maximum response. See figure 6 containing surface plot and its corresponding 2-D contour plot of MRR versus Speed & Depth of Cut at a holding value of feed on 750 mm/min.

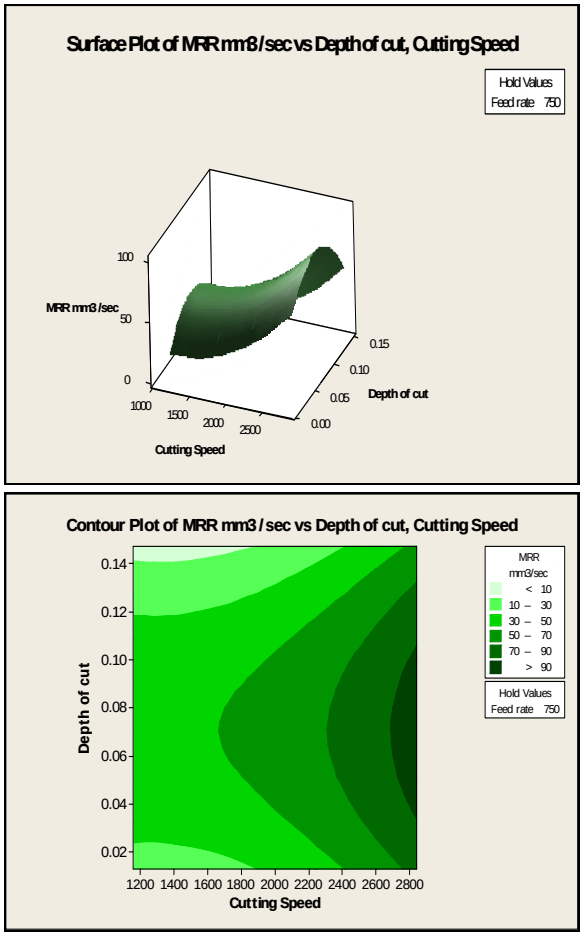

Fig. 6. Surface and Contour Plots of MRR Vs Depth of Cut & Cutting Speed

Contour plots are basically orthographic views of 3-D plot and consists of colored regions of input variables bearing different value of output response. Like dark green region of above plot reflects the area having values of Feed and Depth of Cut where MRR may be reached up to 90 mm^3/sec or more. On the same pretext figure 7 demonstrates the surface plot and contour plot of MRR Vs Cutting Speed & Feed at holding value of Depth of Cut on 0.081 mm.

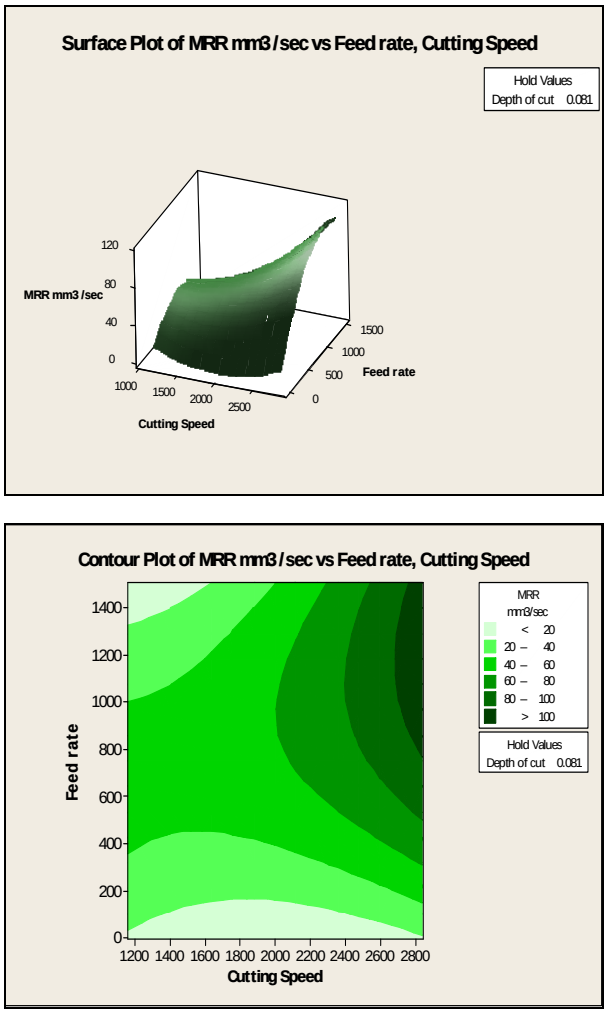

Figure 7. Surface and Contour Plots of MRR Vs Cutting Speed & Feed

At the end, Minitab has created an Estimated Regression Coefficients for MRR in terms of its significant factors and their interactions, as detailed below in Table 4.

Term	Coef
Cutting Speed	-0.0854685
Feed rate	0.0505547
Depth of cut	1197.02
Cutting Speed × Cutting Speed	2.17672E-05
Feed rate × Feed rate	-6.38724E-05
Depth of cut × Depth of cut	-7571.13
Cutting Speed × Feed rate	4.09922E-05
Cutting Speed × Depth of cut	-0.0125684
Feed rate × Depth of cut	-0.141797

Table 4: Estimated Regression Coefficients for MRR using data in uncoded units

3.3 Optimization Equation of MRR :

MRR = -0.0854685 (Cutting Speed) + 0.0505547 (Feed) - 1197.02 (Depth) + 2.17672E-05 (Cutting Speed) ² - 6.38724E-05 (Feed Rate) ² - 7571.13 (Depth of cut) ² - 0.141797 (Feed x Depth)

The coefficient of each factor reflects its weightage with MRR and its positive or negative sign signifies the respective proportionality. Feed rate and Depth of Cut seems to be highly impacting factors along with its interaction, as far as high MRR is in question. After analyzing the data of experiments, software has provided the solution at 98% composite desirability that at Cutting Speed at 2840.9 rpm, Feed of 818.8 mm/min and Depth of Cut of 0.06 mm, maximum MRR of 103.905(mm^3/sec) is achieved.

Operation	Speed (rpm)	Feed (mm/min)	Depth of Cut (mm)	MRR (mm^3/sec)
Finishing Case	2840.9	818.8	0.06	103.905

Table 5. Optimization Values of RSM

4. CONCLUSION

Based on the conducted experiments and accomplished analysis, the material removal is effectively predicted by using spindle speed, feed rate, and depth of cut as the input variables. The optimized values 2840.9 rpm, 818.8 mm/min and 0.06 mm were obtained for cutting speed, feed and depth of cut respectively. The maximum material removal rate was noticed under these set of parameters. A volume material removal rate of 103.905 mm^3/sec was achieved. The average actual Material removal rate value was obtained as 44.05 mm^3/min. The depth of cut and feed rate and their interaction are significant factors in the material removal rate model. RSM provide a very good process modeling. It provides the better data coverage value. The excellent accuracy (nearly null error) of the RSM optimization procedure is observed during finishing machining.

5. REFERENCES

[1] Sadiq, S. N., Raguraman, T. R., Kumar, D. T. , Rajasekaran, R., Kannan, T. T. M.: Optimization of milling parameters of OHNS steel using tialn coated cutter by design of experiment technique, International Journal of Mechanical Engineering and Robotic Reearch, Volume number 3 (1), 2014.

[2] Soleymani Yazdi, M.R.,Khorram, A.: Modeling and Optimization of Milling Process by using RSM and ANN methods, IACSIT International Journal of Engineering and Technology, Volume number 2 (5), p.p. 474-480, 2010.

[3] Moshat, S., Datta, S., Bandyopadhyay, A., Kumar Pal, P.,: Optimization of CNC end milling process parameters using PCA-based taguchi method, International Journal of Engineering, Science and Technology,Volume number 2 (1), p.p. 92-102, 2010.

[4] Župerl, U., Cuš, F., Gecevskaa, V.: Optimization of characteristic parameters in milling by using PSO

evolution technique, Elsevier Journal of Materials Processing Technology, Vol. 10 (1), p.p. 560-567, 2010.
[5] Saffar, R. J.,. Razfar, M.R., Salimi, A.H., Khani, M.M.: Optimization of machining parameters to minimize tool deflection in the end milling operation using genetic algorithm, World Applied Sciences Journal, Volume number 6 (1), p.p. 64-69, 2009.
[6] Ahmad, N., Tanaka, T., Saito, Y.: Optimization of cutting parameters for end milling operation by soap based genetic algorithm, Proceedings of the International Conference on Mechanical Engineering, p.p.1-5, Dhaka, Bangladesh, Dec. 27-29 2005, No.05-204, ICME05-AM-08.
[7] Camuscu, N., Aslan, E.: A comparative study on cutting tool performance in end milling of AISI D3 tool steel, Elsevier Journal of Materials Processing Technology, Volume number 170, p.p. 121-126, 2005.
[8] Koshy, P., Dewes, R.C., Aspinwall, D.K.: High speed end milling of hardened AISI D2 tool steel (58 HRC) Elsevier Journal of Materials Processing Technology, Volume number 127, p.p. 266-273, 2002.
[9] Singh, B.J., Sodhi, H.S.: Parametric optimisation of CNC turning for Al-7020 with RSM, International Journal of Operations Research, Volume number 20 (2), p.p. 180-206, 2014.
[10] Box, G.E.P., Wilson, K.B.: On the experimental attainment of optimum conditions, Journal of the Royal Statistical Society, Volume number B13, p.p. 1-45, 1951.
[11] Montgomery, D.C..: Design and Analysis of Experiments, John Wiley & Sons, New York, 1997.
[12] Montgomery, D.C., Peck, E.A., Vining, G.G.: Introduction to Linear Regression Analysis, 3rd ed. New York, John Wiley, 2000.
[13] Box, G. E. P., Draper, N. R.: Empirical Model Building and Response Surfaces, John Wiley & Sons, New York, NY, USA, 1991.
[14] Myers, R.H., Montgomery, D.C.: Response Surface Methodology, John Wiley & Sons, New York, 1995.
[15] Cornell, J.A.: How to Apply Response Surface Methodology, The ASQC Basic References in Quality Control: Statistical Techniques, Volume number 8, ASQC, Wisconsin, 1990.
[16] Srikanth, T., Kamala, V.: A Real Coded Genetic Algorithm for Optimization of Cutting Parameters in Turning IJCSNS International Journal of Computer Science Network Security, Volume number 8(6), p.p.189-193, 2008.
[17] Thamizhmanii, S., Saparudin, S., Hasan, S.: Analyses of Surface Roughness by Turning process using Taguchi method, Journal of Achievements in Materials and Manufacturing Engineering, Volume number 20(1-2), pp.503-506, 2007.

Authors:

Gurmeet Singh, Assistant Professor, Department of Mechanical Engineering, Chandigarh University, Gharuan, Mohali, Punjab, India

[*]**Harjit Singh Mangat, Assistant Professor,** Department of Mechanical Engineering, Baba Banda Singh Bahadur Engineering College, Fatehgarh Sahib, Punjab, India affiliated to Punjab Technical University, Kapurthala, Punjab, India

Home Address: V.P.O- Ghaloti, Tehsil- Payal, District- Ludhiana, State- Punjab, Country- India, Pin Code- 141419.

Official Address: Baba Banda Singh Bahadur Engineering College, Fatehgarh Sahib, Punjab, India- 140407.

Harsimran Singh Sodhi, Assistant Professor, Department of Mechanical Engineering, Chandigarh University, Gharuan, Mohali, Punjab, India

E-mail: gurmeetsinghdec30@gmail.com
mangat84@gmail.com (Correspondence E-mail)
harsimransinghsodhi@yahoo.com

[*]**(Corresponding Author)**

Journal of Production Engineering
Vol.17 No.2

Original Scientific Paper

Madić, M., Gecevska, V., Radovanović, M., Petković, D.

MULTI-CRITERIA ECONOMIC ANALYSIS OF MACHINING PROCESSES USING THE WASPAS METHOD

Received: 26 Septebmer 2014 / Accepted: 22 October 2014

Abstract: *The selection of the most suitable machining process for a given machining application is not straightforward and requires consideration of a number of techno-technological and economic criteria. Therefore is often viewed as a multi-criteria decision making (MCDM). This paper is focused on multi-criteria economic analysis of various machining processes by applying recently developed MCDM method, i.e. weighted aggregated sum product assessment (WASPAS) method. By using available data from literature MCDM model consisting of eight different machining processes and five economical criteria was defined. In order to determine relative significance of considered criteria a pairwise comparison matrix was applied.*
Key words: *multi-criteria decision making, machining process selection, economic analysis, WASPAS*

Višekriterijumska ekonomska analiza procesa obrade primenom metode WASPAS. *Izbor najpogodnijeg procesa obrade nije jednostavan zadatak jer zahteva razmatranje niza tehno-tehnoloških i ekonomskih kriterijuma. Iz ovih razloga se često posmatra kao problem višekriterijumske analize. U ovom radu je izvršena višekriterijumska analiza različitih procesa obrade u odnosu na ekonomske kriterijume primenom metode WASPAS. Koristeći dostupne podatke iz literature razvijen je model višekriterijumske analize koju uključuje osam različitih procesa obrade i pet ekonomskih kriterijuma.U cilju određivanja relativne značajanosti razmatranih kriterijuma korišćena je matrica upoređenja po parovima.*
Ključne reči: *višekriterijumska analiza, izbor procesa obrade, ekonomska analiza, WASPAS*

1. INTRODUCTION

Machining technologies change the form of raw materials or semi-finished products by conventional machining, forming, non-conventional machining or some other type of processing in order to obtain assembly or finished parts. Conventional machining processes are processes in which the tool removes material from the workpiece in the form of chips thereby creating a certain part with defined shape, dimensions and surface quality [1]. In recent years there is increasing usage of advanced and newer materials with improved technological properties. As machining of these materials by conventional machining processes gives rise to problems such as high cutting forces and temperatures and rapid tool wear, in today's modern industry non-conventional machining processes take an important place. The application of non-conventional machining processes involves the use of energy in direct form, e.g. mechanical energy by abrasive water jet machining, heat energy by laser and plasma machining, thermoelectric energy by electric discharge machining, etc. A unique characteristic of these processes is that there is no direct contact between the tool and the workpiece, as well as the ability to concentrate large amounts of energy per unit area [2].

Currently, all machining processes should satisfy severe production requirements, including productivity, efficiency and surface quality, and additionally reliability, energy consumption and ecological standards [3]. Each machining process is a complex multi-input/multi-output process characterized by its unique process capabilities, advantages and limitations. Which machining process will be used for a particular machining application depends on a number of criteria including price, production volume, desired quality, etc. In order to deal with a number of conflicting criteri, decision makers often apply multi-criteria decision making (MCDM) methods which have been proven as powerful mathematical tools for solving selection problems in manufacturing environment.

Previous studies reported the application of different MCDM methods such as analytic hierarchy process (AHP), fuzzy AHP, technique for order preference by similarity to ideal solution (TOPSIS), preference ranking organization method for enrichment evaluation (PROMETHEE), evaluation of mixed data (EVAMIX), multi-objective optimization on the basis of ratio analysis (MOORA) method, etc. These methods were applied for solving different MCDM problems in manufacturing environment such as selection of cutting fluids [4], selection of non-conventional machining processes [5, 6], selection of rapid prototyping process [7], selection of machine tool [8], selection of the tool insert [9], selection of intelligent manufacturing systems [10], and other applications [11].

This paper focuses on multi criteria analysis of various machining processes considering economics. An attempt has been made to explore the applicability of recently developed MCDM method, i.e. weighted aggregated sum product assessment (WASPAS) method for solving such type of MCDM problems.

Firstly, using the available data from literature [12], a MCDM model consisting of eight different machining processes and five parameters influencing economy (criteria) was defined. A pairwise comparison matrix of the AHP method was then used to determine the relative significance of considered criteria.

2. SELECTION OF MACHINING PROCESSES CONSIDERING ECONOMICS

Each machining process has a specific application field to which is best suited. However, machining process application fields are often overlapped, so that some machining operations can be achieved by two or more processes. The final selection of the best machining process for a given application is a complex process and involves the careful consideration of several factors such as desired shape and size of the product, properties of materials, quality of the machined product, and the cost of machining [12]. When large production volumes are to be machined, the final decision about selection of the machining process is predominantly influenced by economic considerations. Apart from the cost of material used, the machining cost include fixed cost, tool cost and its setup cost, variable cost, labor cost, etc. [3].

The procedures for calculating the machining costs differ significantly for various machining processes due to differing mechanisms associated with them [12]. One of the main parameters that influence economics is the cutting speed. As the cutting speed is increased, machining time is decreased which results in reduced labor cost. However, cutting speed cannot be increased above some optimal values, since excessive increase in cutting speed may results in adverse effects. For example, in laser cutting increase in cutting speed may result in incomplete cut or deterred surface finish. Similarly, in turning, increase in cutting speed may result in rapid tool wear resulting in higher tool cost and its setup cost. In general when machining a certain material using a machining process there exist set of optimal machining process parameters. Relative economic comparison of various machining processes is presented in Table 1 [12].

As can be seen from Table 1, performance of each machining process regarding five criteria (CI, TF, PR, RE and TW) is given linguistically. In order to apply a MCDM method for comparison of machining processes considering these criteria one need to convert these linguistic terms into crisp (real) values. In this paper this was performed in the range [0, 1] by using the 5-point fuzzy scale [11]. In this scale, crisp value for linguistic term "very low" is 0.115, and on the other hand crisp value for linguistic term "very high" is 0.895. Crisp values of linguistic terms "low", "medium" and "high" have crisp values of 0.295, 0.495 and 0.695, respectively.

3. WASPAS METHOD

Weighted aggregated sum product assessment (WASPAS) method for solving MCDM problems was proposed by Zavadskas et al. [13] in 2012. The main procedure of the WASPAS method solving MCDM problems includes several steps.

Step 1. Set the initial decision matrix.

Step 2. Normalization of the decision matrix by using following equations:

$$\bar{x}_{ij} = x_{ij} / \max_i x_{ij} \qquad (1a)$$

$$\bar{x}_{ij} = \min_i x_{ij} / x_{ij} \qquad (1b)$$

where x_{ij} is the assessment value of the i-th alternative with respect to the j-th criterion, and eqs. 1a and 1b are used for maximization and minimization criteria, respectively.

Step 3. The total relative importance of i-th alternative, based on weighted sum method (WSM), is calculated as follows [14]:

$$Q_i^{(1)} = \sum_{j=1}^{n} \bar{x}_{ij} \cdot w_j \qquad (2)$$

Step 4. The total relative importance of i-th alternative, based on weighted product method (WPM), is calculated as follows:

$$Q_i^{(2)} = \prod_{j=1}^{n} \bar{x}_{ij}^{w_j} \qquad (3)$$

Step 5: In order to have increased ranking accuracy and effectiveness of the decision making process, in the WASPAS method, a more generalized equation for determining the total relative importance of alternatives is developed as below [13]:

$$Q_i = \lambda \cdot Q_i^{(1)} + (1-\lambda) \cdot Q_i^{(2)} \qquad (4)$$

where λ=0,0.1,...,1.

Machining process	Parameter influencing economy				
	CI	TF	PR	RE	TW
CM	low	low	low	very low	low
USM	low	low	low	high	medium
AJM	very low	low	low	high	low
ECM	very high	medium	medium	low	very low
CHM	medium	low	high	medium	very low
EDM	medium	high	low	high	high
PAM	very low	low	very low	very low	very low
LBM	medium	low	very low	very high	very low
CM – conventional machining; USM – ultra sonic machining; AJM – abrasive jet machining; ECM – electrochemical machining; CHM – chemical machining; EDM – electric discharge machining; PAM – plasma arc machining; LBM – laser beam machining; CI – capital investment; TF – Tooling/fixtures; PR – power requirements; RE – removal efficiency; TW – tool wear					

Table 1. Relative economic comparison of various machining processes [12]

Now, the candidate alternatives are ranked based on the Q values, i.e. the best alternative would be that one having the highest Q value. When the value of λ is 0, WASPAS method is transformed to WPM, and when λ is 1, it becomes WSM [14].

4. RESULTS AND DISCUSSION

4.1 Determining relative significance of criteria

In order to determninr relative significance of the considered criteria in decision matrix AHP method was applied. The salient advantage of the method is that it prevents inconsistency in determining criteria weights.

The Saaty 9-point preference scale [11] is used in the AHP for constructing the pairwise comparison matrix. Based on preferences the following pairwise comparison matrix was constructed (Table 2).

By using the geometric mean method criteria weights were obtained as w=[0.51, 0.076, 0.0846, 0.25, 0.0788].

	CI	TF	PR	RE	TW
CI	1	5	5	3	7
TF	0.2	1	1	0.2	1
PR	0.2	1	1	0.33	1
RE	0.33	5	3	1	3
TW	0.14	1	1	0.33	1

Table 2. Pairwise comparison matrix of criteria

It is observed that capital investment (CI) and removal efficiency (RE) are assigned the greatest importance. To ensure consistency of preference while determining criteria weights, a consistency check was performed. For five considered criteria i.e. for random index of 1.11, consistency index and consistency ratio values of 0.021 and 0.019 were obtained, respectively.

4.2 Application of the WASPAS method

Since linguistic terms, used to express the performance of each machining process regarding economics, have already been converted into crisp (real) values, the application of the WASPAS method starts with normalization of the decision matrix using eqs. 1a and 1b. Subsequently, total relative importance of alternatives as per WSM and WPM are calculated by using eqs 2 and 3, respectively. Finally, joint criterion of optimality of the WASPAS method is calculated by using equation 5. Table 3 provides the values of total relative importance (performance scores) for all the considered alternatives for a λ value of 0.5.

	$Q_i^{(1)}$	$Q_i^{(2)}$	Q	Rank
CM	0.371212	0.31747	0.371212	7
USM	0.520804	0.477862	0.520804	4
AJM	0.844425	0.804793	0.844425	1
ECM	0.292013	0.22602	0.292013	8
CHM	0.426109	0.351777	0.426109	5
EDM	0.391139	0.334619	0.391139	6
PAM	0.782134	0.598729	0.782134	2
LBM	0.608455	0.474988	0.608455	3

Table 3. Computational details of the WASPAS method for a λ value of 0.5

As could be seen from Table 3 by applying the WASPAS method, the ranking of the various machining processes considering economics is obtained as AJM-PAM-LBM-USM-CHM-EDM-CM-ECM. It is observed that AJM is determined as the most economical process. It is revealed that PAM is the second best choice, and that LBM is third choice. ECM is obtained as the least preferred machining process.

Figure 1 shows the effect of varying values of λ on total relative importance values and rankings of the considered machining processes.

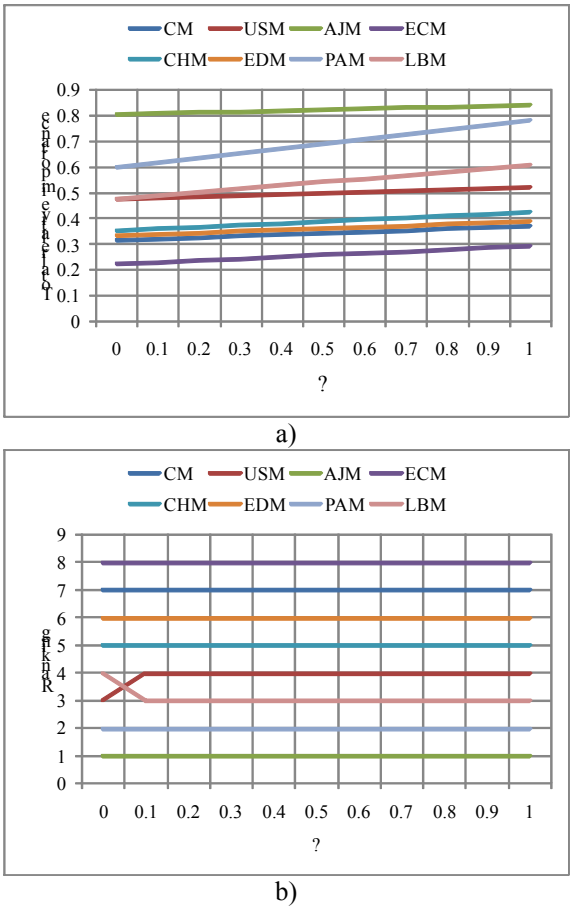

Fig. 1. Variations of total relative importance (Q) and ranking of various machining processes with respect to λ

From Figure 1 it could be observed that a higher total relative importance values are achieved for the higher value of λ, i.e. when WASPAS method behaves like WSM. Also, the rankings of the two most preferred machining processes that is AJM and PAM and two leas least preferred alternatives that is CM and ECM remain unaffected for different values of λ. However in the case of USM and LBM, different values of λ produced different rankings. For λ=0, LBM is determined as the fourth and USM is determined as third alternative, while for λ=0.1 rankings of LBM and USM is reversed. However, on the basis of the conducted analyses it is evident that the obtained ranking of machining processes considering economics is stable to perturbations in values of λ.

In relation to the conducted analysis, as noted by Dahotre and Harimkar [12], in critical applications highest quality of the product must be obtained irrespective of the machining cost and this should be

considered while selecting the most suitable machining process. Similarly, in less critical applications a machining process that can achieve acceptable product quality level at the lowest cost can be considered as the most appropriate.

Apart from the conducted multi criteria analysis it should be noted that for a given workpiece material, required part geometries and surface quality some machining processes are often viewed as the best one. For example rotational ultrasonic machining is best machining process for advanced ceramics [15], while WEDM process evolved as best machining process for producing complicate parts with very good surface finish and dimensional accuracy [16].

5. CONCLUSION

In this paper recently developed MCDM method, i.e. WASPAS method was applied for the purpose of multi-criteria economic analysis of various machining processes. The obtained results from multi-criteria economic analysis suggested that AJM is the best alternative, followed by PAM and LBM. ECM obtained lowest rankings due to very high investments cost as well as low removal efficiency. The effect of parameter λ on the ranking performance revealed the fact that there exists strong resistance against rank reversal of the considered alternatives.

Selection of a particular machining process is very important task in manufacturing environment. Comprehensive analysis of this complex problem for a given machining application should consider material type and required geometries, tolerances and surface finish, design requirements, process capabilities, cost and productivity and this will be future research scope. Also, for further research, the results of this study can be compared with that of other MCDM methods.

6. REFERENCES

[1] Radovanović, M.: *Tehnologija mašinogradnje-obrada rezanjem*, Univerzitet u Nišu, Mašinski fakultet, Niš, 2002.

[2] Kovačević, M., Madić, M., Radovanović, M., Rančić, D.: *Software prototype for solving multi-objective machining optimization problems: Application in non-conventional machining processes*, Expert Systems with Applications, Vol. 41, No. 13 p.p. 5657-5668, 2014.

[3] Grzesik, W.: *Advanced machining processes of metallic materials*, Elsevier, 2008.

[4] Abhang, L.B., Hameedullah, M.: *Selection of lubricant using combined multiple attribute decision-making method*, Advances in Production Engineering and Management, Vol. 7, No. 1, p.p. 39-50, 2012.

[5] Karande, P., Chakraborty, S.: *Application of PROMETHEE-GAIA method for non-traditional machining processes selection*, Management Science Letters, Vol. 2, No. 1, p.p. 2049-2060, 2012.

[6] Temuçin, T., Tozan, H., Valíček, J., Harničárová, M.: *A fuzzy based decision support model for non-traditional machining process selection*, Tehnički vjesnik, Vol. 20, No. 5, p.p. 787-793, 2013.

[7] Byun, H.S., Lee, K.H.: *A decision support system for the selection of a rapid prototyping process using the modified TOPSIS method*, International Journal of Advanced Manufacturing Technology, Vol. 26, No. 1, p.p. 1338-1347, 2005.

[8] Taha, Z., Rostam, S.: *A fuzzy AHP–ANN-based decision support system for machine tool selection in a flexible manufacturing cell*, The International Journal of Advanced Manufacturing Technology, Vol. 57, No. 5-8, p.p. 719-733, 2011.

[9] Patel, N., Patel, R.K., Patel, U.J., Patel, B.P.: *Insert selection for turning operation on CNC turning centre using MADM methods*, International Journal of Latest Trends in Engineering and Technology, Vol. 1, No. 3, p.p. 49-59, 2012.

[10] Mandal, U.K., Sarkar, B.: *Selection of best intelligent manufacturing system (IMS) under fuzzy moora conflicting MCDM environment*, International Journal of Emerging Technology and Advanced Engineering, Vol. 2, No. 9, p.p. 301-310, 2012.

[11] Rao, R.V.: *Decision making in the manufacturing environment: using graph theory and fuzzy multiple attribute decision making methods*. Springer, 2007.

[12] Dahotre, N.B., Harimkar, S.: *Laser fabrication and machining of materials*, Springer, 2008.

[13] Zavadskas, E.K., Turskis, Z., Antucheviciene, J., Zakarevicius, A.: *Optimization of weighted aggregated sum product assessment*, Electronics and Electrical Engineering, Vol. 122, No. 6, p.p. 3-6, 2012.

[14] Chakraborty, S., Zavadskas, E.K.: *Applications of WASPAS method in manufacturing decision making*, Informatica, Vol. 25, No. 1, p.p. 1-20, 2014.

[15] Li, Z.C., Cai, L.W., Pei, Z.J., Treadwel, C.: *Edge chipping reduction in rotary ultrasonic machining of ceramics: finite element analysis and experimental verification*, International Journal of Machine Tool and Manufacture , Vol. 46, No. 5. p.p. 1469-1477, 2006.

[16] Sudhakara, D., Prasanthi, G.: Review of research trends: process parametric optimization of wire electrical discharge machining (WEDM), International Journal of Current Engineering and Technology, Vol. 2, No. 1. p.p. 131-140, 2014.

Authors: **Dr. Miloš Madić, Prof. Dr. Miroslav Radovanović, MSc Dušan Petković.**, University of Niš, Faculty of Mechanical Engineering in Niš, Aleksandra Medvedeva 14, 18 000 Niš, Serbia, Phone: +381 18 500-687, Fax: +381 18 588-244;

Prof. Dr. Valentina Gecevska, University in Skopje, Faculty of Mechanical Engineering, Karpos II bb, 1000 Skopje, Macedonia, Phone: + 389 2 3099 249, Fax: + 389 2 3099 298;

E-mail: madic@masfak.ni.ac.rs
valentina.gecevska@mf.edu.mk
mirado@masfak.ni.ac.rs
dulep@masfak.ni.ac.rs

Journal of Production Engineering
Vol.17 No.2

Original Scientific Paper

Lukić, D., Milošević, M., Borojević, S., Vukman, J., Đurđev, M.

APPLICATION OF MULTI-CRITERIA DECISION MAKING FOR MANUFACTURING PROCESS EVALUATION AND SELECTION

Received: 12 November 2014 / Accepted: 27 November 2014

Abstract: *Selection of manufacturing process is one of the most difficult decisions in product development and is mainly conditioned by technological, economic and organizational criteria. In such situations, in addition to a large number of criteria, occurs also a number of alternatives, all of which makes the problem of evaluation and selection more complex. Therefore, the selection of optimal manufacturing process comes down to the problem of multi-criteria decision making. In this paper, process of multi-criteria evaluation and selection of best manufacturing process solution using the developed module of conceptual CAPP system is shown.*
Key words: *Multi-criteria decision making, Manufacturing processes, CAPP*

Primena višekriterijumskog odlučivanja za ocenu i izbor tehnoloških procesa izrade. *Izbor tehnološkog procesa je jedna od najtežih odluka u razvoju novih proizvoda, i uslovljen je, uglavnom, tehničko-tehnološkim, ekonomskim i organizacionim kriterijumima. U takvim situacijama se pored velikog broja kriterijuma javlja i veći broj alternativa, što sve zajedno čini problem vrednovanja i izbora mnogo složenijim. Shodno tome, izbor optimalnog tehnološkog procesa se svodi na problem višekriterijumskog odlučivanja.*
U ovom radu prikazan je postupak višekriterijumskog vrednovanja i izbora najpovoljnijeg rešenja tehnološkog procesa izrade, primenom razvijenog modula konceptualnog CAPP sistema.
Ključne reči: *Višekriterijumsko odlučivanje, Tehnološki procesi, CAPP*

1. INTRODUCTION

The task of developing and mastering a new product is a multidimensional problem which determines the working condition and exploitation requirements, product's functionality and conditions that define the society and market, as well as the manufacturing process within the constraints of production. Development level of the manufacturing technologies, on the one hand, and demand characteristics of modern markets, on the other hand, determine the basic tasks of modern manufacturing, where the question is no longer "Is it possible to manufacture something?" but "What is the optimal manufacturing process?".

For selection of best process plan for manufacturing a product, multi-criteria decision making (MCDM) methods are succesfully used. In this paper process of multi-criteria evaluation and selection of best manufacturing process solution using the developed module of conceptual CAPP system is shown, with verification on the example of outer ring of roller bearing, according to manufacturing conditions of specific production system.

2. BASICS OF MANUFACTURING PROCESS SELECTION

Selection of manufacturing process is one of the most difficult decisions in product development and is mainly conditioned by technological, economic and organizational criteria. Therefore, the selection of optimal manufacturing process comes down to the problem of MCDM [1,2].

Problem of selection of basic manufacturing processes represents one of the fundamental tasks within design for manufacturing – DfM, concerned by many authors, such as [1,2,3,4,5,6]. In the references, this area is called as Conceptual Process Planning-CPP [7], and the corresponding software systems are known as Conceptual CAPP [8]. Some of the developed systems in this area are described in more detail in [9,10]: CAMPS (Computer-Aided Material and Process Selection), EPSS (Expert Processing Sequence Selector), CMS (Cambridge Materials Selector) i CPS (Cambridge Process Selector), COMPASS (Computer Oriented Material, Processes and Apparatus Selection System), MaMPS (Material and Manufacturing Process Selection), MAS (Manufacturing Advisory Service), DFMA (Design for Manufacture and Assembly), TeamSET and others.

Figure 1 presents algorithm for selection of basic manufacturing processes, which essentially contains the most important selection stages that are common for most of developed methodologies.

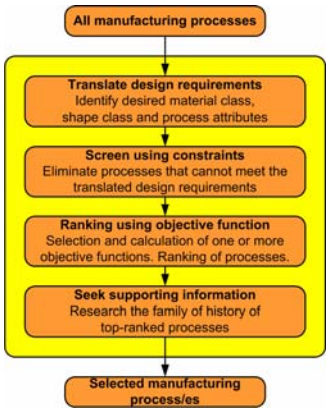

Fig. 1. Flow chart of the procedure for manufacturing process selection [1]

In the **first stage** of translating product design requirements, the task is to define:

- *The requirements that are expected from the process,*
- *Constraints within the desired material class, shape class and process attributes are identified, and*
- *Criteria for manufacturing process evaluation and selection.*

In the **second stage**, also called as feasibility phase [2], set constraints are checked and unsuitable processes are eliminated. This phase is usually analytically realized by table searching which consists of matrix defined manufacturing process capabilities or constraints considering product, manufacturing and process characteristics. The most common criteria are type of material, shape, quantity, accuracy, etc.

In the **third**, optimization stage, ranking of potential manufacturig processes is performed according to defined optimization criterion/ia, i.e. objective function/s. The most common optimization criteria are manufacturing time and cost and product quality.

In the **fourth stage** the highest ranked processes are thoroughly analyzed and tested in order to obtain additional and confirmatory information about the quality of selections. The potential adverse effects are considered, and if some major deficiencies are determined, the following process by rank is adopted.

3. MODULE FOR MULTI-CRITERIA MANUFACTURING PROCESSES EVALUATION AND SELECTION

According to developed general and functional model of technological preparation of manufacturing [11,12] within the conceptual design stage of manufacturing process planning, four basic activities are realized:

(1) *manufacturability analysis of product design,*
(2) ***selection of basic manufacturing processes,***
(3) *selection of basic manufacturing resources, and*
(4) *manufacturing time and cost estimation.*

Based on this model the corresponding conceptual CAPP system is developed, figure 2, namely, DfM software solution, which comprises the module for selection of basic manufacturing processes.

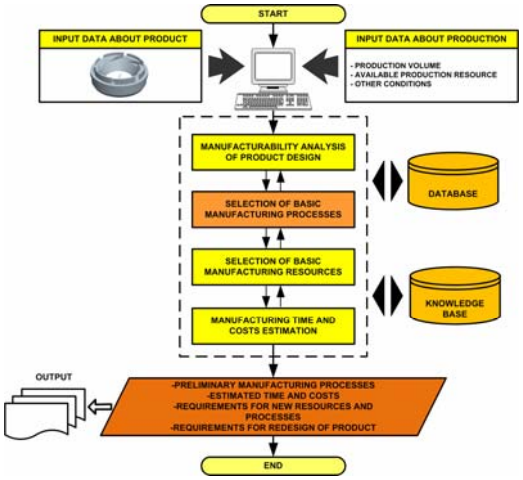

Fig. 2. Algorithm structure of the conceptual CAPP system [12,13]

Within the developed software solution of considered module, tasks are solving and related to defining and selection of basic manufacturing processes for producing parts, as well as assesment or evaluation and ranking of alternative variants of these manufacturing processes. Software solution algorithm of this module is shown in Figure 3.

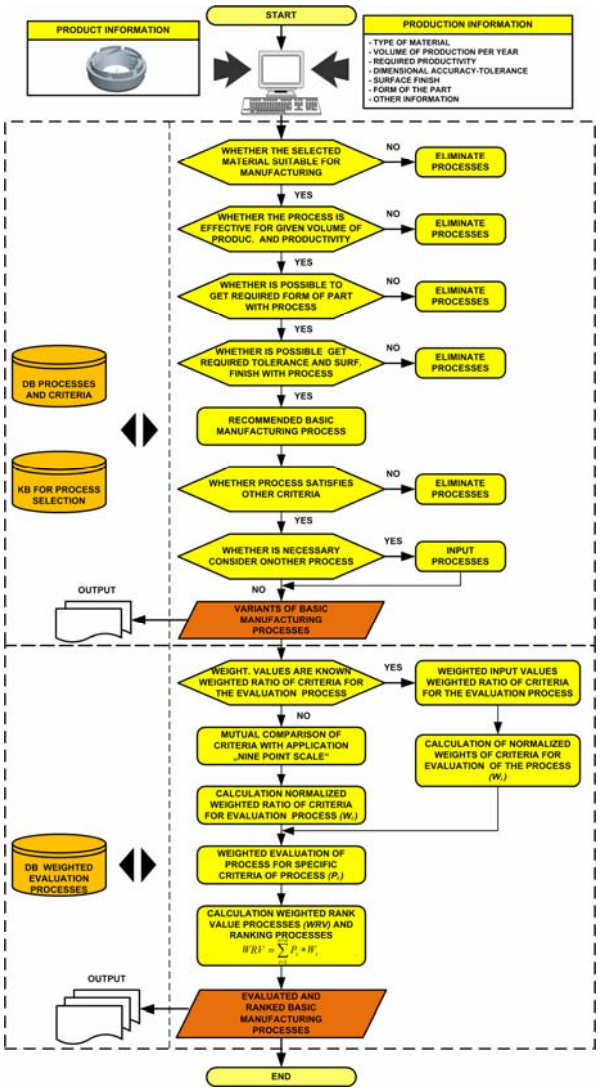

Fig. 3. Algorithm structure of software solution module for manufacturing process selection [12]

The basis for development of this module are related to realization of two key stages (second and third on Figure 1). Within the feasibility stage (stage 2), rules for the process selection based on the certain criteria are established, such as type of material, economical application of processes for the planned production volume, processing quality, accuracy, productivity, cost, etc.

After the elimination of processes that do not meet the criteria, the optimization stage is realized (stage 3), within which evaluation and ranking of manufacturing processes is performed. In the present case system for evaluation of manufacturing processes by ASM (American Society for Metals) is adopted [3], which includes the following evaluation criteria W_i: (A) production cycle time, (B) process flexibility, (C) material utilization, (D) quality and (E) operating costs.

Process evaluation (WRV) is performed according to formula (1), by which the order of importance of the processes, namely, their ranking, is determined. According to the reference data [2,3 etc.], weighted process scores (Pi) for considered criteria A÷D are defined.

$$WRV = \sum_{i=1}^{n} (P_i) \times (W_i) \qquad (1)$$

- *WRV – weighted rank values of the processes,*
- *n – total number of criteria,*
- *Pi – weighted process score for specific criterion,*
- *Wi – weight coefficient of criterion.*

Definition, or calculation of weighted coefficients of mentioned criteria (Wi) within this software solution can be performed in two ways:

a) By normalizing freely estimated weighted values of weight coefficients,

b) Mutual comparison of criteria with each other (9-point scale) and calculation of normalized weight coefficients by using the methodology which is applied to the AHP method [14].

4. SELECTION OF BASIC MANUFACTURING PROCESSES FOR THE BEARING OUTER RING

Basic input data for software solution of conceptual CAPP system refer to data from the drawings of outer ring of roller bearing, fig. 4. On this figure selection of suitable software solution module was performed.

Fig. 4. Input mask in conceptual CAPP system

In order to select possible variants of process for manufacturing bearing outer ring, suitable input data are entered, figure 5:

- *Type of material: Alloy steel (Č.4146)*
- *Annual production volume: Var.1 (100-1000 parts/yr.) and Var.2 (1000-10000 parts/yr.)*
- *Required productivity: low to 10 (parts/hour)*
- *Dimensional accuracy (level of dimensional tolerance): high (<0,13mm)*
- *Surface quality: high (<Ra=1,6μm (N7))*

These data also represents the criteria for elimination and selection of basic (primary) manufacturing processes, based on developed rules in the knowledge base. Software solution provides performing of manual elimination of some primary manufacturing processes, based on additional criteria such as specific labor, equipment and tool cost, then mass and wall thickness of part sections etc.

Based on these constraints and constraints of the manufacturing system itself for variant 1, two alternatives are selected, conventional and CNC machining.

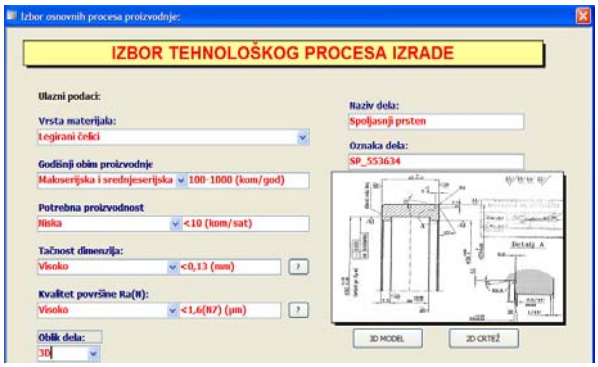

Fig. 5. Input data in module for selection of basic manufacturing processes

Figure 6 represents relative evaluation criteria and calculated values of weight coefficients for evaluation of alternative processes for manufacturing the bearing outer ring, according to method (b).

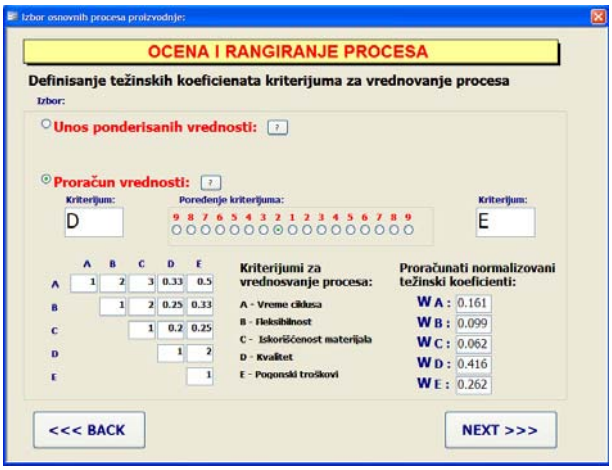

Fig. 6. Calculation of weight coefficients for evaluation of alternative solutions - Var1 - method (b)

After defining the weight coefficients for process evaluation, the calculation of the weighted rank value of processes (WRV) is performed according to formula (1). Figure 7 shows outputs of evaluation of alternative processes for manufacturing bearing outer ring, in case when method (b) for defining the weight coefficients is applied, according to Figure 6.

Fig.7. Results of evaluation and ranking of alternative processes for manufacturing the bearing ring - Var1

In the case of variant 2 when required production volume is 1000-10000 parts/year, alternative processing on CNC machines and automats are adopted by this software solution. For the present case, determination of weight coefficients by using other methods, i.e. comparing criteria with each other using scale "nine points", is performed, figure 8.

Figure 9 represents outputs of evaluation of these alternative primary processes for manufacturing the bearing ring.

Fig.8. Calculation of weight coefficients for the evaluation of alternative solutions - Var2 - method (b)

Fig.9. Results of evaluation and ranking of alternative processes for manufacturing the bearing ring – Var2

Based on these results, it can be concluded that for the given input data for the first variant of production quantity machining on CNC machines represents better solution, while for the second variant automats are better option. This is additionaly confirmed by application of software solution module for production cost estimation in paper [15].

5. CONCLUSION

Manufacturing process planning is one of the most important activities in the development of quality products and production time and cost reduction. Multi-criteria decision making methods (MCDM) are succesfully used for selection of optimal processes for part manufacture.

This paper briefly presents the basic foundation for the development of software solution module for multi-criteria selection of manufacturing processes, as piece of the conceptual CAPP systems, and its application for the selection of the optimal basic process for manufacturing the roller bearing outer ring.

6. REFERENCES

[1] Ashby, M.F.: *Materials Selection in Mechanical Design*, Butterworth-Heinemann, 2005.

[2] Creese, R.C.: *Introduction to Manufacturing Processes and Materials*, Marcel Dekker, Inc., New York, 1999.

[3] ASM Handbook: *Material Selection and Design*, *Vol. 20*, ASM, Ohio, 1997.

[4] Boothroyd, G., Dewhurst, P., Knight, W.: *Product Design for Manufacture and Assembly*, 2nd edition, Marcel Dekker, New York, 2002.

[5] Bralla, J. G.: *Design for Manufacturability Handbook*, 2nd Edition. McGraw-Hill, New York, 1998.

[6] Corrado, P.: *Design for Manufacturing: A structured Approach*, Butterworth-Heinemann, Woburn, 2001.

[7] Feng, S., Zhang Y.: *Conceptual Process Planning–A definition and functional decomposition, Manufacturing Science and Engineering*, Proceedings of the International Mechanical Engineering Congress and Exposition, Vol.10, pp. 97-106, 1999.

[8] Luttervelt, C.A.: *Research Challenges in CAPP*, Production Engineering and Computers, Vol. 4, No. 5, FME, Belgrade, pp. 5-18, 2002.

[9] Febransyah, A.: *A Feature-based Approach to Automating High-Level Process Planning*, Doctoral thesis, Faculty of North Carolina State University, 2001.

[10] Todić, V., Lukić, D., Milošević, M., Jovičić, G., Vukman, J.: *Manufacturability of product design regarding suitability for manufacturing and assembly (DfMA)*, Journal of Production engineering, Vol. 16, No. 1, pp. 47-50, 2013.

[11] Lukić, D., Todić, V., Milošević, M.: *Model of Modern Technological Production Preparation*, Proceedings in Manufacturing Systems, Vol. 5, No. 1, pp. 15-22, 2010.

[12] Lukić, D.: *Development of a General Technological Preparation of Production Model*, Doctoral thesis, Faculty of Technical Science, 2012. (In serbian)

[13] Lukić D., Todić V., Milošević M., Jovičić G., Vukman J.: *Software development for conceptual process planning*, 11th Anniversary International conference an accomplisments in Electrical and Mechanical Engineering and Information Technology, FME, Banja Luka, pp. 375-381, 2013.

[14] Saaty, T.L.: *Multi-criteria Decision Making: The Analytic Hierarchy Process*, Pittsburgh, PA: RWS Publication, 1990.

[15] Lukić D., Todić V., Milošević M., Vukman J., Jovičić G.: *Verification of The Development Conceptual CAPP System on The Example of Roller Bearings*, 11th Anniversary International conference an accomplisments in Electrical and Mechanical Engineering and Information Technology, FME, Banja Luka, pp. 383-388, 2013.

Authors: **Assist. Professor Dr. Dejan Lukić, Assist. Professor Dr. Mijodrag Milošević, MS.c Jovan Vukman, MS.c Mića Đurđev,** University of Novi Sad, Faculty of Technical Sciences, Department for Production Engineering, Trg Dositeja Obradovica 6, 21000 Novi Sad, Serbia, Phone.: +381 21 485-2331, Fax: +381 21 454-495.

MS.c Stevo Borojević, assistent, University of Banja Luka, Faculty of Mechanical Engineering, Vojvode Stepe Stepanovica 71, 78000 Banja Luka, Republika Srpska, BiH, Phone.: +387 51 433 068

E-mail: lukicd@uns.ac.rs; mido@uns.ac.rs; vukman@uns.ac.rs; mdjurdjev@live.com; stevoborojevic@hotmail.com;

Note: This paper is part of a research on project "Modern approaches to the development of special bearings in mechanical engineering and medical prosthetics," TR 35025, supported by the Ministry of Education, Science and Technological Development, Republic of Serbia

Journal of Production Engineering
Vol.17 No.2

Preliminary Note

Abhimanu S. and Datta C.K

POLICY FOR MINIMIZATION OF SCRAP IN A PRODUCTION LINE WITH IMMEDIATE FEEDBACK AND MULTI SERVER WORKSTATIONS

Received: 01 September 2014 / Accepted: 13 October 2014

Abstract: *In this paper, we are studying to estimate the amount of scrap in a production line caused by unsuccessful processing of items at various processing units. We are studying to obtain mathematical expression to give the scrap amount. We have considered a production line consisting of an arbitrary number of processing units, all arranged in a series along a straight line. At each of the processing units, we have provided the facility of re-processing of a job/item at the same processing unit if its processing is not done correctly at that processing unit, and there is still chance of its processing once more at the same processing unit. We have considered multi server facility at each of the processing units. Arrival of jobs at the first processing unit is supposed to be according to Poisson rule and service times at all the processing units are supposed to be exponentially distributed.*
Key words: *Network of Queues, Processing Units, multi Server Queues, Immediate Feedback, Scrap*

Politika minimizacije otpada na proizvodnoj liniji sa trenutnom povratnom vezom u multi serverskom okruženju za sve proizvodne jedinice. *U ovom radu data je procena količine otpada na proizvodnoj liniji izazvana nakon neuspešne obrade predmeta na različitim proizvodnim jedinicama. Izveden je matematički izraz za dobijanje količine otpada. Proizvodna linija se sastoji od proizvoljnog broja proizvodnih jedinica poređane duž prave linije. Na svakoj proizvodnoj jedinici obezbeđen je objekat za doradu predmet, i ako obrada nije korektna postoji šansa za njegovu doradu na istoj proizvodnoj jedinici. Smatra se da na svakoj proizvodnoj jedinici se nalazi multi server. Dolazeći predmeti na prvoj proizvodnoj jedinici treba da budu u skladu sa Poasonovim pravilom i svim obradnim vremenima proizvodnih jedinica koje imaju eksponencijalnu distribuciju.*
Ključne reči: *Čekajuća mreža, proizvodne jedinice, multi server, trenutna povratna sprega, otpad*

1. INTRODUCTION

A production line is a sequence of a finite number of processing units arranged in a specific order (fig. 1). At each of the processing units, service may be provided by one person or one machine that is called single- server facility, or it can be provided by more than one persons or more than one machines that is called multi-server facility at the respective processing units. In this paper we have considered multi-server facility at each of the processing units. At each of the processing units, a specific type of processing is performed i.e. at different processing units material is processed differently. At a processing unit, the processing times of different jobs or items are independent and are distributed exponentially around a certain value, called mean processing time [1].

In a production line the processing of raw material or a job starts at the first processing unit. It is processed for a certain time interval at the first processing unit and then it is transferred to the second processing unit for other type of processing, if it's processing is done correctly at the first processing unit. This sequence is followed until the processing at the last processing unit is over. In a production line raw material is processed at a series of processing units one after the other and finally it is transformed into finished goods ready for use.

End of processing at each of the processing units give rise to the following three possibilities:

a) Processing at a unit is done correctly and the job or material is transferred to the next processing unit for other type of processing.

b) Processing at a unit is not done correctly but can be reprocessed once more at the same processing unit.

c) Processing at a unit is neither done correctly nor it can be reprocessed at the same processing unit i.e. this job or material is lost, in this situation the job or material is rejected and put into the scrap.

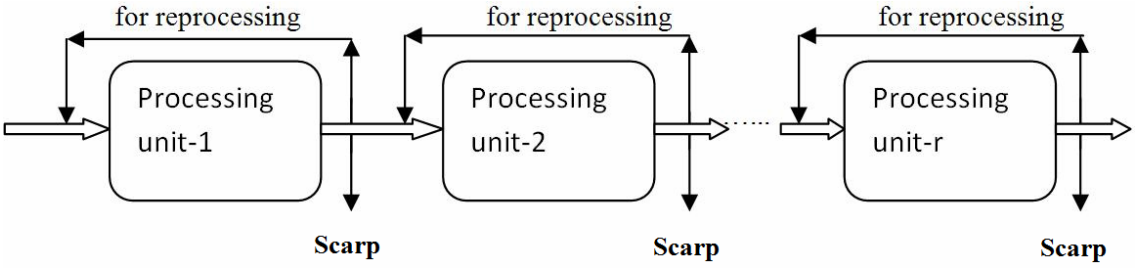

Fig.1. General Production line

2. LITERATURE SURVEY

A Queuing theory is a branch of applied mathematics that deals with phenomenon of waiting lines and arises from the use of powerful mathematical analysis to describe production processes. A lot of work has been done on the applications of Queuing Theory to study and analyze the production systems. After 1920, a lot of work has been done for developing the Queuing Theory as well as on its applications to model various phenomenons. Queuing theory's history goes back nearly 100 years. Johannsen's "WaitingTimes and Number of Calls" (an article published in 1907 and reprinted in Post Office Electrical Engineers Journal, London, October, 1910) seems to be the first paper on the subject. But the method used in this paper was not mathematically exact and therefore, from the point of view of exact treatment, the paper that has historic importance is A. K. Erlang's, "The Theory of Probabilities and Telephone Conversations" (Nyt tidsskrift for Matematik, B, 20 (1909), p. 33). Several researches have made efforts to apply queuing theory to model manufacturing systems. We are making effort to apply this theory to determine a policy to minimize the amount of scrap, which is produced due to ill-processing of material or jobs at various workstations of the production line. Many researchers have considered the queues in series having infinite queuing space before each servicing unit. [2] T. L. Saaty, in his book "Elements of Queuing Theory" has discussed various queuing models and their measures of performances. [3] R. R. P. Jackson, (1954) has found the steady state solution of a network of two queues in series. [4] R. R. P. Jackson, (1956) found the steady state solution of a serial network of arbitrary number of queues. [5] K. L. Arya, had found that the steady state distribution of queue length taking two queues in the system, where each of the two non-serial servers is separately in service with the other two non-serial servers. [6] O. P. Sharma studied the stationary behavior of a finite space queuing model consisting of queues in series. He had found the steady state solution of serial network of queues with multi server facility and infinite waiting space. In our model, we have introduced immediate-feedback at each of the processing units. [7] J. R. Jackson has discussed the network of queues. Arrivals to the first processing unit are according to Poisson rule and service times at each of the processing units are exponentially distributed. . [8] Trivedi, Kishor. S., in his book "Probability & Statistics with Reliability, Queuing and Computer Science Applications" has discussed the network of queues and has found the steady state solution of serial network of queues. [9] U. N. Bhat has discussed the steady state behavior of queues and found the steady state solution of a serial network of an arbitrary number of queues. [10] Leonard Kleinrock in his book "Queueing Systems, Computer Applications" vol.-1, has found the steady state probability distribution of number of units in the system. [11] Gross D , Harris CM in their book "Fundamentals of Queuing Theory" have discussed major queuing models. [12] J. Walrand in his book "An Introduction to Queuing Networks" has discussed a queuing system with immediate feedback and has suggested how the parameters change when immediate feedback is removed. [13] M. P.,GROOVER, in his book "Automation, Production Systems, and Computer-Integrated Manufacturing" has discussed various kinds of assembly line/ production line. [14] Curry Guy L, Feldman Richard M , in their book "Manufacturing System Modeling and Analysis, have discussed the M/M/1 queuing model with applications.

3. MODELING NOTATIONS

Maximum we consider a production line as shown in fig.2 consisting of an arbitrary number(r) of processing units arranged in a series in a specific order. Each of the processing units has multi- server facility and immediate feedback.

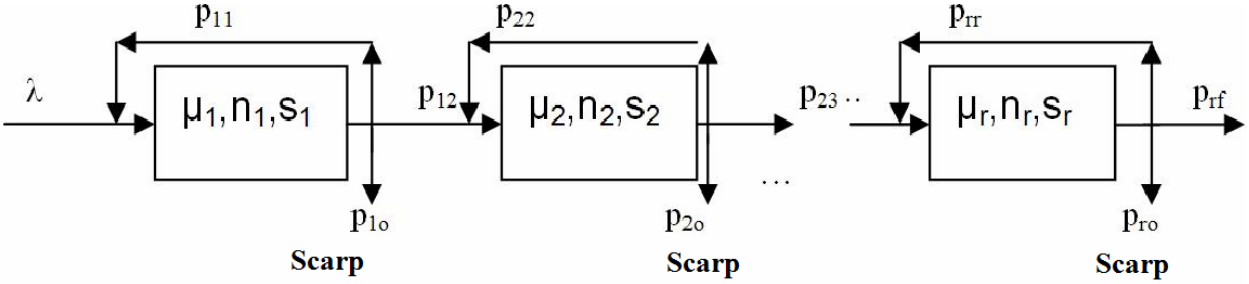

Fig.2. Proposed production line

λ - Mean arrival rate to the first processing unit from an infinite source, following Poisson's rule.

μ_i - Mean service rate of an individual server at the i^{th} processing unit having exponentially distributed service times.

s_i - Number of servers at the i^{th} processing unit

n_i - Number of unprocessed jobs before the i^{th} processing unit waiting for service, including one in service, if any, at any time t

$p_{i,i+1}$ - Probability that the processing of a job or material at the i^{th} processing unit is done correctly and it is transferred to the $(i+1)^{st}$ processing unit $p_{i,i}$ - Probability that the processing of a job or material at the i^{th} processing unit is not done correctly but it can be reprocessed once more, so, it is transferred to the same processing unit for processing once more.

$p_{i,o}$ - Probability that the processing of a job or material at the i^{th} processing unit is neither done correctly nor it remains suitable for reprocessing.

$P(n_1, n_2, ...n_r, t)$ - Probability that there are n_1 jobs waiting for processing before the first processing unit, including one in service, if any, n_2 jobs before the second processing unit waiting for service including one in service, if any, and so on, n_r jobs before the r^{th} processing unit waiting for service including one in service, if any at time t, with $n_i \geq 0 (1 \leq i \leq r)$, and $\mathrm{P}(n_1, n_2, ...n_r, t)$=0, if some n_i <0 (because number of jobs cannot be negative).

Queuing Network: An interconnected collection of stations in which customers move from one station to another requesting service called queuing network, where each station consists of a queue where customers (or jobs) wait for service.

The above production line can be represented by a serial network of queues (Fig. 3) in which each workstation is equivalent to a queue with the same number of similar servers and the same numbers of jobs waiting for service.

In the above serial network of queues, each queue has immediate feedback. To analyze this serial network of queues firstly we remove the immediate feedback.

After removing the immediate feedback, the above serial network of queues is replaced by one, as follows:

Here $\mu_i^{'} = \mu_i (1 - p_{i,i})$, [11] is the effective service at the i^{th} processing unit after the removal of the immediate feedback.

And the respective probabilities become as follows:

$$q_{i,o} = \frac{p_{i,o}}{(1 - p_{i,i})}, q_{i,i+1} = \frac{p_{i,i+1}}{(1 - p_{i,i})} \quad (1)$$

Under the steady state conditions, we have [1, 8, 10]:

$$\left[\lambda + s_1\mu_1^{'} + s_2\mu_2^{'} + ... + s_r\mu_r^{'}\right].$$

$$\mathrm{P}(n_1, n_2, ...n_r) = \lambda \mathrm{P}(n_1 - 1, n_2 n_3, ...n_r) +$$

$$\sum_{i=1}^{r} s_i\mu_i^{'}.q_{i,i+1}.P(n_1, n_2, ...n_i + 1, n_{i+1} - 1, ...n_r) +$$

$$\sum_{i=1}^{r} s_i\mu_i^{'}.q_{i,o}.P(n_1, n_2, ...n_i + 1.n_{i+1}, ...n_r) \quad (2)$$

4. SOLUTION FOR INFINITE QUEUING SYSTEM

Under the steady state conditions all the queues behave independently and thus the solution of steady state equation in product form is given by

$$\mathrm{P}(n_1, n_2, ...n_r) = \prod_{i=1}^{r} (1 - \rho_i)\rho_i^{n_i} \quad (3)$$

where $n_i \geq 0 (1 \leq i \leq r)$ and $\rho_i < 1 \ (1 \leq i \leq r)$.

If any $\rho_i \ (1 \leq i \leq r) > 1$ then the stability is disturbed and the behavior of the system will not remain stationary consequently solution will not be given by Eq. (3) [1, 5, 7, 8, 10, 13].

Here, we have

$$\rho_i = \frac{\lambda_i}{s_i\mu_i^{'}},$$

where $\lambda_i = \lambda \prod_{k=1}^{i} \frac{p_{k-1,k}}{(1 - p_{k-1,k-1})}, \quad p_{0,0} = 0$

Thus

$$\rho_i = \frac{\lambda}{s_i\mu_i} \prod_{k=1}^{i} \frac{p_{k-1,k}}{(1 - p_{k,k})}, \quad (4)$$

with $p_{0,1} = 1$.

It is observed that

$$\sum_{i=1}^{r} \lambda_i.q_{i,o} + \lambda_r.q_{r,f} = \lambda \quad (5)$$

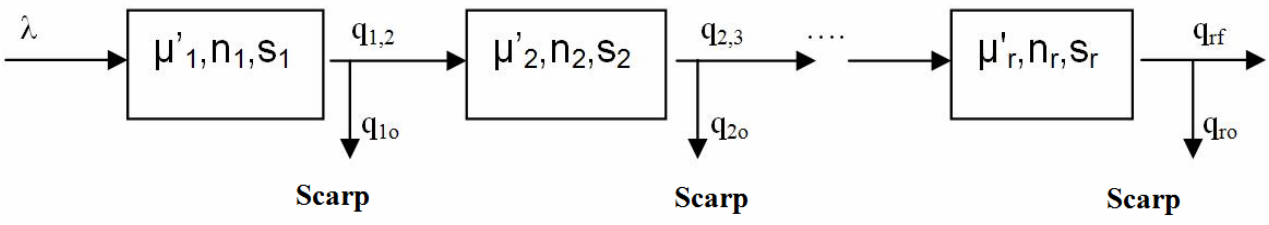

Fig.3. Equivalent serial network of queues representing the production line

5. AVERAGE AMOUNT OF SCRAP

As we start the production line, its first workstation starts working and the output of this workstation is checked for quality. If the processing of the job is done correctly, then it is transferred to the second workstation. If its processing is not done correctly, but it still possesses the quality for reprocessing once more at the same workstation, then it is reprocessed at the first workstation. If the processing at the first workstation is neither done correctly nor it possesses the quality for reprocessing at the first workstation, then it is rejected and put into the scrap. This quality check is performed at all the workstations in the production line. Finally, the work part/a job/material is processed at the last workstation. In this way, the jobs/work parts, which are not processed correctly as well as they do not have the quality required for reprocessing, are useless and put into the scrap.

Under steady state condition, A, the amount of scrap produced per unit of time is:

A= The amount of scrap obtained from all the workstations of the production line (due to unsuccessful processing of material/a job/a work part),

= Sum of amounts of scrap obtained at all of the workstations of the production line,

= amount of scrap obtained at the first workstation + amount of scrap obtained at the second workstation + ...,

... + amount of scrap obtained at the last workstation.

$$A = \lambda\, q_{1,o} + \lambda\, q_{1,2}\, q_{2,o} + \ldots + \lambda\, q_{1,2}\, q_{2,3} \ldots q_{r-1,r}\, q_{r,o}$$

$$= \sum_{i=1}^{r} \lambda\, q_{1,2}.q_{2,3}...q_{i-1,i} q_{i,o}\,, \text{ with } q_{0,1} = 1$$

$$= \lambda \sum_{i=1}^{r} \frac{p_{1,2}}{(1-p_{1,1})} \frac{p_{2,3}}{(1-p_{2,2})} \cdots \frac{p_{i-1,i}}{(1-p_{i-1,i-1})} \frac{p_{i,o}}{(1-p_{i,i})},$$

with $p_{0,0} = 0$, *and* $p_{0,1} = 1$

$$= \lambda \sum_{i=1}^{r} \prod_{k=1}^{i} \left(\frac{p_{k-1,k}}{1-p_{k-1,k-1}} \right) \frac{p_{i,o}}{(1-p_{i,i})} \qquad (6)$$

6. MINIMIZATION OF SCRAP

The scrap as given by the equation (6) can be minimized by minimizing each term in the summation given by the equation (6).

This we can do in two ways:

(i) By minimizing the numerator i.e. by minimizing the terms. Thus, one way of minimizing the scrap is the installation of machines with minimum rejection rate.

(ii) By maximizing the denominators i.e. by maximizing the terms in the denominators or by minimizing the values of scarp. Thus, another way of minimizing the scrap is the installation of machines with minimum reprocessing rate.

Finally, the scrap in the production line can be minimized by installing machines with minimum rejection rate and minimum reprocessing rate.

7. ACKNOWLEDGEMENT

I am thankful to the management and director of BPIT for providing a very conducive environment as well as to my colleague faculty members for invaluable suggestions and discussions.

8. REFERENCES

[1] Singh, A., Datta, C.K.: *Loss Minimization Policy for a Production Line with Immediate Feedback and Multi Server Facility at all Processing Units*, Journal of Production Engineering, vol. 16, No. 2013.

[2] Saaty, T. L.: Elements of Queuing Theory. McGraw-Hill, New York, 1961.

[3] Jackson, R. R. P.: *Queuing Systems with Phase Type Service,* Operations Research Quarterly, Vol. 5, No. 2, pp. 109-120, 1954.

[4] Jackson, R. R. P.: *Some equilibrium Results for the Queueing Process Ek/ M/I*, Journal of the Royal Statistical Society, 1956.

[5] Arya,K. L.: *Study of a Network of Serial and Non-serial Servers with Phase Type Service and Finite Queuing Space*, Journal of Applied Probability, Vol. 9, No.1, pp. 198-201, 1972.

[6] Sharma,O. P.: *A Model for Queues in Series*, Journal of Applied Probability, Vol.10, No.3, pp. 691-696, 1973.

[7] Jackson, J. R.: *Networks of waiting lines*, Oper. Res., 5, pp. 518-521, 1957.

[8] Trivedi, Kishor. S.: *Probability & Statistics with Reliability,* Queuing and Computer Science Applications. Wiley India, (P.) Ltd., 4435/7, Ansari Road, Daryaganj, New Delhi, 2002.

[9] Bhat, U. Narayan: *An Introduction to Queuing Theory*. Birkhäuser Boston, pp.144-147, 2008.

[10] Leonard Kleinrock: *Queueing Systems*, Computer Applications, Volume 2 , Wiley Interscience, pp. 147-152, 1976.

[11] Gross. D, Harris C.M.: *Fundamentals of Queuing Theory.* John-Wiley, New York, pp.220-226, 1985.

[12] Warland, J.: *An Introduction to Queuing Networks*, Prentice Hall, Englewood Clifs, New Jersey, USA, pp.160, 1998.

[13] GROOVER, M. P.: *Automation, Production Systems, and Computer-Integrated Manufacturing*, Pearson Education, Delhi, India, 2004.

[14] Curry Guy L., Feldman Richard, M.: *Manufacturing System*, Springer-Verlag Berlin Heidelberg, pp.77-80, 2011.

Authors: **Mr. Abhimanu Singh**, Research Scholar at Faculty of Technology, university of Delhi, Delhi, India, Assistant Professor at BPIT, Rohini, Delhi, India. **Prof., Dr., C. K. Datta,** Deptt. of Mechanical Engineering, PDM College of Engineering, Bahadurgarh, Haryana, India(Formerly Professor in Production Engineering at Delhi Technological University, Delhi, India).

E-Mail: asingh19669@yahoo.co.in

Journal of Production Engineering
Vol.17 No.2

Preliminary Note

Żurawski, Ł., Kapłonek, W.

VISION SYSTEMS USED FOR THE ASSESSMENT OF THE MEASUREMENT ACCURACY OF LINEAR AND ROTATING TABLES WITH STEPPING MOTORS

Received: 25 September 2014 / Accepted: 15 October 2014

Abstract: *In this work, a simple method for determining the deviation of displacement and rotation for measurement tables with stepper motors has been described. During the tests a system for control of the tables equipped with an 8-bit AVR microcontroller ATMEGA16-16PI by Atmel was used. Also, an experimental setup based on a vision system for observation and digital image acquisition of the displacement of the stage macrometer, with a nominal length of 1 mm, was used. The experiments were carried out for three different values of the traverse and rotational speed. The results showed that the tested measurement tables with stepper motors, exhibited numerous deviations of displacement and rotation occurring relative to the nominal dimension. These results were statistically analysed. On the basis of this analysis frequencies of occurrence of the deviation values were determined and are detailed in the final part of the work.*
Key words: *Displacement deviation, rotation deviation, measurement accuracy, stepper motor, vision system*

Optički sistem za procenu merne tačnosti linearnih i rotacionih stolova sa koračnim motorom. *U ovom radu je opisan jednostavan metod za određivanje odstupanja pozicioniranja i rotacije mernih stolova sa koračnim motorima. Tokom testa je korišćen sistem za kontrolu stolova sa 8 - bitnim AVR mikrokontrolerom ATMEGA16-16PI proizvođača Atmel. Takođe je korišćen i eksperimentalni optički sistem za praćenje i akviziciju digitalnih slika odstupanja makrometra, nominalne dužine 1 mm. Eksperimenti su sprovedeni za tri različite vrednosti brzine pozicioniranja i rotacije. Rezultati su pokazali da je testirani merni sto imao razna odstupanja pri pozicioniranju i rotaciji realtivnoj na nominalnu dimenziju. Ovi rezultati su statistički analizirani. Na osnovu analize frekvencije pojave odstupanja, određene su vrednosti iste i detaljno prikazane u završnom delu rada.*
Ključne reči: *Zapreminsko odstupanje , rotaciono odstupanje , tačnost merenja , koračni motor , optički sistem*

1. INTRODUCTION

Current market NC (*Numerical Control*)/CNC (*Computerized Numerical Control*) machine tools [1,2] are constructed of modules with modern kinematic and structural solutions [3]. A modular design with flexible configuration of components, enables effective machining of a number of materials currently used in modern automotive and aerospace industries. The modules are presented during various stages of repair. For example, for CNC tooling systems turning and milling are used, among others, in the following modules:

- direct tool holders (adapters) – mounted directly in the tool head or spindle,
- indirect tool holders (adapters) – giving the desired reach of the machining tool,
- tool holders – fixing the classic tool or tip of the folding tool with a cutting blade.

Typical solutions used in the NC/CNC technological machines are the modules based on the rolling rail guides, screw-rolling guides and direct transmissions that have different numbers of headstocks with additional independent control drives.

The above mentioned modules are also present in linear and rotating measurement tables with stepper motors [4]. In order to obtain accurate displacements of workpieces mounted on the tables proper procedures must be used. Such tests require the designation of displacement and rotational deviations as well carrying out their statistical analysis.

2. EXPERIMENTAL TESTS

2.1 Main goal of the experimental tests

The main goal was to develop a methodology for testing measurement tables equipped with stepper motors. This methodology also required calculation of displacement and rotational deviations as well as the carrying out of their statistical analysis.

2.2 Characteristics of the experimental setup

The experimental setup was based on a vision system equipped with a color CCD camera CAM-620C by Camstar (Poland). The optical system, consisted of a tube tube lens (ϕ = 46.5 mm, l = 200 mm), a set of 4 spacer rings (2 – ϕ = 46.5 mm, l = 15 mm + 2 – ϕ = 46.5 mm, l = 30 mm) and an objective lens Helios 44M-4 by KMZ (Russia). All of these devices were used in conjunction with the camera. The general characteristics of the CCD camera CAM-620C and objective lens Helios 44M-4 are given in Tabs. 1 and 2 respectively.

Parameter	Value
Detector	1/3" Sony Exview HAD CCD
Picture Elements	PAL: 500(H)×582(V), NTSC: 510(H)×492(V)
Horizontal resolution	480TV lines
Minimum illumination	0.01 lux / F1.2
Electric shutter	1/50(1/60)~1/100.000 s

Table 1. The general characteristics of the color CCD camera CAM-620C by Camstar

The vision system was mounted on a steel base with the dimensions 380×310×20 mm. Platforms with 2 tables, both equipped with stepper motors, were fixed to the aforementioned base.

Parameter	Value
Focal lenght	58 mm
Aperture	f/2.0-f/16
Angle of view	40°28'
Mount	42, K
Optical resolution	38/19 lines/mm
Transmittance	0.80

Table 2. The general characteristics of the objective lens Helios 44M-4 by KHZ

These platforms with stepper motors allowed for the realization of linear displacements. Table 1, with dimensions of 300×80 mm, enabled the realisation of longitudinal displacements in the range of 0 to 170 mm, with a screw pitch of 0.5 mm. Table 2, with dimensions of 250×80 mm, allow for the realisation of transverse displacements. Both tables were driven by stepper motors (step angle: 1.8°) type 42BYG020 by Kysan Electronics (China). For control of the motors the system based on 8-bit AVR microcontroller ATMEGA16-16PI, by Atmel (USA), was used. On the top side of the control system a digital display was placed which gave the values of displacement (in microns) and rotation (in ° of the plane angle) of the table. On that set of tables was mounted the rotary table (ϕ = 90 mm, h = 110 mm), equipped (depending on configuration) with 1 or 2 stage micrometers. In this case a stage object micrometer for transmitted light produced by LOMO (Russia) was used. An element, developed in accordance with GOST 7513-55 standard, was a transparent glass plate with 1 mm long scale having 0.01 mm scale factor. This glass plate with scale was protected by 0.17 mm cover glass and glued into a steel holder with dimensions of 76×26×2 mm. The general view of this setup is presented in Fig. 1a, whereas the general view of one used in tests stage object micrometers is presented in Fig. 2.

Fig. 2. General view of a stage object micrometer produced by LOMO (Russia) used in the tests

Connection between the microcontroller and the PC workstation was made possible by using a standard RS-232 port. The HyperTerminal from Microsoft Windows XP® was helpful during the entering of commands controlling the movement of the stepper motors on the measurement tables. A list of typical commands are given in Tab. 3.

For the acquisition of digital images the authors developed an application in the LabVIEW 7.1 environment produced by National Instruments (USA) [5].

2.3 Methodology and results of the experimental tests

The experiments were carried out for 2 configurations of the system, presented in Fig. 1b-c. In Configuration I the measurement accuracy of a linear table was determined, whereas in Configuration II it was the measurement accuracy of a rotary table. For each configuration the measurements were carried out for 3 different values of the traverse and rotational speeds. Each measurement was carried out 30 times in the distance between the points A and B of a stage object micrometer. This situation is shown in Fig. 3.

During the determining of the linear table measurement accuracy the measurement range was 74628 steps, which after conversion (1 step – displacement of 1.25 μm) gave a length of 93.285 mm. The movement of the rotating table was realized according to a clockwise

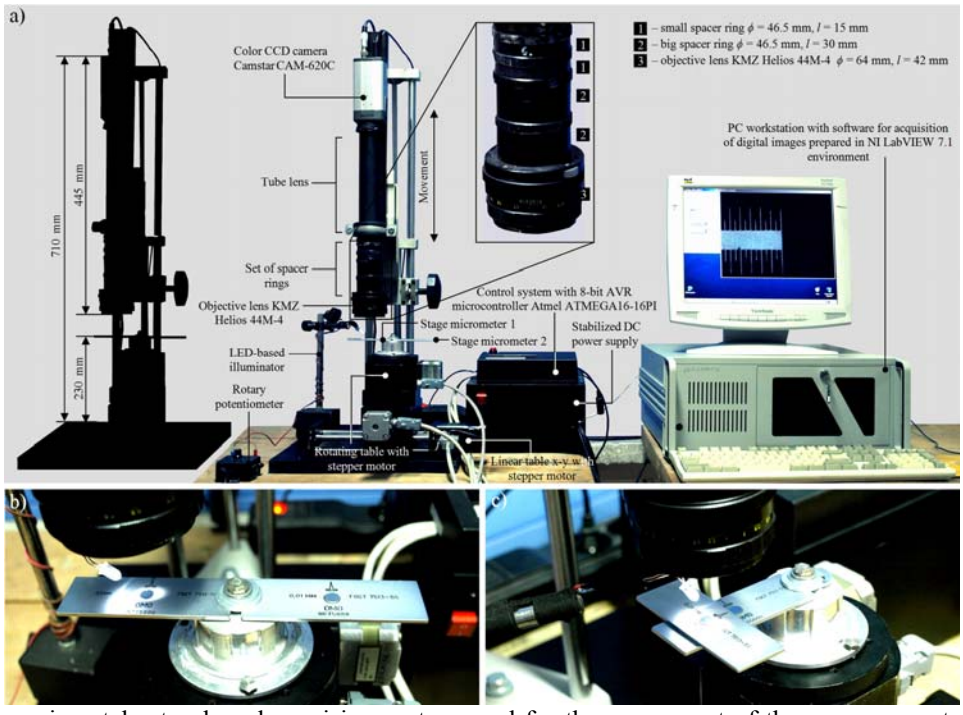

Fig. 1. The experimental setup based on vision system used for the assessment of the measurement accuracy of a linear and rotating tables with stepping motor: a) general view of the system, b) system in Configuration I for measurement accuracy of a linear table, c) system in Configuration II for measurement accuracy of a rotary table

Command	Description
X+"numerical value"	The displacement of the linear table by a positive numerical value with regard to the *x* axis
X–"numerical value"	The displacement of the linear table by a negative numerical value with regard to the *x* axis
O+"numerical value"	The rotation of the rotational table by a positive numerical value
O–"numerical value"	The rotation of the rotational table by a negative numerical value
Spee="numerical value"	The setting of speed in a range from 0 to 255 (standard value 220), arbitrary units
Reset	Resetting the table, the current setting is replaced by the coordinates 0.0
Stop	Stopping the table
Back	Reversing to the zero position

Table 3. The commands used to control the stepper motors

motion. In this case a single measure was included consisting 5 full turns (1800°). In the Tabs. 4-5 giving the range available to set values "spee" speed. These values were converted and given their units. For the traverse speed of the linear table the values are as follows: 150 = 10 mm/ min, 220 = 30 mm/min and 245 = 66 mm/min, whereas for the rotary table they were: 150 = 0.22 r/min, 220 = 0.65 r/min and 245 = 2.14 r/min.

Tabs. 4-5 also give the results of the statistical analysis that was carried out simultaneously. The analysis included the values of the arithmetic mean, variance as well as standard deviation for the data obtained from the measurements. The authors additionally determined the value of the gauge capability index (scatter index) [6] from the given equation (1) for the linear and rotary table. This index is referred to in the following equation (2).

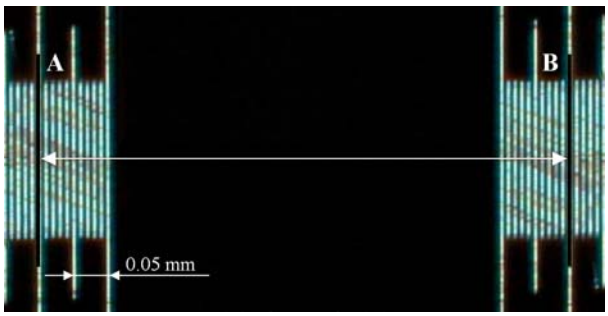

Fig. 3. Example view of movement in the distance A-B realized by two object stage micrometers used in Configuration II of the linear table

$$C_g = \frac{0.2 \cdot T}{6 \cdot s_g} = \frac{0.2\,(USL - LSL)}{6 \cdot s_g}, \qquad (1)$$

$$0.2\,T = 0.2\,(USL - LSL), \qquad (2)$$

where: s_g – standard deviation, T – tolerance, USL – upper size limit, LSL – lower size limit

Traverse speed	Deviation value for displacement of the linear table, mm					
	Arithmetic mean	Variance	Standard deviation	Tolerance	Min.	Max.
n_t = 10 mm/min	0.0296	0.0008	0.0294	1.1797	–0.02	0.08
n_t = 30 mm/min	0.0483	0.0008	0,0296	1.1869	–0.01	0.12
n_t = 66 mm/min	0.0426	0.0012	0.0350	1.4006	–0.02	0.11

Table 4. Statistical analysis of the measurement results for the linear table

Rotational speed	Deviation value for rotation of the rotary table, minutes of arc (1/60°)					
	Arithmetic mean	Variance	Standard deviation	Tolerance	Min.	Max.
n_r = 0.22 r/min	0.3487	7.7191	2.7783	111.133 (1.85°)	–4.96	4.96
n_r = 0.65 r/min	–0.5693	5.1034	2.259	90.363 (1,5°)	–4.4	3.85
n_r = 2.14 r/min	–1.9113	7.0346	2.6522	106.091 (1.76°)	–7.18	4.4

Table 5. Statistical analysis of the measurement results for the rotary table

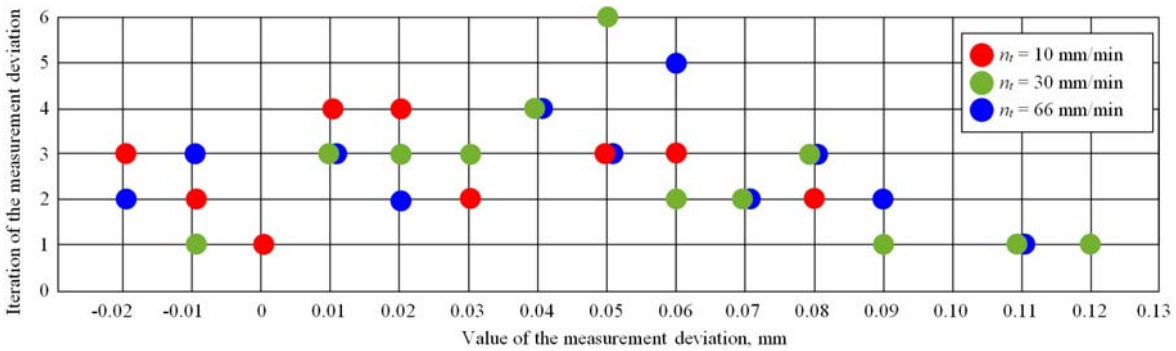

Fig. 4. The frequency of measurement deviation for linear table

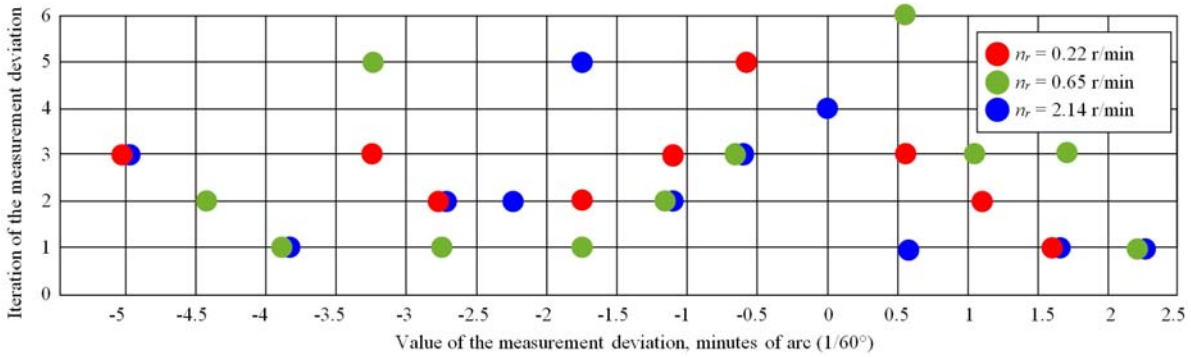

Fig. 5. The frequency of measurement deviation for rotary table

The results obtained were in the range of -0.02 to 0.12 mm for the linear table and -5 to 2.5 minutes of arc for the rotary table. Figs. 4-5 present the incidence of deviations of the measuring values calculated for the tested tables.

Analysis of the values of deviations presented for the linear table (Fig. 4), shows there is a high concentration in the range of positive values. The lowest number of deviations (9) was found for n_t = 10 mm/min, while the highest (12) for n_t = 30 mm/min. The interval of the highest number of iterations between the values 0.01 and 0.09 mm was observed. The highest number of iterations (6) was found for the deviation of the value 0.05 mm at n_t = 30 mm/min. The average value of the deviation for a linear table was 0.04 mm.

Fig. 5 presents the results of measurements of deviations obtained for the rotary table. In this case, most of the results were centred around the range of negative values. The lowest number of deviations (9) was found for n_r = 0.22 r/min, while the highest (11) for other rotational speeds. The highest number of iterations (6) was found for the deviation of the value 0.5 minutes of arc at n_r = 0.65 r/min. The average value of the deviation for a rotary table was -0.94 minutes of arc. The results obtained show that deviations during operation of the tested measuring tables (regardless of their type) were found. On the basis of data generated by these analyses, there are questions to be asked about the proper operation of the device..The calculated value of the gauge capability index may also prove helpful in this regard. For those tables tested during this work the value is 1.33, which indicates it meets the objectives of the SPC (*Statistical Process Control*) [7,8]. This means that both devices can be used for carrying out measurements, in which the observed values of deviations will not have a substantial effect on the results obtained.

3. CONCLUSION

The issues presented in this paper constituted a relatively important problem at the intersection of modern manufacturing technology and the metrology of geometrical quantities. Determination of the displacement and rotation deviations for tested measurement tables enables reliable information about their metrological parameters to be obtained, which is important from the point of view of their application.

The authors intend to continue research into the subjects presented in the present work. The next activities will focus on, among others, designing and constructing a module for monitoring of wear of the cutting inserts. The development of such a module will increase the likelihood of obtaining a useful measuring device, which is necessary for the correct diagnosis of cutting tools used in modern highly efficient machining processes.

4. REFERENCES

[1] Suh, S-H. et al.: *Theory and Design of CNC Systems,* Springer-Verlag, London, UK, 2008.
[2] Mattson, M.: *CNC Programming: Principles and Application,*. Delmar, Clifton Park, USA, 2009.
[3] Agrawal, P. M., Pate, V. J.: *CNC Fundamentals and Programming,* Charotar Publishing, Anand, India, 2009.
[4] Overby, A.: *CNC Machining Handbook: Building, Programming, and Implementation,* McGraw Hill, New York, USA, 2011.
[5] Kapłonek, W., Żurawski, Ł.: *Assessment of the Milled Surface Microroughness by Optical Measurement Methods and Computer Image Analysis,* Advances in Materials Science, 8(16), p.p. 36-43, 2008. (in polish)
[6] Sałaciński, T.: *Analysis of Tools and Measurement Systems Capabilities,* Journal of Machine Engineering, 17(2), p.p. 74-83, 2012. (in polish)
[7] Oakland, J. S.: *Statistical Process Control (6th Edition),* Butterworth-Heinemann, Burlington, USA, 2007.
[8] Ge, Z., Song, Z.: *Multivariate Statistical Process Control: Process Monitoring Methods and Applications,* Springer-Verlag, London, 2013.

Authors:
Dr. Łukasz Żurawski, Ph.D, ME, Koszalin University of Technology, Faculty of Mechanical Engineering, Subject Group of Monitoring Technological Processes, Racławicka 15-17, 75-620 Koszalin, Poland, Phone: +48 94 3478312, Fax: +48 94 3426753, E-mail: lukasz.zurawski@tu.koszalin.pl

Dr. Wojciech Kapłonek, Ph.D, ME, Koszalin University of Technology, Faculty of Mechanical Engineering, Department of Production Engineering, Subject Group of Metrology and Quality, *Racławicka 15-17, 75-620 Koszalin, Poland, Phone: +48 94 3478233, Fax: +48 94 3426753,*
E-mail: wojciech.kaplonek@tu.koszalin.pl

Journal of Production Engineering
Vol.17 No.2

Preliminary Note

Šebo, J., Rosenfelderová, T.

CONDITIONS AND FACTORS AFFECTING SUITABILITY OF REUSE AND RECYCLING AS OPTIONS FOR THE HANDLING WITH UNNEEDED MOBILE PHONES

Received: 27August 2014 / Accepted: 30 September 2014

Abstract: *The contribution deals with the reuse and recycling as options for handling with unneeded mobile phones. The aim is to assess the socio-economic and environmental conditions and factors affecting the reuse and recycling of mobile phones. Among the important factors and conditions can be classified growth in the number of mobile phones sold, reducing the mobile phone using time, rapid technological developments in the field of mobile phones, a small percentage of collected unneeded mobile phones, environmental awareness, legislative environment, the availability of the most advanced recycling technologies, content of precious commodities in mobile phone, geological availability of the commodities, market prices of metals and other commodities, the demand for second-hand mobile phones, flexibility of renovation companies, environmental impacts of recycling, recyclability of materials, the content of toxic substances in the mobile phone.*
Key words: *reuse, recycling, refurbishment, renovation, mobile phone*

Uslovi i faktori koji utiču na mogućnost ponovne upotrebe i reciklaže, kao opcije za ophođenje sa nepotrebnim mobilnim telefonima. *Ovde je predstavljen doprinos ponovne upotrebe i reciklaže kao opcije ophođenja sa nepotrebnim mobilnim telefonima . Cilj je da se procene socio - ekonomski i ekološki uslovi i faktori koji utiču na ponovnu upotrebu i reciklažu mobilnih telefona . Među važne faktore i uslove se može svrstati rast prodaje mobilnih telefona te smanjenje vremena posedovanja mobilnog telefona, brz tehnološki razvoj u oblasti mobilnih telefona, mali procenat prikupljanja odbačenih mobilnih telefona, ekološka svest, zakonodavno okruženje, dostupnost najnaprednijih reciklažnih tehnologija, sadržaj dragocenih materijala u mobilnom telefonu, geološka dostupnost materijala, tržišna cena metala i drugih materijala, potražnja polovnih mobilnih telefona, fleksibilnost kompanija za renoviranje, uticaj reciklaže na životnu sredinu , reciklabilnost materijala, sadržaj toksičnih supstanci u mobilnom telefonu .*
Ključne reči: *ponovna upotreba , reciklaža , obnavljanje, renoviranje , mobilni telefon*

1. INTRODUCTION

Consumer electronics are now an integral part of everyday life for many of us. It is estimated that on average each person owns 24 pieces of various electrical and electronic equipment, this includes for example: TV, refrigerators, mobile phones, laptops, freezers, washing machines and other. Nowadays people are governed by trend, according to which the latest is best, which of course does not always reflect reality. Even if our currently used equipment is still far from reaching the end of its life we just place it in this category of and we look about for the newer devices, which automatically results in huge amounts of WEEE. According to various studies, it was found that in 2012 it was produced 54 million tons of WEEE worldwide. In Europe is calculated with 20 kg of WEEE per person over 5 years. [1,2] In addition, more than 70% of unnecessary consumer electronics consumers usually stored at home three to five years. They consider that these devices still have some value, but that assumption is wrong. With the rapid development of electronic technology, their residual value drops rapidly. [3]
Another reason why deal with unnecessary EEE is that they could contain up to 60 different types of components (materials) that can be classified as valuable. EEE belong to the category of major consumers of large amounts of precious and special metals. From most of EEE can these precious metals (e.g. gold, platinum, silver, zinc and palladium) be recovered. Group of the most valuable substances is usually contained in the printed circuit board. [4] From these scarce resources, however, only very small portion is recovered, which is related also to the fact that different countries have different legal regulations and also use various recycling technologies.
In dealing with unnecessary or end-of-life EEE, we can consider the following alternatives:

a) reuse of functional devices (with or without renovation),
b) reuse and recycling of the components and materials,
c) disposal (landfilling, incineration, or other)

2. SPECIFICS OF MOBILE PHONES REUSE

Unlike for other electronic and electrical equipment reuse of mobile phones (hereinafter MP) were prosperous industry. In the first decade of the 21st century existed in the U.S., UK and possibly in other developed countries rather profitable schemes of MP renovations intended mainly for third markets (mostly developing countries). During this period, up to 65% of collected MP in the United States were reused (about 50% in the UK) [5]. We understand here "reuse" as the further use of the product for the same purpose for which it was produced. Whether collected MP should be reused depends on several factors. Renovation can range from simple refurbishing (polishing, new packaging, etc.), software upgrade, minor repairs (e.g.

replacement of damaged components) to demanding renovation. The extent and nature of the renovation is selected according to which of these methods has the largest profitability. Usually, the most profitable is minimum of processing, since labor costs are large in relation to the selling price of renovated MP. Since a certain percentage of the collected MP is not suitable for reuse, they are sent for recycling.

3. SPECIFICS OF MOBILE PHONES RECYCLING

Despite the similarity in the management of other types of EEE, management unneeded or end-of-life MP has two essential specifics. MPs have a huge increase in sales, suggesting the need for an efficient solutions of already unneeded or end-of-life MPs . According to Strategy Analytics today 4.6 billion people owns MP, with the largest increase in sales of mobile phones in Africa, India and China. [6] The total number of mobile phones sold worldwide in 2014 is estimated at 1.9 billion (Fig. 1). There is also shortening of MPs using life, thereby increasing the number of unnecessary MP. MP using life, which accounted for roughly three years in 1991, dropping to 18 months in 2002 and today is probably even lower, and manufacturers believe that the technical lifetime of MP is about 10 years. [5] The second distinctive feature is very popular purchase of second hand. More mobile phones nowadays is reused as recycled. [5] According to estimates, however, in world measure the recycling gets only about 1%. [6] The surveys also point to the fact that the owners of electronic products after their use, from whatever reason, have lack of knowledge about how to proceed with unnecessary EEE. [5]

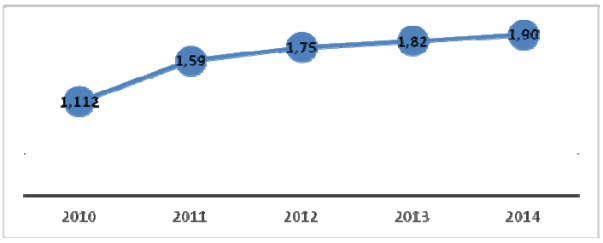

Fig. 1. Number of sold mobile phones in recent years in the world in billions. [based on data from company Gartner] (Note: data do not include information about smartphones or iPhones)

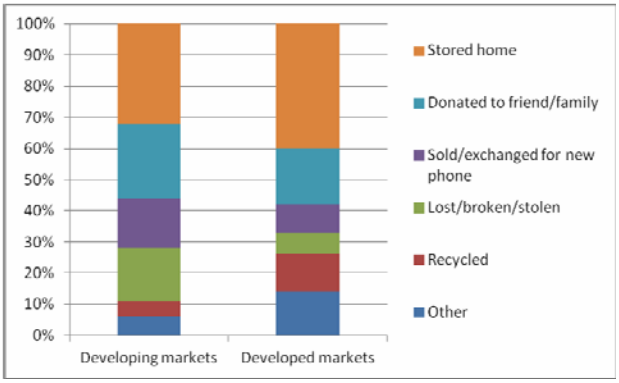

Fig. 2. How people handle their useless MP (modified according to [7])

Recycling process of the mobile phone is quite similar to other electronic devices. MPs are disassembled and with assistance of separation, metallurgical and chemical processes are recovered various metals. Separated plastic parts may be used for the production of granulate. [6] Battery and flame retardants require separate handling and they complicate recycling.

4. SOCIO - ECONOMIC CONDITIONS AND FACTORS OF MOBILE PHONE REUSE AND RECYCLING

Some activities related to the MPs reuse and recycling are voluntary and ecologically motivated but some of them are stimulated by profit or legislation. Some studies (e.g. [8]) indicate a significant profit potential of renovation for expensive MP models and also covering of MP recycling cost by recycling revenues. When reusing MP the main source of revenues are income from the sale of refurbished or renovated MP and when recycling MP metals sales (especially precious) at commodity markets. In the world operate several commercial renovation company engaged in refurbishing, renovation and selling of used MP (for example. ReCellular, USA or Greener Solutions, United Kingdom). In order to be profitable renovation company, it need to use effective planning methods and tools capable of dealing with the specifics of acquiring unneeded MP, refurbishment, renovation and distribution processes. These tools should enable them to effectively restructure operations in view of the rapidly changing product, process and market conditions. The most often changing input parameters are the type and quantity of mobile phones offered on the market. In Western Europe, the average replacement cycles of MP less than 18 months and more than 100 new phone models every year, it can be assumed that customize the program for the renovation is required several times during the year. [9]

The low percentage of returned MP to place, for where is ensured an appropriate way of handling with them is one of the factors influencing the reuse and recycling. One of the surveys was executed in Finland, Italy, France, Germany, Russia, Sweden, UK, UAE, USA, Nigeria, China, India and Brazil revealed that only 3% of people recycle their mobile phones, two thirds reported that do not even know how to recycle their old MP and 71% did not know where to recycled. [7, 10] With the collection is also related problem that people often are not at all informed and if they briefly captures somewhere the topic of recycling (or reuse) MP the practical steps very little motivated. Problem is also collection form, which should be economically efficient and environmentally sound.

The second crucial factor affecting in particular MP recycling is the trend of the amount of precious metals in the MP and the prices of these metals (especially gold) on world commodity markets. Unnecessary EEE are often classified based on their gold content. MPs belong to the category with a medium (100-400 ppm) or high (above 400 ppm) gold value. [11] As shown in Figure 3 the value of the gold contained in the MP

depends both on the actual price of gold as well as the content in MP. In contrast to the presented graph, which presents a slight decrease in the gold content in MPs from 2003 to 2007, the study [13] presents the findings that nowadays manufacturers prefer gold as a component of the PCB, due to easier recovery compared to copper. According to Umicore gold recycling is economically and environmentally advantageous compared to metal recycling. [12] In addition to gold, the MP contains also a small number of other precious metals as silver and palladium. Regarding the amount of metal is most represented in MP copper (about 15% of MP weight [13]).

Another factor influencing in particular MP recycling is use of metals in the production of MPs , most of which belong to the "critical". Critical metals are important for the industrial production and are often limited by geological availability and economic factors. [11] These are metals that are economically and strategically important for the countries.

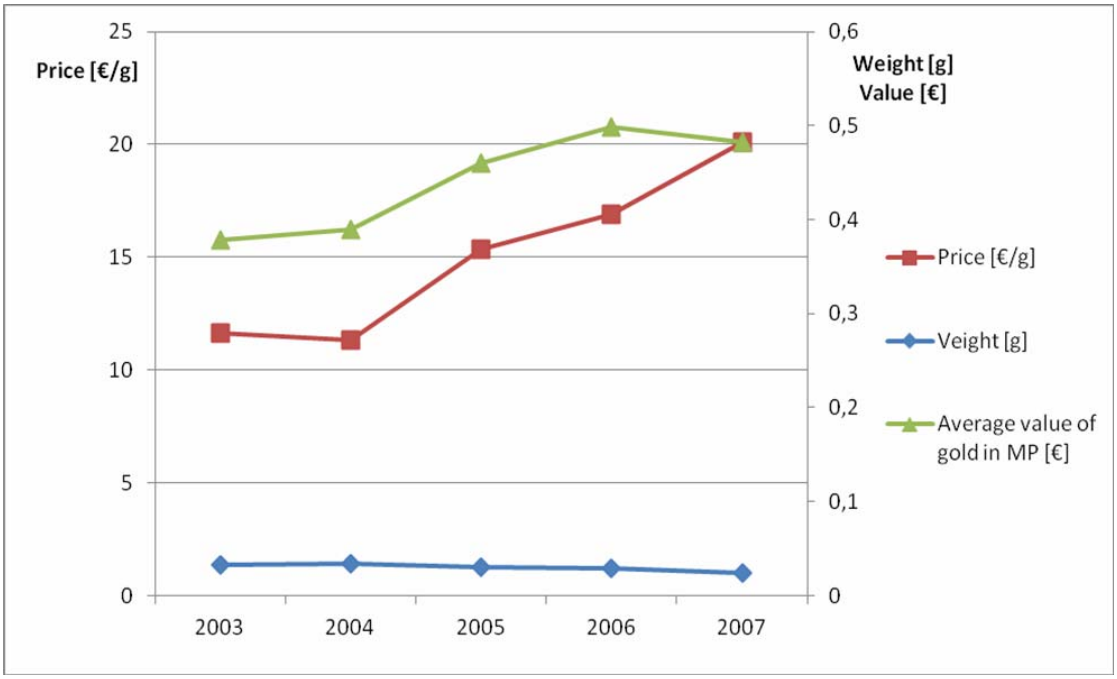

Fig. 3 Comparison of the average value of the gold in the MP according to the amount of gold in the MP and gold price in the commodity market (prepared on the basis of the data from [5, 14, 15, 16, 17])

5. ENVIRONMENTAL IMPACTS OF MOBILE PHONES IN RELATION TO THEIR REUSE AND RECYCLING

In terms of saving natural resources and reducing greenhouse gas emissions, the director for environmental affairs of Nokia Markus Tertho said that "if each user of mobile phones brought back just one unused device, we would save 240,000 tons of raw materials and reduce greenhouse gas emissions at the same extent as if we put 4 million cars out of the traffic". [10] This argument, however, cannot be considered an exhaustive answer to the question whether it is environmentally advantageous extract new raw materials or recycle MPs and obtain secondary raw materials.

In terms of direct impact on the environment and health materials contained in MP have negative impact at a certain level of concentration. It is not known that they are harmful in the case of a mobile phone in sound conditions, but when reaching the end-of-life or in lack of proper disposal they pose a threat. Through various studies it was demonstrated, that the harmful substances get into the soil and groundwater. These are, for example, lead, antimony, copper, nickel, chromium, mercury, cadmium and arsenic. These substances have been linked to a number of health problems. [18,19,20]

6. OUTLINE OF THE OPTIONS FOR ADDRESSING THE PROBLEMS ASSOCIATED WITH REUSE AND RECYCLING OF MOBILE PHONES BY CHANGING THE STRUCTURE (DESIGN) MOBILE PHONE

In terms of MP design to minimize impacts on the environment would be appropriate to establish the concept of reusable MP (or modular phone (note: currently one such concept is introduced by Motorola)). Also, avoiding of mixing different materials and components (or use recyclable materials and components), the use of standardized types of plastic and omission of toxic materials may improve recycling outcomes. Battery as potentially hazardous waste should also be easily dismantled. Of course these measures in design shall not excessively raise the price of MP and thus limit its potential for mass use. Mass use of modular telephones could also affect the amount of unnecessary MP, but one great force, which may be against is questionable variability and trendiness of modular design of MP.

7. CONCLUSION

The need to address the effective management of MP has been gaining strength with the increased

number of MP and the rate of obsolescence. One of the prerequisites for proper handling with MP is also adequate legislation and possession of the latest recycling technologies, which, however, from country to country may differ significantly. Finding economically and environmentally sound solutions for the handling with MP involves consideration of incorporating MP reuse and recycling in the life cycle of this product. Each of these alternatives, which also may supplement each other, has certain advantages and disadvantages, under certain conditions. Reuse is generally in terms of environmental priorities preferred alternative prior to recycling, while in the case of MPs is also economically profitable for expensive MP models. Reuse is, however, sensitive to the demand for refurbished and renovated MP and refurbishment and renovation require flexible planning, technical equipment and staff and operation and distribution processes. For the survival of the business model of renovation companies will also be essential to be able effectively include suitable enhancements (e.g. software upgrade, etc.) to refurbished or renovated MPs to increase their sale potential. MP recycling is from economical view capable to cover recycling costs by generated revenues. Its revenues are very dependent on the actual prices of precious metals (especially of gold). As for the quantity of secondary materials, in a significant quantity may be obtained from MP especially copper and plastics. Most metals in MP, however, belong to strategically important metals, what increases the importance of recovering. Some parts and materials as battery and flame retardants require separate disposal and they complicate recycling. Benefit of recycling is avoiding of deposition of MPs to the landfills and thereby prevents release of harmful substances into soil and groundwater. The problem connected with both alternatives is small percentage (about 1%) of collected unnecessary MP worldwide. One response to the problems with increasing amounts of unnecessary MPs is creation of the concept of modular MP (e.g. by Motorola), which has the potential to affect the MP reuse and recycling and mitigate the negative impacts on the environment, but its mass spread is our view so far prevented by demand for such MP in regard to questionable variability and trendiness of the design.

Acknowledgement:
This contribution has been supported by research grant VEGA 1/0879/13 (Agilné, trhu sa prispôsobujúce podnikové systémy s vysokoflexibilnou podnikovou štruktúrou).

8. REFERENCES

[1] LEWIS. T.: World's E-Waste to Grow 33% by 2017, Says Global Report, Live Science, December 2013 [online], [cit. 21.3.2014], dostupné na internete: http://www.livescience.com/41967-world-e-waste-to-grow-33-percent-2017.html

[2] NAMIAS J.: The future of elektronic waste recycling in the United States, Columbia University [ongline], [cit.15.3.2014], dostupné na internete: http://www.seas.columbia.edu/earth/wtert/sofos/Namias_Thesis_07-08-13.pdf

[3] KANG. Hai-Yong, SCHOENUNG J. M., Electronic waste recycling: A review of U.S.infrastructure and technology options, Resources, Conservation and Recycling 45 (2005) 368–400 [online], citované:[12.12.2013], dostupné na internete: https://wiki.umn.edu/pub/ESPM3241W/S11TopicSummaryTeamOne/Electronic_waste_recyclingA_review_of_U.S._infrastructure_and_technology_options.pdf

[4] SCHLUEP. M. at.al.: Recycling – from e-waste to recources, Sustainable Innovation and Technology Transfer Industrial Sector Studies, UNEP, July 2009 (1-90) [online] , [cit. 22.3.2014], dostupné na internete: http://www.unep.org/pdf/Recycling_From_e-waste_to_resources.pdf

[5] GEYER, R., 2010: The economics of cell phone reuse and recycling, Adv Manuf Technol, 47:515–52, DOI 10.1007/s00170-009-2228-z [online], citované: [18.12.2013], dostupné na internete: http://download.springer.com/static/pdf/463/art%253A10.1007%252Fs00170-009-2228-z.pdf?auth66=1397807200_1fc9c4ab99dedb114de92d61a8fa6c04&ext=.pdf

[6] Recyklácia mobilov. Recyklácia – magazín ASEKOL 1/2011 (online) [cited 2013-18-04] http://www.asekol.sk/sk/download/spotrebitelia/casopis-recyklacia/recyklacia201101.pdf

[7] TASKEN P.: Electronics Waste: Recycling of Mobile Phones, Postu-Consumer Waste Recycling and Optimal Production, Prof. Enri Damanhuri (Ed.), ISBN:978-953-51-0632-6, [online], [cit. 16.3.2014], dostupné na internete: http://www.intechopen.com/books/post-consumer-waste-recycling-and-optimal-production/electronics-waste-recycling-of-mobile-phones

[8] LANZILOTTO. A, GNONI. G.M.: System Dynamics Model for Sustainability Analysis of Mobile Phone Reverse Logistics, International Conference on Industrial Engineering and Operations Management Istanbul, Turkey, July 3 – 6, 2012 (1644 - 1653) [online], [cit. 21.3.2014], dostupné na internete: http://iieom.org/ieom2012/pdfs/390.pdf

[9] FRANKE, C.: Remanufacturing of mobile phones—capacity, program and facility adaptation planning, The International Jouranl of Management Science, Omega 34 (2006) 562 – 570 [online], citovavné: [20.12.2013], dostupné na internete: http://ac.els-cdn.com/S0305048305000241/1-s2.0-S0305048305000241-main.pdf?_tid=12ee51ca-c07e-11e3-849f-00000aab0f27&acdnat=1397113526_42601876df75c50d7062806ed4956e5a

[10] PETERS. M.: What happens with old mobile phones?, LetsGoMobile [online], [cit. 11.1.2013], dostupné na internete: http://www.letsgomobile.org/en/3707/old-phones/

[11] OECD: Case Study on Critical Metals in Mobile Phones Final Report, 2012 (1-87) [online], [cit.13.3.2014], dostupné na internete: http://www.oecd.org/env/waste/Case%20Study%20on%20Critical%20Metals%20in%20Mobile%20Phones.pdf
[12] Umicore Precious Metal Refining: Materials we treat, 2014 [online], citované: [7.5.2014], dostupné na internete: http://www.preciousmetals.umicore.com/recyclables/eScrap/MaterialsWeTreat/
[13] WIENEROVÁ V.: Návrh skladby chráněné dílny, včetně materiálového toku odpadů a komponentů, UPEI FSI VUT BRNO, Bakalárska práca, Brno 2009
[14] ALSHAYEB. M, KUSCH. S.: End of Life of Electronic Communication Devices in the Context of Strategies to Decouple Resources Use from Economic Growth, Conference of Informatics and Management Sciences, (2013) 133 - 137 [online], citované: [21.3.2014], dostupné na internete: http://www.sigrid.de/mediapool/55/553823/data/Alsheyab_Kusch_ICTIC 2013_Proceedings.pdf
[15] ALAFARA A. BABA, at. al.: Recovery of valuable metals from spent Mobile Phone Wastes. Part I: Dissolution Kinetics Evaluation, Pelagia Research Library, Advances in Applied Science Research, 2011, 2 (2): 117-127 [online], citované: [18.12.2013], dostupné na internete: http://pelagiaresearchlibrary.com/advances-in-applied-science/vol2-iss2/AdASR-2011-2-2-117-127.pdf
[16] Silver Price Ounce: current silver prices per ounce and silver prices history [online], citované: [29.3.2014], dostupné na internete: http://www.silverpriceoz.com/
[17] Gold price ounce: current gold prices ounce and gold prices history [online], citované [22.3.2014], dostupné na internete: http://www.goldpriceoz.com/
[18] The secret life series, A project of INFORM, Cell Phones, [online], [cit. 17.3.2014], dostupné na internete: http://www.informinc.org/pages/images/INFORM_The_Secret_Life_of_Cell_Phones.pdf
[19] Waste from electrical and electronic equipment, Citizens information, [online], citované: [4.12.2013], dostupné na internete: http://www.citizensinformation.ie/en/environment/waste_management_and_recycling/waste_from_electric_and_electronic_equipment.html
[20] NC State University: Electronics are banned from the landfill [online], citované: [3.12.2013], dostupné na internete: http://recycling.ncsu.edu/learnmore/electronics.php

***Authors*:**
Ing. Juraj Šebo, PhD., Tímea Rosenfelderová, Technical University of Košice, Faculty of Mechanical Engineering, Department of Industrial Engineering and Management, Nemcovej 32, 04200 Košice, Slovak Republic, Phone.: +421 55 6023241
E-mail: juraj.sebo@tuke.sk

INSTRUCTIONS FOR CONTRIBUTORS

No. of pages:	4 DIN A4 pages
Margins:	left: 2,5 cm
	right: 2 cm
	top: 2 cm
	bottom: 2 cm
Font:	Times New Roman
Title:	Bold 12, capitals
Abstract:	Italic 10
Headings:	Bold 10, capitals
Subheadings:	Bold 10, small letters
Text:	Regular 10
Columns:	Equal column width with 0,7 cm spacing
Spacing:	Single line spacing
Formulae:	Centered and numerated from 1 in ascending order. Equations must be typed in Equation Editor, with following settings: Style>Math – Times New Roman Size>Full 12pt, Subscript/Superscript 7pt, Symbol 18 pt
Figures:	High quality, numerated from 1 in ascending order (e.g.: Fig.1, Fig. 2 etc.); Figures and tables can spread over both two columns, please avoid photographs and color prints
Tables:	Numerated from 1 in ascending order (e.g..: Tab. 1, Tab. 2, etc.)
References:	Numerated from [1] in ascending order; cited papers should be marked by the number from the reference list (e.g. [1], [2, 3] ...)
Submission:	**Papers prepared in MS Word format should be e-mailed to: pkovac@uns.ac.rs, savkovic@uns.ac.rs**
Notice:	**Papers are to be printed in Journal of Production Engineering** Sample paper with detailed instructions can be found at: **http://www.jpe.ftn.uns.ac.rs/**

FOR MORE INFORMATION, PLEASE CONTACT:

Prof. Pavel Kovač, PhD, MEng.
Borislav Savković, *MSc. Assistant*
FACULTY OF TECHNICAL SCIENCES
Department for Production Engineering
Trg Dositeja Obradovica 6
21000 Novi Sad
Serbia
Tel.: (+381 21) 485 23 24; 485 23 20 ; 450 366;
Fax: (+381 21) 454 495
E-mail: pkovac@uns.ac.rs, savkovic@uns.ac.rs
http://www.jpe.ftn.uns.ac.rs/